Networked and Event-Triggered Control Systems

Tijs Donkers

disc

Networked and Event-Triggered Control Systems

PROEFSCHRIFT

ter verkrijging van de graad van doctor aan de
Technische Universiteit Eindhoven, op gezag van de
rector magnificus, prof.dr.ir. C.J. van Duijn, voor een
commissie aangewezen door het College voor
Promoties in het openbaar te verdedigen
op donderdag 27 oktober 2011 om 16.00 uur

door

Mattheus Cornelius Franciscus Donkers

geboren te Eindhoven

Dit proefschrift is goedgekeurd door de promotor:

prof.dr.ir. W.P.M.H. Heemels

Copromotor:
dr.ir. N. van de Wouw

Contents

Summary

Networked and Event-Triggered Control Systems

In this thesis, control algorithms are studied that are tailored for platforms with limited computation and communication resources. The interest in such control algorithms is motivated by the fact that nowadays control algorithms are implemented on small and inexpensive embedded microprocessors and that the sensors, actuators and controllers are connected through multipurpose communication networks. To handle the fact that computation power is no longer abundant and that communication networks do not have infinite bandwidth, the control algorithms need to be either robust for the deficiencies induced by these constraints, or they need to optimally utilise the available computation and communication resources. In this thesis, methodologies for the design and analysis of control algorithms with such properties are developed.

Networked Control Systems: In the first part of the thesis, so-called networked control systems (NCSs) are studied. The control algorithms studied in this part of the thesis can be seen as conventional sampled-data controllers that need to be robust against the artefacts introduced by using a finite bandwidth communication channel. The network-induced phenomena that are considered in this thesis are time-varying transmission intervals, time-varying delays, packet dropouts and communication constraints. The latter phenomenon causes that not all sensor and actuator data can be transmitted simultaneously and, therefore, a scheduling protocol is needed to orchestrate when to transmit what data over the network. To analyse the stability of the NCSs, a discrete-time modelling framework is presented and, in particular, two cases are considered: in the first case, the transmission intervals and delays are assumed to be upper and lower bounded, and in the second case, they are described by a sequence of continuous random variables. Both cases are relevant. The former case requires a less detailed description of the network behaviour than the latter case, while the latter results in a less conservative stability analysis than the former. This allows to make a tradeoff between modelling accuracy (of network-induced effects) and conservatism in the stability analysis. In both cases, linear plants and controllers are considered and the NCS is modelled as a discrete-time switched linear parameter-varying system. To assess the stability of this system, novel polytopic overapproximations are developed, which allows the stability of the NCS to be studied using a finite number of linear matrix inequalities. It will be shown that this approach reduces conservatism significantly with respect to existing results in the literature and allows for studying larger classes of controllers, including discrete-time dynamical output-based controllers. Hence, the main contribution of this part of the thesis is the de-

velopment of a new and general framework to analyse the stability of NCSs subject to four network-induced phenomena in a hardly conservative manner.

Event-Triggered Control Systems: In the second part of the thesis, so-called event-triggered control (ETC) systems are studied. ETC is a control strategy in which the control task is executed after the occurrence of an external event, rather than the elapse of a certain period of time as in conventional periodic sampled-data control. In this way, ETC can be designed to only provide control updates when needed and, thereby, to optimally utilise the available computation and communication resources. This part of the thesis consists of three main contributions in this appealing area of research.

The first contribution is the extension of the existing results on ETC towards dynamical output-based feedback controllers, instead of state-feedback control, as is common in the majority of the literature on ETC. Furthermore, extensions towards decentralised event triggering are presented. These extensions are important for practical implementations of ETC, as in many control applications full state measurements are not available for feedback, and sensors and actuators are often physically distributed, which prohibits the use of centralised event-triggering conditions. To study the stability and the $\mathcal{L}_\infty$-performance of this ETC system, a modelling framework based on impulsive systems is developed. Furthermore, for the novel output-based decentralised event-triggering conditions that are proposed, it is shown how nonzero lower bounds on the minimum inter-event times can be guaranteed and how they can be computed.

The second contribution is the proposition of the new class of periodic event-triggered control (PETC) algorithms, where the objective is to combine the benefits that, on the one hand, periodic sampled-data control and, on the other hand, ETC offer. In PETC, the event-triggering condition is monitored periodically and at each sampling instant it is decided whether or not to transmit the data and to use computation resources for the control task. Such an event-triggering condition has several benefits, including the inherent existence of a minimum inter-event time, which can be tuned directly. Furthermore, the fact that the event-triggering condition is only verified at the periodic sampling times, instead of continuously, makes it possible to implement this strategy in standard time-sliced embedded software architectures. To analyse the stability and the $\mathcal{L}_2$-performance for these PETC systems, methodologies based on piecewise-linear systems models and impulsive system models will be provided, leading to an effective analysis framework for PETC.

Finally, a novel approach to solving the codesign problem of both the feedback control algorithm and the event-triggering condition is presented. In particular, a novel way to solve the minimum attention and anytime attention control problems is proposed. In minimum attention control, the 'attention' that a control task requires is minimised, and in anytime attention control, the

performance under the 'attention' given by a scheduler is maximised. In this context, 'attention' is interpreted as the inverse of the time elapsed between two consecutive executions of a control task. The two control problems are solved by formulating them as linear programs, which can be solved efficiently in an online fashion. This offers a new and elegant way to solve both the minimum attention control problem and the anytime attention control problem in one unifying framework.

The contributions presented in this thesis can form a basis for future research explorations that can eventually lead to mature system theories for both NCSs and ETC systems, which are indispensable for the deployment of NCSs and ETC systems in a large variety of practical control applications.

1

Introduction

1.1   Networked and Event-Triggered Control Systems

A current trend in control engineering is to no longer implement control algorithms on dedicated computation platforms having dedicated communication channels. Instead, control algorithms are nowadays implemented on embedded microprocessors [91], which communicate with the sensors and actuators using (shared) communication networks. This results in larger flexibility and maintainability of the control system, as modifying control algorithms and adding control loops becomes easier. These advantages form some of the reasons why this control architecture is applied in conventional passenger cars, in which more and more data is transmitted over a controller area network (CAN) [84]. Furthermore, besides the enhanced flexibility and maintainability, the embedded and networked control architecture allows the control system to have less wiring, with the extremum of being completely wireless. This is especially beneficial for large-scale systems, e.g., mines [141], manufacturing/production lines [97], chemical plants [123], water distribution networks [25] and distributed power generation systems [18]. In some cases even, wiring the control systems is impossible, e.g., in cooperative control of unmanned aerial vehicles (UAVs) [110], vehicle platoons on motorways [48, 106], or in tele-operated haptic systems [70, 93]. Hence, control systems that use embedded microprocessors and communication networks can already be found in a large variety of practical applications and the deployment of these control systems is believed to even grow in the near future. In fact, the development of control strategies that are tailored for embedded microprocessors and communication networks is considered as one of the important challenges in control theory [98], as this will further reinforce this trend.

Despite the aforementioned advantages, using embedded microprocessors and (shared) communication networks causes the closed-loop system to exhibit behaviour that it would not exhibit when employing dedicated computation platforms and dedicated communication channels. This is caused by the fact that the computation power is not abundant on embedded microprocessors, and communication networks do not have infinite bandwidth. Furthermore, the control task has to share computation and communication resources with other tasks, which makes the availability of these resources time varying and possibly uncertain. Still, control algorithms are typically designed under the assumption that sufficient computation and/or communication resources are available, as this allows control algorithms to be designed and analysed using well-developed 'classical' techniques, see, e.g., [8, 27, 118, 148]. This leads, however, to over-utilisation of the available resources and requires over-provisioned hardware, which is not desirable in a competitive market where the overall cost price of a system should often be as low as possible.

Therefore, control algorithms are needed that are designed to ensure a desired control performance, while taking the restrictions of the implementation explicitly into account. There are, in principle, two ways of doing this: (i) designing control algorithm with a traditional structure that are robust against the consequences induced by the imperfect implementation environment (to a certain extent), or (ii) designing control algorithms that reduce the computation and communication resources needed to execute the control task. In the literature, the former approach is studied in the field of networked control systems (NCSs), and the latter is studied in the field of event-triggered control systems (ETCSs). Both these approaches are studied in this thesis. The motivation for studying both these approaches in a single thesis comes from the fact that they both take scarcity of the resources available for control explicitly into account.

1.1.1 Networked Control Systems

NCSs are systems in which the control loops are closed over a real-time communication network. The fact that controllers, sensors, and actuators are connected through a multipurpose network introduces new challenges, caused by the packet-based data exchange between different parts of the network. Compared to a traditional control system, see Figure 1.1a, the fact that the communication network has only a finite bandwidth causes the outputs of the controller u and the outputs of the plant y not to be exactly equal to the inputs of the plant $\hat{u}$ and the inputs of the controller $\hat{y}$, respectively, see Figure 1.1b. Therefore, the control algorithm has to be robust against the artefacts introduced by the communication network that cause $u \neq \hat{u}$ and $y \neq \hat{y}$. Generally speaking, these artefacts can be categorised into the following five types.

(a) Traditional Control System

(b) Networked Control System with $y \neq \hat{y}$ and $u \neq \hat{u}$
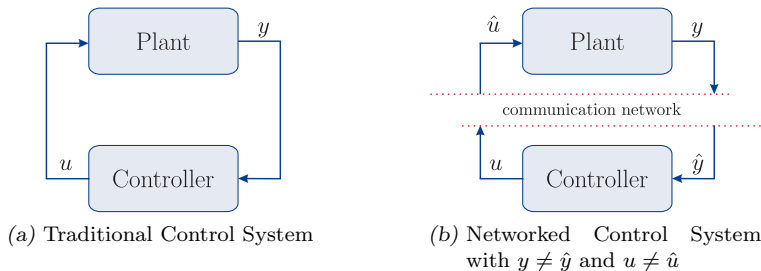
Figure 1.1: A Traditional versus a Networked Control System Schematic.

Quantisation of the transmitted signals: Quantisation occurs because the transmitted data is sent in packets that only have a finite word length.

Packet dropouts: Transmissions may fail, due to collisions of packets with others or because the data gets corrupted in the physical layer of the network, causing a message to never arrive or to become unreadable.

Varying sampling/transmisson intervals (jitter): In NCSs, each network node has only a limited processing power and the local clocks typically have a low accuracy. Therefore, the time instants at which the data is sampled and transmitted is inaccurate, which causes the transmission/sampling interval to be uncertain and time varying.

Varying transmission delays (latencies): Sampling and transmitting data, and executing the control algorithm take a certain (nonzero) amount of time. Besides the fact that these operations cannot be performed infinitely fast, the network and the computation resources can also be partially occupied by other tasks and the data can be routed differently at every transmission. This introduces nonzero and time-varying transmission delays.

Communication constraints: When several sensors and actuators have to communicate over a shared network, it is generally impossible to transmit all sensor and actuator signals simultaneously. This introduces the need for a scheduling protocol that orchestrates when a node is given access to the network and is allowed to transmit its data.

It is generally known that any of these phenomena can degrade closed-loop performance or, even worse, can harm closed-loop stability of the control system, see, e.g., [31]. It is therefore important to know how these effects influence

stability and performance in a quantitative way. Extensive overviews of the existing literature that studies these phenomena are given in Chapters 2 and 3. A general observation obtained from these literature surveys is that most of the results in the literature only consider a few of the aforementioned phenomena, while ignoring the others. As in reality all these phenomena are present simultaneously, it is important to have a single framework for the modelling, the stability analysis and the controller synthesis for NCSs in which the joint presence of all the aforementioned phenomena can be studied.

1.1.2   Event-Triggered Control Systems

Event-triggered control (ETC), see [6, 9, 59, 64], is a control strategy in which the control task is executed after the occurrence of an external event, rather than after the elapse of a fixed period of time as in conventional periodic control. As such, the ETC algorithm consists of two parts: the feedback controller that computes the plant inputs based on sampled and transmitted plant outputs, and the event-triggering mechanism (ETM) that determines when, and which, outputs of the plant and the controller have to be transmitted, see Figure 1.2. A typical ETM invokes transmissions of (some of) the outputs of the plant and the controller when a certain event-triggering condition is violated and, when properly designed, it is such that these transmissions only take place when needed from a stability and performance point of view, thereby reducing the utilisation of the available computation and communication resources.

Closely related to ETC is self-triggered control [130]. In self-triggered control, the ETM is such that the time instant that the violation of the event-triggering condition is pre-computed using previously sampled and transmitted data and knowledge on the plant dynamics. This has the advantage that there is no need for (continuously) monitoring violations of the event-triggering condition and the ETM as depicted in Figure 1.2 can be considered to be emulated in software. The name 'self-triggered' comes from the fact that it is not really an 'external event', but rather the controller itself that determines the next time instant to transmit. Self-triggered control uses similar techniques to analyse stability and performance, and can be considered as a special case of ETC.

Although the advantages of ETC are well-motivated and practical applications show its potential, relatively few theoretical results exist that study ETCS in a mathematically rigourous way. An overview of the few existing results on ETC will be given in Chapter 4. The main reason for the absence of a comprehensive theory is the fact that the system behaviour of ETCSs is intrinsically hybrid, i.e., it has both continuous as well as discrete behaviour, which makes their analysis difficult. Still, the recent developments in hybrid system theory, see, e.g., [50, 55], offer opportunities for maturing the event-triggered system theory, so that it can support the deployment of ETC in practice. Be-
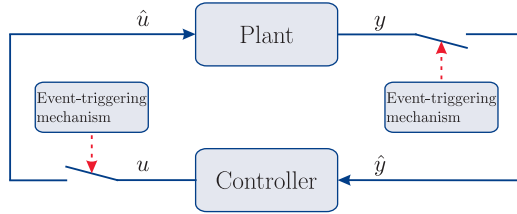
Figure 1.2: An Event-Triggered Control System Schematic.

sides the absence of a mature system theory for ETC, also the ETC strategies that currently exist in the literature have limitations that hamper their wide application in practice.

A first limitation is that most of the existing results on ETC consider state-feedback controllers, which is an unrealistic assumption as in many control applications full state measurements are not available for feedback. Furthermore, in most works in ETC, a centralised ETM is used, meaning that the ETM has an event-triggering condition, which invokes, when violated, simultaneous transmissions of all the outputs of the plant and controller. Typically, such a centralised ETM requires access to all the sensor and actuator data to decide when to transmit data, which might be prohibitive as actuators, sensors and controllers can be physically distributed. Therefore, the existing results on ETC have to be extended so that dynamical output-based controllers and decentralised ETMs can be studied. In such a decentralised ETM, only parts of the inputs and outputs are transmitted when a local event-triggering condition, which uses only locally available sensor or actuator data, is violated. Note that there exist some preliminary results on ETC that use dynamical output-based feedback controllers, however an analysis of the minimum time between two subsequent events, the so-called minimum inter-event time, is not available for these works. Having such a (nonzero) minimum inter-event time is important, as this allows us to guarantee an upper bound on the number of events within a certain time interval. Being able to bound the number of events within a certain time interval is important as our primary reason to make control systems event-triggered is to save computation and communication resources.

The second limitation is that the implementation of event-triggered controllers on digital platforms requires continuous monitoring of all the outputs. As often proposed in the literature, this can be done using dedicated analogue hardware. However, if instead ETC could be implemented without the need for dedicated hardware and it could work on more traditional time-sliced architecture of the embedded software, deploying ETC in practice becomes a lot easier. In other words, an ETC algorithm is needed that can be implemented using more traditional time-sliced software architectures, while still preserving the benefits of reduced utilisation of computation and communication resources.

A final limitation of the existing results on ETC is that all these results use an 'emulation-based approach', by which we mean that the feedback controller is designed assuming an ideal (non-event-triggered) implementation, while, subsequently, the ETM is designed (based on the feedback controller resulting from the first step of the design procedure). As a consequence, during the design of the feedback controller, no knowledge of the ETM is incorporated at all. Clearly, simultaneously designing both could leads to more optimal ETCSs than the ones obtained using a sequential design approach.

Overcoming the limitations discussed above, together with a corresponding systematic analysis and design framework, greatly enhances the dissemination of ETC in control engineering practice significantly.

1.2   Objectives and Contributions

From the discussion above, we can conclude that both fields of NCSs and ETCSs have several major open problems and the theories for NCSs and ETCSs are far from being comprehensive. We will, therefore, address these aforementioned open problems in this thesis, thereby making a significant step towards such comprehensive theories.

1.2.1   Networked Control Systems

As discussed in Section 1.1.1, there is currently a strong need for a unifying framework that allows the stability and the performance of NCSs to be studied when it is simultaneously subject to all the mentioned network-induced phenomena. Some results exist that are able to study the joint presence of several network-induced phenomena. In particular, time-varying transmission intervals, time-varying delays and communication constraints are studied in [26, 62]. However, these results use a continuous-time controller, which can of course be discretised, but it is of high practical relevance to directly study discrete-time controllers. In addition, the results presented in [26, 62] have a certain level of conservatism and cannot exploit specific structure, such as linearity, being present in the control problem at hand.

In this thesis, we will, therefore, develop a framework for stability analysis of NCSs that are subject to time-varying transmission intervals, time-varying delays and communication constraints. The occurrence of packet dropouts can be included by (implicitly) modelling them as prolongations of the transmission intervals, see, e.g. [113]. The framework is sufficiently rich to allow for extensions in the direction of the inclusion of, for instance, quantisation and analysis of the closed-loop performance, but these are left for future research (even though some preliminary work regarding the inclusion of quantisation is reported in [89]). The framework we will present is based on discrete-time switched and parameter-varying models for NCSs, where the switching is due

to the scheduling protocol, which is needed because of the communication constraints, and the varying parameters are due to the unknown and time-varying transmission intervals and delays. The fact that we use a discrete-time modelling framework allows the considered dynamical output-based controller to be given in continuous time, as is commonly done in the existing NCS literature, as well as in discrete time, which is more useful in the practical implementation of NCSs, as already argued above. We will focus on linear plants and controllers and consider two cases. In the first case, the transmission intervals and delays are assumed to be within certain (given) bounds and, in the second case, they are described by a sequence of random continuous variables, satisfying a (given) probability distribution. Note that the former case requires less information of the network behaviour than the latter case (for instance, the probability density function does not have to be known exactly, but only its support), while the latter results in a less conservative stability analysis than the former as it can incorporate more detailed knowledge. This makes both cases relevant. We will provide techniques for assessing the stability of the NCS using polytopic overapproximations and linear matrix inequalities (LMIs) [19]. Moreover, we will show that this approach reduces conservatism significantly with respect to existing results in the literature, meaning that we can now guarantee stability for NCSs for which such guarantees could not be given before.

1.2.2 Event-Triggered Control Systems

In Section 1.1.2, we observed that the theory on ETC is far from being comprehensive and that, in striving for such a comprehensive theory, several contributions are needed. We will make some of those contributions in this thesis.

The first contribution is the development of dynamical output-based event-triggered controllers. As mentioned in Section 1.1.2, the fact that the controller is based on output feedback instead of state feedback requires nontrivial extensions of existing ETMs in order to guarantee a nonzero minimum time between two subsequent events. Furthermore, since sensors and actuators, which can be grouped into nodes, can be physically distributed, centralised ETMs are often prohibitive and, therefore, there is a need for decentralised ETMs. We will propose a novel output-based decentralised ETC strategy that has nonzero minimum inter-event times and we will study the closed-loop stability and the $\mathcal{L}_\infty$-performance of the resulting ETCS. We provide a computational procedure to compute a lower bound on the minimum inter-event time of each node. Furthermore, we will model the event-triggered control system as an impulsive system, thereby explicitly describing the behaviour of the event-triggered control system, which leads to improved stability guarantees, compared to the existing results in the ETC literature.

The second contribution in the area of ETC is the proposition of an ETC strategy that alleviates the need for dedicated hardware for its implementation.

We will do this by striking a balance between periodic sampled-data control and event-triggered control, which will lead to so-called periodic event-triggered control (PETC) algorithms that preserve the advantages of reduced resource usage on the one hand, while the event-triggering conditions have a periodic character on the other hand. The most important benefit of the strategy is that it can be implemented using a more traditional time-sliced software architecture. To analyse the stability and the $\mathcal{L}_2$-performance of the proposed PETC algorithm, we will propose novel methodologies. These methodologies will be based on discrete-time piecewise-linear system models, on discrete-time perturbed system models and on impulsive system models, leading to an effective analysis framework for PETC.

Finally, we will make a first step towards solving the codesign problem for ETC, i.e., the joint design of the feedback controller and the ETM. In particular, we aim at designing a control algorithm that yields both the controller output and the next sampling and transmission instant, given a sampled measurement. Hence, the resulting control algorithm can be perceived as a self-triggered control algorithm [130], but the method also has strong relations to another existing approach in the literature, see [3, 21], being 'minimum attention control', where 'attention' is interpreted as the inverse of the time elapsed between two consecutive transmissions of the controller outputs. In minimum attention control, the 'attention' that a control task requires is minimised given certain performance requirements. A related problem is that of 'anytime attention control' [3], where the control objective is to maximise the performance under the 'attention' given by a scheduler. Hence, anytime attention control aims at finding a control value that optimises a certain performance criterion, given a sampled measurement and a given next sampling and transmission instant. We will show that the problem formulation of minimum attention control is similar to that of anytime attention control and, therefore, we will provide a unifying framework leading to the same solution strategy for both problems. Both resulting control algorithms will be in the form of a linear program that can be solved efficiently online.

1.3   Outline of the Thesis

This thesis consists of two parts, which in turn, consist of two and three chapters, respectively. Each of these chapters is based entirely on a research paper and is therefore self contained. As a consequence, each individual chapter can be read independently.

Part I: Networked Control Systems

Chapter 2:   In this chapter, we present the discrete-time modelling approach to analyse stability of NCSs subject to time-varying transmission intervals,

time-varying delays, communication constraints, and assume that the transmission intervals and delays are upper and lower bounded. This chapter is based on [40], of which a preliminary version appeared as [41].

Chapter 3: This chapter extends the framework presented in Chapter 2 to study stability of NCSs, in which now the transmission intervals and delays are modelled as a sequence continuous random variables, and the occurrence of packet dropouts is modelled as a Markov chain. This chapter is based on [39], of which a preliminary version appeared as [38].

Part II: Event-Triggered Control Systems

Chapter 4: The contribution of this chapter is to extend the existing results in the literature on state-feedback controllers to dynamical output-based controllers and providing an analysis framework based on impulsive systems. This chapter is based on [37], of which a preliminary version appeared as [36].

Chapter 5: The new class of periodic event-triggered controllers is introduced in this chapter. This chapter is based on [57], of which a preliminary version appeared as [58].

Chapter 6: In Chapter 6, we present a novel approach to design minimum attention and anytime attention control algorithms for linear systems. This chapter is based on [42].

Finally, we reflect on the work presented in this thesis by drawing conclusions and giving recommendations for future research in Chapter 7.

Besides the topics covered in this thesis, the research presented in to this thesis also led to a framework to analyse and design stochastic model predictive controllers [17], a methodology to synthesise decentralised observer-based controllers [13, 14], a comparison of several modelling approaches for packet dropouts [113], a comparison of several convex overapproximation techniques [63], and first results on the inclusion of quantisation in the discrete-time modelling framework for NCSs [89].

1.4 Publications

The research leading to this thesis, also lead to the following publications.

Journals Publications:

- M.C.F. Donkers, W.P.M.H. Heemels, N. van de Wouw and L. Hetel, Stability Analysis of Networked Control Systems using a Switched Linear Systems Approach. *IEEE Trans. Autom. Control*, 56:2101–2115, 2011.

- M.C.F. Donkers, W.P.M.H. Heemels, D. Bernadini, A. Bemporad and V. Shneer. Stability Analysis of Stochastic Networked Control Systems. *Accepted for Automatica*, 2011.

- M.C.F. Donkers and W.P.M.H. Heemels, Output-Based Event-Triggered Control with Guaranteed $\mathcal{L}_\infty$-gain and Improved and Decentralised Event-Triggering. *Conditionally accepted for IEEE Trans. Autom. Control*, 2011.

- W.P.M.H. Heemels, M.C.F. Donkers and A.R. Teel, Periodic Event-Triggered Control. *Submitted for journal publication*, 2011.

- N.W. Bauer, M.C.F. Donkers, W.P.M.H. Heemels and N. van de Wouw, Decentralized observer-based control via networked communication. *Submitted for journal publication*, 2011.

- S.J.L.M. van Loon, M.C.F. Donkers, W.P.M.H. Heemels and N. van de Wouw, Stability analysis of networked and quantized control systems: A Switched Linear Systems Approach. *Submitted for journal publication*, 2011.

Book Chapters:

- M.C.F. Donkers, L. Hetel, W.P.M.H. Heemels, N. van de Wouw and M. Steinbuch, Stability Analysis of Networked Control Systems using a Switched Linear Systems Approach. In Lecture Notes in Computer Science. *Hybrid Systems: Computation and Control*, pages 150–164, Springer Verlag, 2009.

Refereed Conference Contributions:

- N.W. Bauer, M.C.F. Donkers, W.P.M.H. Heemels and N. van de Wouw, An approach to observer-based decentralized control under periodic protocols. In *Proc. American Control Conf.*, pages 2125 – 2131, 2010.

- D. Bernadini, M.C.F. Donkers, A. Bemporad and W.P.M.H. Heemels, A Model Predictive Control Approach for Stochastic Networked Control Systems, In *Proc. IFAC Workshop Distributed Estimation & Control in Networked Systems*, pages 7 – 12, 2010.

- M.C.F. Donkers and W.P.M.H. Heemels, Output-Based Event-Triggered Control with Guaranteed $\mathcal{L}_\infty$-gain and Improved Event-Triggering. In *Proc. IEEE Conf. Decision & Control*, pages 3246 – 3251, 2010.

- M.C.F. Donkers, W.P.M.H. Heemels, D. Bernadini, A. Bemporad and V. Shneer. Stability Analysis of Stochastic Networked Control Systems. In *Proc. American Control Conf.*, pages 3684 – 3689, 2010.

- W.P.M.H. Heemels, N. van de Wouw, R. Gielen, M.C.F. Donkers, L. Hetel, S. Olaru, M. Lazar, J. Daafouz and S. I. Niculescu, Comparison of Overapproximation Methods for Stability Analysis of Networked Control Systems. In *Proc. Conf. Hybrid Systems: Computation and Control*, pages 181 – 190, 2010.

- J.J.C. van Schendel, M.C.F. Donkers, W.P.M.H. Heemels and N. van de Wouw, On Dropout Modelling for Stability Analysis of Networked Control Systems. In *Proc. American Control Conf.*, pages 555 – 561, 2010.

- M.C.F. Donkers, P. Tabuada and W.P.M.H. Heemels, On the minimum attention control problem for linear systems: a linear programming approach. In *Proc. IEEE Conf. Decision & Control*, 2011.

- W.P.M.H. Heemels, M.C.F. Donkers and A.R. Teel, Periodic Event-Triggered Control Based on State Feedback. In *Proc. IEEE Conf. Decision & Control*, 2011.

Part I

Networked Control Systems

2

Stability Analysis of Networked Control Systems using a Switched Linear Systems Approach[1]

Abstract − In this chapter, we study the stability of networked control systems (NCSs) that are subject to time-varying transmission intervals, time-varying transmission delays, packet dropouts and communication constraints. Communication constraints impose that, per transmission, only one node can access the network and send its information. The order in which nodes send their information is orchestrated by a network protocol, such as, the round-robin (RR) and the try-once-discard (TOD) protocol. In this chapter, we generalise the mentioned protocols to novel classes of so-called 'periodic' and 'quadratic' protocols. By focussing on linear plants and controllers, we present a modelling framework for NCSs based on discrete-time switched linear uncertain systems. This framework allows the controller to be given in discrete time as well as in continuous time. To analyse stability of such systems for a range of possible transmission intervals and delays, we propose a new procedure to obtain a convex overapproximation in the form of a polytopic system with norm-bounded additive uncertainty. We show that this approximation can be made arbitrarily tight in an appropriate sense. Based on this overapproximation, we derive stability results in terms of linear matrix inequalities (LMIs). We illustrate our stability analysis on the benchmark example of a batch reactor and show how this leads to tradeoffs between different protocols, allowable ranges of transmission intervals and delays.

---

[1]This chapter is based on [40].

2.1 Introduction

Networked control systems (NCSs) are systems in which control loops are closed over a real-time communication network. The fact that controllers, sensors, and actuators are not connected through point-to-point connections, but through a multipurpose network offers advantages, such as increased system flexibility, ease of installation and maintenance, and decreased wiring and cost. However, networking the control system also introduces new challenges, caused by the packet-based data exchange between different parts of the network. Therefore, control algorithms are needed that can handle the communication imperfections and constraints caused by the packet-based communication. The control community is widely aware of this fact, as is evidenced by the broad attention NCSs have received recently, see, e.g., the overview papers [67, 128, 144, 147].

In general, network-induced communication imperfections and constraints can be categorised into five types:

(i) Quantisation errors in the transmitted signals, due to the finite word length of the transmitted packets.

(ii) Packet dropouts, due to unreliable transmissions.

(iii) Variable sampling/transmission intervals.

(iv) Variable transmission delays.

(v) Communication constraints, i.e., not all sensor and actuator signals can be transmitted at the same time.

It is generally known that any of these phenomena can degrade closed-loop performance or, even worse, can harm closed-loop stability of the control system. It is therefore important to know how these effects influence the stability properties.

Systematic approaches to analyse stability of NCSs subject to only one of these network-induced imperfections are well developed. For instance, the effects of quantisation are studied in [22, 35, 61, 86, 101], of packet dropouts in [88, 117, 119], of time-varying transmission intervals and delays in [12, 45, 69, 96, 122], and [31, 43, 49, 68, 76, 100, 146], respectively, and of communication constraints in [20, 34, 72, 109]. However, since in NCSs typically all the aforementioned limitations and constraints are present simultaneously, it is relevant to study the consequences of all these phenomena in a common framework. Unfortunately, fewer results are available that study combinations of these imperfections. References that simultaneously consider *two* types of network-induced imperfections are given in Table 2.1. Furthermore, [102] considers imperfections of type (i), (iii), (v) and [29] studies type (ii), (iii) and (iv) simultaneously. In this chapter, we will focus on the stability of NCSs with

Table 2.1: References that study two network-induced imperfections simultaneously.

&	(iv)	(v)
(i)	[87]	
(ii)	[30, 145]	
(iii)	[99, 142]	[24, 41, 103, 132, 134]

time-varying transmission intervals and delays and the presence of communication constraints, i.e., type (iii), (iv) and (v) phenomena.

Stability of NCSs subject to communication constraints, time-varying transmission intervals and transmission delays has already been considered in [26, 62]. The communication constraints impose that, per transmission, only one node can access the network and send its information and, hence, a protocol is needed to orchestrate when a certain communication node is given access to the network. Given a protocol, such as the round-robin (RR) and the try-once-discard (TOD) protocol, the mentioned papers provide criteria for computing the so-called maximum allowable transmission interval (MATI) and the maximum allowable delay (MAD). Stability is guaranteed as long as the actual transmission intervals and delays are always smaller than the MATI and MAD, respectively. The difference between the work in [62] and [26], is that in the latter a delay compensation scheme is proposed. This delay compensation requires time stamping of the messages and sending future control signals in larger packets, which is not needed in the more basic *emulation based* approach, as in [62] and the earlier work without transmission delays in [24, 41, 102, 103, 125, 132, 134]. Furthermore, the results in [26] have the drawback that they are not applicable to the commonly used Round-Robin protocol, while [62] is.

The work presented in [26, 62] both apply to general nonlinear plants and controllers and are based on a continuous-time modelling paradigm related to impulsive systems as in [50]. However, neither [26], nor [62] include the possibility that the controller is formulated in discrete time. The case of discrete-time controllers has been considered in [34], however, assuming that the transmission interval is constant and that delays are absent. Another feature of [26, 62] is that, in these works, zero lower bounds on the transmission intervals h_k and delays τ_k are considered (i.e., $h_k \in (0, h_{\text{MATI}}]$, $\tau_k \in [0, \tau_{\text{MAD}}]$). The ability to handle discrete-time controllers and nonzero lower bounds on the transmission intervals and delays is highly relevant from a practical point of view, because controllers are typically implemented in a digital and, thus, discrete-time form. Furthermore, finite communication bandwidth always introduce nonzero lower bounds on the transmission intervals and transmission delays. This motivates

the need for studying these situations as well, preferably in a nonconservative manner. Although the work presented in [26, 62] is very general and can accommodate for many nonlinear NCSs, their results cannot reduce conservatism when a certain structure is present in the NCS, such as linearity of the controller and plant.

In this chapter, we focus on linear plants and linear controllers and study the stability of the corresponding NCS in the presence of communication constraints, time-varying transmission intervals and time-varying delays, where the latter two possibly have a *nonzero* lower bound. We will also comment on how to accommodate for packet dropouts. Moreover, we allow for both a continuous-time as well as a *discrete-time* controller, which requires a different modelling paradigm than in [26, 62], and in the work without transmission delays, [24, 41, 103, 132, 134]. In particular, we provide techniques for assessing stability of the NCS with time-varying transmission intervals $h_k \in [\underline{h}, \overline{h}]$ and time-varying transmission delays $\tau_k \in [\underline{\tau}, \overline{\tau}]$ for two well-known protocols, namely, the round-robin (RR) protocol and the try-once-discard (TOD) protocol, and their generalisations. These generalisations consist of the classes of 'periodic' and 'quadratic' protocols, which are formally introduced here. In contrast with [26, 62], we apply a *discrete-time* modelling framework that leads to a switched linear system model with exponential uncertainty. To properly handle this exponential uncertainty, we provide a polytopic overapproximation for this system. This overapproximation is obtained using a novel procedure that combines ideas from gridding [45, 122] and norm bounding [12, 43, 69]. Unlike other methodologies for obtaining a convex overapproximation, see, e.g., [12, 31, 43, 45, 49, 69, 122] and the overview paper [63], we provide a proof that the newly proposed procedure can be made arbitrarily tight in an appropriate sense. Using this overapproximated system, we can assess stability using newly developed conditions based on linear matrix inequalities (LMIs). We will show the effectiveness of the presented approach on the benchmark example of a batch reactor as used in [24, 34, 41, 62, 103, 125, 134], as well. Moreover, we will show that the linearity of plant and controller can indeed be exploited, which leads to a significant reduction of conservatism with respect to the existing approaches.

The remainder of this chapter is organised as follows. After introducing the necessary notational conventions used in this chapter, we introduce the model of the NCS in Section 2.2 and propose a method to write it as a discrete-time switched linear uncertain system. We also state a precise problem formulation. Subsequently, in Section 2.3, we provide a procedure to overapproximate the NCS model by a polytopic system with norm-bounded uncertainty. In Section 2.4, we provide conditions for stability of the NCS in terms of LMIs and reflect in Section 2.5 on the conservatism this approach introduces. Finally, we illustrate the stability results using a numerical benchmark example in Section 2.6 and draw conclusions in Section 2.7. Appendix A.1 contains the proofs of the

more technical lemmas and theorems.

2.1.1   Nomenclature

The following notational conventions will be used. $\mathbb{R}_+$ denotes the set of non-negative real numbers. $\mathrm{diag}(A_1, \ldots, A_n)$ denotes a block-diagonal matrix with the entries $A_1, \ldots, A_n$ on the diagonal and $A^\top \in \mathbb{R}^{m \times n}$ denotes the transposed of matrix $A \in \mathbb{R}^{n \times m}$. For a vector $x \in \mathbb{R}^n$, we denote by x^i the i-th and by $\|x\| := \sqrt{x^\top x}$ its Euclidean norm. We denote by $\|A\| := \sqrt{\lambda_{\max}(A^\top A)}$ the spectral norm of the matrix $A \in \mathbb{R}^{n \times m}$, which is the square-root of the maximum eigenvalue of the matrix $A^\top A$. For brevity, we sometimes write symmetric matrices of the form $\begin{bmatrix} A & B \\ B^\top & C \end{bmatrix}$, as $\begin{bmatrix} A & B \\ \star & C \end{bmatrix}$. Finally, by $\lim_{s \downarrow t}$ and $\lim_{s \uparrow t}$, we denote the limit as s approaches t from above and below, respectively, and the convex hull and interior of a set $\mathcal{A}$ are denoted by $\mathrm{co}\mathcal{A}$ and $\mathrm{int}\mathcal{A}$, respectively.

2.2   NCS Model and Problem Statement

In this section, we present the model describing the networked control systems (NCSs), subject to communication constraints, time-varying transmission intervals and delays. We will later comment on how this model can accommodate for packet dropouts. Let us consider the linear time-invariant (LTI) continuous-time plant given by

$$\begin{cases} \frac{\mathrm{d}}{\mathrm{d}t} x^p(t) = A^p x^p(t) + B^p \hat{u}(t) \\ \qquad y(t) = C^p x^p(t), \end{cases} \tag{2.1}$$

where $x^p \in \mathbb{R}^{n_p}$ denotes the state of the plant, $\hat{u} \in \mathbb{R}^{n_u}$ the most recently received control variable, $y \in \mathbb{R}^{n_y}$ the (measured) output of the plant and $t \in \mathbb{R}_+$ the time. The controller, also an LTI system, is assumed to be given in either continuous time by

$$\begin{cases} \frac{\mathrm{d}}{\mathrm{d}t} x^c(t) = A^c x^c(t) + B^c \hat{y}(t) \\ \qquad u(t) = C^c x^c(t) + D^c \hat{y}(t), \end{cases} \tag{2.2a}$$

or in discrete time by

$$\begin{cases} x^c_{k+1} = A^c x^c_k + B^c \hat{y}_k \\ u(t_k) = C^c x^c_k + D^c \hat{y}(t_k). \end{cases} \tag{2.2b}$$

In these descriptions, $x^c \in \mathbb{R}^{n_c}$ denotes the state of the controller, $\hat{y} \in \mathbb{R}^{n_y}$ the most recently received output of the plant and $u \in \mathbb{R}^{n_u}$ denotes the controller output. At transmission instant $t_k, k \in \mathbb{N}$, (parts of) the outputs of the plant $y(t_k)$ and controller $u(t_k)$ are sampled and are transmitted over the
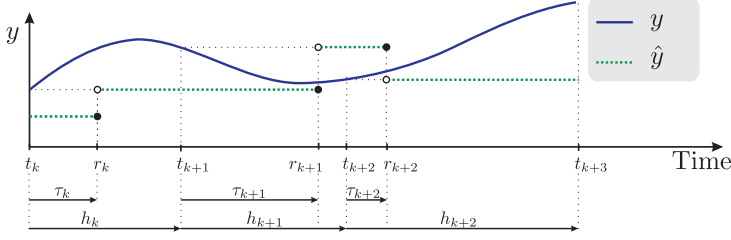
Figure 2.1: Illustration of a typical evolution of y and $\hat{y}$.

network. We assume that they arrive at instant r_k, called the arrival instant. The situation described above is illustrated in Fig. 2.1. In the case we have a discrete-time controller (2.2b), the states of the controller x^c_{k+1} are updated using $\hat{y}_k := \lim_{t \downarrow r_k} \hat{y}(t)$, i.e., as in [34], directly after $\hat{y}$ is updated. Note that in this case, the update of x^c_{k+1} in (2.2b) has to be performed in the time interval $(r_k, t_{k+1}]$.

Let us now explain in more detail the functioning of the network and define these 'most recently received' $\hat{y}$ and $\hat{u}$ exactly, see also [24, 34, 41, 62, 103, 132, 134]. The plant is equipped with sensors and actuators that are grouped into N nodes. At each transmission instant t_k, $k \in \mathbb{N}$, one node, denoted by $\sigma_k \in \{1, \ldots, N\}$, obtains access to the network and transmits its corresponding values. These transmitted values are received and implemented on the controller or the plant at arrival instant r_k. As in [62], a transmission only occurs after the previous transmission has arrived, i.e., $t_{k+1} > r_k \geqslant t_k$, for all $k \in \mathbb{N}$. In other words, we consider the sampling interval to be lower bounded and the delays to be smaller than the transmission interval. After each transmission and reception, the values in $\hat{y}$ and $\hat{u}$ are updated with the newly received values, while the other values in $\hat{y}$ and $\hat{u}$ remain the same, as no additional information is received. This leads to the constrained data exchange expressed as

$$\begin{cases} \hat{y}(t) = \Gamma^y_{\sigma_k} y(t_k) + (I - \Gamma^y_{\sigma_k})\hat{y}(t_k) \\ \hat{u}(t) = \Gamma^u_{\sigma_k} u(t_k) + (I - \Gamma^u_{\sigma_k})\hat{u}(t_k) \end{cases} \tag{2.3}$$

for all $t \in (r_k, r_{k+1}]$. The matrix $\Gamma_{\sigma_k} := \mathrm{diag}(\Gamma^y_{\sigma_k}, \Gamma^u_{\sigma_k})$ is a diagonal matrix, given by

$$\Gamma_i = \mathrm{diag}(\gamma_{i,1}, \ldots, \gamma_{i,n_y+n_u}). \tag{2.4}$$

when $\sigma_k = i$. In (2.4), the elements $\gamma_{i,j}$, with $i \in \{1, \ldots, N\}$ and $j \in \{1, \ldots, n_y\}$, are equal to one, if plant output y^j is in node i, elements $\gamma_{i,j+n_y}$, with $i \in \{1, \ldots, N\}$ and $j \in \{1, \ldots, n_u\}$, are equal to one, if controller output u^j is in node i, and are zero elsewhere.

The value of $\sigma_k \in \{1, \ldots, N\}$ in (2.3) indicates which node is given access to the network at transmission instant t_k, $k \in \mathbb{N}$. Indeed, (2.3) reflects that

the values in $\hat{u}$ and $\hat{y}$ corresponding to node σ_k are updated just after r_k, with the corresponding transmitted values at time t_k, while the others remain the same. A scheduling protocol determines the sequence $(\sigma_0, \sigma_1, \ldots)$ and particular protocols will be made explicit later.

The transmission instants t_k, as well as the arrival instants r_k, $k \in \mathbb{N}$ are not necessarily distributed equidistantly in time. Hence, both the transmission intervals $h_k := t_{k+1} - t_k$ and the transmission delays $\tau_k := r_k - t_k$ are varying in time, as is also illustrated in Fig. 2.1. We assume that the variations in the transmission interval and delays are bounded and are contained in the sets $[\underline{h}, \overline{h}]$ and $[\underline{\tau}, \overline{\tau}]$, respectively, with $\overline{h} \geqslant \underline{h} > 0$ and $\overline{\tau} \geqslant \underline{\tau} \geqslant 0$. Since we assumed that each transmission delay τ_k is smaller than the corresponding transmission interval h_k, we have that $(h_k, \tau_k) \in \Theta$, for all $k \in \mathbb{N}$, where

$$\Theta := \left\{ (h, \tau) \in \mathbb{R}^2 \mid h \in [\underline{h}, \overline{h}], \tau \in [\underline{\tau}, \min\{h, \overline{\tau}\}) \right\}. \qquad (2.5)$$

Remark 2.2.1. *In the above reasoning, we implicitly assumed that packet loss does not occur, similar to, e.g., [24, 34, 132, 134]. However, we could accommodate for packet dropouts by modelling them as prolongations of the transmission interval, as done in [62, 103]. This means that if we assume that there is a bound $\delta \in \mathbb{N}$ on the maximum number of successive dropouts, and we have stability of the NCS for $(h_k, \tau_k) \in \Theta$, for all $k \in \mathbb{N}$, in the case without dropouts, then the NCS with dropouts is still guaranteed to be stable for $(h_k, \tau_k) \in \Theta'$, for all $k \in \mathbb{N}$, where*

$$\Theta' := \left\{ (h, \tau) \in \mathbb{R}^2 \mid h \in [\underline{h}, \overline{h}'], \tau \in [\underline{\tau}, \min\{h, \overline{\tau}\}) \right\} \qquad (2.6)$$

in which $\overline{h}' := \frac{\overline{h}}{\delta + 1}$.

2.2.1 The NCS as a Switched Uncertain System

To analyse stability of the NCS described above, we transform it into a discrete-time model. In this framework, we need a discrete-time equivalent of (2.1) and also of (2.2a) in case a continuous-time controller is used. To arrive at this description, let us first define the network-induced error as

$$\begin{cases} e^y(t) := \hat{y}(t) - y(t) \\ e^u(t) := \hat{u}(t) - u(t). \end{cases} \qquad (2.7)$$

The discrete-time switched uncertain system can now be obtained by describing the evolution of the states between t_k and $t_{k+1} = t_k + h_k$. In order to do so, we define $x_k^p := x^p(t_k)$, $u_k := u(t_k)$, $\hat{u}_k := \lim_{t \downarrow r_k} \hat{u}(t)$ and $e_k^u := e^u(t_k)$. Since $\hat{u}$, as in (2.3), is a piecewise-constant left-continuous signal, i.e., $\lim_{s \uparrow t} \hat{u}(s) = \hat{u}(t)$, we can write $\hat{u}_{k-1} = \lim_{t \downarrow r_{k-1}} \hat{u}(t) = \hat{u}(r_k) = \hat{u}(t_k)$. This allows us to write

the exact discretisation of (2.1) as follows:

$$x_{k+1}^p = e^{A^p h_k} x_k^p + \int_0^{h_k} e^{A^p(h_k - s)} B^p \hat{u}(t_k + s) \mathrm{d}s$$

$$= e^{A^p h_k} x_k^p + \int_0^{\tau_k} e^{A^p(h_k - s)} \mathrm{d}s B^p \hat{u}_{k-1} + \int_{\tau_k}^{h_k} e^{A^p(h_k - s)} \mathrm{d}s B^p \hat{u}_k. \quad (2.8)$$

As (2.3) and (2.7) yield $\hat{u}_{k-1} = u_k + e_k^u$ and $\hat{u}_{k-1} - \hat{u}_k = \Gamma_{\sigma_k}^u e_k^u$, (2.8) can be rewritten as

$$x_{k+1}^p = e^{A^p h_k} x_k^p + \int_{h_k - \tau_k}^{h_k} e^{A^p s} \mathrm{d}s B^p \hat{u}_{k-1} + \int_0^{h_k - \tau_k} e^{A^p s} \mathrm{d}s B^p \hat{u}_k$$

$$= e^{A^p h_k} x_k^p + \int_0^{h_k} e^{A^p s} \mathrm{d}s B^p \hat{u}_{k-1} + \int_0^{h_k - \tau_k} e^{A^p s} \mathrm{d}s B^p (\hat{u}_k - \hat{u}_{k-1})$$

$$= e^{A^p h_k} x_k^p + \int_0^{h_k} e^{A^p s} \mathrm{d}s B^p (u_k + e_k^u) - \int_0^{h_k - \tau_k} e^{A^p s} \mathrm{d}s B^p \Gamma_{\sigma_k}^u e_k^u. \quad (2.9)$$

A discretised equivalent of (2.2a) is obtained in a similar fashion by defining $x_k^c := x^c(t_k)$, $y_k := y(t_k)$, $e_k^y := e^y(t_k)$, $\hat{y}_k := \lim_{t \downarrow r_k} \hat{y}(t)$, and observing $\hat{y}_{k-1} = \hat{y}(t_k)$, and is given by

$$x_{k+1}^c = e^{A^c h_k} x_k^c + \int_0^{h_k} e^{A^c s} \mathrm{d}s B^c (y_k + e_k^y) - \int_0^{h_k - \tau_k} e^{A^c s} \mathrm{d}s B^c \Gamma_{\sigma_k}^y e_k^y. \quad (2.10)$$

We now present three different models, each describing a particular NCS. The first and the second model cover the situation where both the plant and the controller outputs are transmitted over the network, differing by the fact that the controller is given by (2.2a) and (2.2b), respectively. In the third model, it is assumed that the controller is given by (2.2a) and that only the plant outputs y are transmitted over the network and u are sent continuously via an ideal nonnetworked connection. We include this particular case, because it is often used in examples in the NCS literature (see, e.g., the benchmark example in [24, 34, 41, 62, 103, 134]) and it allows us to compare our methodology to the existing ones.

A) The NCS model with controller (2.2a)***:***   For an NCS having controller (2.2a), the complete NCS model is obtained by combining (2.3), (2.7), (2.9), and (2.10) and defining

$$\bar{x}_k := \begin{bmatrix} x_k^{p\top} & x_k^{c\top} & e_k^{y\top} & e_k^{u\top} \end{bmatrix}^\top. \quad (2.11)$$

This results in the discrete-time model given by

$$\bar{x}_{k+1} = \underbrace{\begin{bmatrix} A_{h_k} + E_{h_k}BDC & E_{h_k}BD - E_{h_k - \tau_k}B\Gamma_{\sigma_k} \\ C(I - A_{h_k} - E_{h_k}BDC) & I - D^{-1}\Gamma_{\sigma_k} + C(E_{h_k - \tau_k}B\Gamma_{\sigma_k} - E_{h_k}BD) \end{bmatrix}}_{=:\tilde{A}_{\sigma_k, h_k, \tau_k}} \bar{x}_k,$$

(2.12)

in which $\tilde{A}_{\sigma_k, h_k, \tau_k} \in \mathbb{R}^{n \times n}$, with $n = n_p + n_c + n_y + n_u$, and

$$A_\rho := \begin{bmatrix} e^{A^p \rho} & 0 \\ 0 & e^{A^c \rho} \end{bmatrix}, \quad B := \begin{bmatrix} 0 & B^p \\ B^c & 0 \end{bmatrix}, \quad C := \begin{bmatrix} C^p & 0 \\ 0 & C^c \end{bmatrix}, \tag{2.13a}$$

$$D := \begin{bmatrix} I & 0 \\ D^c & I \end{bmatrix}, \quad E_\rho := \begin{bmatrix} \int_0^\rho e^{A^p s} \mathrm{d}s & 0 \\ 0 & \int_0^\rho e^{A^c s} \mathrm{d}s \end{bmatrix}, \quad \rho \in \mathbb{R}. \tag{2.13b}$$

B) The NCS model with controller (2.2b)***:*** For an NCS having controller (2.2b), the complete NCS model is obtained by combining (2.2b), (2.3), (2.7), and (2.9), also resulting in (2.12), in which now

$$A_\rho := \begin{bmatrix} e^{A^p \rho} & 0 \\ 0 & A^c \end{bmatrix}, \quad B := \begin{bmatrix} 0 & B^p \\ B^c & 0 \end{bmatrix}, \quad C := \begin{bmatrix} C^p & 0 \\ 0 & C^c \end{bmatrix}, \tag{2.14a}$$

$$D := \begin{bmatrix} I & 0 \\ D^c & I \end{bmatrix}, \quad E_\rho := \begin{bmatrix} \int_0^\rho e^{A^p s} \mathrm{d}s & 0 \\ 0 & I \end{bmatrix}, \quad \rho \in \mathbb{R}. \tag{2.14b}$$

C) The NCS model if only y ***is transmitted over the network:*** In this case we assume that only the outputs of the plant are transmitted over the network and the controller communicates its values continuously and without delay. We therefore have that $u(t) = \hat{u}(t)$, for all $t \in \mathbb{R}_+$, which allows us to combine (2.1) and (2.2a), yielding

$$\begin{bmatrix} \dot{x}^p(t) \\ \dot{x}^c(t) \end{bmatrix} = \begin{bmatrix} A^p & B^p C^c \\ 0 & A^c \end{bmatrix} \begin{bmatrix} x^p(t) \\ x^c(t) \end{bmatrix} + \begin{bmatrix} B^p D^c \\ B^c \end{bmatrix} \hat{y}(t). \tag{2.15}$$

Since $\hat{y}$ is still updated according to (2.3), we can describe the evolution of the states between t_k and $t_{k+1} = t_k + h_k$ in a similar fashion as in (2.9). In this case, (2.11) reduces to

$$\bar{x}_k := \begin{bmatrix} x_k^{p\top} & x_k^{c\top} & e_k^{y\top} \end{bmatrix}^\top, \tag{2.16}$$

resulting in (2.12), in which

$$A_\rho := e^{\left(\begin{bmatrix} A^p & B^p C^c \\ 0 & A^c \end{bmatrix} \rho \right)}, \quad B := \begin{bmatrix} B^p D^c \\ B^c \end{bmatrix}, \quad C := \begin{bmatrix} C^p & 0 \end{bmatrix}, \tag{2.17a}$$

$$D := I, \quad E_\rho := \int_0^\rho e^{\left(\begin{bmatrix} A^p & B^p C^c \\ 0 & A^c \end{bmatrix} s \right)} \mathrm{d}s, \quad \rho \in \mathbb{R}. \tag{2.17b}$$

2.2.2 Protocols as a Switching Function

Based on the previous modelling steps, the NCS is formulated as a discrete-time switched uncertain system (2.12). In this framework, protocols are considered as the switching function determining σ_k. We consider two commonly used protocols, see [24, 41, 62, 103, 125, 132, 134], namely the try-once-discard (TOD) and the round-robin (RR) protocol and generalise these into two novel classes of protocols, named 'quadratic' and 'periodic' protocols.

A) Quadratic Protocols: A quadratic protocol is a protocol, for which the switching function can be written as

$$\sigma_k = \arg \min_{i \in \{1,\ldots,N\}} \bar{x}_k^\top P_i \bar{x}_k, \tag{2.18}$$

where P_i, $i \in \{1,\ldots,N\}$, are certain given matrices. In case two nodes have the same minimal values, one of them can be chosen arbitrarily. In fact, the well-known TOD protocol, sometimes also called the maximum-error-first (MEF) protocol, belongs to this class of protocols. In this protocol, the node that has the largest network-induced error, i.e., the difference between the most recently transmitted values and its current values of the signals corresponding to the node, is granted access to the network. We can arrive at the TOD protocol by adopting the following structure in the P_i matrices:

$$P_i = \bar{P} - \text{diag}(0, \Gamma_i), \tag{2.19}$$

in which Γ_i, $i \in \{1,\ldots,N\}$, is given by (2.4). Furthermore, if we define $\tilde{e}_k^i := \Gamma_i e_k$, where $e_k := [e_k^{y\top}, e_k^{u\top}]^\top$, (2.18) becomes

$$\sigma_k = \arg \min \left\{ -e_k^\top \Gamma_1 e_k, \ldots, -e_k^\top \Gamma_N e_k \right\} = \arg \max \left\{ \|\tilde{e}_k^1\|, \ldots, \|\tilde{e}_k^N\| \right\}, \tag{2.20}$$

which is the TOD protocol.

B) Periodic Protocols: Another class of protocols that is considered in this chapter is the class of so-called periodic protocols. A periodic protocol is a protocol that satisfies for some $\tilde{N} \in \mathbb{N}$

$$\sigma_{k+\tilde{N}} = \sigma_k \tag{2.21}$$

for all $k \in \mathbb{N}$. $\tilde{N}$ is then called the period of the protocol. Actually, the well-known RR protocol belongs to this class and is defined by

$$\{\sigma_1, \ldots, \sigma_N\} = \{1, \ldots, N\}, \tag{2.22}$$

and period $\tilde{N} = N$, i.e., during each period of the protocol every node has access to the network exactly once.

The above modelling approach now provides a description of the NCS system in the form of a *discrete-time switched linear uncertain system* given by (2.12) and one of the protocols, characterised by (2.18) or (2.21). The system switches between N linear uncertain systems and the switching is due to the fact that only one node accesses the network at each transmission instant. The uncertainty is caused by the fact that the transmission intervals and the transmission delays $(h_k, \tau_k) \in \Theta$ are varying over time.

2.2.3   Stability of the NCS

The problem studied in this chapter is to determine the stability of the continuous-time NCS, given by (2.1), (2.2a) or (2.2b), (2.3), and (2.7), with protocols satisfying (2.18) or (2.21) given the bounds $[\underline{h}, \overline{h}]$ and $[\underline{\tau}, \overline{\tau}]$, or to find bounds that guarantee stability. Let us now formally define stability for this continuous-time NCS.

Definition 2.2.2. *The continuous-time NCS given by* (2.1), (2.2a) *or* (2.2b), (2.3), *and* (2.7), *with protocols satisfying* (2.18) *or* (2.21), *having states* $\bar{x}(t) := \begin{bmatrix} x^{p\top}(t) & x^{c\top}(t) & e^{y\top}(t) & e^{u\top}(t) \end{bmatrix}^{\top} \in \mathbb{R}^n$, *is said to be* uniformly globally exponentially stable *(UGES) if there exist* $c_c, \beta_c > 0$, *such that for any initial condition* $\bar{x}(0)$, *any sequence of transmission intervals* $(h_0, h_1, \ldots)$, *and any sequence of transmission delays* $(\tau_0, \tau_1, \ldots)$, *with* $(h_k, \tau_k) \in \Theta$, *for all* $k \in \mathbb{N}$, *it holds that*

$$\|\bar{x}(t)\| \leqslant c_c \|\bar{x}(0)\| e^{-\beta_c t}, \quad \forall \, t \in \mathbb{R}_+. \tag{2.23}$$

Stability of the continuous-time NCS can be analysed by assessing stability of the discrete-time uncertain switched linear system (2.12) with switching functions satisfying (2.18) or (2.21), as we will show. Let us now formally define stability of this discrete-time system.

Definition 2.2.3. *System* (2.12) *with switching sequences satisfying* (2.18) *or* (2.21) *is said to be* uniformly globally exponentially stable *(UGES) if there exist* $c_d, \beta_d > 0$, *such that for any initial condition* $\bar{x}_0 \in \mathbb{R}^n$, *any sequence of transmission intervals* $(h_0, h_1, \ldots)$, *and any sequence of transmission delays* $(\tau_0, \tau_1, \ldots)$, *with* $(h_k, \tau_k) \in \Theta$, *for all* $k \in \mathbb{N}$, *it holds that*

$$\|\bar{x}_k\| \leqslant c_d \|\bar{x}_0\| e^{-\beta_d k}, \quad \forall \, k \in \mathbb{N}. \tag{2.24}$$

Since the discrete-time switched uncertain linear system (2.12) with switching sequences satisfying (2.18) or (2.21) is formulated in discrete time, we can only assess stability at the transmission instants. However, states of the plant (2.1) and controller (2.2a) actually evolve in continuous time. In the next lemma, we state that UGES of the discrete-time NCS model implies UGES of the continuous-time NCS.

Lemma 2.2.4. *The discrete-time system* (2.12) *with switching sequences satisfying* (2.18) *or* (2.21) *is UGES, if and only if the continuous-time NCS given by* (2.1), (2.2a) *or* (2.2b), (2.3), *and* (2.7), *with protocols satisfying* (2.18) *or* (2.21) *is UGES.*

Proof. The proof is given in Appendix A.1.   □

This lemma states that it suffices to consider the discrete-time model (2.12) with switching sequences satisfying (2.18) or (2.21) to assess UGES of the continuous-time NCS system.

2.3   Obtaining a Convex Overapproximation

In the previous section, we obtained an NCS model in the form of a switched uncertain system. However, the form as in (2.12) is not really convenient to develop efficient techniques for stability analysis due to the nonlinear dependence of $\tilde{A}_{\sigma_k, h_k, \tau_k}$ on the uncertain parameters h_k and τ_k. Therefore, we will provide a procedure that overapproximates system (2.12) by a polytopic system with a norm-bounded additive uncertainty of the form

$$\bar{x}_{k+1} = \Big(\sum_{l=1}^{L} \alpha_k^l \bar{A}_{\sigma_k, l} + \bar{B} \Delta_k \bar{C}_{\sigma_k} \Big) \bar{x}_k, \qquad (2.25)$$

where $\bar{A}_{\sigma, l} \in \mathbb{R}^{n \times n}$, $\bar{B} \in \mathbb{R}^{n \times m}$, $\bar{C}_\sigma \in \mathbb{R}^{m \times n}$, for $\sigma \in \{1, \dots, N\}$ and $l \in \{1, \dots, L\}$, with L the number of vertices of the polytope. Furthermore, $\alpha_k = [\alpha_k^1 \, \dots \, \alpha_k^L]^\top \in \mathcal{A}$, $k \in \mathbb{N}$, denotes an unknown time-varying vector with

$$\mathcal{A} = \Big\{ \alpha \in \mathbb{R}^L \, \Big| \, \sum_{l=1}^{L} \alpha^l = 1, \alpha^l \geqslant 0, l \in \{1, \dots, L\} \Big\} \qquad (2.26)$$

and $\Delta_k \in \boldsymbol{\Delta}$, $k \in \mathbb{N}$, where $\boldsymbol{\Delta}$ is a norm-bounded set of matrices in $\mathbb{R}^{m \times m}$ that describes the additive uncertainty. This additive uncertainty can have some specific structure, as we will see below. The model (2.25) should be an overapproximation of (2.12) in the sense that for all $\sigma \in \{1, \dots, N\}$, it holds that

$$\big\{ \tilde{A}_{\sigma, h, \tau} \, \big| \, (h, \tau) \in \Theta \big\} \subseteq \Big\{ \sum_{l=1}^{L} \alpha^l \bar{A}_{\sigma, l} + \bar{B} \Delta \bar{C}_\sigma \, \Big| \, \alpha \in \mathcal{A}, \Delta \in \boldsymbol{\Delta} \Big\}. \qquad (2.27)$$

In this chapter, we use the gridding idea of [45, 122] to obtain, for a fixed σ, $\bar{A}_{\sigma, l}$ by evaluating $\tilde{A}_{\sigma, h, \tau}$ of (2.12) at a collection of selected pairs of transmission intervals and transmission delays $(\tilde{h}_l, \tilde{\tau}_l) \in \Theta$, $l \in \{1, \dots, L\}$. Hence, we take $\bar{A}_{\sigma, l} := \tilde{A}_{\sigma, \tilde{h}_l, \tilde{\tau}_l}$ in (2.25), with $l \in \{1, \dots, L\}$. However, contrary to

[45, 122], we choose to allow for convex combinations of the vertices, whereas in [45, 122] the system switches between the vertices only. Moreover, we construct a norm-bounded additive uncertainty $\Delta \in \mathbf{\Delta}$ to capture the remaining approximation error, as done in, e.g., [12, 43, 69]. By comparing $\tilde{A}_{\sigma,h,\tau}$ with the convex combinations of the vertices instead of with the vertices alone, we obtain smaller bounds on the additive uncertainty than in [12, 43, 45, 122].

By specifying $(\tilde{h}_l, \tilde{\tau}_l)$, $l \in \{1, \ldots, L\}$, and thereby determining $\bar{A}_{\sigma,l}$, it only remains to show how to choose $\bar{B}\Delta\bar{C}_\sigma$ in (2.25) and $\mathbf{\Delta}$ in order to satisfy (2.27). This additive uncertainty is used to capture the approximation error between the original system (2.12) and the polytopic system

$$\bar{x}_{k+1} = \sum_{l=1}^{L} \alpha_k^l \bar{A}_{\sigma_k,l} \bar{x}_k. \tag{2.28}$$

In order for (2.27) to hold, for each triple (σ, h, τ), with $\sigma \in \{1, \ldots, N\}$ and $(h, \tau) \in \Theta$, there should exist some $\alpha \in \mathcal{A}$ and $\Delta \in \mathbf{\Delta}$, such that

$$\tilde{A}_{\sigma,h,\tau} - \sum_{l=1}^{L} \alpha^l \bar{A}_{\sigma,l} = \bar{B}\Delta\bar{C}_\sigma. \tag{2.29}$$

Hence, we should determine the worst-case distance between the real system (2.12) and the polytopic system (2.28), leading to an upper bound on the approximation error. To obtain such an upper bound, we partition Θ into M triangles $\mathcal{S}_1, \ldots, \mathcal{S}_M$, see Fig. 2.2, and we compare $\tilde{A}_{\sigma,h,\tau}$, for $(h, \tau) \in \mathcal{S}_m$, with $\{\sum_{j=1}^{3} \tilde{\alpha}^j \bar{A}_{\sigma,l_j^m} \mid \sum_{j=1}^{3} \tilde{\alpha}^j = 1, \ \tilde{\alpha}^j \geqslant 0, j \in \{1, 2, 3\}\}$, where $(\tilde{h}_{l_j^m}, \tilde{\tau}_{l_j^m})$, $j = \{1, 2, 3\}$, denote the vertices (with vertex index $l_j^m \in \{1, \ldots, L\}$, $j \in \{1, 2, 3\}$ and $m \in \{1, \ldots, M\}$) of triangle $\mathcal{S}_m$. This allows us to construct the right-hand side of (2.29) by computing the worst-case distance. Note that it is always possible to partition Θ into triangles, as Θ is a convex polytope. We will, however, also provide a systematic procedure to obtain a suitable partitioning.

A specific feature of the overapproximation presented in this chapter is that, contrary to [12, 31, 43, 45, 49, 69, 122], it can be made arbitrarily tight, i.e., besides that (2.27) holds, it also holds that

$$\left\{ \sum_{l=1}^{L} \alpha^l \bar{A}_{\sigma,l} + \bar{B}\Delta\bar{C}_\sigma \;\middle|\; \alpha \in \mathcal{A}, \Delta \in \mathbf{\Delta} \right\}$$
$$\subseteq \mathrm{co}\big\{\tilde{A}_{\sigma,h,\tau} \,\big|\, (h, \tau) \in \Theta\big\} + \big\{\bar{\Delta} \mid \|\bar{\Delta}\| \leqslant \varepsilon\,\big\}, \tag{2.30}$$

for each $\sigma \in \{1, \ldots, N\}$, in which $\varepsilon > 0$ can be chosen arbitrarily small. This can be achieved by increasing the number of pairs $(\tilde{h}_l, \tilde{\tau}_l) \in \Theta$, $l \in \{1, \ldots, L\}$, in a well-distributed fashion. The fact that (2.30) can be ensured to hold for an arbitrarily small $\varepsilon > 0$ is important, as it allows us to show that the existence of
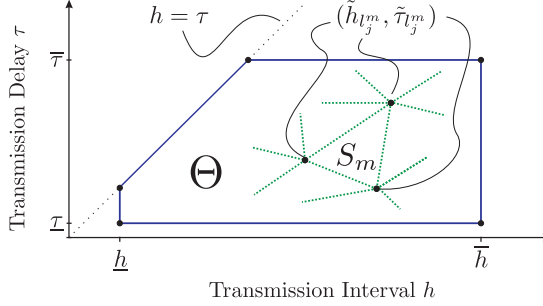
Figure 2.2: The partitioning of Θ into triangles $\mathcal{S}_m$.

a Lyapunov function of a particular type for (2.12) is equivalent to the existence of a Lyapunov function of the same type for (2.25). Since we will indeed show that (2.30) can be guaranteed for any choice of $\varepsilon > 0$, we can let the introduced conservatism in the overapproximation vanish. We will formalise this result in Section 2.5.

We now formalise the procedure to obtain a convex overapproximation as outlined above. The procedure results in a tight overapproximation, by adding pairs $(\tilde{h}_l, \tilde{\tau}_l) \in \Theta$ until $\varepsilon \leqslant \varepsilon_u$ is achieved for an user-specified threshold $\varepsilon_u > 0$, such that (2.30) holds with $\varepsilon \leqslant \varepsilon_u$.

Procedure 2.3.1.

Step 1 *Choose a desired $\varepsilon_u > 0$. Furthermore, select distinct pairs $(\tilde{h}_l, \tilde{\tau}_l) \in \Theta$, $l \in \{1, \ldots, L\}$, such that co $\mathcal{G} = \Theta$, where $\mathcal{G} = \cup_{l=1}^{L}\{(\tilde{h}_l, \tilde{\tau}_l)\}$. Now partition Θ into M triangles $\mathcal{S}_m$, $m \in \{1, \ldots, M\}$, such that, for each $\mathcal{S}_m \in \mathcal{H}$, where $\mathcal{H} = \{\mathcal{S}_1, \ldots, \mathcal{S}_M\}$, it holds that*

$$\mathcal{S}_m = \text{co}\{(\tilde{h}_{l_1^m}, \tilde{\tau}_{l_1^m}), (\tilde{h}_{l_2^m}, \tilde{\tau}_{l_2^m}), (\tilde{h}_{l_3^m}, \tilde{\tau}_{l_3^m})\}, \tag{2.31}$$

where $l_j^m \in \{1, \ldots, L\}$, $j \in \{1, 2, 3\}$. Hence, $(\tilde{h}_{l_j^m}, \tilde{\tau}_{l_j^m}) \in \mathcal{G}$, $j \in \{1, 2, 3\}$ are the vertices of the triangle $\mathcal{S}_m$. Moreover, for all $m, p \in \{1, \ldots, M\}$ and $p \neq m$, $\text{int}\mathcal{S}_p \cap \text{int}\mathcal{S}_m = \emptyset$, $\cup_{m=1}^{M}\mathcal{S}_m = \Theta$, and $\text{int}\mathcal{S}_m \neq \emptyset$, i.e., the triangles form a (nonoverlapping) partitioning of Θ and have nonempty interiors.

Step 2 *Define*

$$\bar{A}_{\sigma,l} := \tilde{A}_{\sigma, \tilde{h}_l, \tilde{\tau}_l} \tag{2.32}$$

for all $\sigma \in \{1, \ldots, N\}$ and $(\tilde{h}_l, \tilde{\tau}_l) \in \mathcal{G}$, $l \in \{1, \ldots, L\}$.

Step 3 *To bound the approximation error, first construct the matrix $\bar{\Lambda}$, that,*

depending on the NCS model defined in Section 2.2.1, is given by

$$\bar{\Lambda} = \begin{cases} \operatorname{diag}(A^p, A^c), & \text{if (2.12) is as in Section 2.2.1.A,} \\ \operatorname{diag}(A^p, 0), & \text{if (2.12) is as in Section 2.2.1.B,} \\ \begin{bmatrix} A^p & B^p C^c \\ 0 & A^c \end{bmatrix}, & \text{if (2.12) is as in Section 2.2.1.C.} \end{cases} \tag{2.33}$$

Decompose the matrix $\bar{\Lambda}$ into its real Jordan form [71], i.e., $\bar{\Lambda} := T\Lambda T^{-1}$, where T is an invertible matrix and

$$\Lambda = \operatorname{diag}(\Lambda_1, \ldots, \Lambda_K) \tag{2.34}$$

with $\Lambda_i \in \mathbb{R}^{n_i \times n_i}$, $i \in \{1, \ldots, K\}$, the i-th real Jordan block of $\bar{\Lambda}$.

Step 4 *Compute for each real Jordan block Λ_i, $i \in \{1, \ldots, K\}$, the worst-case approximation error of all triangles $\mathcal{S}_m \in \mathcal{H}$, $m \in \{1, \ldots, M\}$, i.e.,*

$$\delta_i^A = \max_{m \in \{1, \ldots, M\}} \max_{\sum_{j=1}^3 \tilde{\alpha}^j = 1, \tilde{\alpha}^j \geqslant 0} \tilde{\delta}_{i,m,\tilde{\alpha}}^A, \tag{2.35a}$$

$$\delta_i^{E_h} = \max_{m \in \{1, \ldots, M\}} \max_{\sum_{j=1}^3 \tilde{\alpha}^j = 1, \tilde{\alpha}^j \geqslant 0} \tilde{\delta}_{i,m,\tilde{\alpha}}^{E_h}, \tag{2.35b}$$

$$\delta_i^{E_{h-\tau}} = \max_{m \in \{1, \ldots, M\}} \max_{\sum_{j=1}^3 \tilde{\alpha}^j = 1, \tilde{\alpha}^j \geqslant 0} \tilde{\delta}_{i,m,\tilde{\alpha}}^{E_{h-\tau}}, \tag{2.35c}$$

in which $\tilde{\alpha} = [\tilde{\alpha}^1 \ \tilde{\alpha}^2 \ \tilde{\alpha}^3]^\top$ and

$$\tilde{\delta}_{i,m,\tilde{\alpha}}^A = \left\| e^{\Lambda_i \sum_{j=1}^3 \tilde{\alpha}^j \tilde{h}_{l_j^m}} - \sum_{j=1}^3 \tilde{\alpha}^j e^{\Lambda_i \tilde{h}_{l_j^m}} \right\|, \tag{2.36a}$$

$$\tilde{\delta}_{i,m,\tilde{\alpha}}^{E_h} = \left\| \sum_{j=1}^3 \tilde{\alpha}^j \int_{\tilde{h}_{l_j^m}}^{\sum_{j=1}^3 \tilde{\alpha}^j \tilde{h}_{l_j^m}} e^{\Lambda_i s} ds \right\|, \tag{2.36b}$$

$$\tilde{\delta}_{i,m,\tilde{\alpha}}^{E_{h-\tau}} = \left\| \sum_{j=1}^3 \tilde{\alpha}^j \int_{\tilde{h}_{l_j^m} - \tilde{\tau}_{l_j^m}}^{\sum_{j=1}^3 \tilde{\alpha}^j (\tilde{h}_{l_j^m} - \tilde{\tau}_{l_j^m})} e^{\Lambda_i s} ds \right\|. \tag{2.36c}$$

For a detailed explanation of the origin of the approximation error bounds, see the proof of Theorem 2.3.2.

Step 5 *Define*

$$\bar{C}_\sigma := \begin{bmatrix} T^{-1} & 0 \\ T^{-1}BDC & T^{-1}BD \\ 0 & -T^{-1}B\Gamma_\sigma \end{bmatrix} \tag{2.37}$$

and

$$\bar{B} := \begin{bmatrix} T & T & T \\ -CT & -CT & -CT \end{bmatrix} \cdot \operatorname{diag}(\delta_1^A I_1, \ldots, \delta_K^A I_K, \delta_1^{E_h} I_1, \ldots,$$

$$\delta_K^{E_h} I_K, \delta_1^{E_{h-\tau}} I_1, \ldots, \delta_K^{E_{h-\tau}} I_K) \tag{2.38}$$

with I_i the identity matrix of size n_i, complying with the i-th real Jordan Block, and compute

$$\varepsilon = \|\bar{B}\| \max_{\sigma \in \{1,\dots,N\}} \{\|\bar{C}_\sigma\|\}. \tag{2.39}$$

Step 6 *In case that $\varepsilon > \varepsilon_u$, meaning that the user-specified tightness of the overapproximation in the sense of* (2.30) *is not achieved we add a pair $(\tilde{h}_{L+1}, \tilde{\tau}_{L+1}) \in \Theta$ to $\mathcal{G}$. In order to determine the specific pair to be added, compute the point $(h, \tau) \in \mathcal{S}_m$, where the maximum approximation error is achieved by solving*

$$(m^\star, \tilde{\alpha}^\star) \in \arg \max_{\substack{m \in \{1,\dots,M\}, \\ \sum_{j=1}^3 \tilde{\alpha}^j = 1, \tilde{\alpha}^j \geqslant 0}} \tilde{\delta}^{j^\star}_{i^\star, m, \tilde{\alpha}} \tag{2.40}$$

in which

$$(i^\star, j^\star) \in \arg \max_{\substack{i \in \{1,\dots,K\}, \\ j \in \{A, E_h, E_{h-\tau}\}}} \delta_i^j, \tag{2.41}$$

and add this new pair $(\tilde{h}_{L+1}, \tilde{\tau}_{L+1}) = \sum_{j=1}^3 \tilde{\alpha}^{\star j}(\tilde{h}_{l_{m^\star}^j}, \tilde{\tau}_{l_{m^\star}^j})$ to the set $\mathcal{G}$, i.e., update $\mathcal{G}$ according to

$$\mathcal{G} := \mathcal{G} \cup \{(\tilde{h}_{L+1}, \tilde{\tau}_{L+1})\}, \tag{2.42}$$

and redefine $L := L + 1$. Furthermore, subdivide the corresponding triangle $\mathcal{S}_{m^\star}$ into smaller triangles and replace $\mathcal{S}_{m^\star}$ by the smaller triangles in the set $\mathcal{H}$, i.e.,

$$\begin{aligned} \mathcal{H} := \big(\mathcal{H}\backslash\mathcal{S}_{m^\star}\big) &\cup \mathrm{co}\{(\tilde{h}_{L+1}, \tilde{\tau}_{L+1}), (\tilde{h}_{l_1^m}, \tilde{\tau}_{l_1^m}), (\tilde{h}_{l_2^m}, \tilde{\tau}_{l_2^m})\} \\ &\cup \mathrm{co}\{(\tilde{h}_{L+1}, \tilde{\tau}_{L+1}), (\tilde{h}_{l_1^m}, \tilde{\tau}_{l_1^m}), (\tilde{h}_{l_3^m}, \tilde{\tau}_{l_3^m})\} \\ &\cup \mathrm{co}\{(\tilde{h}_{L+1}, \tilde{\tau}_{L+1}), (\tilde{h}_{l_2^m}, \tilde{\tau}_{l_2^m}), (\tilde{h}_{l_3^m}, \tilde{\tau}_{l_3^m})\}, \quad (2.43) \end{aligned}$$

redefine[2] $M := M + 2$, and repeat the procedure from Step 2.

Step 7 *In case $\varepsilon \leqslant \varepsilon_u$, the user-specified tightness of the overapproximation is achieved and the resulting uncertainty set $\boldsymbol{\Delta} \subseteq \mathbb{R}^{3(n_p+n_c)\times 3(n_p+n_c)}$ is given by*

$$\boldsymbol{\Delta} = \big\{\mathrm{diag}(\Delta^1, \dots, \Delta^{3K}) \mid \Delta^{i+jL} \in \mathbb{R}^{n_i \times n_i}, \|\Delta^{i+jL}\| \leqslant 1,$$
$$i \in \{1, \dots, K\}, j \in \{0, 1, 2\}\}. \tag{2.44}$$

---

[2]In case one of the smaller triangles satisfies int $\mathrm{co}\{(\tilde{h}_{L+1}, \tilde{\tau}_{L+1}), (\tilde{h}_{l_i^m}, \tilde{\tau}_{l_i^m}), (\tilde{h}_{l_j^m}, \tilde{\tau}_{l_j^m})\} = \emptyset$ for some $i, j \in \{1, 2, 3\}$, meaning that $(\tilde{h}_{L+1}, \tilde{\tau}_{L+1})$ lies on one of the edges of $\mathcal{S}_{m^\star}$, then this triangle is not added to the set $\mathcal{H}$, and the number of triangles in the partitioning increases according $M := M + 1$.

Theorem 2.3.2. *Consider the NCS given by (2.12) where $(h_k, \tau_k) \in \Theta$, $k \in \mathbb{N}$, with Θ as in (2.5). If system (2.25) is obtained by following Procedure 2.3.1 for some user-specified $\varepsilon_u > 0$, then (2.27) holds and thus (2.25) is an overapproximation of (2.12). Furthermore, the overapproximation is ε-tight, in the sense that (2.30) holds, with ε given by (2.39) and $\varepsilon \leqslant \varepsilon_u$.*

Proof. The proof is given in Appendix A.1. $\qquad\qquad\qquad\square$

Remark 2.3.3. *In the special case that $\underline{h} = \overline{h}$ or that $\underline{\tau} = \overline{\tau}$, Procedure 2.3.1 has to be modified slightly. This is because we proposed to form triangles $\mathcal{S}_m$, $m \in \{1, \ldots, M\}$, having the property that $\mathrm{int}\mathcal{S}_m \neq \emptyset$, which is not possible when $\underline{h} = \overline{h}$ or $\underline{\tau} = \overline{\tau}$. Instead, in this case, we partition Θ into M line-segments $\mathcal{S}_1, \ldots, \mathcal{S}_M$, such that, for each $\mathcal{S}_m$, $m \in \{1, \ldots, M\}$, it holds that*

$$\mathcal{S}_m = \mathrm{co}\{(\tilde{h}_{l_1^m}, \tilde{\tau}_{l_1^m}), (\tilde{h}_{l_2^m}, \tilde{\tau}_{l_2^m})\}, \tag{2.45}$$

where $(\tilde{h}_{l_j^m}, \tilde{\tau}_{l_j^m})$, $j \in \{1, 2\}$, now denote the vertices of the line segment $\mathcal{S}_m$. All other properties of $\mathcal{S}_m$, $m \in \{1, \ldots, M\}$, still hold and the remainder of the procedure can be applied mutatis mutandis.

UGES of the NCS system given by (2.1), (2.2a) or (2.2b), (2.3), and (2.7), with protocols satisfying (2.18) or (2.21), with $(h_k, \tau_k) \in \Theta$, $k \in \mathbb{N}$, can now be guaranteed by proving UGES of (2.25), with switching sequences satisfying (2.18) or (2.21), $\alpha_k \in \mathcal{A}$, and $\Delta_k \in \boldsymbol{\Delta}$, $k \in \mathbb{N}$, using the result of Lemma 2.2.4 and the fact that (2.25) is a (tight) overapproximation of (2.12).

2.4 Stability of Switched Systems with Parametric Uncertainty

In the previous sections, we discussed the NCS model and introduced a way to overapproximate it by a switched polytopic system with norm-bounded uncertainty. Given this switched uncertain system, we can analyse whether a switching sequence, as induced by a protocol, renders the switched system UGES.

We will start with so-called quadratic protocols that include the well-known TOD protocol as a particular case. The analysis is based on extensions of the ideas in [47], in which only switched linear systems without any form of uncertainty are considered. Hence, generalisations are needed to include switched polytopic systems with norm-bounded uncertainties as in (2.25). After the stability analysis for the quadratic protocols and the TOD protocol as a special case, we will also show how we can analyse stability for periodic protocols, having the RR protocol as a special case.

2.4.1   Quadratic Protocols

In this section, we assume that the switching function is given by (2.18). To analyse the stability of (2.25) having this switching function, we introduce the non-quadratic Lyapunov function

$$V(\bar{x}_k) = \min_{i \in \{1,\dots,N\}} \bar{x}_k^\top P_i \bar{x}_k = \min_{\nu \in \mathcal{N}} \bar{x}_k^\top \sum_{i=1}^{N} \nu_i P_i \bar{x}_k, \tag{2.46}$$

where

$$\mathcal{N} := \Big\{ \nu \in \mathbb{R}^N \,\Big|\, \sum_{i=1}^{N} \nu_i = 1, \nu_i \geqslant 0, i \in \{1,\dots,N\} \Big\}. \tag{2.47}$$

Furthermore, we introduce the class $\mathcal{M}$ of so-called Metzler matrices $\Pi = \{\pi_{ji}\}$ given by

$$\mathcal{M} := \Big\{ \Pi \in \mathbb{R}^{N \times N} \,\Big|\, \sum_{j=1}^{N} \pi_{ji} = 1, \pi_{ji} \geqslant 0, i,j \in \{1,\dots,N\} \Big\}, \tag{2.48}$$

and the set of matrices

$$\mathcal{R} = \big\{ \mathrm{diag}(r_1 I_1, \dots, r_K I_K, r_{K+1} I_1, \dots, r_{2K} I_K,$$
$$r_{2K+1} I_1, \dots, r_{3K} I_K) \in \mathbb{R}^{3(n_p+n_c) \times 3(n_p+n_c)} \mid r_i > 0 \big\}, \tag{2.49}$$

where I_i is an identity matrix of size n_i.

   The main result of this section is presented in the following theorem.

Theorem 2.4.1. *Assume that there exist a matrix $\Pi = \{\pi_{ji}\} \in \mathcal{M}$, positive definite matrices P_i, and matrices $R_{i,l} \in \mathcal{R}$, $i \in \{1,\dots,N\}$ and $l \in \{1,\dots,L\}$, satisfying*

$$\begin{bmatrix} P_i & 0 & \bar{A}_{i,l}^\top \sum_{j=1}^{N} \pi_{ji} P_j & \bar{C}_i^\top R_{i,l} \\ \star & R_{i,l} & \bar{B}^\top \sum_{j=1}^{N} \pi_{ji} P_j & 0 \\ \star & \star & \sum_{j=1}^{N} \pi_{ji} P_j & 0 \\ \star & \star & \star & R_{i,l} \end{bmatrix} \succ 0, \tag{2.50}$$

for all $i \in \{1,\dots,N\}$ and $l \in \{1,\dots,L\}$. Then, the switching law (2.18) renders the system (2.25) UGES. Consequently, the NCS given by (2.1), (2.2a) or (2.2b), (2.3), and (2.7) is also UGES if the switching law (2.18) is employed as the protocol.

Proof. The proof is given in Appendix A.1.   □

Remark 2.4.2. *The results of Theorem 2.4.1 can be exploited in two ways: (i) For the design of a stabilising protocol. Then the conditions in (2.50) are not LMIs, but bilinear matrix inequalities (BMIs) due to the presence of the*

product of π_{ji} and P_j. Although literature on solving BMIs is available, see, e.g., [51, 56, 73], solving BMIs is considered to be of a high numerical complexity. (ii) Stability analysis for a given protocol. *In the situation that the matrices P_i, $i \in \{1, \ldots, N\}$, are completely given for a particular quadratic protocol, the conditions (2.50) are LMIs in $\Pi \in \mathcal{M}$ and $R_{i,l} \in \mathcal{R}$, for all $i \in \{1, \ldots, N\}$ and $l \in \{1, \ldots, L\}$.*

2.4.2 The TOD Protocol

In Section 2.2.2, we showed that by suitable choice of P_i, $i \in \{1, \ldots, N\}$, as in (2.19), the TOD protocol is a specific quadratic protocol. We can therefore use the result of Theorem 2.4.1 to determine the allowable range of transmission intervals and transmission delays of the NCS using the TOD protocol. This result is formalised in the following corollary, in which

$$\overline{\mathcal{M}} := \Big\{ \mathrm{diag}(0, \sum_{j=1}^{N} \pi_{ji} \Gamma_j) \in \mathbb{R}^{n \times n} \Big| \sum_{j=1}^{N} \pi_{ji} = 1, \pi_{ji} \geqslant 0, i, j \in \{1, \ldots, N\} \Big\}. \tag{2.51}$$

Corollary 2.4.3. *Assume that there exist matrices $\bar{\Pi}_i \in \overline{\mathcal{M}}$, $i \in \{1, \ldots, N\}$, a matrix P, matrices $R_{i,l} \in \mathcal{R}$, $i \in \{1, \ldots, N\}$ and $l \in \{1, \ldots, L\}$, satisfying*

$$\begin{bmatrix} P - \mathrm{diag}(0, \Gamma_i) & 0 & \bar{A}_{i,l}^{\top}(P - \Pi_i) & \bar{C}_i^{\top} R_{i,l} \\ \star & R_{i,l} & \bar{B}^{\top}(P - \Pi_i) & 0 \\ \star & \star & P - \Pi_i & 0 \\ \star & \star & \star & R_{i,l} \end{bmatrix} \succ 0, \tag{2.52}$$

for all $i \in \{1, \ldots, N\}$ and $l \in \{1, \ldots, L\}$, with Γ_i, as in (2.4). Then, the system (2.25) with (2.20) is UGES. Consequently, the NCS, given by (2.1), (2.2a) or (2.2b), (2.3), and (2.7), with the TOD protocol (2.20) is also UGES.

Proof. The proof follows directly from Theorem 2.4.1 and the fact that P_i is structured as in (2.19). Therefore, it holds that $\sum_{j=1}^{N} \pi_{ji} P_j =: P - \Pi_i$. □

2.4.3 Periodic protocols and the RR Protocol

We will now analyse another class of communication protocols, namely the periodic protocols, with the RR protocol as a special case. Hence, we need to analyse stability of the system (2.25) with a switching sequence induced by (2.21) or (2.22). This system is essentially a $\tilde{N}$-periodic uncertain system. For this system, we introduce positive definite matrices P_i, $i \in \{1, \ldots, N\}$, and a time-dependent periodic Lyapunov function given by

$$V_k(\bar{x}_k) = \bar{x}_k^{\top} P_k \bar{x}_k, \quad \text{and} \quad V_{k+\tilde{N}}(\bar{x}_{k+\tilde{N}}) = V_k(\bar{x}_k). \tag{2.53}$$

We can now present the main result of this section.

Theorem 2.4.4. *Assume that there exist positive definite matrices P_i, $i \in \{1, \ldots, \tilde{N}\}$, and matrices $R_{i,l} \in \mathcal{R}$, $i \in \{1, \ldots, N\}$ and $l \in \{1, \ldots, L\}$, satisfying*

$$\begin{bmatrix} P_i & 0 & \bar{A}_{\sigma_i,l}^\top P_{i+1} & \bar{C}_{\sigma_i}^\top R_{i,l} \\ \star & R_{i,l} & \bar{B}^\top P_{i+1} & 0 \\ \star & \star & P_{i+1} & 0 \\ \star & \star & \star & R_{i,l} \end{bmatrix} \succ 0, \tag{2.54}$$

where $P_{\tilde{N}+1} := P_1$, for all $i \in \{1, \ldots, \tilde{N}\}$ and $l \in \{1, \ldots, L\}$. Then, the system (2.25) with (2.22) is UGES and consequently, the NCS as given by (2.1), (2.2a) or (2.2b), (2.3), and (2.7) with a periodic protocol (2.21) is UGES.

Proof. The proof follows the same lines of reasoning as the proof of Theorem 2.4.1. □

2.5 Nonconservativeness of the Overapproximation

Given the results of the previous sections, it is now natural to ask if and how conservative the presented methodology is. The answer is given by the following result, showing that if the original system (2.12) (without any overapproximation), with protocol (2.18) or (2.21), is UGES in the sense that a Lyapunov function of a particular type exists, given by (2.46) or (2.53), respectively, the presented procedure based on the overapproximation will guarantee stability and will find a respective Lyapunov function, given that the overapproximation of (2.12) is sufficiently tight, i.e., (2.30) holds for a sufficiently small $\varepsilon > 0$. Therefore, making a convex overapproximation, according to Procedure 2.3.1, introduces no conservatism in the stability analysis as presented in the previous section.

In the following theorem, we will show the result for the NCS model (2.12) with protocol (2.18). A similar result holds for the NCS model (2.12) with protocol (2.21).

Theorem 2.5.1. *Suppose system (2.12), with protocol (2.18), has a Lyapunov function of the form (2.46), i.e., there exist a matrix $\Pi = \{\pi_{ji}\} \in \mathcal{M}$ and positive definite matrices P_i, $i \in \{1, \ldots, N\}$, such that*

$$\tilde{A}_{i,h,\tau}^\top \sum_{j=1}^N \pi_{ji} P_j \tilde{A}_{i,h,\tau} - P_i \preceq -\gamma I, \tag{2.55}$$

for all $i \in \{1, \ldots, N\}$ and $(h, \tau) \in \Theta$, and some $\gamma > 0$. Then, there exists an ε_0, such that for any ε-tight overapproximation satisfying (2.30), with $0 < \varepsilon \leqslant \varepsilon_0$, the conditions of Theorem 2.4.1 hold.

Proof. The proof is given in Appendix A.1. □

This result states that the convex overapproximation does not introduce conservatism when analysing UGES using mode-dependent quadratic Lyapunov functions.

2.6 Illustrative Example

In this section, we illustrate the presented theory using a well-known benchmark example in the NCS literature, see, e.g., [24, 34, 62, 103, 134], consisting of a model of a batch reactor. The linearised batch reactor is given by (2.1), with

$$
\left[\begin{array}{c|c} A^p & B^p \\ \hline C^p & \end{array}\right] = \left[\begin{array}{cccc|cc} 1.380 & -0.208 & 6.715 & -5.676 & 0 & 0 \\ -0.581 & -4.290 & 0 & 0.675 & 5.679 & 0 \\ 1.067 & 4.273 & -6.654 & 5.893 & 1.136 & -3.146 \\ 0.048 & 4.273 & 1.343 & -2.104 & 1.136 & 0 \\ \hline 1 & 0 & 1 & -1 & & \\ 0 & 1 & 0 & 0 & & \end{array}\right]. \tag{2.56}
$$

The continuous-time controller considered in [24, 34, 62, 103, 134] is given by (2.2a), with

$$
\left[\begin{array}{c|c} A^c & B^c \\ \hline C^c & D^c \end{array}\right] = \left[\begin{array}{cc|cc} 0 & 0 & 0 & 1 \\ 0 & 0 & 1 & 0 \\ \hline -2 & 0 & 0 & -2 \\ 0 & 8 & 5 & 0 \end{array}\right]. \tag{2.57}
$$

First, we will analyse the continuous-time NCS as also used in [24, 62, 103, 134]. As done in these references, we consider the TOD and RR protocol and assume that the controller is directly connected to the actuator, i.e., only the two outputs are transmitted via the network. Since communication delays are only considered in [62], and gives in absence of delays (i.e., $\underline{\tau} = \overline{\tau} = 0$) the same results as in [24], we compare our results with [62]. This will show that our results provide significantly less conservative bounds on the uncertain transmission intervals and transmission delays than earlier results in the literature. Secondly, we illustrate that our framework can equally well deal with discrete-time controllers, a larger number of nodes than used in previous examples in the literature, and a nonzero lower bound on the transmission interval.

2.6.1 Continuous-Time Controller

In order to assess the bounds on the allowable transmission intervals and delays, we first define our NCS model as in Section 2.2.1.C. This model appropriately describes the situation as discussed in this example, where only the plant outputs y are transmitted over the network and u are sent continuously via a nonnetworked connection. Then, we derive the uncertain polytopic system
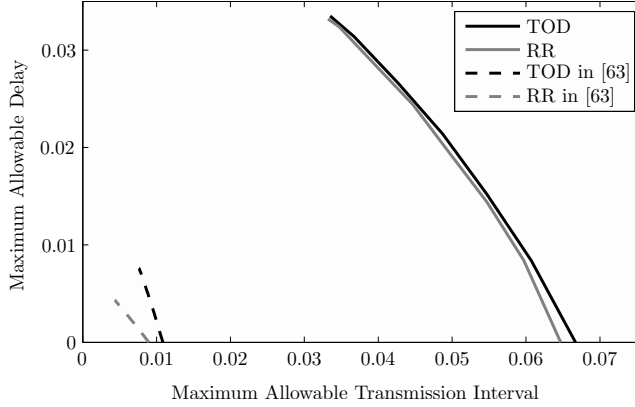
Figure 2.3: Tradeoff curves between allowable transmission intervals and transmission delays for two different protocols.

(2.25) that overapproximates the NCS model (2.12), using Procedure 2.3.1. As in [62], we try to obtain combinations of $\bar{h}$ and $\bar{\tau}$ for which the NCS is stable, and we assume that $\underline{\tau} = 0$, and we take $\underline{h} = 10^{-3}$. We cannot make $\underline{h}$ too small, because, by doing so, $\tilde{A}_{\sigma_k, h_k, \tau_k}$, as in (2.12), approaches the identity matrix and LMI solvers run into numerical problems, as the system becomes close to unstable. Note that [24, 62, 103, 134] also use nonzero lower bound on the transmission intervals to prevent Zeno behaviour, although, this lower bound can be taken arbitrarily small. Using Procedure 2.3.1, we obtain a convex overapproximation, in which we choose $\varepsilon_u = 2$ as decreasing ε_u does not change the results in this example. Using the obtained overapproximation, we can check for which combinations of $\bar{h}$ and $\bar{\tau}$, the LMIs in Corollary 2.4.3 and Theorem 2.4.4 are feasible. This results for each $\bar{\tau}$ in the maximum achievable $\bar{h}$ (or vice versa) for which the LMIs in Corollary 2.4.3 and Theorem 2.4.4 are satisfied. This results in tradeoff curves, as shown in Figure 2.3. These tradeoff curves can be used to impose or select a suitable network with a certain communication delay and a certain allowable transmission interval.

Moreover, in Figure 2.3, also the tradeoff curves as obtained in [62] are given. We conclude that our proposed methodology is less conservative than the one in [62]. More interestingly, in case there is no delay, i.e., $\underline{\tau} = \bar{\tau} = 0$, the maximum allowable transmission interval $\bar{h}$ obtained in [24], which provide the least conservative results known in literature so far, was $\bar{h} = 0.0108$, while we obtain $\bar{h} = 0.0665$. In [134], $\bar{h}$ was estimated (using simulations) to be approximately 0.08 for the TOD protocol. Furthermore, for the RR protocol, [24] provides the bound $\bar{h} = 0.009$ in the delay-free case, while we obtain $\bar{h} = 0.0645$. Also in [134], for a constant transmission interval, i.e. $\underline{h} = \bar{h}$, the bound 0.0657 was obtained for the RR protocol. The case where the trans-
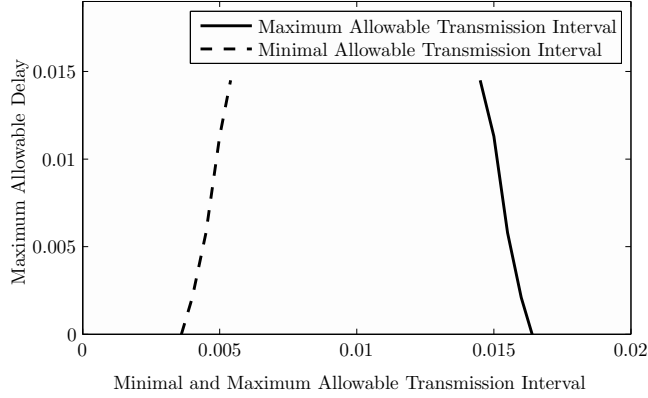
Figure 2.4: Tradeoff curves between allowable transmission intervals and transmission delays.

mission interval is constant, provides an upper bound on the true maximum allowable transmission interval (MATI). We can therefore conclude that for this example, our methodology reduces conservatism significantly in comparison to existing methodologies and even approximates known estimates of the true MATI closely.

2.6.2 Discrete-Time Controller

Next, we compute $\underline{h}$, $\overline{h}$, $\underline{\tau}$, and $\overline{\tau}$ for the NCS with a discrete-time controller as in (2.2b). Contrary to the example presented above, and all examples considered in [24, 62, 103, 134], we now designate a node to each single sensor and actuator, resulting in an NCS with four nodes. By doing so, we try to point out that our methodology is also suitable to study more complex problems. In this example, the controller is given by an exact discretisation of the continuous-time controller (2.2a) with matrices (2.57) using a zero-order hold and assuming a nominal transmission interval $h_{\text{nom}} = 0.01$ and a bounded variation h_{var} around this nominal transmission interval. We assume that $\underline{\tau} = 0$ and $\underline{h} \neq 0$, i.e., transmissions can be infinitely fast, but do not occur infinitely often. In this example, we select $\underline{h} = h_{\text{nom}} - h_{\text{var}}$ and $\overline{h} = h_{\text{nom}} + h_{\text{var}}$, where $2h_{\text{var}} > 0$ determines the range of allowable transmission intervals and we only consider the RR protocol.

After obtaining a convex overapproximation using Procedure 2.3.1, in which we have taken $\varepsilon_u = 0.02$, and assessing stability using the results of Theorem 2.4.4, we can now plot for each $\overline{\tau}$, the largest range, determined by $\underline{h} = h_{\text{nom}} - h_{\text{var}}$ and $\overline{h} = h_{\text{nom}} + h_{\text{var}}$, for which UGES is guaranteed. In this example, we take $h_{\text{nom}} = 0.01$, which results in the tradeoff curve as shown in Figure 2.4.

2.7   Conclusions

In this chapter, we studied the stability of networked control systems (NCSs) that are subject to communication constraints, time-varying transmission intervals and time-varying delays, and packet dropouts. We analysed the stability of the NCS when the communication sequence is determined by one of the protocols in the newly introduced classes of quadratic protocols or periodic protocols, having the well-known try-once-discard (TOD) and the round-robin (RR) as special cases. This analysis was based on a discrete-time switched linear uncertain system to model the NCS. A new and efficient convex over-approximation was proposed that allows us to analyse stability using a finite number of linear matrix inequalities. We presented an automated procedure to obtain the overapproximation and we formally showed that the convex overapproximation can be made arbitrarily tight and does not introduce conservatism. On a benchmark example, we illustrated the advantages and the effectiveness of the developed theory. In particular, we showed that stability can be guaranteed for a much larger maximum allowable transmission interval and maximum allowable transmission delay, when compared to the existing results in the literature. In addition, our results can be applied for stability analysis of NCS with *discrete-time* controllers and *nonzero* lower bounds on the transmission intervals and delays, which could not be analysed before even though they are highly relevant for practical implementations of networked controllers.

Future work focusses on studying the case where delays are not restricted to be smaller than the transmission interval, on the inclusion of quantisation effects of the sensor and actuator signals on the closed-loop stability and performance, and on co-design methods of the controller and the protocol.

3

Stability Analysis of Stochastic Networked Control Systems[1]

Abstract – In this chapter, we study the stability of networked control systems (NCSs) that are subject to time-varying transmission intervals, time-varying transmission delays, packet dropouts and communication constraints. Communication constraints impose that, per transmission, only one sensor or actuator node can access the network and send its information. Which node is given access to the network at a transmission time is orchestrated by a so-called network protocol. The transmission intervals and transmission delays are described by a sequence of *continuous* random variables, which is in contrast with many existing stochastic approaches that only allow a finite or countable number of transmission intervals and/or delays. The complexity that the continuous character of the probability distribution introduces, is overcome using a novel convex overapproximation technique that preserves the available probabilistic information. By focussing on linear plants and controllers and quadratic, periodic and stochastic protocols, we present a modelling framework for NCSs based on discrete-time linear switched and parameter-varying systems. Stability (in the mean-square) of these systems is analysed using a new stochastic computational technique and a finite number of linear matrix inequalities. On a benchmark example of a batch reactor, we illustrate the developed theory.

---

[1]This chapter is based on [39].

3.1 Introduction

Modelling, analysis, and controller design of networked control systems (NCSs) have recently received considerable attention in the literature, as is evidenced by the overview papers, e.g., [4, 67, 144, 147], and the book [16]. The main reason for this attention is the many advantages that NCSs offer, such as reduced system wiring and increased flexibility. A drawback of networking the control system is, however, that it becomes subject to time-varying delays, time-varying transmission intervals, packet dropouts, and that communication is constrained, (i.e., it is no longer possible to transmit all sensor and actuator signals at every transmission instant). Most of the literature studies the effects of only some of the phenomena, while ignoring the others. Clearly, it is important to consider the combined presence of time-varying delays and time-varying transmission intervals, packet dropouts and communication constraints, as in any practical NCS they will be present simultaneously.

Despite the importance of studying the combined presence of the mentioned network-induced phenomena, only few results exist that provide a framework that allows studying these phenomena simultaneously. For instance, time-varying transmission intervals and communication constraints (and, less explicitly, packet dropouts) has been considered in [103, 134] and time-varying transmission intervals, time-varying delays, (again less explicitly, packet dropouts) and communication constraints in [26, 40, 62]. The mentioned papers provide methods for computing the so-called maximum allowable transmission interval (MATI) and maximum allowable delays (MAD), given a certain network protocol that determines which sensor and/or actuator information is sent at a transmission instant. Stability is guaranteed as long as the actual transmission intervals and delays are always smaller than the MATI and MAD, respectively. Three other network induced phenomena, namely time-varying transmission intervals, time-varying delays and packet dropouts, are considered in [29, 99, 142], in which stability is analysed for the case that the number of consecutive dropouts are upper bounded, and bounds on the transmission intervals and delays are available.

A common feature of the aforecited references is that conditions for stability are derived, given bounds on the various network phenomena. In many situations, however, transmission intervals, delays and packet dropouts can be described as random phenomena, modelled using probability distributions. Unfortunately, fewer stability results are available in this context. A common approach found in literature, see, e.g., [96, 114, 115, 138, 143, 146], is to take a finite or countable set of possible transmission intervals and delays and attribute probabilities to each element of the set. In this way, a discrete probability distribution is obtained and the NCS can be effectively modelled as a Markov jump system [32]. It is, however, not possible to make any statements about stability when a *continuous* probability distribution is given and, con-

sequently, the number of elements in the set is not finite or countable. Other approaches are taken in [105], in which a delay-dependent controller is proposed, and in [95], which discusses so-called 'model-based control'. We will, as in [5, 124], focus on the more basic 'emulation-based' approach, i.e., we assume the controller to be designed to stabilise the plant without considering the network and we study how this controller behaves in the presence of the stochastic network.

In this chapter, we focus on linear plants and linear controllers and study the stability (in the mean-square) of NCSs in the presence of communication constraints, time-varying transmission intervals, time-varying delays and dropouts, which the latter three are described by an independent and identically distributed sequence of random variables and in which the delays are assumed to be smaller than the transmission intervals. Contrary to [96, 114, 115, 138, 143, 146], we allow for *continuous* probability distributions with possibly infinite supports, as in [5, 124]. In particular, the techniques we provide are applicable to any distribution whose tail is exponentially bounded and, thereby, includes the exponential distribution that was studied in [124] as a special case. Furthermore, we consider three classes of protocols, namely: the class of quadratic network protocols, of which the well-known try-once-discard (TOD) protocol is a special case, the class of periodic protocols, which includes the round-robin (RR) protocol and was also studied in [5], and the stochastic protocol, which was introduced in [124]. Next to treating a more general setup than in [5, 124], the essential difference between [5, 124] and the work presented in this chapter is that [5, 124] use a continuous-time modelling paradigm, while we apply a *discrete-time* modelling framework that leads to a switched linear system model that is stochastically parameter varying. We propose novel convex overapproximation techniques, which are used to handle continuous probability distributions, and newly developed linear matrix inequalities (LMIs) to guarantee stability (in the mean-square) of NCSs with the transmission intervals and delays satisfying a continuous probability distribution. Note that in this chapter, we consider the simultaneous presence of all the aforementioned network effects, whereas in [5, 96, 114, 115, 124, 138, 143, 146] only some of them are considered. We will show the effectiveness of the presented approach on the benchmark example of a batch reactor as also used in [5, 40, 62, 124].

The remainder of this chapter is organised as follows. After introducing the necessary notational conventions used in this chapter, we introduce the model of the NCS in Section 3.2 and propose a method to write it as a discrete-time switched linear parameter-varying system. We also state a precise problem formulation. In Section 3.3, we provide a procedure to obtain a convex overapproximation of NCS systems with time-varying transmission intervals and time-varying transmission delays, which preserves the probabilistic information present in the probability distribution. This result will be used in the conditions for stability of NCS that we present in Section 3.4. In Section 3.5,

we will formally proof the fact that employing the convex overapproximation technique presented in this chapter does not introduce any conservatism. Finally, we illustrate the stability results using a numerical benchmark example in Section 3.6 and draw conclusions in Section 3.7. Appendix A.2 contains the proofs of the lemmas and theorems.

3.1.1   Nomenclature

The following notational conventions will be used. $\text{diag}(A_1, \ldots, A_N)$ denotes a block-diagonal matrix with the entries $A_1, \ldots, A_N$ on the diagonal, $A^\top \in \mathbb{R}^{m \times n}$ denotes the transposed of the matrix $A \in \mathbb{R}^{n \times m}$, and $\lambda_{\max}(A)$ and $\lambda_{\min}(A)$ denote the maximum and minimum eigenvalue of a symmetric matrix $A \in \mathbb{R}^{n \times n}$, respectively. For a vector $x \in \mathbb{R}^n$, we denote by x^i the i-th component and by $\|x\| := \sqrt{x^\top x}$ its Euclidean norm. For a matrix $A \in \mathbb{R}^{n \times m}$, we denote by $\|A\| := \sqrt{\lambda_{\max}(A^\top A)}$ its spectral norm. For brevity, we sometimes write symmetric matrices of the form $\begin{bmatrix} A & B \\ B^\top & C \end{bmatrix}$, as $\begin{bmatrix} A & B \\ \star & C \end{bmatrix}$. By $\lim_{s \downarrow t}$ and $\lim_{s \uparrow t}$, we denote the limit as s approaches t from above or below, respectively. The convex hull and interior of a set $\mathcal{A}$ are denoted by $\text{co}\mathcal{A}$ and $\text{int}\mathcal{A}$, respectively, and the indicator function of a set $\mathcal{A} \subseteq \mathbb{R}^n$ is the function $\mathbf{1}_\mathcal{A} : \mathbb{R}^n \to \{0, 1\}$ that satisfies $\mathbf{1}_\mathcal{A}(x) = 1$ if $x \in \mathcal{A}$, and $\mathbf{1}_\mathcal{A}(x) = 0$ if $x \notin \mathcal{A}$. A polytope is the convex hull of finitely many points. The probability distribution of a random variable x, taking values in $\mathbb{R}^n$, is given in terms of the probability measure μ, which satisfies $\mu(\mathbb{R}^n) = 1$. We assume that the measure μ can be decomposed into a continuous component μ_c and a discrete component μ_d, i.e., $\mu = \mu_c + \mu_d$, where $\mu_c(\mathcal{A}) = \int_\mathcal{A} p_c(\omega)\mathrm{d}\omega$ for some Lebesgue-integrable probability density function (pdf) $p_c : \mathbb{R}^n \to \mathbb{R}_+$ and where $\mu_d(\mathcal{A}) = \sum_{i \in \{j \,|\, a_j \in \mathcal{A}\}} p_{d,i}$, for some finite or countable set of isolated atom points $\{a_i \,|\, i \in \mathcal{I}\}$ and a corresponding set of weights $\{p_{d,i} \,|\, i \in \mathcal{I}\}$, where $\mathcal{I} \subseteq \mathbb{N}$. This probability measure μ defines the probability that the event $x \in \mathcal{A}$ occurs, denoted by $\Pr(x \in \mathcal{A}) := \mu(\mathcal{A})$, and defines the expected value of $f(x)$, for a mapping $f : \mathbb{R}^n \to \mathbb{R}^m$, as $\mathbb{E}(f(x)) := \int_{\mathbb{R}^n} f(\omega)p_c(\omega)\mathrm{d}\omega + \sum_{i=1}^\infty f(a_i)p_{d,i}$.

3.2   NCS Model and Problem Statement

In this section, we present the model describing networked control systems (NCSs) subject to communication constraints, time-varying transmission intervals and delays. We will later comment on how this model can accommodate for packet dropouts. Let us consider the linear time-invariant (LTI) continuous-time plant given by

$$\begin{cases} \frac{\mathrm{d}}{\mathrm{d}t}x^p(t) = A^p x^p(t) + B^p \hat{u}(t) \\ \quad y(t) = C^p x^p(t), \end{cases} \tag{3.1}$$
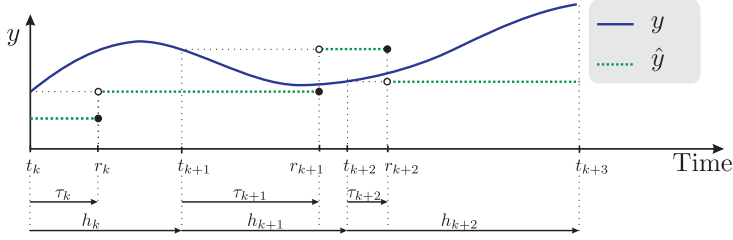
Figure 3.1: Illustration of a typical evolution of y and $\hat{y}$.

where $x^p \in \mathbb{R}^{n_p}$ denotes the state of the plant, $\hat{u} \in \mathbb{R}^{n_u}$ the most recently received control variable, $y \in \mathbb{R}^{n_y}$ the (measured) output of the plant and $t \in \mathbb{R}_+$ the time. The controller, also an LTI system, is assumed to be given in either continuous time by

$$\begin{cases} \frac{\mathrm{d}}{\mathrm{d}t} x^c(t) = A^c x^c(t) + B^c \hat{y}(t) \\ \quad u(t) = C^c x^c(t) + D^c \hat{y}(t), \end{cases} \tag{3.2a}$$

or in discrete time by

$$\begin{cases} x^c_{k+1} = A^c x^c_k + B^c \hat{y}_k \\ u(t_k) = C^c x^c_k + D^c \hat{y}(t_k). \end{cases} \tag{3.2b}$$

In these descriptions, $x^c \in \mathbb{R}^{n_c}$ denotes the state of the controller, $\hat{y} \in \mathbb{R}^{n_y}$ the most recently received output of the plant and $u \in \mathbb{R}^{n_u}$ denotes the controller output. At transmission instant $t_k, k \in \mathbb{N}$, (parts of) the outputs of the plant $y(t_k)$ and the controller $u(t_k)$ are sampled and are transmitted over the network. We assume that they arrive after a delay τ_k at instant $r_k := t_k + \tau_k$, called the arrival instant, see Fig. 3.1. In the case we have a discrete-time controller (3.2b), the states of the controller x^c_{k+1} are updated using $\hat{y}_k := \lim_{t \downarrow r_k} \hat{y}(t)$, i.e., as in [34, 40], directly after $\hat{y}$ is updated. Note that in this case, the update of x^c_{k+1} in (3.2b) has to be performed in the time interval $(r_k, t_{k+1}]$.

Let us now explain in more detail the functioning of the network and define these 'most recently received' $\hat{y}$ and $\hat{u}$ exactly. The plant is equipped with sensors and actuators that are grouped into N nodes. At each transmission instant t_k, $k \in \mathbb{N}$, one node, denoted by $\sigma_k \in \{1, \ldots, N\}$, gets access to the network and transmits its corresponding values. These transmitted values are received and implemented on the controller and/or the plant at arrival instant r_k. As in [62], a transmission only occurs after the previous transmission has arrived, i.e., $t_{k+1} > r_k \geqslant t_k$, for all $k \in \mathbb{N}$, where $t_0 = 0$. In other words, we consider the delays to be smaller than the transmission interval. After each transmission and reception, the values in $\hat{y}$ and $\hat{u}$ are updated with the newly received information, while the other values in $\hat{y}$ and $\hat{u}$ remain the same, as no

additional information is received. This leads to the constrained data exchange expressed as

$$\begin{cases} \hat{y}(t) = \Gamma_{\sigma_k}^y y(t_k) + (I - \Gamma_{\sigma_k}^y)\hat{y}(t_k) \\ \hat{u}(t) = \Gamma_{\sigma_k}^u u(t_k) + (I - \Gamma_{\sigma_k}^u)\hat{u}(t_k) \end{cases} \tag{3.3}$$

for all $t \in (r_k, r_{k+1}]$. The matrix $\Gamma_{\sigma_k} := \text{diag}(\Gamma_{\sigma_k}^y, \Gamma_{\sigma_k}^u)$ is a diagonal matrix, given by

$$\Gamma_i = \text{diag}(\gamma_{i,1}, \ldots, \gamma_{i,n_y+n_u}), \tag{3.4}$$

when $\sigma_k = i$. In (3.4), the elements $\gamma_{i,j}$, with $i \in \{1, \ldots, N\}$ and $j \in \{1, \ldots, n_y\}$, are equal to one, if plant output y^j is in node i, elements $\gamma_{i,j+n_y}$, with $i \in \{1, \ldots, N\}$ and $j \in \{1, \ldots, n_u\}$, are equal to one, if controller output u^j is in node i, and are zero elsewhere.

The value of $\sigma_k \in \{1, \ldots, N\}$ in (3.3) indicates which node is given access to the network at transmission instant t_k, $k \in \mathbb{N}$. Indeed, (3.3) reflects that the values in $\hat{u}$ and $\hat{y}$ corresponding to node σ_k are updated just after r_k, with the corresponding transmitted values at time t_k, while the others remain the same. A scheduling protocol determines the sequence $(\sigma_0, \sigma_1, \ldots)$ and particular protocols will be made explicit below.

In this chapter, we consider the case that both the transmission intervals $h_k := t_{k+1} - t_k > 0$, $k \in \mathbb{N}$, and the transmission delays $\tau_k := r_k - t_k \geqslant 0$, $k \in \mathbb{N}$, are varying in time. Since we assumed that $t_{k+1} > r_k$, for all $k \in \mathbb{N}$, we have that $\tau_k < h_k$. Furthermore, we assume that the transmission intervals and transmission delays are described by an independent and identically distributed (iid) sequence of (possibly) continuous random variables. These assumptions are made explicit below.

Assumption 3.2.1. *For each $k \in \mathbb{N}$, the transmission interval h_k and the transmission delay τ_k are continuous random variables, characterised by a probability distribution that satisfies $\Pr\big((h, \tau) \in \Theta\big) = 1$, where*

$$\Theta \subseteq \left\{ (h, \tau) \in \mathbb{R}^2 \mid h > 0, \ 0 \leqslant \tau < h \right\}. \tag{3.5}$$

Furthermore, the sequence of transmission intervals and delays $\{(h_k, \tau_k)\}_{k \in \mathbb{N}}$ is iid.

3.2.1 Incorporating Packet Dropouts

In the model presented above, we only considered communication constraints, time-varying transmission intervals and delays. It can, however, easily be adapted to accommodate for packet dropouts as well. To do so, we divide the transmissions into successful and failed ones, and model the sequence of transmissions by a two-state Markov process, as was also done in [2, 74, 140]. This model, which is depicted in Fig. 3.2, is also known as the Gilbert-Elliot model and has two states, namely, the 'packet received' state ($d_k = 1$) and
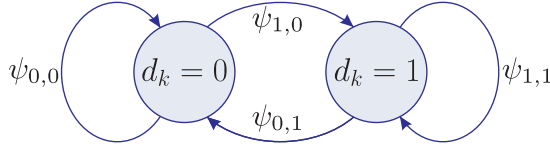
Figure 3.2: The Gilbert-Elliot model of packet dropouts.

the 'packet dropped' state ($d_k = 0$). The conditional probability that a packet is received or dropped $d_k \in \{0, 1\}$ at time t_k, given that the previous one is dropped or received $d_{k-1} \in \{0, 1\}$, is given by

$$\Pr(d_k = i | d_{k-1} = j) = \psi_{i,j} \tag{3.6}$$

for all $k \in \mathbb{N}\backslash\{0\}$, where $\psi_{0,j} + \psi_{1,j} = 1$ for all $j \in \{0, 1\}$, and it is assumed that $d_0 = 1$.

In this Gilbert-Elliot model, the probability that exactly δ successive packets are dropped before one is received equals $\psi_{1,0}\psi_{0,0}^{\delta-1}\psi_{0,1}$ for $\delta > 0$ and the probability that two subsequent packets arrive equals $\psi_{1,1}$. Now by only considering the successful transmissions and redefining the transmission interval as the time between two subsequent successful transmissions, as also done in [62, 103], packet dropouts can be incorporated in the NCS model. As a result, the probability that the interval between two subsequent successful transmission and the transmission delay satisfy $(h, \tau) \in \mathcal{Q}$, for some $\mathcal{Q} \subseteq \mathbb{R}^2$, becomes

$$\Pr\big((h, \tau) \in \mathcal{Q}\big) = \psi_{1,1}\Pr\big((h_1, \tau) \in \mathcal{Q}\big) + \sum_{\delta=1}^{\infty} \psi_{1,0}\psi_{0,0}^{\delta-1}\psi_{0,1}\Pr\big((\sum_{i=1}^{\delta+1} h_i, \tau) \in \mathcal{Q}\big). \tag{3.7}$$

In the remainder of the chapter, we will assume that the given probability distribution incorporates the information on the packet-dropout probability as outlined above.

3.2.2   The NCS as a Time-Varying Switched System

To analyse the stability of the NCS described above, we transform it into a discrete-time model. In this framework, we need a discrete-time equivalent of (3.1). To arrive at this description, let us first define the network-induced error as

$$\begin{cases} e^y(t) := \hat{y}(t) - y(t) \\ e^u(t) := \hat{u}(t) - u(t). \end{cases} \tag{3.8}$$

The stochastically parameter-varying discrete-time switched system can now be obtained by describing the evolution of the states between t_k and $t_{k+1} = t_k + h_k$.

In order to do so, we define $x_k^p := x^p(t_k)$, $u_k := u(t_k)$, $\hat{u}_k := \lim_{t\downarrow r_k} \hat{u}(t)$ and $e_k^u := e^u(t_k)$. Since $\hat{u}$, as in (3.3), is a left-continuous piecewise constant signal, i.e. $\lim_{s\uparrow t} \hat{u}(s) = \hat{u}(t)$, we can write $\hat{u}_{k-1} = \lim_{t\downarrow r_{k-1}} \hat{u}(t) = \hat{u}(r_k) = \hat{u}(t_k)$. Now using the fact that (3.3) and (3.8) yield $\hat{u}_{k-1} = u_k + e_k^u$ and $\hat{u}_{k-1} - \hat{u}_k = \Gamma_{\sigma_k}^u e_k^u$, we can write the exact discretisation of (3.1) as follows:

$$x_{k+1}^p = e^{A^p h_k} x_k^p + \int_0^{h_k} e^{A^p s} \mathrm{d}s B^p(u_k + e_k^u) - \int_0^{h_k-\tau_k} e^{A^p s} \mathrm{d}s B^p \Gamma_{\sigma_k}^u e_k^u. \quad (3.9)$$

A discretised equivalent of (3.2a) is obtained in a similar fashion. By defining $x_k^c := x^c(t_k)$, $y_k := y(t_k)$, $e_k^y := e^y(t_k)$, $\hat{y}_k := \lim_{t\downarrow r_k} \hat{y}(t)$, and observing that $\hat{y}_{k-1} = \hat{y}(t_k)$, it holds that

$$x_{k+1}^c = e^{A^c h_k} x_k^c + \int_0^{h_k} e^{A^c s} \mathrm{d}s B^c(y_k + e_k^y) - \int_0^{h_k-\tau_k} e^{A^c s} \mathrm{d}s B^c \Gamma_{\sigma_k}^y e_k^y. \quad (3.10)$$

We now present three different models each describing a particular setup for the NCS. The first and the second model cover the situation where both the plant and the controller outputs are transmitted over the network, differing by the fact that the controller is given by (3.2a) and (3.2b), respectively. In the third model, it is assumed that the controller is given by (3.2a) and that only the plant outputs y are transmitted over the network and u are sent continuously via an ideal nonnetworked connection. We include this particular case, because it is often used in examples in the NCS literature, (see, e.g., the benchmark example in [5, 34, 40, 41, 62, 103, 124, 134]).

A) The NCS model with controller (3.2a)**:** For an NCS having controller (3.2a), the complete NCS model is obtained by combining (3.3), (3.8), (3.9), and (3.10) and defining

$$\bar{x} := \begin{bmatrix} x^{p\top} & x^{c\top} & e^{y\top} & e^{u\top} \end{bmatrix}^\top. \quad (3.11)$$

This results in the discrete-time model

$$\bar{x}_{k+1} = \underbrace{\begin{bmatrix} A_{h_k} + E_{h_k} BDC & E_{h_k} BD - E_{h_k-\tau_k} B\Gamma_{\sigma_k} \\ C(I - A_{h_k} - E_{h_k} BDC) & I - D^{-1}\Gamma_{\sigma_k} + C(E_{h_k-\tau_k} B\Gamma_{\sigma_k} - E_{h_k} BD) \end{bmatrix}}_{=:\tilde{A}_{\sigma_k,h_k,\tau_k}} \bar{x}_k,$$

$$(3.12)$$

with $\bar{x}_k = \bar{x}(t_k)$, in which $\tilde{A}_{\sigma_k,h_k,\tau_k} \in \mathbb{R}^{n\times n}$, with $n = n_p + n_c + n_y + n_u$, and

$$A_\rho := \begin{bmatrix} e^{A^p \rho} & 0 \\ 0 & e^{A^c \rho} \end{bmatrix}, \quad B := \begin{bmatrix} 0 & B^p \\ B^c & 0 \end{bmatrix}, \quad C := \begin{bmatrix} C^p & 0 \\ 0 & C^c \end{bmatrix} \quad (3.13\text{a})$$

$$D := \begin{bmatrix} I & 0 \\ D^c & I \end{bmatrix}, \quad E_\rho := \begin{bmatrix} \int_0^\rho e^{A^p s} \mathrm{d}s & 0 \\ 0 & \int_0^\rho e^{A^c s} \mathrm{d}s \end{bmatrix}, \quad \rho \in \mathbb{R}. \quad (3.13\text{b})$$

B) The NCS model with controller (3.2b)***:*** The complete NCS model is obtained by combining (3.2b), (3.3), (3.8), and (3.9), and defining $\bar{x} := [x^{p\top} \ x^{c\top} \ e^{y\top} \ e^{u\top}]^\top$. This also results in the discrete-time model (3.12), in which now

$$A_\rho := \begin{bmatrix} e^{A^p \rho} & 0 \\ 0 & A^c \end{bmatrix}, \quad B := \begin{bmatrix} 0 & B^p \\ B^c & 0 \end{bmatrix}, \quad C := \begin{bmatrix} C^p & 0 \\ 0 & C^c \end{bmatrix}, \tag{3.14a}$$

$$D := \begin{bmatrix} I & 0 \\ D^c & I \end{bmatrix}, \quad E_\rho := \begin{bmatrix} \int_0^\rho e^{A^p s} \mathrm{d}s & 0 \\ 0 & I \end{bmatrix}, \quad \rho \in \mathbb{R}. \tag{3.14b}$$

C) The NCS model if only y ***is transmitted over the network:*** In this case we assume that only the outputs of the plant are transmitted over the network and the controller communicates its values continuously and without delay. We therefore have that $u(t) = \hat{u}(t)$, for all $t \in \mathbb{R}_+$, which allows us to combine (3.1) and (3.2a), yielding

$$\begin{bmatrix} \dot{x}^p(t) \\ \dot{x}^c(t) \end{bmatrix} = \begin{bmatrix} A^p & B^p C^c \\ 0 & A^c \end{bmatrix} \begin{bmatrix} x^p(t) \\ x^c(t) \end{bmatrix} + \begin{bmatrix} B^p D^c \\ B^c \end{bmatrix} \hat{y}(t). \tag{3.15}$$

Since $\hat{y}$ is still updated according to (3.3), we can describe the evolution of the states between t_k and $t_{k+1} = t_k + h_k$ in a similar fashion as in (3.9). In this case, (3.11) reduces to

$$\bar{x} := \begin{bmatrix} x^{p\top} & x^{c\top} & e^{y\top} \end{bmatrix}^\top, \tag{3.16}$$

also resulting in (3.12), in which now

$$A_\rho := e^{\left(\begin{bmatrix} A^p & B^p C^c \\ 0 & A^c \end{bmatrix} \rho\right)}, \quad B := \begin{bmatrix} B^p D^c \\ B^c \end{bmatrix}, \quad C := \begin{bmatrix} C^p & 0 \end{bmatrix}, \tag{3.17a}$$

$$D := I, \quad E_\rho := \int_0^\rho e^{\left(\begin{bmatrix} A^p & B^p C^c \\ 0 & A^c \end{bmatrix} s\right)} \mathrm{d}s, \quad \rho \in \mathbb{R}. \tag{3.17b}$$

3.2.3 Protocols as a Switching Function

Based on the previous modelling steps, the NCS is formulated as a stochastically parameter-varying discrete-time switched linear system (3.12). In this framework, protocols are considered as the switching function determining σ_k, $k \in \mathbb{N}$. We consider three classes of protocols, namely quadratic and periodic protocols, as introduced in [40], and stochastic protocols, as introduced in [124].

A) Quadratic Protocols: A quadratic protocol is a protocol, for which the switching function can be written as

$$\sigma_k = \arg \min_{i=1,\dots,N} \bar{x}_k^\top P_i \bar{x}_k, \tag{3.18}$$

where P_i, $i \in \{1, \ldots, N\}$, are certain given matrices. In case two or more nodes have the same minimal values, one of them can be chosen arbitrarily. As was shown in [40], the well-known try-once-discard (TOD) protocol, see, e.g., [62, 134], belongs to this class of protocols. In the TOD protocol, the node that has the largest network-induced error, i.e., the largest difference between the latest transmitted values and the current values of the signals corresponding to the node, is granted access to the network. The TOD protocol can be modelled as in (3.18) by adopting the following structure in the P_i matrices:

$$P_i = \bar{P} - \mathrm{diag}(0, \Gamma_i), \qquad (3.19)$$

in which Γ_i, $i \in \{1, \ldots, N\}$, is given by (3.4) and $\bar{P}$ is some arbitrary matrix. Indeed, if we define $\tilde{e}_k^i := \Gamma_i e_k$, being the error corresponding to node i (extended with zeros on the entries that do not correspond to node i), where $e_k := [e_k^{y\top}, e_k^{u\top}]^\top$, (3.18) becomes

$$\sigma_k = \arg\min \left\{ -e_k^\top \Gamma_1 e_k, \ldots, -e_k^\top \Gamma_N e_k \right\} = \arg\max \left\{ \|\tilde{e}_k^1\|, \ldots, \|\tilde{e}_k^N\| \right\}, \quad (3.20)$$

which is the TOD protocol.

B) Periodic Protocols: Another class of protocols that is considered in this chapter is the class of so-called periodic protocols. A periodic protocol is a protocol that satisfies for some $\tilde{N} \in \mathbb{N}$

$$\sigma_{k+\tilde{N}} = \sigma_k, \quad \text{for all } k \in \mathbb{N}. \qquad (3.21)$$

$\tilde{N}$ is then called the period of the protocol. The well-known round-robin (RR) protocol belongs to this class of protocols and is defined by

$$\{\sigma_1, \ldots, \sigma_N\} = \{1, \ldots, N\}, \qquad (3.22)$$

and period $\tilde{N} = N$, i.e., during each period of the protocol every node has access to the network exactly once.

C) Stochastic Protocols: The third class of protocols that is considered in this chapter is the class of stochastic protocols. Contrary to the quadratic and periodic protocol, in which the resulting switching function is deterministic, the stochastic protocol determines $\sigma_k \in \{1, \ldots, N\}$ through a Markov chain. The conditional probability that node i, $i \in \{1, \ldots, N\}$, gets access to the network at time t_k, given the value of $\sigma_{k-1} \in \{1, \ldots, N\}$, is given by

$$\Pr(\sigma_k = i | \sigma_{k-1} = j) = \pi_{ij} \quad \text{for all } k \in \mathbb{N}\backslash\{0\}, \qquad (3.23)$$

where $\sum_{i=1}^{N} \pi_{ij} = 1$ for all $j \in \{1, \ldots, N\}$, and $\sigma_0 \in \{1, \ldots, N\}$ is assumed to be given.

For each of the three classes of protocols, the above modelling approach now provides a description of the NCS in the form of a *stochastically parameter-varying discrete-time switched linear system* given by (3.12) and one of the protocols, characterised by (3.18), (3.21) or (3.23).

3.2.4 Stability of the NCS

The problem studied in this chapter is to analyse stability of the stochastically parameter-varying discrete-time switched linear system (3.12) with protocols (3.18), (3.21) or (3.23) and the transmission intervals and transmission delays satisfying Assumption 3.2.1. Let us now formally define stability for the NCS.

Definition 3.2.2. *The continuous-time NCS given by* (3.1), (3.2b), (3.3), *and* (3.8), *with protocols satisfying* (3.18), (3.21) *or* (3.23), *is said to be* uniformly globally mean-square exponentially stable *(UGMSES) if there exist* $c_c, \beta_c > 0$, *such that for any initial condition* $\bar{x}(0)$, *for a sequence of random variables* $\{(h_k, \tau_k)\}_{k \in \mathbb{N}}$, *and for all* $t \in \mathbb{R}_+$ *it holds that*

$$\mathbb{E}\left(\|\bar{x}(t)\|^2\right) \leqslant c_c \|\bar{x}(0)\|^2 e^{-\beta_c t}. \tag{3.24}$$

Stability of the *continuous-time* NCS can be analysed by assessing stability of the *discrete-time* uncertain switched linear system (3.12) with switching functions satisfying (3.18), (3.21) or (3.23), as we will show below. Before doing so, let us formally define stability of this discrete-time system.

Definition 3.2.3. *System* (3.12) *with switching sequences satisfying* (3.18), (3.21) *or* (3.23) *is said to be* uniformly globally mean-square exponentially stable *(UGMSES) if there exist* $c_d, \beta_d > 0$, *such that for any initial condition* $\bar{x}_0 \in \mathbb{R}^n$, *for a sequence of random variables* $\{(h_k, \tau_k)\}_{k \in \mathbb{N}}$, *and for all* $k \in \mathbb{N}$, *it holds that*

$$\mathbb{E}\left(\|\bar{x}_k\|^2\right) \leqslant c_d \|\bar{x}_0\|^2 e^{-\beta_d k}. \tag{3.25}$$

Since the switched uncertain linear system (3.12) with switching sequences satisfying (3.18), (3.21) or (3.23) is formulated in discrete time, we can only assess stability at the transmission instants. However, we will show that UGMSES of the discrete-time model implies UGMSES of the continuous-time NCS in the sense of Definition 3.2.2 under an assumption on the probability distribution. To prove this, we first need a technical lemma.

Lemma 3.2.4. *The continuous-time system, given by* (3.1), (3.2a) *or* (3.2b), (3.3) *and* (3.8) *with protocols satisfying* (3.18), (3.21) *or* (3.23) *is UGMSES, if the discrete-time system* (3.12) *with switching sequences satisfying* (3.18), (3.21) *or* (3.23) *is UGMSES, Assumption 3.2.1 is satisfied, the probability distribution for* (h, τ) *satisfies* $\mathbb{E}(e^{\bar{\lambda} h}) < c_h$, *for some* $\bar{\lambda} > 0$ *and some* $c_h > 0$, *and*

there exists a function $\gamma : \mathbb{R}_+ \to \mathbb{R}_+$, satisfying $\mathbb{E}(\gamma(h)) < c_\gamma$, for some $c_\gamma > 0$, such that the solutions of (3.1), (3.2a) or (3.2b), (3.3) and (3.8) satisfy

$$\|\bar{x}(t_k + \tilde{t})\|^2 \leqslant \gamma(h_k)\|\bar{x}(t_k)\|^2, \tag{3.26}$$

for all $\tilde{t} \in (0, h_k]$, $k \in \mathbb{N}$.

Proof. The proof is given in Appendix A.2. $\qquad\square$

In order to prove the main result of this section, we make the following assumption on the probability distribution for (h, τ).

Assumption 3.2.5. *There exists a constant $\bar{\lambda}$, such that $\bar{\lambda} > \max\{0, \lambda_{\max}(\bar{\Lambda}^\top + \bar{\Lambda})\}$, with*

$$\bar{\Lambda} = \begin{cases} \mathrm{diag}(A^p, A^c), & \text{if (3.12) is as in Section 3.2.2.A,} \\ \mathrm{diag}(A^p, 0), & \text{if (3.12) is as in Section 3.2.2.B,} \\ \begin{bmatrix} A^p & B^p C^c \\ 0 & A^c \end{bmatrix}, & \text{if (3.12) is as in Section 3.2.2.C,} \end{cases} \tag{3.27}$$

such that the probability distribution of (h, τ) satisfies $\mathbb{E}(e^{\bar{\lambda}h}) < c_h$, for some $c_h > 0$.

Assumption 3.2.5 excludes all probability distributions whose tails are not exponentially bounded, so-called heavy-tailed probability distributions, see, e.g., [7]. However, when the random variable (h, τ) has an exponentially bounded probability distribution, such as the Uniform, the Normal, and the Gamma distribution, stability can be analysed using the results presented in this chapter. This makes the results presented in this chapter more general than the results of [124], in which only exponential distributions are discussed. In the next theorem, we state that UGMSES of the discrete-time NCS model implies UGMSES of the continuous-time NCS, given that Assumptions 3.2.1 and 3.2.5 are satisfied.

Theorem 3.2.6. *Assume the discrete-time system (3.12) with switching sequences satisfying (3.18), (3.21) or (3.23) is UGMSES and Assumptions 3.2.1 and 3.2.5 are satisfied. Then, the corresponding continuous-time NCS given by (3.1), (3.2b), (3.3), and (3.8), with protocols satisfying (3.18), (3.21) or (3.23) is also UGMSES.*

Proof. The proof can be found in Appendix A.2. $\qquad\square$

This theorem states that it suffices to consider the discrete-time model (3.12) with switching sequences satisfying (3.18), (3.21) or (3.23) to assess UGMSES of the continuous-time NCS system.

3.3 Obtaining a Convex Overapproximation

In the previous section, we obtained an NCS model in the form of a stochastically parameter-varying discrete-time switched linear system. In the stability conditions developed in the next section, we will employ techniques originally developed for the situation in which the time-varying transmission intervals and delays are contained in some bounded set $\bar{\Theta}$, i.e., $(h_k, \tau_k) \in \bar{\Theta}$ for all $k \in \mathbb{N}$ without any probability information, as discussed in Chapter 2. As in Chapter 2, the matrix $\tilde{A}_{\sigma_k, h_k, \tau_k}$ depends nonlinearly on the uncertain parameters h_k and τ_k, which is not convenient for stability analysis. To make the system amenable for analysis, in Chapter 2 a procedure was given to overapproximate $\tilde{A}_{\sigma_k, h_k, \tau_k}$ by a polytopic system with norm-bounded additive uncertainty, i.e.,

$$\bar{x}_{k+1} = \left(\sum_{l=1}^{L} \alpha_k^l \bar{A}_{\sigma_k, l} + \bar{B} \Delta_k \bar{C}_{\sigma_k} \right) \bar{x}_k, \qquad (3.28)$$

where $\bar{A}_{\sigma, l} \in \mathbb{R}^{n \times n}$, $\bar{B} \in \mathbb{R}^{n \times q}$, $\bar{C}_\sigma \in \mathbb{R}^{q \times n}$, for $\sigma \in \{1, \ldots, N\}$ and $l \in \{1, \ldots, L\}$, with L the number of vertices of the polytope. The vector $\alpha_k = [\alpha_k^1 \ \ldots \ \alpha_k^L]^\top \in \mathcal{A}$, $k \in \mathbb{N}$, is time varying with

$$\mathcal{A} = \left\{ \alpha \in \mathbb{R}^L \,\middle|\, \sum_{l=1}^{L} \alpha^l = 1, \ \alpha^l \geqslant 0 \ \forall \ l \in \{1, \ldots, L\} \right\} \qquad (3.29)$$

and $\Delta_k \in \boldsymbol{\Delta}$, $k \in \mathbb{N}$, where

$$\boldsymbol{\Delta} = \left\{ \operatorname{diag}(\Delta^1, \ldots, \Delta^Q) \in \mathbb{R}^{q \times q} \,\middle|\, \Delta^i \in \mathbb{R}^{q_i \times q_i}, \|\Delta^i\| \leqslant 1 \ \forall \ i \in \{1, \ldots, Q\} \right\}. \qquad (3.30)$$

The system (3.28) is constructed to be an overapproximation of (3.12), in the sense that for all $\sigma \in \{1, \ldots, N\}$, it holds that

$$\left\{ \tilde{A}_{\sigma, h, \tau} \mid (h, \tau) \in \Theta \right\} \subseteq \left\{ \sum_{l=1}^{L} \alpha^l \bar{A}_{\sigma, l} + \bar{B} \Delta \bar{C}_\sigma \mid \alpha \in \mathcal{A}, \Delta \in \boldsymbol{\Delta} \right\}. \qquad (3.31)$$

The approach presented in Chapter 2, based on (3.31), is not suitable in the context here, as this would remove all information present in the probability distribution of (h, τ). We therefore propose a new procedure that also preserves the probabilistic information contained in the probability distribution. Therefore, we propose to partition Θ into triangles $\mathcal{S}_m$, $m \in \{1, \ldots, M\}$, and make overapproximations of $\tilde{A}_{\sigma_k, h_k, \tau_k}$ for each individual triangle $\mathcal{S}_m$. This allows us to assign a probability $\bar{p}_m = \Pr\big((h, \tau) \in \mathcal{S}_m\big)$ to each triangle and adopt this information in the subsequent stability analysis. Roughly speaking, the (possibly) continuous probability distribution is approximated by a discrete probability distribution that assigns probabilities to (h, τ) to each triangle $\mathcal{S}_m$ in the partitioning of Θ. Since it is in general not possible to achieve a partitioning satisfying $\cup_{m=1}^{M} \mathcal{S}_m = \Theta$, (as we use a *finite* number of bounded triangles $\mathcal{S}_m$, $m \in \{1, \ldots, M\}$, and Θ may be an unbounded set), we introduce

a parameter $h^\star$ and partition only the set $\{(h, \tau) \in \Theta \mid h \leqslant h^\star\}$ into triangles $\mathcal{S}_m$, i.e., $\cup_{m=1}^M \mathcal{S}_m := \{(h, \tau) \in \Theta \mid h \leqslant h^\star\}$. This will result in a 'tail' of the probability distribution $\mathcal{Q} := \Theta \setminus \cup_{m=1}^M \mathcal{S}_m$ that is not partitioned into triangles. We will, however, propose a stability analysis method that incorporates this tail $\mathcal{Q}$, by exploiting that this parameter $h^\star$ can be chosen a sufficiently large. Now inside each triangle $\mathcal{S}_m$, the matrix set $\{\tilde{A}_{\sigma,h,\tau} \mid (h, \tau) \in \mathcal{S}_m\}$ is overapproximated, according to the procedure presented in [40], in the sense that for each $\mathcal{S}_m$, $m \in \{1, \ldots, M\}$, and for all $\sigma \in \{1, \ldots, N\}$ it holds that

$$\left\{\tilde{A}_{\sigma,h,\tau} \mid (h, \tau) \in \mathcal{S}_m\right\} \subseteq \left\{\textstyle\sum_{l=1}^L \alpha^l \bar{A}_{\sigma,m,l} + \bar{B}_m \Delta \bar{C}_\sigma \mid \alpha \in \mathcal{A}, \Delta \in \mathbf{\Delta}\right\}, \quad (3.32)$$

where now $\bar{A}_{\sigma,m,l} \in \mathbb{R}^{n \times n}$, $\bar{B}_m \in \mathbb{R}^{n \times q}$.

A specific feature of the approach presented in this chapter is that, similar to [40], the approximation can be made arbitrarily tight, by selecting a sufficiently large $h^\star > 0$, and by making every triangle $\mathcal{S}_m$ sufficiently small. To properly explain what we mean by triangles that are 'sufficiently small', let us introduce the notion of diameter of a set $\mathcal{S} \subseteq \mathbb{R}^2$ as

$$\operatorname{diam}\mathcal{S} := \sup_{v,w \in \mathcal{S}} \|v - w\|. \quad (3.33)$$

By choosing $h^\star > 0$ sufficiently large, and by choosing the diameter of the triangles $\mathcal{S}_m$, $m \in \{1, \ldots, M\}$, smaller than ε, i.e., by choosing $\operatorname{diam}\mathcal{S}_m \leqslant \varepsilon$, for some sufficiently (small) $\varepsilon > 0$, we can show that the existence of a Lyapunov function of a particular type for (3.12) is equivalent to the existence of a Lyapunov function of the same type for (3.28) for all $\sigma \in \{1, \ldots, N\}$ and all $m \in \{1, \ldots, M\}$. Therefore, we can let the introduced conservatism in the overapproximation vanish by making the partitioning sufficiently refined. We will formalise this result in Section 3.5.

Let us now formalise the procedure to obtain the convex overapproximation as outlined above. For a formal proof that the following procedure indeed results in an overapproximation, in the sense that (3.32) holds, the reader is referred to Chapter 3.

Procedure 3.3.1.

- *Given constants $h^\star > 0$ and $\varepsilon > 0$, choose M triangles $\mathcal{S}_m \subseteq \Theta$, $m \in \{1, \ldots, M\}$, satisfying*

$$\mathcal{S}_m = \operatorname{co}\{(\tilde{h}_{m,1}, \tilde{\tau}_{m,1}), (\tilde{h}_{m,2}, \tilde{\tau}_{m,2}), (\tilde{h}_{m,3}, \tilde{\tau}_{m,3})\}, \quad (3.34)$$

  where $(\tilde{h}_{m,l}, \tilde{\tau}_{m,l})$, $l \in \{1, 2, 3\}$ denote the vertices of the triangle $\mathcal{S}_m$, such that

  1. $\Pr\left((h, \tau) \in (\mathcal{S}_p \cap \mathcal{S}_m)\right) = 0$, for all $m, p \in \{1, \ldots, M\}$ and $p \neq m$,

2. $\text{diam}\mathcal{S}_m \leqslant \varepsilon$, *for all* $m \in \{1, \ldots, M\}$,

3. $\cup_{m=1}^{M} \mathcal{S}_m := \{(h, \tau) \in \Theta \mid h \leqslant h^\star\}$.

- *Compute* $\bar{p}_m = \text{Pr}\big((h, \tau) \in \mathcal{S}_m\big)$ *for all* $m \in \{1, \ldots, M\}$.

- *Define*

$$\bar{A}_{\sigma,m,l} := \tilde{A}_{\sigma,\tilde{h}_{m,l},\tilde{\tau}_{m,l}}, \tag{3.35}$$

for all $\sigma \in \{1, \ldots, N\}$ *and* $(\tilde{h}_{m,l}, \tilde{\tau}_{m,l})$, $m \in \{1, \ldots, M\}$, $l \in \{1, 2, 3\}$.

- *To bound the approximation error, decompose the matrix* $\bar{\Lambda}$*, as in* (3.27)*, into its real Jordan form [71], i.e.,* $\bar{\Lambda} := T\Lambda T^{-1}$*, where* T *is an invertible matrix and*

$$\Lambda = \text{diag}(\Lambda_1, \ldots, \Lambda_K) \tag{3.36}$$

with $\Lambda_i \in \mathbb{R}^{n_i \times n_i}$*,* $i \in \{1, \ldots, K\}$*, the* i*-th real Jordan block of* $\bar{\Lambda}$*. Now compute for each real Jordan block* Λ_i*,* $i \in \{1, \ldots, K\}$*, the worst case approximation error, i.e.*

$$\delta_{i,m}^{A} = \max_{\alpha \in \mathcal{A}} \left\| e^{\Lambda_i \sum_{l_1=1}^{3} \alpha^{l_1} \tilde{h}_{m,l_1}} - \sum_{l_2=1}^{3} \alpha^{l_2} e^{\Lambda_i \tilde{h}_{m,l_2}} \right\|, \tag{3.37a}$$

$$\delta_{i,m}^{E_h} = \max_{\alpha \in \mathcal{A}} \left\| \sum_{l_1=1}^{3} \alpha^{l_1} \int_{\tilde{h}_{m,l_1}}^{\sum_{l_2=1}^{3} \alpha^{l_2} \tilde{h}_{m,l_2}} e^{\Lambda_i s} ds \right\|, \tag{3.37b}$$

$$\delta_{i,m}^{E_{h-\tau}} = \max_{\alpha \in \mathcal{A}} \left\| \sum_{l_1=1}^{3} \alpha^{l_1} \int_{\tilde{h}_{m,l_1} - \tilde{\tau}_{m,l_1}}^{\sum_{l_2=1}^{3} \alpha^{l_2}(\tilde{h}_{m,l_2} - \tilde{\tau}_{m,l_2})} e^{\Lambda_i s} ds \right\|. \tag{3.37c}$$

For a detailed explanation of the origin of the approximation error bounds, the reader is referred to Chapter 2.

- *Finally, define*

$$\bar{C}_\sigma := \begin{bmatrix} T^{-1} & 0 \\ T^{-1}BDC & T^{-1}BD \\ 0 & -T^{-1}B\Gamma_\sigma \end{bmatrix} \tag{3.38}$$

and

$$\bar{B}_m := \begin{bmatrix} T & T & T \\ -CT & -CT & -CT \end{bmatrix} \cdot \text{diag}(\delta_{1,m}^{A} I_1, \ldots, \delta_{K,m}^{A} I_K,$$
$$\delta_{1,m}^{E_h} I_1, \ldots, \delta_{K,m}^{E_h} I_K, \delta_{1,m}^{E_{h-\tau}} I_1, \ldots, \delta_{K,m}^{E_{h-\tau}} I_K), \tag{3.39}$$

with I_i *the identity matrix of size* n_i*, complying with the* i*-th real Jordan block. The additive uncertainty set* $\boldsymbol{\Delta} \subseteq \mathbb{R}^{3(n_p+n_c) \times 3(n_p+n_c)}$ *is now given by*

$$\boldsymbol{\Delta} = \big\{\text{diag}(\Delta^1, \ldots, \Delta^{3K}) \mid \Delta^{i+jK} \in \mathbb{R}^{n_i \times n_i}, \|\Delta^{i+jK}\| \leqslant 1$$
$$\forall\, i \in \{1, \ldots, K\}, j \in \{0, 1, 2\}\big\}. \tag{3.40}$$

Remark 3.3.2. *In the special case that there exists an h_{nom} or a τ_{nom} such that $p(h, \tau) = 0$, either for all $h \neq h_{nom}$ or for all $\tau \neq \tau_{nom}$, i.e., the transmission interval or delay is constant, Procedure 3.3.1 can be modified slightly. This is because we proposed to form triangles $\mathcal{S}_m \subseteq \Theta \subset \mathbb{R}^2$, $m \in \{1, \ldots, M\}$, whereas Θ can be considered a line segment in this case. Instead of triangles, we propose to form line-segments $\mathcal{S}_m \subseteq \Theta$, $m \in \{1, \ldots, M\}$, in this case such that for each $\mathcal{S}_m$, $m \in \{1, \ldots, M\}$, it holds that*

$$\mathcal{S}_m = \mathrm{co}\{(\tilde{h}_{m,1}, \tilde{\tau}_{m,1}), (\tilde{h}_{m,2}, \tilde{\tau}_{m,2})\}, \tag{3.41}$$

where $(\tilde{h}_{m,l}, \tilde{\tau}_{m,l})$, $l \in \{1, 2\}$, now denote the vertices of the line segment $\mathcal{S}_m$. All other properties of $\mathcal{S}_m$, $m \in \{1, \ldots, M\}$ still hold and the remainder of the procedure can be applied mutatis mutandis.

In this chapter, we will adopt the procedure to obtain an overapproximation of the NCS model from Chapter 2, resulting in the procedure presented above. All the theory presented in the next section also applies if the overapproximation is obtained by other techniques, see, e.g., [63] for an overview and a thorough comparison of all the existing overapproximation techniques. However, in Chapter 2, it was proven that the overapproximation adopted here can be made arbitrarily tight and, therefore, does not introduce any conservatism.

3.4   Stability of NCSs with Stochastic Uncertainty

In Section 3.2, we discussed the NCS model and, in Section 3.3, we proposed a technique to overapproximate it by a switched polytopic system with a norm-bounded uncertainty. In this section, we will use the overapproximation derived in the previous section to develop conditions to verify UGMSES of the NCS model (3.12) with switching sequences satisfying (3.18), (3.21) or (3.23) and the transmission intervals and delays are given by an sequence of random variables satisfying Assumption 3.2.1 and 3.2.5.

We will start with so-called quadratic protocols and analyse stability using the ideas in [47], in which only switched linear systems without any form of uncertainty are considered. Then, we will also show how we can analyse stability for periodic protocols. Finally, the stability analysis for the stochastic protocols is presented using ideas from [32], in which stability analysis for discrete-time Markov jump linear systems is analysed, again without any form of uncertainty. In all cases, we need two intermediate results.

Lemma 3.4.1. *Let Assumption 3.2.1 hold. The system* (3.12) *with switching functions satisfying* (3.18), (3.21) *or* (3.23) *is UGMSES if there exist a*

Lyapunov function $V : \mathbb{R}^n \times \mathbb{N} \to \mathbb{R}_+$ *and scalars* $b_1, b_2, b_3 > 0$ *satisfying*[2]

$$b_1 \|\bar{x}\|^2 \leqslant V(\bar{x}, k) \leqslant b_2 \|\bar{x}\|^2 \tag{3.42a}$$

$$\mathbb{E}[V(\tilde{A}_{\sigma_k, h_k, \tau_k} \bar{x}, k+1)] - V(\bar{x}, k) \leqslant -b_3 \|\bar{x}\|^2 \tag{3.42b}$$

for all $\bar{x} \in \mathbb{R}^n$ *and all* $k \in \mathbb{N}$.

Proof. The proof is given in Appendix A.2. $\qquad\square$

Lemma 3.4.2. *Let Assumptions 3.2.1 and 3.2.5 hold, and let a symmetric matrix* $\tilde{P}$ *and a set* $\mathcal{Q} \subseteq \Theta$ *be given. It holds for each* $i \in \{1, \ldots, N\}$ *that*

$$\mathbb{E}\big(\tilde{A}_{i,h,\tau}^{\top} \tilde{P} \tilde{A}_{i,h,\tau} \mathbf{1}_{\mathcal{Q}}(h, \tau)\big) \preceq \lambda_{\max}(\tilde{P}) \upsilon_i \mathbb{E}\big(\rho(h) \mathbf{1}_{\mathcal{Q}}(h, \tau)\big) I, \tag{3.43}$$

in which

$$\upsilon_i = (\|\tilde{A}_{i,0,0}\| + \|\tilde{B}\| \, \|\tilde{C}_i\|)^2 \tag{3.44}$$

with $\tilde{A}_{i,h,\tau}$, *as defined in (3.12),*

$$\tilde{B} := \begin{bmatrix} I & I & I \\ -C & -C & -C \end{bmatrix}, \qquad \tilde{C}_i := \begin{bmatrix} I & 0 \\ BDC & BD \\ 0 & B\Gamma_i \end{bmatrix}, \tag{3.45}$$

and

$$\rho(h) = \max\{1, \big(e^{\frac{1}{2}\lambda_{\max}(\bar{\Lambda}^{\top} + \bar{\Lambda})h} + 1\big)^2, \int_0^h e^{\lambda_{\max}(\bar{\Lambda}^{\top} + \bar{\Lambda})s} \mathrm{d}s\}. \tag{3.46}$$

Proof. The proof is given in Appendix A.2. $\qquad\square$

3.4.1 Quadratic Protocols

In this section, we analyse the class of quadratic protocols given by (3.18) of which the TOD protocol is a special case. To analyse the stability of (3.12) having this switching function, we introduce the non-quadratic Lyapunov function

$$V(\bar{x}_k) = \min_{i=1,\ldots,N} \bar{x}_k^{\top} P_i \bar{x}_k = \min_{\nu \in \mathcal{N}} \bar{x}_k^{\top} \sum_{i=1}^{N} \nu_i P_i \bar{x}_k, \tag{3.47}$$

where

$$\mathcal{N} := \Big\{ \nu \in \mathbb{R}^N \Big| \sum_{i=1}^{N} \nu_i = 1, \nu_i \geqslant 0 \ \forall \ i \in \{1, \ldots, N\} \Big\}. \tag{3.48}$$

---

[2]Note that for quadratic and periodic protocols, the expected value is taken with respect to h_k and τ_k. For stochastic protocols, however, the expected value is taken with respect to h_k, τ_k and σ_{k+1}, as the Lyapunov function V on time $k+1$, depends on σ_{k+1}, which is a random variable, see (3.23).

Furthermore, we introduce the class $\mathcal{M}$ of so-called Metzler matrices $\Pi = \{\pi_{ji}\}$, $i, j \in \{1, \ldots, N\}$, given by

$$\mathcal{M} := \Big\{ \Pi \in \mathbb{R}^{N \times N} \,\Big|\, \sum_{j=1}^{N} \pi_{ji} = 1 \,\forall\, i \in \{1, \ldots, N\}, \pi_{ji} \geqslant 0 \,\forall\, i, j \in \{1, \ldots, N\} \Big\},$$

(3.49)

and the set of matrices given by

$$R \in \mathcal{R} = \big\{ \text{diag}(r_1 I_1, \ldots, r_K I_K, r_{K+1} I_1, \ldots, r_{2K} I_K,$$
$$r_{2K+1} I_1, \ldots, r_{3K} I_K) \in \mathbb{R}^{3(n_p + n_c) \times 3(n_p + n_c)} \mid r_i > 0 \big\}, \quad (3.50)$$

where I_i is an identity matrix of size n_i.

The main result of this section is presented in the following theorem, in which conditions for UGMSES for the NCS system with a quadratic protocol are given.

Theorem 3.4.3. *Let Assumptions 3.2.1 and 3.2.5 hold and let the system (3.12) with a switching function satisfying (3.18), a probability distribution for (h, τ) and positive definite matrices P_i as in (3.18) be given. Suppose there exist a convex overapproximation obtained by Procedure 3.3.1, a matrix $\Pi = \{\pi_{ji}\} \in \mathcal{M}$, positive scalars μ_i satisfying $\sum_{j=1}^{N} \pi_{ji} P_j \preceq \mu_i I$, matrices $U_{i,m}$, and matrices $R_{i,m,l} \in \mathcal{R}$, for $i \in \{1, \ldots, N\}$, $m \in \{1, \ldots, M\}$, and $l \in \{1, \ldots, L\}$, satisfying the LMIs*

$$\begin{bmatrix} U_{i,m} & 0 & \sqrt{\bar{p}_m} \bar{A}_{i,m,l}^{\top} \sum_{j=1}^{N} \pi_{ji} P_j & C_i^{\top} R_{i,m,l} \\ \star & R_{i,m,l} & \sqrt{\bar{p}_m} \bar{B}_m^{\top} \sum_{j=1}^{N} \pi_{ji} P_j & 0 \\ \star & \star & \sum_{j=1}^{N} \pi_{ji} P_j & 0 \\ \star & \star & \star & R_{i,m,l} \end{bmatrix} \succ 0, \qquad (3.51)$$

for all $i \in \{1, \ldots, N\}$, $m \in \{1, \ldots, M\}$, $l \in \{1, \ldots, L\}$, in which $\bar{p}_m = \Pr\big((h, \tau) \in \mathcal{S}_m\big)$, and satisfying

$$P_i - \sum_{m=1}^{M} U_{i,m} - \mu_i \upsilon_i \mathbb{E}\big(\rho(h) \mathbf{1}_{\mathcal{Q}}(h, \tau)\big) I \succeq 0, \qquad (3.52)$$

for all $i \in \{1, \ldots, N\}$, in which $\mathcal{Q} := \Theta \backslash (\cup_{m=1}^{M} \mathcal{S}_m)$, and υ_i and $\rho(h)$ are defined as in (3.44) and (3.46), respectively. Then, the switching law (3.18) renders the system (3.12) UGMSES. Consequently, the continuous-time NCS given by (3.1), (3.2b), (3.3), and (3.8) is also UGMSES if the switching law (3.18) is employed as the protocol.

Proof. The proof is given in Appendix A.2. $\qquad\qquad\square$

We will briefly comment on Theorem 3.4.3. Firstly, the stability of (3.12) is guaranteed for h_k and τ_k, $k \in \mathbb{N}$, satisfying a continuous probability distribution, because the probability distribution is 'approximated' by assigning $\bar{p}_m := \Pr\big((h,\tau) \in \mathcal{S}_m\big)$ to each polytope $\mathcal{S}_m$, $m \in \{1,\dots,M\}$. Secondly, in case the $h^\star$ can be chosen such that $\Pr\big((h,\tau) \in \mathcal{Q}\big) = 0$, where $\mathcal{Q} := \Theta \backslash (\cup_{m=1}^{M} \mathcal{S}_m)$, the conditions in (3.52) simplify since $\mathbb{E}\big(\rho(h)\mathbf{1}_{\mathcal{Q}}(h,\tau)\big) = 0$. This is possible, if there exists an upper-bound on the transmission intervals. Finally, for the TOD protocol the matrices P_i still contain a free variable $\bar{P}$. This freedom $\bar{P}$ in modelling the TOD protocol can be exploited as the conditions in (3.51) are still LMIs in $\bar{P}$ as well. This can be shown by applying the ideas of Corollary 2.4.3 of Chapter 2.

3.4.2 Periodic protocols

We will now analyse another class of network protocols, namely the periodic protocols, with the RR protocol as a special case. Hence, we need to analyse stability of the system (3.28) with a switching sequence satisfying (3.21). This system is essentially a $\tilde{N}$-periodic uncertain system. For this system, we introduce positive definite matrices P_i, $i \in \{1,\dots,N\}$, and a time-dependent periodic Lyapunov function given by

$$V(\bar{x}_k, k) = \bar{x}_k^\top P_{k \bmod \tilde{N}} \, \bar{x}_k, \tag{3.53}$$

where $k \bmod \tilde{N}$ denotes k modulo $\tilde{N}$, which is the remainder of the division of k by $\tilde{N}$.

Theorem 3.4.4. *Let Assumptions 3.2.1 and 3.2.5 hold and let the system (3.12) with a switching function satisfying (3.21) and a probability distribution for (h, τ) be given. Suppose there exist a convex overapproximation obtained by Procedure 3.3.1, positive definite matrices P_i, positive scalar μ_i, satisfying $P_i \preceq \mu_i I$, matrices $U_{i,m}$, and matrices $R_{i,m,l} \in \mathcal{R}$, $i \in \{1,\dots,\tilde{N}\}$, $m \in \{1,\dots,M\}$, and $l \in \{1,\dots,L\}$, satisfying the LMIs*

$$\begin{bmatrix} U_{i,m} & 0 & \sqrt{\bar{p}_m} \bar{A}_{\sigma_i,m,l}^\top P_{i+1} & C_{\sigma_i}^\top R_{i,m,l} \\ \star & R_{i,m,l} & \sqrt{\bar{p}_m} \bar{B}_m^\top P_{i+1} & 0 \\ \star & \star & P_{i+1} & 0 \\ \star & \star & \star & R_{i,m,l} \end{bmatrix} \succ 0, \tag{3.54}$$

for all $i \in \{1,\dots,\tilde{N}\}$, $m \in \{1,\dots,M\}$, $l \in \{1,\dots,L\}$, where $P_{\tilde{N}+1} := P_1$ and $\bar{p}_m = \Pr\big((h,\tau) \in \mathcal{S}_m\big)$, and satisfying

$$P_i - \sum_{m=1}^{M} U_{i,m} - \mu_{i+1} \upsilon_i \mathbb{E}\big(\rho(h)\mathbf{1}_{\mathcal{Q}}(h,\tau)\big) I \succeq 0, \tag{3.55}$$

for all $i \in \{1, \ldots, \tilde{N}\}$, in which $\mathcal{Q} := \Theta \backslash (\cup_{m=1}^{M} \mathcal{S}_m)$, $\mu_{N+1} := \mu_1$, and υ_i and $\rho(h)$ are defined as in (3.44) and (3.46), respectively. Then, the switching law (3.21) renders the system (3.12) UGMSES. Consequently, the continuous-time NCS given by (3.1), (3.2b), (3.3), and (3.8) is also UGMSES if the switching law satisfying (3.21) is employed as the protocol.

Proof. The proof follows the same lines of reasoning as the proof of Theorem 3.4.3 and is therefore omitted. $\qquad \square$

3.4.3   Stochastic Protocols

Finally, we will analyse stability for the stochastic protocol. Hence, we need to analyse stability of the system (3.28) with a switching sequence satisfying (3.23), which can be done by introducing positive definite matrices P_i, $i \in \{1, \ldots, N\}$, and a node-dependent Lyapunov function of the form

$$V(\bar{x}_k, k) = \bar{x}_k^{\top} P_{\sigma_k} \bar{x}_k. \tag{3.56}$$

Theorem 3.4.5. *Let Assumptions 3.2.1 and 3.2.5 hold and let the system (3.12) with a switching function satisfying (3.23) and a probability distribution for (h, τ) be given. Suppose there exist a convex overapproximation obtained by Procedure 3.3.1, positive definite matrices P_i, positive scalars μ_i satisfying $\sum_{j=1}^{N} \pi_{ji} P_j \preceq \mu_i I$, matrices $U_{i,m}$, and matrices $R_{i,m,l} \in \mathcal{R}$, $i \in \{1, \ldots, N\}$, $m \in \{1, \ldots, M\}$, and $l \in \{1, \ldots, L\}$, satisfying (3.51), for all $i \in \{1, \ldots, N\}$, $m \in \{1, \ldots, M\}$, $l \in \{1, \ldots, L\}$, in which $\bar{p}_m = \Pr\big((h, \tau) \in \mathcal{S}_m\big)$, and satisfying (3.52), for all $i \in \{1, \ldots, N\}$, in which $\mathcal{Q} := \Theta \backslash (\cup_{m=1}^{M} \mathcal{S}_m)$, and υ_i and $\rho(h)$ are defined as in (3.44) and (3.46), respectively. Then, the switching law (3.23) renders the system (3.12) UGMSES. Consequently, the NCS given by (3.1), (3.2b), (3.3), and (3.8) is also UGMSES if the switching law (3.23) is employed as the protocol.*

Proof. The proof follows the same lines of reasoning as the proof of Theorem 3.4.3 and is therefore omitted. $\qquad \square$

As was also observed in [47] for switched linear systems, the conditions of Theorem 3.4.3 and Theorem 3.4.5 are similar, with the only difference that in Theorem 3.4.5 the scalars π_{ij}, $i, j \in \{1, \ldots, N\}$ are given by the stochastic protocol, see (3.23), whereas in Theorem 3.4.3 the matrices P_i, $i \in \{1, \ldots, N\}$, are given by the quadratic protocol.

3.5   Nonconservatism of the Stability Analysis

Given the results of the previous sections, it is now natural to ask if and how conservative the presented methodology is. The answer is given by the following result, showing that if the original system (3.12) (without any overapproximation), with protocol satisfying (3.18), (3.21) or (3.23), is mean-square

stable in the sense that a Lyapunov function exists, given by (3.47), (3.53), or (3.56), respectively, the presented procedure based on the overapproximation will guarantee mean-square stability and will find a respective Lyapunov function, given a sufficiently large $h^\star > 0$, and a sufficiently small $\varepsilon > 0$. Therefore, making a convex overapproximation, according to Procedure 3.3.1, introduces no conservatism in the stability analysis (given a certain class of Lyapunov functions) presented in the previous section.

In the following theorem, we will show the result for the NCS model (3.12) with protocol (3.18). Similar results hold for the NCS model (3.12) with protocol (3.21) and protocol (3.23).

Theorem 3.5.1. *Suppose system* (3.12)*, with protocol* (3.18)*, has a Lyapunov function of the form of* (3.47)*, i.e., there exist a matrix* $\Pi = \{\pi_{ji}\} \in \mathcal{M}$ *and positive definite matrices* P_i, $i \in \{1, \dots, N\}$*, such that*

$$\mathbb{E}\big(\tilde{A}_{i,h,\tau}^\top \sum_{j=1}^{N} \pi_{ji} P_j \tilde{A}_{i,h,\tau}\big) - P_i \preceq -\gamma I, \qquad (3.57)$$

for all $i \in \{1, \dots, N\}$*, and some* $\gamma > 0$*. Then, there exists an* $h_0^\star > 0$ *such that for any* $h^\star > h_0^\star$ *there is an* ε_0 *(depending on* $h_0^\star$*) such that for any convex overapproximation obtained using Procedure 3.3.1 with constants* $h^\star$ *and* ε*, where* $0 < \varepsilon < \varepsilon_0$*, the conditions of Theorem 3.4.3 hold.*

Proof. The proof is given in Appendix A.2. □

This result states that the convex overapproximation does not introduce conservatism when analysing stability using mode-dependent quadratic Lyapunov functions, provided that $h^\star$ (capturing the tail of the probability distribution) is sufficiently large, and the triangles $\mathcal{S}_m$, $m \in \{1, \dots, M\}$, are sufficiently small.

3.6 Illustrative Example

In this section, we illustrate the presented theory using a well-known benchmark example in the NCS literature [5, 40, 62, 124, 134], consisting of a linearised model of a batch reactor. The details of the linearised model of the batch reactor model and the controller can be found in the aforementioned references.

In [5, 40, 62, 124, 134], it was assumed that the controller is given in *continuous time* and it is directly connected to the actuator, i.e., only the two outputs are transmitted via the network. We will consider here the TOD protocol and assume, for simplicity, that delays are absent, i.e., $\Pr\big((h, \tau) \in \Theta\big) = 1$, where $\Theta = \{(h, \tau) \in \mathbb{R}^2 \,|\, h > 0, \tau = 0\}$. Furthermore, we let $\Pr\big((h, \tau) \in \mathcal{S}\big) = \int_{\hat{\mathcal{S}}} p(h)\mathrm{d}h$, for some $\mathcal{S} \subseteq \Theta$, where $\hat{\mathcal{S}} = \{h \in \mathbb{R} \,|\, (h, 0) \in \mathcal{S}\}$ and $p(h)$ denotes

a marginal probability density function (mpdf). In this example, we consider two different mpdf for the transmission intervals, namely the uniform mpdf

$$p(h) = \begin{cases} \frac{1}{c_2 - c_1} & \text{for } c_1 \leqslant h \leqslant c_2 \\ 0 & \text{elsewhere} \end{cases} \tag{3.58}$$

with $c_1 = 10^{-5}$ and $c_2 = 0.11$ and the Gamma mpdf

$$p(h) = \begin{cases} \frac{1}{(c_3 - 1)! \, (c_4)^{c_3}} h^{c_3 - 1} e^{-\frac{h}{c_4}} & \text{for } h > 0 \\ 0 & \text{elsewhere} \end{cases} \tag{3.59}$$

with $c_3 = 10$ and $c_4 = 0.006$. The resulting mpdfs are shown in Fig. 3.3.

In order to assess stability, we first define our NCS model as in Section 3.2.2.C. This model appropriately describes the situation as discussed in this example, where only the plant outputs y are transmitted over the network and the controller outputs u are sent continuously via a nonnetworked connection. We then derive the uncertain polytopic system (3.28) and $\bar{p}_m$, using Procedure 3.3.1. For the uniform distribution, we choose $h^\star = 0.11$ and $\varepsilon = \frac{0.11}{80}$, yielding $\mathcal{S}_m = [(\frac{0.11}{80}(m-1), 0), (\frac{0.11}{80}m, 0)]$, $m \in \{1, \ldots, 80\}$, and for the Gamma distribution, we choose $h^\star = 0.25$ and $\varepsilon = \frac{0.25}{30}$, yielding $\mathcal{S}_m = [(\frac{0.25}{30}(m-1), 0), (\frac{0.25}{30}m, 0)]$, $m \in \{1, \ldots, 30\}$. The values for the parameters $h^\star$ and ε are chosen such that, increasing $h^\star$ and decreasing ε does not significantly change the results in this example. We can now derive the uncertain polytopic system (3.28), satisfying (3.32). To obtain $\bar{A}_{i,l,m}$, $\bar{B}_m$, and $\bar{C}_i$, we use the overapproximation technique presented in [40], in which we use two grid points for each $\mathcal{S}_m$. In Fig. 3.3, we also illustrate for the Gamma distribution the partitioning of h in polytopes $\mathcal{S}_m$ and the resulting (scaled) $\bar{p}_m$. We now check the matrix inequalities of Theorem 3.4.3, using the structure of the P_i-matrices as in (3.19). Using this procedure we obtain a feasible solution of LMIs of Theorem 3.4.3, on the basis of which we conclude that the TOD protocol stabilises the NCS when the transmission intervals are given by an iid sequence of random variables satisfying the aforementioned probability distributions. The computation time required to compute the overapproximation and to find feasible solutions to the LMIs on a standard desktop computer[3] is 180 seconds for the uniform distribution and 36 seconds for the Gamma distribution.

Chapter 2, we obtained a 'robust' range of allowable transmission intervals, i.e., $h_k \in [10^{-3}, 0.066]$, $k \in \mathbb{N}$, which includes all probability distributions for which it holds that $\Pr\big((h, \tau) \in \Theta\big) = 1$ where $\Theta := \{(h, \tau) \in \mathbb{R}^2 \,|\, 10^{-3} < h \leqslant 0.066, \tau = 0\}$. Therefore, we can conclude that incorporating probabilistic

---

[3]The authors have used a Windows PC running at 3GHz with 4GB RAM, and MATLAB 2007B and SEDUMI 1.3 for this numerical example. The number of LMIs that need to be verified is $2 \times 2 \times 80 + 2 + 2 = 324$ for the Uniform distrubution, and $2 \times 2 \times 30 + 2 + 2 = 124$ for the Gamma distribution.
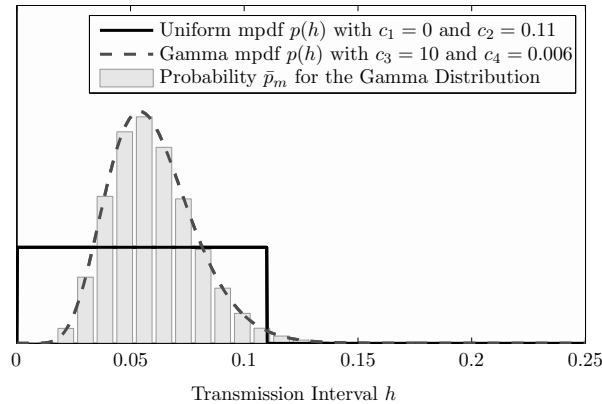
Figure 3.3: Illustration of the considered mpdfs, and the approximation of the Gamma distribution.

information on the distribution of the transmission intervals is very useful as it can be used to prove stability for situations not contained in the case that was studied in Chapter 2.

3.7   Conclusions

In this chapter, we studied networked control systems (NCSs) that are subject to communication constraints, time-varying transmission intervals and time-varying delays, and packet dropouts. In particular, we analysed the stability of the NCS when the transmission intervals and transmission delays are described by an independent and identically distributed sequence of *continuous* random variables, and the communication sequence is determined by a quadratic, periodic, or stochastic protocol. This analysis was based on a stochastically parameter-varying discrete-time switched linear system model of the NCS. We derived conditions for stability (in the mean-square sense) by adopting techniques for convex overapproximation, which are now used as a way to handle continuous probability distributions. This convex overapproximation technique was extended such that the probabilistic information as present in the probability distribution is preserved, and yields LMI-based conditions for stability. On a benchmark example, we showed that by incorporating probabilistic information on the transmission intervals and delays and packet dropouts, stability can now be guaranteed for situations not covered by earlier results in the literature.

Future work will focuss on studying the case where delays are not restricted to be smaller than the transmission interval, on the inclusion of quantisation effects of the sensor and actuator signals, and on co-design methods of the controller and the protocol.

Part II

Event-Triggered Control Systems

4

Output-Based Decentralised Event-Triggered Control with Guaranteed $\mathcal{L}_\infty$-gain[1]

Abstract – Most event-triggered controllers available nowadays are based on static state-feedback controllers. As in many control applications full state measurements are not available for feedback, it is the objective of this chapter to propose event-triggered dynamical output-based controllers. The fact that the controller is based on output feedback instead of state feedback does not allow for straightforward extensions of existing event-triggering mechanisms if a minimum time between two subsequent events has to be guaranteed. Furthermore, since sensor and actuator nodes can be physically distributed, centralised event-triggering mechanisms are often prohibitive and, therefore, we will propose a decentralised event-triggering mechanism. This event-triggering mechanism invokes transmission of the outputs in a node when the difference between the current values of the outputs in the node and their previously transmitted values becomes 'large' compared to the current values and an additional threshold. For such event-triggering mechanisms, we will study closed-loop stability and $\mathcal{L}_\infty$-performance and provide bounds on the minimum time between two subsequent events generated by each node, the so-called inter-event time of a node. This enables us to make tradeoffs between closed-loop performance on the one hand and communication load on the other hand, or even between the communication load of individual nodes. In addition, we will model the event-triggered control system using an impulsive system.As a result, we will

---

[1]This chapter is based on [37].

be able to guarantee stability and performance for improved event-triggered controllers with larger minimum inter-event times than existing results in the literature. We illustrate the developed theory using three numerical examples.

4.1 Introduction

In many control applications nowadays, the controller is implemented on a digital platform. In such an implementation, the control task consists of sampling the outputs of the plant and computing and implementing new actuator signals. Typically, the control task is executed periodically, since this allows the closed-loop system to be analysed and the controller to be designed using the well-developed theory on sampled-data systems, see, e.g., [8, 27]. Although periodic sampling is preferred from an analysis and design point of view, it is sometimes less preferable from a resource allocation point of view. Namely, executing the control task at times when no disturbances are acting on the system and the system is operating desirably is clearly a waste of computation resources. Moreover, in case the measured outputs and/or the actuator signals have to be transmitted over a shared (and possibly wireless) network, unnecessary utilisation of the network (or power consumption of the wireless radios) is introduced. To mitigate the unnecessary waste of communication and computation resources, an alternative to periodic control, namely, event-triggered control has been proposed, see [6, 9, 59, 64]. Event-triggered control is a control strategy in which the control task is executed after the occurrence of an external event, generated by some well-designed event-triggering mechanism, rather than the elapse of a certain period of time as in conventional periodic control. As experimental results show, see, e.g., [6, 9, 59, 64, 65, 83, 85, 111, 127], event-triggered control is capable of reducing the number of control task executions, while retaining a satisfactory closed-loop performance.

Although the advantages of ETC are well-motivated and practical applications show its potential, relatively few theoretical results exist that study ETC systems, see, e.g., [10, 44, 46, 60, 66, 81, 90, 94, 107, 126, 136]. In these references, several different event-triggering mechanisms and control strategies are proposed. For instance, in [10, 66], an impulsive control action is applied to the system that resets the state to the origin every time the state of the plant exceeds a certain threshold. The analysis is performed for first-order stochastic systems, as analysis of larger-dimensional systems is difficult, and it is shown that the variance of the state is smaller when compared to a sampled-data controller, while having approximately the same number of control updates. Another interesting approach to event-triggered control is presented in [44, 46, 90], in which the system is controlled in open loop, using an 'input generator' that uses a prediction of the plant states to produce a control signal. These predicted states are only corrected in case the true plant state deviates too much from its predicted value. Such a deviation can be caused by disturbances, [46, 90],

or by the fact that the plant model is incorrect [44].

A more basic 'emulation-based approach' is taken in [60, 81, 107, 126, 136]. By emulation-based, we mean that the controller is designed without considering the event-triggered nature of the control system, and, subsequently, an event-triggering mechanism is designed to ensure that the event-triggered control system is stable, has some guaranteed lower bound on the performance and some guaranteed upper bound on the number of events within a certain time interval. The differences between the work discussed in [60, 81, 107, 126, 136] lies in the fact that in [60, 136] the influence of unknown disturbances are studied, whereas in [81, 107, 126] only stabilisation is considered. Another difference is the condition that generates the events. In [60], events are generated in case the state of the plant is a larger than a certain threshold, in [126, 136] when the relative difference between the state of the plant and the previously sampled state violates a certain threshold, and in [81, 107] when the absolute difference between the state of the plant and the previously sampled state violates a certain threshold.

An important observation to be made about the aforecited works is that most of them consider state-feedback controllers, which assumes that all the plant states can be measured. To the best of the authors' knowledge, the only theoretical result on event-triggered control using dynamical output-based controllers is presented in [81]. However, an analysis of the minimum time between two subsequent events, the so-called inter-event time, is not available for [81] and, thereby, guarantees on the upper bound on the number of events cannot be made. Furthermore, extending the event-triggering mechanisms in [126, 136] to output-based controllers is not straightforward, since for these event-triggering mechanisms, no minimum inter-event time can be shown to exist, even though they have a guaranteed minimum inter-event time for state-feedback controllers. For any event-triggered control system to be useful, we need such a lower bound on the inter-event time, as our primary reason to make control systems event-triggered is to save computation and communication resources.

In this chapter, we analyse *stability and $\mathcal{L}_\infty$-performance* of event-triggered control systems for given *dynamical output-based controllers*. We consider the case where the sensors and actuators, which can be grouped into nodes, and controllers can be physically distributed. This causes a centralised event-triggering mechanism to be prohibitive. Namely, a centralised event-triggering mechanism determines when to transmit data based on (current) information from all the outputs of the plant and controller, which requires this information to be available for this centralised event-triggering mechanism at all times and without any delays. This means that node data has to be transmitted to this centralised event-triggering mechanism continuously, which is undesirable when the objective is to reduce utilisation of communication resources. To resolve this issue, we will propose a decentralised event-triggering mechanism, in which

events are triggered on the basis of local information only, and sharing of node data between different (physically distributed) parts of the control system is not needed. Inspired by [126], we propose an event-triggering mechanism that invokes transmission of the controller or the plant outputs of a node when the difference between the current values in the node and its previously transmitted values becomes 'large' compared to the current values and an additional threshold. This additional threshold ensures that each node has a nonzero minimum inter-event time, which allows us to guarantee a bound on the total number of transmissions. Interestingly, the event-triggering mechanism presented in this chapter can be seen as a unification of the event-triggering mechanisms proposed in [126, 136] and [81, 94, 107].

As a second contribution of this chapter, we propose to model the event-triggered control system as an impulsive system, see, e.g., [50, 55].Furthermore, we extend the framework presented in [126] towards output-feedback controllers and $\mathcal{L}_\infty$-performance, and we formally show that the impulsive systems framework provides stability guarantees for event-triggering mechanisms that result in larger minimum inter-event times than the extended results of [126]. These stability conditions will be based on linear matrix inequalities (LMIs), so that efficient verification is possible. We will provide three numerical examples to demonstrate various aspects of the developed theory. In particular, we will illustrate that the guaranteed lower bounds on the minimum inter-event times are indeed improved with respect to existing results in literature and that the inclusion of a nonzero threshold in the event-triggering mechanism is necessary to guarantee a positive minimum inter-event time for each node.

The remainder of this chapter is organised as follows. After introducing the necessary notational conventions, we introduce the model of the decentralised output-based event-triggered control system in Section 4.2. We analyse its stability and its $\mathcal{L}_\infty$-gain properties in Section 4.3, and in Section 4.4 we provide a way to compute the lower bound on the minimum inter-event time of each node. In Section 4.5, we extend the work of [126] towards output-based dynamical controllers and $\mathcal{L}_\infty$-performance, and present a theorem that states that the impulsive system formulation of the event-triggered control problem allows us to guarantee stability and performance for event-triggered controllers with at least the same minimum inter-event times as the results based on the reasoning of [126]. Finally, the presented theory is illustrated by numerical examples in Section 4.6 and we draw conclusions in Section 4.7. Appendix A.3 contains the proofs of the more technical lemmas and theorems.

4.1.1   Nomenclature

For a vector $x \in \mathbb{R}^n$, we denote by $\|x\| := \sqrt{x^\top x}$ its 2-norm, and by $x_{\mathcal{J}}$ the subvector formed by all components of x in the index set $\mathcal{J} \subseteq \{1, \ldots, n\}$.

For a symmetric matrix $A \in \mathbb{R}^{n \times n}$, $\lambda_{\max}(A)$ and $\lambda_{\min}(A)$ denote the max-

imum and minimum eigenvalue of A, respectively. For a matrix $A \in \mathbb{R}^{n \times m}$, we denote by $A^\top \in \mathbb{R}^{m \times n}$ the transposed of A, and by $\|A\| := \sqrt{\lambda_{\max}(A^\top A)}$ its induced 2-norm. Furthermore, by $A_{\mathcal{J}\bullet}$ and $A_{\bullet\mathcal{J}}$, we denote the submatrices formed by taking all the rows of A in the index set $\mathcal{J} \subseteq \{1, \ldots, n\}$, and by taking all the columns of A in the index set $\mathcal{J} \subseteq \{1, \ldots, m\}$, respectively. By $\mathrm{diag}(A_1, \ldots, A_N)$, we denote a block-diagonal matrix with the entries $A_1, \ldots, A_N$ on the diagonal, and for brevity we write symmetric matrices of the form $\begin{bmatrix} A & B \\ B^\top & C \end{bmatrix}$ as $\begin{bmatrix} A & \star \\ B^\top & C \end{bmatrix}$.

For a signal $w : \mathbb{R}_+ \to \mathbb{R}^n$, where $\mathbb{R}_+$ denotes the set of nonnegative real numbers, we denote by $\|w\|_{\mathcal{L}_p} = (\int_0^\infty \|w(t)\|^p \mathrm{d}t)^{1/p}$ its $\mathcal{L}_p$-norm for $p \in \mathbb{N}$, provided that the integral is finite, and by $\|w\|_{\mathcal{L}_\infty} = \mathrm{ess\,sup}_{t \in \mathbb{R}_+} \|w(t)\|$ its $\mathcal{L}_\infty$-norm. Furthermore, we define the set of signals with a finite $\mathcal{L}_p$-norm as $\mathcal{L}_p := \{w : \mathbb{R}_+ \to \mathbb{R}^n \mid \|w\|_{\mathcal{L}_p} < \infty\}$ for $p \in \mathbb{N} \cup \{\infty\}$. Finally, for a signal $w : \mathbb{R}_+ \to \mathbb{R}^n$ we denote the limit from above at time $t \in \mathbb{R}_+$ by $w^+(t) = \lim_{s \downarrow t} w(s)$, provided that it exists.

4.2 Event-Triggered Control

In this section, we present the event-triggered control problem and model the event-triggered control system as an impulsive system.

4.2.1 Problem Formulation

Let us consider a linear time-invariant (LTI) plant given by

$$\begin{cases} \frac{\mathrm{d}}{\mathrm{d}t} x_p = A_p x_p + B_p \hat{u} + B_w w, \\ \quad y = C_p x_p, \end{cases} \tag{4.1}$$

where $x_p \in \mathbb{R}^{n_p}$ denotes the state of the plant, $\hat{u} \in \mathbb{R}^{n_u}$ the input applied to the plant, $w \in \mathbb{R}^{n_w}$ an unknown disturbance and $y \in \mathbb{R}^{n_y}$ the output of the plant. The plant is controlled using a continuous-time LTI controller given by

$$\begin{cases} \frac{\mathrm{d}}{\mathrm{d}t} x_c = A_c x_c + B_c \hat{y}, \\ \quad u = C_c x_c, \end{cases} \tag{4.2}$$

where $x_c \in \mathbb{R}^{n_c}$ denotes the state of the controller, $\hat{y} \in \mathbb{R}^{n_y}$ the input of the controller, and $u \in \mathbb{R}^{n_u}$ the output of the controller. We assume that the controller is designed to render (4.1) and (4.2) with $y(t) = \hat{y}(t)$ and $u(t) = \hat{u}(t)$, for all $t \in \mathbb{R}_+$, asymptotically stable, i.e., an 'emulation-based' approach is taken.

In this chapter, however, we consider the case where the controller is implemented in a sampled-data fashion, which causes $y(t) \neq \hat{y}(t)$ and $u(t) \neq \hat{u}(t)$ for

almost all $t \in \mathbb{R}_+$. In particular, we study decentralised event-triggered control which means that the outputs of the plant and controller are grouped into N nodes and the outputs of node $i \in \{1, \ldots, N\}$ are only sent at the transmission instants $t_{k_i}^i$, $k_i \in \mathbb{N}$. Hence, at transmission instant $t_{k_i}^i$, node i transmits its respective entries in y and u, and the corresponding entries in $\hat{y}$ and $\hat{u}$ are updated accordingly, while the other entries in $\hat{y}$ and $\hat{u}$ remain the same. Such constrained data exchange can be expressed as

$$\hat{v}^+(t_{k_i}^i) = \Gamma_i v(t_{k_i}^i) + (I - \Gamma_i)\hat{v}(t_{k_i}^i), \tag{4.3}$$

in which $v = [y^\top \ u^\top]^\top$, $\hat{v} = [\hat{y}^\top \ \hat{u}^\top]^\top$, and

$$\Gamma_i = \mathrm{diag}(\gamma_i^1, \ldots, \gamma_i^{n_y + n_u}), \tag{4.4}$$

for all $i \in \{1, \ldots, N\}$. In between transmissions, we use a zero-order hold, i.e.,

$$\frac{\mathrm{d}}{\mathrm{d}t}\hat{v}(t) = 0, \quad \text{for all} \quad t \in \mathbb{R}_+ \backslash \left(\bigcup_{i=1}^N \{t_{k_i}^i \,|\, k_i \in \mathbb{N}\} \right). \tag{4.5}$$

In (4.4), the elements γ_i^j, with $i \in \{1, \ldots, N\}$ and $j \in \{1, \ldots, n_y\}$, are equal to 1 if plant output y_j is in node i and are 0 elsewhere, the elements $\gamma_i^{j+n_y}$, with $i \in \{1, \ldots, N\}$ and $j \in \{1, \ldots, n_u\}$, are equal to 1 if controller output u_j is in node i and are 0 elsewhere. We assume that for each $j \in \{1, \ldots, n_y + n_u\}$, it holds that $\sum_{i=1}^N \gamma_i^j > 0$, i.e., we assume that each sensor and actuator is at least in one node[2]. Furthermore, we assume that at time $t = 0$, it holds that $\hat{v}(0) = v(0)$. This can be accomplished by transmitting all sensor and actuator data at the time the system is deployed[3]. In the case that $t_{k_i}^i = t_{k_j}^j$ for some $k_i, k_j \in \mathbb{N}$ and some $i, j \in \{1, \ldots, N\}$, we assume that the updates as in (4.3) take place simultaneously or directly after one another in a negligible amount of time. Obviously, the order of updating is irrelevant as can be seen from (4.3). Moreover, note that performing multiple successive transmissions at one time instant has exactly the same effect as doing these updates simultaneously.

In a conventional sampled-data implementation, the transmission times are distributed equidistantly in time and are the same for each node, meaning that $t_{k_i+1}^i = t_{k_i}^i + h$, for all $k_i \in \mathbb{N}$ and all $i \in \{1, \ldots, N\}$, and for some constant transmission interval $h > 0$, and that $t_k^i = t_k^j$, for all $k \in \mathbb{N}$ and all $i, j \in \{1, \ldots, N\}$. In event-triggered control, however, these transmissions are orchestrated by a decentralised event-triggering mechanism, as is shown in Figure 4.1. We consider a decentralised event-triggering mechanism that invokes transmissions of node data when the difference between the current

---

[2]In case a sensor or actuator is not in any node, meaning that this sensor or actuator is, effectively, not part of the control loop, we simply remove the corresponding input or output from the plant and controller model.

[3]This assumption could be removed, but it would introduce additional technicalities later. For reasons of readability, we opted to work under this rather mild and natural assumption.
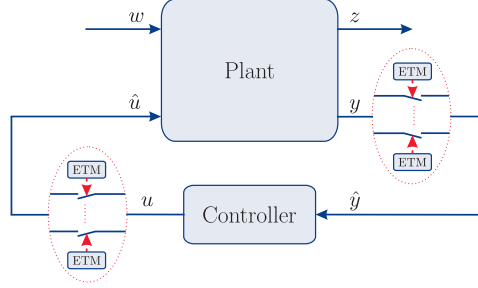
Figure 4.1: Event-triggered Control Schematic, indicating the event-triggering mechanisms (ETM).

values of outputs and their previously transmitted values becomes too large in an appropriate sense. In particular, the event-triggering mechanism proposed in this chapter, results in transmitting the outputs of the plant or the controller in node $i \in \{1, \ldots, N\}$ at times $t^i_{k_i}$, satisfying

$$t^i_{k_i+1} = \inf\{t > t^i_{k_i} \mid \|e_{\mathcal{J}_i}(t)\|^2 = \sigma_i\|v_{\mathcal{J}_i}(t)\|^2 + \varepsilon_i\}, \tag{4.6}$$

and $t^i_0 = 0$, for some $\sigma_i, \varepsilon_i \geqslant 0$. In these expressions, $e_{\mathcal{J}_i}$ and $v_{\mathcal{J}_i}$ denote the subvectors formed by taking the elements of the signals e and v, respectively, that are in the set $\mathcal{J}_i = \{j \in \{1, \ldots, n_y + n_u\} \mid \gamma^j_i = 1\}$, and

$$e(t) = \hat{v}(t) - v(t) \tag{4.7}$$

denotes the error induced by the event-triggered implementation of the controller at time $t \in \mathbb{R}_+$. Hence, the event-triggering mechanism (4.6), which is based on local information available at each node, is such that when for some $i \in \{1, \ldots, N\}$, it holds that $\|e_{\mathcal{J}_i}(t)\|^2 = \sigma_i\|v_{\mathcal{J}_i}(t)\|^2 + \varepsilon_i$, i.e., the norm of the error induced by the event-triggered implementation of the signals in node i becomes 'too large' for the first time, node i transmits its corresponding signal in $v(t)$ and, thus, the signal $\hat{v}(t)$ is updated according to (4.3). This implies that $e^+(t^i_{k_i}) = (I - \Gamma_i)e(t^i_{k_i})$ and thus $e^+_{\mathcal{J}_i}(t^i_{k_i}) = 0$. Using this update law, and the aforementioned assumption that $\hat{v}(0) = v(0)$, yielding $e(0) = 0$, we can observe that the error induced by the event-triggered control scheme satisfies

$$\|e_{\mathcal{J}_i}(t)\|^2 \leqslant \sigma_i\|v_{\mathcal{J}_i}(t)\|^2 + \varepsilon_i, \tag{4.8}$$

for all $t \in \mathbb{R}^+$ and all $i \in \{1, \ldots, N\}$.

The main objective of this chapter is to determine σ_i and ε_i for all $i \in \{1, \ldots, N\}$, such that the closed-loop event-triggered system is stable in an appropriate sense and a certain level of disturbance attenuation is guaranteed, while the number of transmissions of the outputs of the plant and the controller

is minimised. Note that for $\varepsilon_i = 0$, $i \in \{1, \ldots, N\}$, the event-triggering conditions in (4.6) can be seen as an extension of the event-triggering mechanism of [126] for output-based controllers, and for $\sigma_i = 0$, $i \in \{1, \ldots, N\}$, it is equivalent to the event-triggering mechanism of [81, 94, 107]. As such, the event-triggering mechanism in (4.6) unifies two earlier proposals, while additionally, output-based controllers and decentralised event triggering are considered.

Remark 4.2.1. *In this chapter, we assume that the controller is given in continuous time as in (4.2). To implement this controller on a digital platform, the following options can be considered: (i) the controller output is obtained by numerical integration, or (ii) the controller output is obtained using a discrete-time equivalent of the continuous-time controller, based on a sampling interval that is (sufficiently) smaller than the smallest inter-event time (see Theorem 4.4.1 below). This, however, means that the event-triggered control strategy presented in this chapter is particularly useful when the objective is to save communication resources and/or battery power of wireless radios, which is important for many (wireless) networked control systems, see, e.g., [4, 16, 67, 147], and is less useful for saving computation resources.*

Remark 4.2.2. *The event-triggering mechanism as discussed above works satisfactory in case the controller is given as in (4.2). However, some issues can arise in case that the controller is given by*

$$
\begin{cases}
\frac{\mathrm{d}}{\mathrm{d}t} x_c = A_c x_c + B_c \hat{y}, \\
\quad u = C_c x_c + D_c \hat{y},
\end{cases}
\tag{4.9}
$$

with $D_c \neq 0$. Namely, suppose that node i contains sensors and node j contains actuators, and that it holds that $t_{k_i}^i = t_{k_j}^j$, for some $k_i, k_j \in \mathbb{N}$, meaning that sensor and actuator data is transmitted simultaneously and thus both $\hat{y}$ and $\hat{u}$ are updated. Now since $\hat{y}$ directly affects u, according to (4.9), we could have that the event-triggering condition of (actuator) node j is again satisfied immediately, resulting in another transmission of actuator node j. Hence, in this case we would have that node j transmits twice at one time instant, which might not be desirable. In [36], this issue is resolved by introducing a transmission protocol that dictates that when one local *event-triggering condition is violated,* all nodes *transmit their data in a synchronised way, in which it is assumed that sensor data is transmitted and implemented, just before the actuator data is transmitted. Although this prevents u to be transmitted twice, this requires that transmissions of all nodes are synchronised, which might be difficult to achieve.*

4.2.2 An Impulsive System Formulation

In this section, we reformulate the event-triggered control system as an impulsive system, see, e.g., [50, 55], of the form

$$\frac{\mathrm{d}}{\mathrm{d}t}\bar{x} = \bar{A}\bar{x} + \bar{B}w, \qquad \text{when } \bar{x} \in \mathcal{C} \tag{4.10a}$$

$$\bar{x}^+ = \bar{G}_i\bar{x}, \qquad \text{when } \bar{x} \in \mathcal{D}_i, \, i \in \{1, \ldots, N\}, \tag{4.10b}$$

where $\bar{x} \in \mathcal{X} \subseteq \mathbb{R}^{n_x}$ denotes the state of the system and $w \in \mathbb{R}^{n_w}$ an external disturbance. The flow and the jump sets are denoted by $\mathcal{C} \subseteq \mathbb{R}^{n_x}$ and $\mathcal{D}_i \subseteq \mathbb{R}^{n_x}$, $i \in \{1, \ldots, N\}$, respectively, and $\mathcal{X} = \mathcal{C} \cup (\bigcup_{i=1}^{N} \mathcal{D}_i)$. Note that the transmission times $t_{k_i}^i$, $k_i \in \mathbb{N}$, as in (4.6), are now related to the event times at which the jumps of $\bar{x}$, according to (4.10b) for $i \in \{1, \ldots, N\}$, take place.

To arrive at a system description of the event-triggered control system (4.1), (4.2), (4.3), (4.5), and (4.6) of the form (4.10), we combine (4.1), (4.2), (4.3), (4.5) and (4.7), and define $\bar{x} := [x^\top \ e^\top]^\top \in \mathbb{R}^{n_x}$, where $x = [x_p^\top \ x_c^\top]^\top$ and $n_x := n_p + n_c + n_y + n_u$, yielding the flow dynamics of the system

$$\frac{\mathrm{d}}{\mathrm{d}t}\bar{x} = \underbrace{\begin{bmatrix} A + BC & B \\ -C(A + BC) & -CB \end{bmatrix}}_{=:\bar{A}} \bar{x} + \underbrace{\begin{bmatrix} E \\ -CE \end{bmatrix}}_{=:\bar{B}} w, \tag{4.11}$$

in which

$$A = \begin{bmatrix} A_p & 0 \\ 0 & A_c \end{bmatrix}, \quad B = \begin{bmatrix} 0 & B_p \\ B_c & 0 \end{bmatrix}, \quad C = \begin{bmatrix} C_p & 0 \\ 0 & C_c \end{bmatrix}, \quad E = \begin{bmatrix} B_w \\ 0 \end{bmatrix}. \tag{4.12}$$

The system 'flows' as long as the event-triggering conditions are not met, i.e., as long as (4.8) holds for all $i \in \{1, \ldots, N\}$, which can be reformulated as $\bar{x} \in \mathcal{C}$, with

$$\mathcal{C} = \{\bar{x} \in \mathbb{R}^{n_x} \,|\, \bar{x}^\top Q_i \bar{x} \leqslant \varepsilon_i \,\forall\, i \in \{1, \ldots, N\}\}, \tag{4.13}$$

and

$$Q_i = \begin{bmatrix} -\sigma_i C^\top \Gamma_i C & 0 \\ 0 & \Gamma_i \end{bmatrix}, \tag{4.14}$$

because $\bar{x}^\top Q_i \bar{x} \leqslant \varepsilon_i$ is equivalent to $\|\Gamma_i e(t)\|^2 \leqslant \sigma_i \|\Gamma_i v(t)\|^2 + \varepsilon_i$, as in (4.8). As mentioned before, when node i transmits its data, a reset according to $e^+ = (I - \Gamma_i)e$ occurs, while x remains the same, i.e., $x^+ = x$, see (4.3). This can be expressed by

$$\bar{x}^+ = \underbrace{\begin{bmatrix} I & 0 \\ 0 & I - \Gamma_i \end{bmatrix}}_{=:\bar{G}_i} \bar{x}, \tag{4.15}$$

for all $\bar{x} \in \mathcal{D}_i$, $i \in \{1, \ldots, N\}$, in which

$$\mathcal{D}_i = \{\bar{x} \in \mathbb{R}^{n_x} \,|\, \bar{x}^\top Q_i \bar{x} = \varepsilon_i\}, \tag{4.16}$$

according to (4.6). Combining (4.11), (4.13), (4.15) and (4.16) yields an impulsive system of the form (4.10).

4.2.3 Special Cases: State Feedback and Centralised Event Triggering

In the existing literature, the event-triggered control problem has mostly been considered for state-feedback controlled systems, see, e.g., [126, 136]. In this case, the controller is given by

$$u = K\hat{x}_p, \tag{4.17}$$

where $\hat{x}_p \in \mathbb{R}^{n_p}$ denotes the most recently sampled state of the plant and is defined in a similar fashion as $\hat{v}$. We can regard this as a special case of the setup presented above. Namely, to formulate the event-triggered control system with controller (4.17) as an impulsive system, we combine (4.1), (4.3), (4.5), (4.6) and (4.17), where we take $C_p = I$ in (4.1), as all states are measurable, and take $v := y = x_p$, $\hat{v} := \hat{y} = \hat{x}_p$ in (4.3), (4.5) and (4.6). In this case, the resulting impulsive model is given by (4.10), with (4.11), (4.13), (4.15) and (4.16), in which $\bar{x} := [x_p^\top \ e^\top]^\top$ and

$$A = A_p, \quad B = B_p K, \quad C = I, \quad E = B_w. \tag{4.18}$$

To arrive at the event-triggering mechanism that was studied [126], we take $N = 1$ and $\Gamma_1 = I$ (i.e., a centralised event-triggering mechanism), and $\varepsilon_1 = 0$.

Remark 4.2.3. *Although we study event-triggering conditions of the form (4.6), which is an extension of the one presented in [126], we can in principle study every event-triggering mechanism with conditions that can be written in the form $\bar{x}^\top Q_i \bar{x} = \varepsilon_i$, such as the ones presented in [135].*

4.3 Stability and $\mathcal{L}_\infty$-gain

In this section, we will study stability of the event-triggered control system in the sense of Lyapunov and its $\mathcal{L}_\infty$-gain. We will first review some basic stability and $\mathcal{L}_\infty$-gain results for impulsive systems of the form (4.10).

4.3.1 Stability and $\mathcal{L}_\infty$-gain of Impulsive Systems

Let us define the notions of stability and of Lyapunov function candidate that can be used to analyse impulsive systems of the form (4.10).

Definition 4.3.1.*[50] Consider the impulsive system, given by (4.10) with $w = 0$ and a compact set $\mathcal{A} \subset \mathcal{X}$.*

- *The set $\mathcal{A}$ is said to be stable for the impulsive system (4.10) with $w = 0$, if for each $\varepsilon > 0$ there exists $\delta > 0$, such that $\min_{x^\star \in \mathcal{A}} \|\bar{x}(0) - x^\star\| \leqslant \delta$ implies $\min_{x^\star(t) \in \mathcal{A}} \|\bar{x}(t) - x^\star(t)\| \leqslant \varepsilon$, for all solutions $\bar{x}$ to the impulsive system (4.10) with $w = 0$ and all t for which the solution $\bar{x}$ is defined.*

- *The set $\mathcal{A}$ is said to be globally attractive if each solution $\bar{x}$ to the impulsive system (4.10), with $w = 0$, satisfies $\min_{x^\star(t) \in \mathcal{A}} \|\bar{x}(t) - x^\star(t)\| \to 0$ as $t \to \infty$.*

- *The set $\mathcal{A}$ is* globally asymptotically stable *for (4.10), with $w = 0$, if it is stable and globally attractive.*

Definition 4.3.2.[50] *Consider the impulsive system, given by (4.10) with $w = 0$, and a compact set $\mathcal{A} \subset \mathcal{X}$. The function $W : \mathcal{X} \to \mathbb{R}$ is a Lyapunov function candidate for the system (4.10) and the set $\mathcal{A}$ if the function W*

(i) is continuous and nonnegative on $(\mathcal{C} \cup \bigcup_{i=1}^N \mathcal{D}_i)\backslash\mathcal{A} \subset \mathcal{X}$,

(ii) is locally Lipschitz on an open set $\mathcal{O}$ satisfying $\mathcal{C}\backslash\mathcal{A} \subset \mathcal{O} \subset \mathcal{X}$,

(iii) satisfies $\lim_{\bar{x} \to \mathcal{A}, \bar{x} \in \mathcal{X}} W(\bar{x}) = 0$, and

(iv) the sublevel sets of W on $\mathcal{X}$ are compact, i.e., the sets $\{\bar{x} \in \mathcal{X} \,|\, W(\bar{x}) \leqslant c_W\}$ are compact for all $c_W > 0$.

To prove global asymptotic stability of the set $\mathcal{A}$ of the system (4.10), we will make use of the following lemma.

Lemma 4.3.3. *Consider the impulsive system (4.10) with $w = 0$ and a compact set $\mathcal{A} \subset \mathcal{X}$ satisfying $\bar{G}_i \bar{x} \in \mathcal{A}$ for all $\bar{x} \in \mathcal{D}_i \cap \mathcal{A}$, $i \in \{1, \ldots, N\}$. Assume that for $w = 0$ and for all $\bar{x} \in \mathcal{X}$, a minimum inter-event time $h_{\min}^i > 0$ exists for each $i \in \{1, \ldots, N\}$, i.e., $t_{k_i+1}^i - t_{k_i}^i \geqslant h_{\min}^i$ for all $k_i \in \mathbb{N}$, and assume there exists a Lyapunov function candidate W for the impulsive system (4.10) with $w = 0$ and the set $\mathcal{A} \subset \mathcal{X}$, such that*

$$\frac{\mathrm{d}W(\bar{x})}{\mathrm{d}\bar{x}} \bar{A}\bar{x} < 0, \;\; \text{for almost all } \bar{x} \in \mathcal{C}\backslash\mathcal{A}, \tag{4.19a}$$

$$W(\bar{G}_i\bar{x}) - W(\bar{x}) \leqslant 0, \;\; \text{for all } \bar{x} \in \mathcal{D}_i\backslash\mathcal{A}, i \in \{1, \ldots, N\}. \tag{4.19b}$$

Then, $\mathcal{A}$ is a globally asymptotically stable set for the system (4.10) with $w = 0$.

Proof. The proof is given in Appendix A.3. $\qquad\square$

Let us now define the notion of the $\mathcal{L}_\infty$-gain of a system, which was studied for LTI systems in, e.g., [1], for which we introduce a performance variable $z \in \mathbb{R}^{n_z}$ given by

$$z = \bar{C}\bar{x} + \bar{D}w, \tag{4.20}$$

for some matrices $\bar{C}$ and $\bar{D}$ of appropriate dimensions.

Definition 4.3.4. *The $\mathcal{L}_\infty$-gain from w to z of the system (4.10), with (4.20), is defined as*

$$\kappa = \inf\{\bar{\kappa} \in \mathbb{R}_+ \,|\, \exists \delta : \mathcal{X} \to \mathbb{R}_+, \;\; \text{such that } \|z\|_{\mathcal{L}_\infty} \leqslant \bar{\kappa}\|w\|_{\mathcal{L}_\infty} + \delta(\bar{x}(0)),$$
$$\text{for all } \bar{x}(0) \in \mathcal{X}, w \in \mathcal{L}_\infty\}, \tag{4.21}$$

in which $\bar{x}$ is a solution to (4.10) with initial condition $\bar{x}(0) \in \mathcal{X}$, and disturbance $w \in \mathcal{L}_\infty$.

4.3.2 Stability and $\mathcal{L}_\infty$-gain of the Event-Triggered Control System

Using the results presented above for impulsive systems of the form (4.10), we now present the main result of this section. The main result consists of conditions for stability of a set $\mathcal{A}$, and an explicit expression of this set $\mathcal{A}$, and an upper bound on the $\mathcal{L}_\infty$-gain for the event-triggered control system (4.10), with (4.11), (4.13), (4.14), (4.15) and (4.16), and (4.20). We will also present conditions that guarantee that $\mathcal{A}$ is a globally asymptotically stable set for this event-triggered control system, for the case where disturbances are absent (i.e., for $w = 0$).

Theorem 4.3.5. *Consider the event-triggered control system (4.10), with (4.11), (4.13), (4.14), (4.15) and (4.16), and (4.20). Moreover, assume that for all $\bar{x}(0) \in \mathcal{X}$ and all $w \in \mathcal{L}_\infty$, a minimum inter-event time $h^i_{\min} > 0$ exists for each $i \in \{1, \ldots, N\}$, i.e., $t^i_{k_i+1} - t^i_{k_i} \geqslant h^i_{\min}$ for all $k_i \in \mathbb{N}$. Now suppose there exist a positive definite matrix $P \in \mathbb{R}^{(n_p+n_c) \times (n_p+n_c)}$, a positive semidefinite matrix $U \in \mathbb{R}^{n_x \times n_x}$, scalars $\alpha, \beta, \kappa > 0$, and $\mu_i, \nu_i \geqslant 0$, $i \in \{1, \ldots, N\}$, satisfying*

$$\begin{bmatrix} \sum_{i=1}^N \mu_i Q_i - \bar{A}^\top \bar{P} - \bar{P}\bar{A} - \alpha\bar{P} & \star \\ \bar{B}^\top \bar{P} & \beta I \end{bmatrix} \succeq 0, \tag{4.22a}$$

$$\begin{bmatrix} \alpha\bar{P} - \bar{C}^\top \bar{C} & \star \\ -\bar{D}^\top \bar{C} & (\kappa^2 - \beta)I - \bar{D}^\top \bar{D} \end{bmatrix} \succeq 0, \tag{4.22b}$$

$$\bar{P} - \bar{G}_i^\top \bar{P}\bar{G}_i - \nu_i Q_i \succeq 0, \tag{4.22c}$$

for all $i \in \{1, \ldots, N\}$, in which $\bar{P} := \mathrm{diag}(P, 0) + U$. Then,

$$\mathcal{A} = \{\bar{x} \in \mathcal{C} \cup (\bigcup_{i=1}^N \mathcal{D}_i) \,|\, \bar{x}^\top \bar{P}\bar{x} \leqslant \sum_{i=1}^N \tfrac{\mu_i \varepsilon_i}{\alpha}\} \tag{4.23}$$

is a globally asymptotically stable set for (4.10) with $w = 0$. Moreover, the $\mathcal{L}_\infty$-gain of (4.10), with (4.20), is smaller than or equal to κ and $\delta(\bar{x}(0))$ in (4.21) can be taken as $\delta(\bar{x}(0)) = (\alpha\bar{x}^\top(0)\bar{P}\bar{x}(0) + \sum_{i=1}^N \mu_i \varepsilon_i)^{1/2}$ for $\bar{x}(0) \in \mathcal{X}$.

Proof. The proof is given in Appendix A.3. $\qquad\square$

Let us now comment on the results presented in Theorem 4.3.5. The first comment is that the assumption in the hypotheses of Theorem 4.3.5 on the existence of a strictly positive minimum inter-event time for each $i \in \{1, \ldots, N\}$ is automatically guaranteed, if $\varepsilon_i > 0$ for all $i \in \{1, \ldots, N\}$ and the LMIs in (4.22) are feasible. This will be shown in Theorem 4.4.1 below. In case that

$\varepsilon_i = 0$ for some $i \in \{1, \ldots, N\}$, the assumption on the existence of a strictly positive minimum inter-event time for each $i \in \{1, \ldots, N\}$ can be violated and the inter-event time $t^i_{k_i+1} - t^i_{k_i}$ can converge to zero. In this case, an infinite number of events can occur in a finite-length time interval (i.e., the impulsive system (4.10) exhibits Zeno behaviour). This can happen at times t when $\|v_{\mathcal{J}_i}(t)\| = 0$ and $\bar{x}(t) \neq 0$, as we will show in Example 2 in Section 4.6. Therefore, we should generally take $\varepsilon_i > 0$ for all $i \in \{1, \ldots, N\}$ to guarantee minimum inter-event times greater than zero.

Another comment regarding Theorem 4.3.5 is that feasibility of (4.22) is only determined by the choice of suitable α, β, κ, and σ_i, $i \in \{1, \ldots, N\}$, as Q_i depends on σ_i, and feasibility is not affected by the choice of ε_i, $i \in \{1, \ldots, N\}$. Hence, once (4.22) is feasible, practical stability (for $w = 0$) and the upper bound κ on the $\mathcal{L}_\infty$-gain are guaranteed. The 'size' of the set $\mathcal{A}$ as in (4.23), (when $w = 0$), is affected by α, κ and σ_i, through the resulting P, as well as ε_i. Hence, after choosing α, κ and σ_i that render the set $\mathcal{A}$ of the event-triggered control system globally asymptotically stable and that guarantee the desired upper bound κ on the $\mathcal{L}_\infty$-gain, the parameters ε_i can be freely chosen to adjust the size of the set $\mathcal{A}$. As we can see from (4.8), this will affect the number of events, enabling us to make trade-offs between the size of the set $\mathcal{A}$ (related to the ultimate bound x reaches as $t \to \infty$ for $w = 0$) and the number of transmissions in each channel. Indeed, larger ε_i, $i \in \{1, \ldots, N\}$, result in fewer events, and thus fewer transmissions, but in a larger set $\mathcal{A}$, (i.e., a larger ultimate bound) when $w = 0$. In fact if ε_i, $i \in \{1, \ldots, N\}$, all approach zero (from above) we have that $\mathcal{A} \to \{0\}$. Hence, the set $\mathcal{A}$ can be made arbitrary small (at the cost of more transmissions). The naive choice to take $\varepsilon_i = 0$, for all $i \in \{1, \ldots, N\}$, seems appealing as it would yield $\mathcal{A} = \{0\}$. However, as argued already above, this might result in zero minimum inter-event times. In some cases, such as the case of a state-feedback controlled system with centralised event triggering as discussed in Section 4.2.3, a strictly positive minimum inter-event times can guaranteed even for $\varepsilon_1 = 0$, and we have that $\mathcal{A} = \{0\}$ is globally asymptotically stable. We will further discuss the minimum inter-event times below. Finally, note that the function δ is also affected by ε_i, also expressing that larger ε_i will result in a larger ultimate bound (even for $w \neq 0$).

In case disturbances are absent ($w = 0$), we can arrive at simpler conditions to guarantee that $\mathcal{A}$ is a globally asymptotically stable set for the event-triggered control system (4.10), with (4.11), (4.13), (4.14), (4.15) and (4.16).

Corollary 4.3.6. *Consider the event-triggered control system (4.10), with (4.11), (4.13), (4.14), (4.15) and (4.16), and $w = 0$. Moreover, assume that for all $\bar{x}(0) \in \mathcal{X}$, a minimum inter-event time $h^i_{\min} > 0$ exists for each $i \in \{1, \ldots, N\}$, i.e., $t^i_{k_i+1} - t^i_{k_i} \geqslant h^i_{\min}$ for all $k_i \in \mathbb{N}$. Now suppose there exist a positive definite matrix $P \in \mathbb{R}^{(n_p+n_c)\times(n_p+n_c)}$, a positive semidefinite matrix*

$U \in \mathbb{R}^{n_x \times n_x}$, *scalars* $\alpha > 0$, *and* $\mu_i, \nu_i \geqslant 0$, $i \in \{1, \dots, N\}$, *satisfying*

$$\sum_{i=1}^{N} \mu_i Q_i - \bar{A}^\top \bar{P} - \bar{P} \bar{A} - \alpha \bar{P} \succeq 0, \tag{4.24a}$$

$$\alpha \bar{P} - \mathrm{diag}(I, 0) \succeq 0 \tag{4.24b}$$

and (4.22c) *for all* $i \in \{1, \dots, N\}$, *where* $\bar{P} := \mathrm{diag}(P, 0) + U$ *and* I *denotes the identity matrix of size* $(n_p + n_c) \times (n_p + n_c)$. *Then, the set* $\mathcal{A}$ *as in* (4.23) *is a globally asymptotically stable set for* (4.10) *with* $w = 0$. *Furthermore,* $\limsup_{t \to \infty} \|x(t)\| \leqslant (\sum_{i=1}^{N} \mu_i \varepsilon_i)^{1/2}$.

Proof. The proof follows the same lines of reasoning as the proof of Theorem 4.3.5. The fact that $\|x(t)\| \to (\sum_{i=1}^{N} \mu_i \varepsilon_i)^{1/2}$ as $t \to \infty$ follows from (A.87), with $w = 0$, and the fact that (4.24b), implies that $\|x(t)\|^2 \leqslant \alpha V(\bar{x}(t))$ for all $t \in \mathbb{R}_+$. $\qquad\square$

Remark 4.3.7. *In this chapter, we particularly study the* $\mathcal{L}_\infty$*-gain from* w *to* z *of the system* (4.10), *with* (4.20), *instead of the* $\mathcal{L}_p$*-gain from* w *to* z, *for some* $p \in \mathbb{N}$, *defined as*

$$\kappa = \inf\{\bar{\kappa} \in \mathbb{R}_+ \mid \exists \delta : \mathcal{X} \to \mathbb{R}_+, \text{ such that } \|z\|_{\mathcal{L}_p} \leqslant \bar{\kappa} \|w\|_{\mathcal{L}_p} + \delta(\bar{x}(0)),$$
$$\text{for all } \bar{x}(0) \in \mathcal{X}, w \in \mathcal{L}_p\}, \tag{4.25}$$

in which $\bar{x}$ *is a solution to* (4.10) *for initial condition* $\bar{x}(0) \in \mathcal{X}$, *and input* $w \in \mathcal{L}_p$. *The reason for focussing on* $\mathcal{L}_\infty$*-gains is that we are generally interested in* $\varepsilon_i > 0$, $i \in \{1, \dots, N\}$, *as this guarantees nonzero minimum inter-event times (see Theorem 4.4.1 below). In this case,* $\mathcal{A} \supset \{0\}$, *and thus* $\bar{x}(t)$ *will not converge asymptotically to the origin for* $w = 0$, *and therefore* $z(t)$ *will typically not converge to zero when* $t \to \infty$. *Hence,* $\|z\|_{\mathcal{L}_p} = \infty$ *for all* $p \neq \infty$. *Consequently, a finite* $\mathcal{L}_p$*-gain for* $p \in \mathbb{N}$ *cannot be guaranteed in case* $\varepsilon_i > 0$, $i \in \{1, \dots, N\}$. *Since the* $\mathcal{L}_\infty$*-gain does not require* $z(t) \to 0$ *when* $t \to \infty$, *but merely that* $z(t)$ *is bounded for all* $t \in \mathbb{R}_+$, *we can arrive at a finite* $\mathcal{L}_\infty$*-gain for the event-triggered control system discussed in this chapter. Note that in case* $\varepsilon_i = 0$, $i \in \{1, \dots, N\}$, *for which in some circumstances it is possible to guarantee that* $h_{\min}^i > 0$, *(e.g., the case of a state-feedback controlled system with centralised event triggering as discussed in Section 4.2.3), the* $\mathcal{L}_p$*-gain might be finite since in this case* $\mathcal{A} = \{0\}$. *In particular, the* $\mathcal{L}_2$*-gain is guaranteed to be smaller than* κ *for the system* (4.10), *with* (4.20) *and* $\varepsilon_i = 0$ *for all* $i \in \{1, \dots, N\}$, *if there exist a positive definite matrix* $P \in \mathbb{R}^{(n_p + n_c) \times (n_p + n_c)}$, *a positive semidefinite matrix* $U \in \mathbb{R}^{n_x \times n_x}$, *such that* $\bar{P} := \mathrm{diag}(P, 0) + U$, *scalars*

$\alpha > 0$, and $\mu_i, \nu_i \geqslant 0$, $i \in \{1, \dots, N\}$, satisfying

$$\begin{bmatrix} \sum_{i=1}^N \mu_i Q_i - \bar{A}^\top \bar{P} - \bar{P}\bar{A} - \alpha\bar{P} & \star & \star \\ \bar{B}^\top \bar{P} & \kappa^2 I & \star \\ \bar{C} & \bar{D} & I \end{bmatrix} \succeq 0, \qquad (4.26\text{a})$$

$$\bar{P} - \bar{G}_i^\top \bar{P} \bar{G}_i - \nu_i Q_i \succeq 0, \qquad (4.26\text{b})$$

for all $i \in \{1, \dots, N\}$. Of course, this result only holds if all the minimum inter-event times $h_{\min}^i$, $i \in \{1, \dots, N\}$, are strictly positive, as was also required in Theorem 4.3.5.

4.4 A Lower Bound on the Inter-Event Times

In this section, we will show that for each node $i \in \{1, \dots, N\}$, the inter-event times $t_{k_i+1}^i - t_{k_i}^i$, $k_i \in \mathbb{N}$, of the event-triggered control system are bounded from below by a strictly positive constant. The existence of a lower bound on the inter-event times for every node means that the total number of transmissions in a finite time interval is bounded from above, which guarantees a certain maximum utilisation of the communication resources. We will show that, although the stability and $\mathcal{L}_\infty$-gain properties of the system hold globally, the guaranteed lower bound on the inter-event times is a local property, in the sense that it depends on the magnitude of the initial condition and the disturbance.

The analysis is based on studying the solutions of (4.10), with (4.11), (4.13), (4.14), (4.15) and (4.16), from $t_{k_i}^i$ to $t_{k_i+1}^i$. To do so, we study the solutions of the auxiliary system

$$\frac{\mathrm{d}}{\mathrm{d}t}\begin{bmatrix} x \\ e_{\mathcal{J}_i} \end{bmatrix} = \begin{bmatrix} I & 0 \\ 0 & \bar{\Gamma}_i^\top \end{bmatrix} \bar{A} \begin{bmatrix} I & 0 \\ 0 & \bar{\Gamma}_i \end{bmatrix} \begin{bmatrix} x \\ e_{\mathcal{J}_i} \end{bmatrix} + \begin{bmatrix} I & 0 \\ 0 & \bar{\Gamma}_i^\top \end{bmatrix} \left(\bar{A} \begin{bmatrix} 0 \\ \bar{\Gamma}_i^c \end{bmatrix} e_{\mathcal{J}_i^c} + \bar{B}w \right) \qquad (4.27)$$

with $e_{\mathcal{J}_i}^+(t_{k_i}^i) = 0$, from $t_{k_i}^i$ to $t_{k_i+1}^i$, for each $i \in \{1, \dots, N\}$. In (4.27), the submatrices $\bar{\Gamma}_i := I_{\bullet \mathcal{J}_i}$ and $\bar{\Gamma}_i^c := I_{\bullet \mathcal{J}_i^c}$, $i \in \{1, \dots, N\}$, are formed by taking the columns of the identity matrix I that are in the set $\mathcal{J}_i = \{j \in \{1, \dots, n_y + n_u\} \mid \gamma_i^j = 1\}$, and in the set $\mathcal{J}_i^c = \{1, \dots, n_y + n_u\} \backslash \mathcal{J}_i$, respectively, and are used to select the signals in e that correspond to node $i \in \{1, \dots, N\}$, i.e., $e_{\mathcal{J}_i} = \bar{\Gamma}_i^\top e$, and that do not correspond to this node, i.e., $e_{\mathcal{J}_i^c} = (\bar{\Gamma}_i^c)^\top e$, respectively. The auxiliary system (4.27), $i \in \{1, \dots, N\}$, is obtained from (4.11), by considering $e_{\mathcal{J}_i^c}$ as external inputs. Hence, the fact that the dynamics of $e_{\mathcal{J}_i^c}$ depend on x and $e_{\mathcal{J}_i}$ is ignored in (4.27), yielding that the solutions to (4.10), with (4.11), (4.13), (4.14), (4.15) and (4.16), from $t_{k_i}^i$ to $t_{k_i+1}^i$ are included in the solutions of (4.27) and $e_{\mathcal{J}_i}^+(t_{k_i}^i) = 0$ from $t_{k_i}^i$ to $t_{k_i+1}^i$, for each $i \in \{1, \dots, N\}$. This fact, and the fact that $e_{\mathcal{J}_i^c}$ in (4.27) satisfies (4.8), will be exploited to derive the lower bound on the minimum inter-event time.

We now present the main result of this section.

Theorem 4.4.1. *Consider the event-triggered control system given by* (4.10), *with* (4.11), (4.13), (4.14), (4.15) *and* (4.16), *with* $\varepsilon_i > 0$ *for all* $i \in \{1, \ldots, N\}$. *For every* $\delta_x \geqslant 0$ *and every* $\delta_w \geqslant 0$, *there exists a strictly positive lower bound on the minimum inter-event times* $h^i_{\min}(\delta_x, \delta_w)$ *for each node* $i \in \{1, \ldots, N\}$, *i.e.,* $t^i_{k_i+1} - t^i_{k_i} \geqslant h^i_{\min}$, *for all* $k_i \in \mathbb{N}$, *for every solution to* (4.10) *with* $\|\bar{x}(0)\| \leqslant \delta_x$, *and* $\|w\|_{\mathcal{L}_\infty} \leqslant \delta_w$. *An explicit expression for a lower bound* $h^i_{\min}$ *is given by*

$$\min\left\{ h > 0 \,\middle|\, \lambda_{\max}\left(\begin{bmatrix} I \\ 0 \end{bmatrix}^\top e^{\begin{bmatrix} I & 0 \\ 0 & \Gamma_i \end{bmatrix} \bar{A}^\top h} Q_i e^{\bar{A} \begin{bmatrix} I & 0 \\ 0 & \Gamma_i \end{bmatrix} h} \begin{bmatrix} I \\ 0 \end{bmatrix} \right) \geqslant \frac{\zeta_i(h)}{\eta} \right\}, \qquad (4.28)$$

in which

$$\zeta_i(h) = \varepsilon_i - \|Q_i\|\left(2\sqrt{\eta\rho_i(h)}\left\|e^{\bar{A}\begin{bmatrix} I & 0 \\ 0 & \Gamma_i \end{bmatrix} h} \begin{bmatrix} I \\ 0 \end{bmatrix}\right\| + \rho_i(h)\right), \qquad (4.29)$$

with

$$\rho_i(h) = h \int_0^h e^{\vartheta s} \mathrm{d}s \left(\|\bar{B}\|\delta_w + \left\|\bar{A}\begin{bmatrix} 0 \\ \Gamma_i^c \end{bmatrix}\right\| \sqrt{\sum_{j \in \mathcal{I}_i} \sigma_j \|\Gamma_j C\|^2 \eta + \varepsilon_j} \right)^2, \qquad (4.30)$$

and $\eta = \frac{\lambda_{\max}(\bar{P})\alpha\delta_x^2 + \beta\delta_w^2 + \sum_{i=1}^N \mu_i\varepsilon_i}{\alpha\lambda_{\min}(P)}$, $\vartheta = \lambda_{\max}\left(\bar{A}\begin{bmatrix} I & 0 \\ 0 & \Gamma_i \end{bmatrix} + \begin{bmatrix} I & 0 \\ 0 & \Gamma_i \end{bmatrix}^\top \bar{A}^\top\right)$, *and* $\mathcal{I}_i := \{1, \ldots, N\} \setminus \{i\}$.

Proof. The proof is given in Appendix A.3. □

The minimum in (4.28) in Theorem 4.4.1 can be solved by computing the maximum eigenvalue of the h-dependent matrix in the condition in (4.28) for increasing $h > 0$ and check when the inequality is satisfied for the first time. This determines for node $i \in \{1, \ldots, N\}$ the lower bound on the inter-event times $h^i_{\min}$, as in (4.28). Even though a minimum inter-event times is guaranteed for each node, no guarantees can be made about the time between two events in different nodes. Still, the lower bound on the inter-event times for all nodes allows guarantee to be made about the total number of events within a certain time interval. The obtained lower bounds decrease as δ_x (related to $\|\bar{x}(0)\|$) increases or as δ_w (related to $\|w\|_{\mathcal{L}_\infty}$) increases, implying that the control task has to be executed more often if the system's initial state is further away from the origin and in case the norm of the disturbance is larger. We will illustrate this observation in Example 3 of Section 4.6. In the special case that C_p and C_c are invertible and the event triggering is centralised, i.e., the number of nodes $N = 1$ and $\Gamma_1 = I$, (implying that Q_1 has full rank), and no disturbances are present, (implying that $\delta_w = 0$), the minimum inter-event time $h^1_{\min} > 0$ even for $\varepsilon_1 = 0$. Furthermore, we have that $\rho_1(h) = 0$, (due to $\delta_w = 0$ and $\mathcal{I}_1 = \emptyset$) and thus that $\zeta_1(h) = 0$, for all $h \in \mathbb{R}_+$, meaning that the obtained bound is independent of δ_x, (and thus independent of $\bar{x}(0) \in \mathcal{X}$). If additionally the controller is given by a state-feedback controller (4.17), the

resulting condition recovers the one presented in Theorem 5.1 in [92]. In this case, the bounds are tight in the sense that for some $k_1 \in \mathbb{N}$, we have that $t_{k_1+1}^1 - t_{k_1}^1 = h_{\min}^1$.

4.5 Improved Event-Triggering Conditions

In the previous sections, we modelled the event-triggered control system as an impulsive system and presented conditions to guarantee its stability and an upper bound on the $\mathcal{L}_\infty$-gain. The reason to take an impulsive system approach is that it explicitly describes the behaviour of the event-triggered control system. This has the favourable consequence that it yields less conservative conditions than the (direct extensions of the) existing results in the literature, such as [126, 136]. To formally demonstrate this statement, we first extend the reasoning of [126] towards dynamical output-based controllers and by including $\mathcal{L}_\infty$-performance, and secondly, we show that the obtained stability conditions can be seen as a special case of the conditions in Theorem 4.3.5 (i.e., using the impulsive system description of the event-triggered control system).

To extend the work of [126], let us consider the following auxiliary system:

$$\begin{cases} \frac{\mathrm{d}}{\mathrm{d}t}x = (A+BC)x + \begin{bmatrix} B & E \end{bmatrix} \begin{bmatrix} e \\ w \end{bmatrix}, \\ \begin{bmatrix} v \\ z \end{bmatrix} = \begin{bmatrix} C \\ C_x \end{bmatrix} x + \begin{bmatrix} 0 & 0 \\ 0 & \bar{D} \end{bmatrix} \begin{bmatrix} e \\ w \end{bmatrix}, \end{cases} \quad (4.31)$$

which is obtained from (4.11) and (4.20) by considering the error e as an external input, instead of as a state variable as in (4.10), and by assuming that the performance output, as in (4.20), is given by $z = C_x x + \bar{D}w$, implying that $\bar{C}$ in (4.20) has the form $\bar{C} = [C_x \ 0]$. As important observation is that in (4.31), the dynamics of e, given by $\frac{\mathrm{d}}{\mathrm{d}t}e = -\frac{\mathrm{d}}{\mathrm{d}t}v = -C(A+BC)x - CBe$, is ignored in (4.31), while it is captured explicitly in the impulsive system (4.10), with (4.11), (4.13), (4.14), (4.15) and (4.16).

System (4.31), with $e = 0$ and $w = 0$, is a globally asymptotically stable LTI system, because of the assumption made in Section 4.2 that the controller stabilises the plant when $\hat{v}(t) = [\hat{y}^\top(t) \ \hat{u}^\top(t)]^\top = [y^\top(t) \ u^\top(t)]^\top = v(t)$ for all $t \in \mathbb{R}_+$, meaning that $A + BC$ is Hurwitz, i.e., it has all the eigenvalues in the left-half complex plane. This ensures that there exist a positive definite storage function of the form $V(x) = x^\top Px$, see, e.g., [139], a (sufficiently small) positive scalar α, (sufficiently large) positive scalars β, κ, satisfying $\beta \geqslant \kappa^2$, and (sufficiently small) positive scalars σ_i, $i \in \{1, \dots, N\}$, that satisfy the dissipation inequality

$$\frac{\mathrm{d}}{\mathrm{d}t}V(x(t)) \leqslant -\alpha V(x(t)) + \beta \|w(t)\|^2 + \sum_{i=1}^{N} \left(\tfrac{1}{\sigma_i}\|e_{\mathcal{J}_i}(t)\|^2 - \|v_{\mathcal{J}_i}(t)\|^2 \right) \quad (4.32)$$

and the inequality

$$\|z(t)\|^2 + (\beta - \kappa^2)\|w(t)\|^2 \leqslant \alpha V(x(t)). \tag{4.33}$$

Now since (4.8) holds, for all $i \in \{1, \dots, N\}$ and all $t \in \mathbb{R}_+$, we have that

$$\sum_{i=1}^{N} \left(\|v_{\mathcal{J}_i}(t)\|^2 + \tfrac{\varepsilon_i}{\sigma_i} - \tfrac{1}{\sigma_i}\|e_{\mathcal{J}_i}(t)\|^2 \right) \geqslant 0, \tag{4.34}$$

and all $t \in \mathbb{R}_+$. Combining this expression with (4.32) yields that

$$\tfrac{\mathrm{d}}{\mathrm{d}t} V(x(t)) \leqslant -\alpha V(x(t)) + \beta\|w(t)\|^2 + \sum_{i=1}^{N} \tfrac{\varepsilon_i}{\sigma_i}, \tag{4.35}$$

which allows us to show that for $w = 0$ and for $V(x(t)) \geqslant \sum_{i=1}^{N} \tfrac{\varepsilon_i}{\sigma_i \alpha}$, it holds that $\tfrac{\mathrm{d}}{\mathrm{d}t} V(x(t)) < 0$, which means that the state x of (4.31), with (4.8), converges asymptotically to the set $\mathcal{A} = \{x \in \mathbb{R}^{n_p + n_c} \,|\, V(x) \leqslant \sum_{i=1}^{N} \tfrac{\varepsilon_i}{\sigma_i \alpha}\}$. Furthermore, using (4.33) and ideas from [1], we can show that the system (4.31), with (4.8), has a finite $\mathcal{L}_\infty$-gain from disturbance w to performance output z. We will formalise this idea in the following theorem.

Theorem 4.5.1. *Assume that there exist scalars* $\alpha, \beta, \kappa, \sigma_i > 0$, $i \in \{1, \dots, N\}$, *and a positive definite matrix* $P \in \mathbb{R}^{(n_p + n_c) \times (n_p + n_c)}$, *satisfying*

$$\begin{bmatrix} -Z - \alpha P - \sum_{i=1}^{N} C^\top \Gamma_i C & \star & \star \\ B^\top P & \sum_{i=1}^{N} \tfrac{1}{\sigma_i} \Gamma_i & \star \\ E^\top P & 0 & \beta I \end{bmatrix} \succeq 0, \tag{4.36a}$$

$$\begin{bmatrix} \alpha P - C_x^\top C_x & \star \\ \bar{D}^\top C_x & (\kappa^2 - \beta)I - \bar{D}^\top \bar{D} \end{bmatrix} \succeq 0. \tag{4.36b}$$

with $Z := (A + BC)^\top P + P(A + BC)$. *Then, the set*

$$\mathcal{A} = \{x \in \mathbb{R}^{n_p + n_c} \,|\, x^\top P x \leqslant \sum_{i=1}^{N} \tfrac{\varepsilon_i}{\sigma_i \alpha}\} \tag{4.37}$$

is a globally asymptotically stable set of the system (4.31) *with* (4.8) *and for* $w = 0$. *Furthermore, the* $\mathcal{L}_\infty$-*gain from* w *to* z *is smaller than or equal to* κ *and* δ *in* (4.21) *can be taken as* $\delta(x(0)) = (\alpha x^\top(0) P x(0) + \sum_{i=1}^{N} \tfrac{\varepsilon_i}{\sigma_i})^{1/2}$ *for all* $x \in \mathbb{R}^{n_p + n_c}$.

Proof. The proof follows directly from the discussion above and the fact that (4.36a) and (4.36b) imply (4.32) and (4.33), respectively. It also follows directly from Theorem 4.5.2 that we will present below. $\qquad \square$

In case the system is controlled by a state-feedback controller (as discussed in Section 4.2.3), the event triggering mechanism is centralised (i.e., $N = 1$ and $\Gamma_1 = I$), and when disturbances are absent ($E = 0$ and $\bar{D} = 0$), the conditions presented in Theorem 4.5.1 provide LMI-based stability conditions that can be used to analyse the stability of the event-triggered control system studied in [126]. Even though the results in [126] are valid for nonlinear systems as well, while we focus in this chapter on linear systems, Theorem 4.5.1 provides a computational procedure that allows us to obtain large values for σ_i and, thus, large values for the inter-event times, whereas [126] only presents existence results and does not provide a constructive (optimisation-based) way to obtain suitable choices for σ_i. Note that obtaining a LMI-based stability analysis for the case studied in [126] is not the main result of this section. Namely, the main result of this section is presented below. This main result states that if Theorem 4.5.1 guarantees global asymptotic stability of the set $\mathcal{A}$, as in (4.37), and guarantees an upper bound κ on the $\mathcal{L}_\infty$-gain for the system (4.31) with (4.8), for some scalars σ_i and the scalars ε_i, $i \in \{1, \ldots, N\}$, then, global asymptotic stability of the same set $\mathcal{A}$ and the same upper-bound κ on the $\mathcal{L}_\infty$-gain can also be guaranteed for the impulsive system (4.10) using Theorem 4.3.5.

Theorem 4.5.2. *Consider the model of the event-triggered control system* (4.31), *with* (4.8), *and the impulsive system formulation of the event-triggered control system* (4.10), *with* (4.11), (4.13), (4.14), (4.15) *and* (4.16), *and* (4.20) *with* $\bar{C} = [C_x \quad 0]$. *If there exists a positive definite matrix* P, *and scalars* $\alpha, \beta, \kappa, \sigma_i > 0$, $i \in \{1, \ldots, N\}$, *satisfying the conditions of Theorem 4.5.1, then* $\bar{P} := \mathrm{diag}(P, 0)$, $U = 0$, $\mu_i = \frac{1}{\sigma_i}$ *and* $\nu_i = 0$, *for all* $i \in \{1, \ldots, N\}$, *satisfy the conditions of Theorem 4.3.5 for the same* α, β, *and* κ.

Proof. The proof is given in Appendix A.3. □

Theorem 4.5.2 formally shows that the conditions based on impulsive system (4.10) are never more conservative than the ones based on system (4.31), as the matrix $\bar{P}$ in Theorem 4.3.5 can have a more general form than $\bar{P} := \mathrm{diag}(P, 0)$, (which was used in the hypothesis of Theorem 4.5.2). Hence, this creates the opportunity to guarantee stability for event-triggering conditions with a larger inter-event time or a smaller upper-bound on the $\mathcal{L}_\infty$-gain. Furthermore, Theorem 4.5.2 also guarantees that the conditions in Theorem 4.3.5 can always be satisfied if all σ_i, $i \in \{1, \ldots, N\}$, are chosen sufficiently small. Namely, for the auxiliary system (4.31) the existence of storage function of the form $V(x) = x^\top P x$ satisfying (4.32) for some positive α, β and σ_i, $i \in \{1, \ldots, N\}$, is guaranteed. Hence, the hypothesis of Theorem 4.5.1 can always be satisfied for some sufficiently small α and σ_i, $i \in \{1, \ldots, N\}$, and some sufficiently large β and κ, which, in turn, implies feasibility of the conditions in Theorem 4.3.5.

4.6 Illustrative Examples

In this section, we illustrate the presented theory using three numerical examples. The first example is taken from [126], in which an unstable plant is stabilised using an event-triggered implementation of a state-feedback controller and a centralised event-triggering mechanism. We will show that by formulating the event-triggered control system as an impulsive system and employing the theory as developed in this chapter, we can guarantee stability for event-triggered control systems with larger minimum inter-event times. In the second example, we stabilise an unstable plant using a dynamical output-based controller and a decentralised event-triggering mechanism to illustrate that indeed output-based controllers and decentralised event triggering can be designed that perform well. In the last example, we consider a stable plant that is subject to disturbances and show that outputs of the plant and the controller are only transmitted when disturbances are acting on the system or during transients, while no transmissions occur when disturbances are absent and the system is in steady state. This is a favourable property that traditional digital control systems with periodic transmissions do not have.

Example 1: Let us consider the numerical example taken from [126]. The plant (4.1) is given by

$$\tfrac{\mathrm{d}}{\mathrm{d}t}x_p = \begin{bmatrix} 0 & 1 \\ -2 & 3 \end{bmatrix} x_p + \begin{bmatrix} 0 \\ 1 \end{bmatrix} u, \tag{4.38}$$

the state-feedback controller is given by (4.17), with $K = \begin{bmatrix} 1 & -4 \end{bmatrix}$, and the event triggering is centralised, i.e., we have that $N = 1$ and $\Gamma_1 = I$. In [126], global asymptotic stability of the origin is guaranteed for $\bar{\sigma} \leqslant 0.055$ for the event-triggering condition $\|e\| = \bar{\sigma}\|x\|$ and was obtained using an alternative approach. This yields $\sigma_1 = 0.055^2 = 0.0030$ and $\varepsilon_1 = 0$ if the event-triggering mechanism is formulated as in (4.6). For this event-triggering mechanism, Theorem 4.4.1, or its counterpart Theorem 5.1 in [92], yields a lower bound on the inter-event times[4] of 0.0318. We now compare this result with the event-triggering mechanism obtained using the results from Section 4.5, i.e., obtained by maximising σ_1 in the conditions of Theorem 4.5.1. Taking this approach allows us to guarantee stability up to $\sigma_1 = 0.0273$, resulting, for $\varepsilon_1 = 0$, in a lower bound on the inter-event times of 0.0840. Therefore, we can conclude that taking the approach as in Section 4.5 already increases the allowable minimum inter-event time with respect to [126]. However, if we analyse stability using the result of Theorem 4.3.5, which is based on the impulsive system formulation, we can guarantee stability of this event-triggered control system up to $\sigma_1 = 0.0588$,

---

[4]Note that for this example, the obtained lower-bound on the minimum inter-event times is tight, as also was observed in Section 4.4.

which yields, for $\varepsilon_1 = 0$, a lower bound on the inter-event times of 0.1136. The increase of inter-event times is expected due to the formal result established in Theorem 4.5.2.

We therefore conclude that by modelling the event-triggered control system using an impulsive model, stability can be guaranteed for event-triggering mechanisms that yield larger minimum inter-event times.

Example 2: Let us now consider the plant (4.1) given by

$$\begin{cases} \frac{\mathrm{d}}{\mathrm{d}t} x_p = \begin{bmatrix} 0 & 1 \\ -2 & 3 \end{bmatrix} x_p + \begin{bmatrix} 0 \\ 1 \end{bmatrix} \hat{u} \\ y = \begin{bmatrix} -1 & 4 \end{bmatrix} x_p, \end{cases} \tag{4.39}$$

and the controller (4.2) given by

$$\begin{cases} \frac{\mathrm{d}}{\mathrm{d}t} x_c = \begin{bmatrix} 0 & 1 \\ 0 & -5 \end{bmatrix} x_c + \begin{bmatrix} 0 \\ 1 \end{bmatrix} \hat{y} \\ u = \begin{bmatrix} 1 & -4 \end{bmatrix} x_c. \end{cases} \tag{4.40}$$

We assume that no disturbances act on the plant, i.e., $B_w = 0$, and, therefore, we simply take $\bar{C} = 0$ and $\bar{D} = 0$. Furthermore, we assume that the system is equipped with an event-triggering mechanisms at both the sensor-to-controller channel and the controller-to-actuator channel, which means that we define $\Gamma_1 = \mathrm{diag}(1,0)$ and $\Gamma_2 = \mathrm{diag}(0,1)$. Hence, we have two nodes. Practical stability of the event-triggered control system (4.1), (4.2), with event-triggering mechanism (4.6), with $\sigma_1 = \sigma_2 = 10^{-3}$, can be guaranteed using the impulsive system formulation (4.10) and the results of Corollary 4.3.6.

If we take $\varepsilon_1 = \varepsilon_2 = 0$, the inter-event times will become zero when $\|v_{\mathcal{J}_i}(t)\| = 0$, at some time $t \in \mathbb{R}^+$ and for some $i \in \{1,2\}$, as was discussed in Section 4.3 and Section 4.4. By simulating the response of the system to the initial condition $\bar{x}(0) = [\frac{25}{2}, \frac{-25}{2}, \frac{-25}{2}, \frac{25}{2}, 0, 0]^\top$, we can observe that indeed the inter-event times converge to zero, see Figure 4.2b, as $\|v_{\mathcal{J}_2}(t)\| = \|u(t)\| \to 0$, see Figure 4.2a. Hence, this illustrates that $\varepsilon_i > 0$ is needed for all $i \in \{1, \ldots, N\}$ to guarantee minimum inter-event times larger than zero.

If we now take $\varepsilon_1 = \varepsilon_2 = 10^{-3}$, Corollary 4.3.6 yields that the states $x(t)$ satisfy $\limsup_{t \to \infty} \|x(t)\| \leqslant 6.4$. Using the result of Theorem 4.4.1, we obtain that if the initial conditions satisfy, e.g., $\|\bar{x}(0)\| \leqslant 25$, a lower bound on the inter-event times $h_{\min}^1 = h_{\min}^2 = 6.5 \cdot 10^{-9}$ is guaranteed for both nodes. When we compare these results with a simulation of the response of the system to the initial condition $\bar{x}(0) = [\frac{25}{2}, \frac{-25}{2}, \frac{-25}{2}, \frac{25}{2}, 0, 0]^\top$, see Figure 4.3, we observe that the states of the plant and the controller indeed converge asymptotically to a vicinity of the origin and that the outputs of the plants and controllers have

(a) The evolution of y (node $i = 1$) and u (node $i = 2$) as a function of time.

(b) The inter-event times for each node as a function of time.
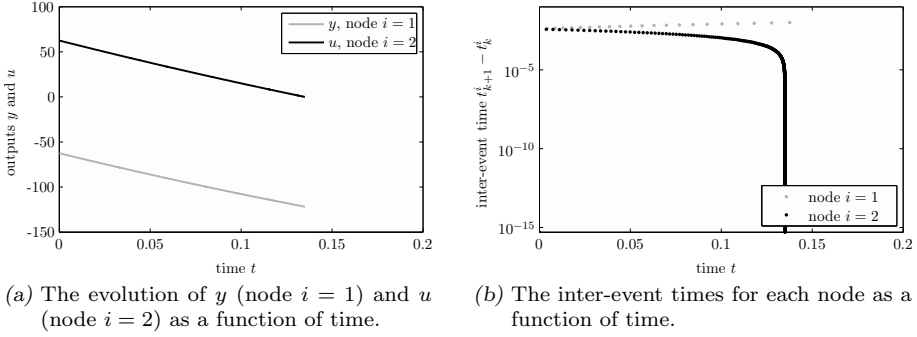
Figure 4.2: Example 2 with $\varepsilon_1 = \varepsilon_2 = 0$.

(a) The evolution of the states of the plant and controller as a function of time.

(b) The inter-event times for each node as a function of time.
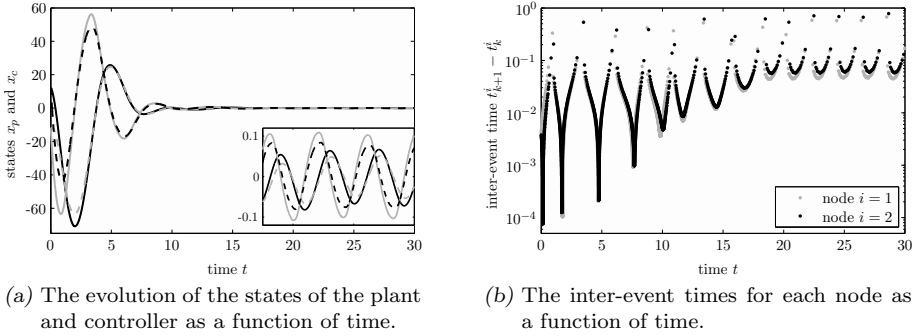
Figure 4.3: Example 2 with $\varepsilon_1 = \varepsilon_2 = 10^{-3}$. Inserted in (a): A close-up of the evolution of the states of the plant and the controller at time $t \in [17.5, 30]$.

to be transmitted less often when the state approaches the origin. However, $x(t)$ even satisfies $\limsup_{t \to \infty} \|x(t)\| \leqslant 0.12$, which is significantly smaller than the predicted upper bound of approximately 6.4. In addition, the observed minimum inter-event time is $h_{\min}^1 \approx h_{\min}^2 \approx 10^{-4}$, which is larger than the predicted value of $6.5 \cdot 10^{-9}$. This seems to hold for many initial conditions satisfying $\|\bar{x}(0)\| < 25$. This shows that, although we can formally prove the existence of a globally asymptotically stable compact set and a nonzero lower bound on the minimal inter-event times, the obtained bounds can still be improved. Improving these bounds is a topic of future research.

Example 3: Let us now consider the (stable) plant (4.1) given by

$$\begin{cases} \frac{\mathrm{d}}{\mathrm{d}t} x_p = \begin{bmatrix} 0 & 1 \\ -2 & -3 \end{bmatrix} x_p + \begin{bmatrix} 0 \\ 1 \end{bmatrix} \hat{u} + \begin{bmatrix} 0 \\ 1 \end{bmatrix} w \\ y = \begin{bmatrix} 1 & 0 \end{bmatrix} x_p, \end{cases} \tag{4.41}$$

and the controller (4.2) given by

$$\begin{cases} \frac{\mathrm{d}}{\mathrm{d}t} x_c = \begin{bmatrix} -2 & 1 \\ -13 & -3 \end{bmatrix} x_c + \begin{bmatrix} -2 \\ -5 \end{bmatrix} \hat{y} \\ u = \begin{bmatrix} 5 & 2 \end{bmatrix} x_c. \end{cases} \tag{4.42}$$

Furthermore, we take $\bar{C} = [1\ 0\ 0\ 0]$ and $\bar{D} = 0$ for the performance output z in (4.20), and assume that the system is equipped with event-triggering mechanisms at both the sensor-to-controller channel and the controller-to-actuator channel. This means that we, again, define $\Gamma_1 = \mathrm{diag}(1, 0)$ and $\Gamma_2 = \mathrm{diag}(0, 1)$. Asymptotic stability of the compact set $\mathcal{A}$ and an upper bound of the $\mathcal{L}_\infty$-gain of the event-triggered control system (4.1), (4.2), with event-triggering mechanism (4.6), with $\sigma_1 = \sigma_1 = 10^{-3}$, can be guaranteed using the impulsive system formulation (4.10) and the results of Theorem 4.3.5. This leads to the smallest upper bound on the $\mathcal{L}_\infty$-gain, given by $\kappa = 0.46$.

When we simulate the response of the system to the initial condition $\bar{x}(0) = 0$ and a disturbance satisfying $\|w(t)\| \leqslant 1$ for time $t \in [0, 10]$ and $\|w(t)\| \leqslant \frac{1}{4}$ for time $t \in [20, 30]$, as shown in Figure 4.4, we obtain the trajectories of z as also shown in Figure 4.4. In this figure, we can observe that the performance output z, as in (4.20), satisfies $\|z(t)\| \leqslant 0.3$ for time $t \in [0, 10]$ and $\|z(t)\| \leqslant 0.09$ for time $t \in [20, 30]$, which satisfies $\|z\|_{\mathcal{L}_\infty} \leqslant \kappa \|w\|_{\mathcal{L}_\infty} + \delta(0) = 0.46 \|w\|_{\mathcal{L}_\infty} + 0.17$, which is an upper bound of the $\mathcal{L}_\infty$-gain of Definition 4.3.4. Furthermore, we can also observe that the inter-event times are larger than 0.022 for $t \in [0, 10]$ and larger than 0.044 for $t \in [20, 30]$. This observation concurs with the result of Section 4.4, which stated that transmissions occur less often if the magnitude of the disturbance is smaller. Finally, since the system (4.41) is stable, it seems that the outputs of the plant and controller only have to be transmitted when disturbances are acting on the system or during transients (i.e., approximately for $t < 10$ and $t > 20$), and no transmissions occur when no disturbances are acting on the system and the systems is close to its steady state. One could say that event-triggered control only acts when it is necessary from a stability or performance point of view, which is a favourable property that makes event-triggered control of high interest. Traditional digital control systems with periodic transmissions do not have this appealing property.
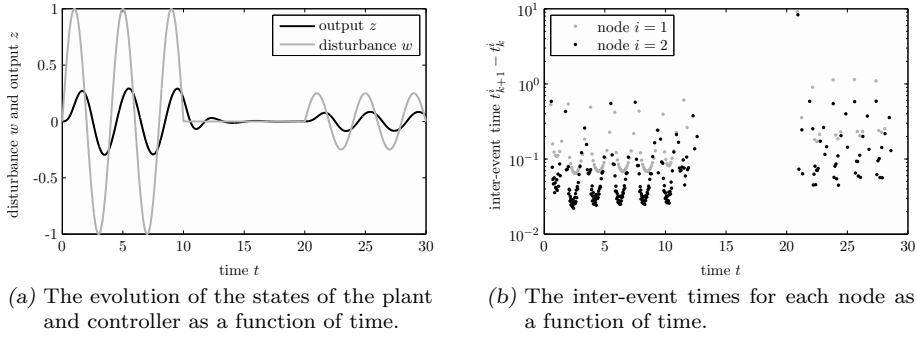
(a) The evolution of the states of the plant and controller as a function of time.

(b) The inter-event times for each node as a function of time.

Figure 4.4: Example 3.

4.7 Conclusions

In this chapter, we studied stability and $\mathcal{L}_\infty$-performance of event-triggered control systems for dynamical output-based controllers having decentralised event-triggering mechanisms. The proposed event-triggering mechanism unifies earlier proposals for event-triggering mechanisms, which were mainly applied to state-feedback controllers. Via an example (Example 2), we showed that direct extensions of existing event-triggering mechanisms for output-based controllers and decentralised event triggering are not applicable, as they result in inter-event times that converge to zero. Such Zeno behaviour is obviously undesirable in practical implementations and, therefore, extensions as proposed in this chapter are necessary.

To analyse the resulting event-triggered control system, we modelled the event-triggered control system as an impulsive system. The stability and $\mathcal{L}_\infty$-performance are then analysed using linear matrix inequalities. In addition, we provided expressions for lower bounds on the minimum inter-event times and we formally proved that by using an impulsive systems approach, stability and $\mathcal{L}_\infty$-performance can be guaranteed for event-triggered controllers with larger inter-event times than existing results in literature. These larger inter-event times ensure less usage of the communication resources. Using three numerical examples, we illustrated the main features of the presented theory. These examples show that indeed larger inter-event times can be obtained, that for unstable systems the outputs of the plants and controllers have to be transmitted less often when the state approaches the origin, and that for stable systems the outputs of the plant and controller only seem to be transmitted when disturbances are acting on the system. Especially, the latter example demonstrates the relevance of event-triggered control: The outputs of the plant and controller are only transmitted when needed from a performance point of

view. This provides significant benefits with respect to traditional sampled-data control systems, in which outputs of the plant and the controller are transmitted periodically.

Future work will focus on obtaining tighter upper bound on the magnitude of the ultimate bound and tighter lower bounds on the inter-event times, on creating codesign methods for the controller and event-triggering mechanism, on including transmission delays, packet dropouts and communication constraints, as are typically studied in the area of networked control systems, as well as making the implementation of the event-triggered control system self-triggered, as was done for state-feedback controllers and centralised event-triggering mechanisms in, e.g., [92, 130, 135].

5

Periodic Event-Triggered Control[1]

Abstract –   Event-triggered control (ETC) is a control strategy that is especially suited for applications where computation and communication resources are scarce. By updating and communicating sensor and actuator data only when needed for stability or performance purposes, ETC is capable of reducing the amount of computations and communications, while still retaining a satisfactory closed-loop performance. In this chapter, a novel ETC strategy is proposed by striking a balance between periodic control and ETC. This leads to so-called periodic event-triggered control (PETC), in which the advantage of reduced resource utilisation is preserved on the one hand, while, on the other hand, the conditions that trigger the events still have a periodic character. The latter aspect has the advantage that the event-triggering condition has to be verified only at the periodic sampling instants, instead of continuously, as in conventional ETC. This offers clear implementation benefits for PETC. Furthermore, it also guarantees a minimum inter-event time of (at least) the sampling interval of the event-triggering condition. The PETC strategies developed in this chapter apply to both static state-feedback and dynamical output-based controllers, as well as for both centralised and decentralised (periodic) event-triggering conditions. To analyse the stability and the $\mathcal{L}_2$-gain properties of the resulting PETC systems, three different approaches will be presented based on (i) piecewise linear systems (ii) discrete-time perturbed linear systems, and (iii) impulsive systems, respectively. Moreover, the advantages and disadvantages

---

[1]This chapter is based on [57].

of each of the three methods will be highlighted. The developed theory will be illustrated using two numerical examples.

5.1   Introduction

In many control applications nowadays, the controller is implemented on a digital platform. In such a digital implementation, the control task consists of sampling the outputs of the plant and computing and implementing new actuator signals. Typically, the control task is executed periodically, since this allows the closed-loop system to be analysed and the controller to be designed using the well-developed theory on sampled-data systems, see, e.g., [8, 27]. Although periodic sampling is preferred from an analysis and design point of view, it is sometimes less preferable from a resource utilisation point of view. Namely, executing the control task at times when no disturbances are acting on the system and the system is operating desirably is clearly a waste of computation resources. Moreover, in case the measured outputs and/or the actuator signals have to be transmitted over a shared (and possibly wireless) network, unnecessary utilisation of the network (or power consumption of the wireless radios) is introduced. To mitigate the unnecessary waste of computation and communication resources as in periodic sampled-data control, an alternative control paradigm, namely event-triggered control (ETC), has been proposed at the end of the nineties [6, 9, 59, 64]. ETC is a control strategy in which the control task is executed after the occurrence of an event, generated by some well-designed event-triggering condition, rather than the elapse of a certain fixed period of time, as in conventional periodic sampled-data control. In this way, ETC is capable of significantly reducing the number of control task executions, while retaining stability and a satisfactory closed-loop performance, as simulation and experimental results show in, e.g., [6, 9, 59, 64, 65, 83, 85, 111, 127].

Although the advantages of ETC are well-motivated and practical applications show its potential, relatively few theoretical results exist that study ETC systems, see, e.g., [10, 36, 46, 60, 66, 81, 90, 94, 107, 126, 136], in which several different ETC strategies are proposed. The main difference between the aforecited papers and the ETC strategy that will be proposed in this chapter is that in the former the event-triggering condition has to be monitored continuously, while in the latter the event-triggering condition is verified only periodically, and every sampling time it is decided whether or not to transmit new measurements and control signals. Only when necessary from a stability or performance point of view, the communication or computation resources are used. As a consequence, this control strategy aims at striking a balance between periodic sampled-data and event-triggered control and therefore we will propose to use the term *periodic event-triggered control* (PETC) for this class of ETC, while we will use the term continuous event-triggered control (CETC) to indicate the existing approaches [10, 36, 46, 66, 81, 90, 94, 107, 126, 136].

By mixing ideas from ETC and periodic sampled-data control, the benefits of reduced resource utilisation are preserved in PETC as transmissions and controller computations are *not* performed periodically, while the event-triggering conditions still have a periodic character. The latter aspect leads to several benefits, including a guaranteed minimum inter-event time of (at least) the sampling interval of the event-triggering condition. Furthermore, as already mentioned, the event-triggering condition has to be verified only at periodic sampling times, making PETC better suited for practical implementations as it can be implemented in more standard time-sliced embedded software architectures, while CETC requires dedicated analogue hardware to detect the events. Another advantage of PETC is that it can be transformed more easily into a self-triggered control variant [92, 130, 135] (at least in the case that the controller is a state-feedback controller), as we will also show in this chapter. Initial attempts towards what we refer here to as PETC were taken in [6, 60, 66], however only for restricted classes of systems and/or controllers (PID, static state feedback, or simple impulse controllers), and for particular event-triggering conditions without providing a general analysis framework.

We will therefore provide a general framework for the introduced class of PETC systems that allows to carry out stability and performance analyses. In fact, we will provide three different analysis approaches, namely: (i) a discrete-time piecewise linear (PWL) system approach, (ii) a discrete-time perturbed linear system approach, and (iii) an impulsive system approach. The first approach adopts PWL models [75, 120] and piecewise quadratic (PWQ) Lyapunov functions, which lead to LMI-based stability conditions for the PETC system. The second method, the one based on perturbed linear systems, can be seen as a discrete-time counterpart of the work in [126], which studied CETC. The essence of this approach is that the difference between the control signal obtained by a standard periodic controller and its event-triggered counterpart can be modelled as a disturbance, resulting in a perturbed linear system. This insight will be used to derive a sufficient condition for stability of the PETC system based on the $\mathcal{H}_\infty$-norm of the perturbed linear system. This leads to a simple stability test, which is, however, more conservative than the stability conditions based on the first approach. The third approach uses impulsive systems [50, 55], which explicitly include the intersample behaviour. Based on this modelling paradigm, we are able to provide guarantees on performance in terms of $\mathcal{L}_2$-gains from disturbance inputs to performance outputs. Besides developing these three analysis methods for PETC, we will also establish formal connections between the methods and highlight their advantages and disadvantages. Finally, we also present methods to compute guaranteed lower bounds on the inter-event times for PETC systems and we show how to convert PETC into self-triggered control [130].

In the first part of the chapter, we will present the three mentioned analysis approaches for the basic setup of state-feedback control system. However, as in

many practical situations not all the states can be measured directly, it is of interest to study output-based dynamic controllers as well, which we will do in the second part of the chapter. Another important issue is related to the question of handling the fact that sensors, actuators and controllers can be physically distributed over a wide area. In fact, a centralised event-triggering mechanism can be prohibitive in this case, as the conditions that generate events would need access to all the plant and controller outputs at every sampling time, which can be an unrealistic assumption in large-scale systems. To resolve this issue, in the second part of the chapter we will also propose decentralised periodic event-triggered conditions for output-based dynamic controllers. We consider both the case that multiple sensors and actuator nodes can transmit their data at the same transmission time, which is possible in case there is no interference during communication of different nodes, as well as the case where a shared communication medium is used and communication constraints prohibit that multiple nodes transmit simultaneously and, hence, the transmissions need to be scheduled by a scheduling protocol.

The remainder of this chapter is organised as follows. After introducing the necessary notational conventions at the end of this section, we introduce PETC and give the problem formulation in Section 5.2. In Section 5.3, the discrete-time PWL system approach, the discrete-time perturbed linear system approach and the impulsive system approach are presented. In Section 5.4, we discuss the advantages and disadvantages of the three different approaches. In Section 5.5, we discuss the minimum inter-event times and the transformation of PETC to self-triggered control, and, in Section 5.6, we will extend the ideas presented in the first part of this chapter towards output-based dynamic controllers and decentralised periodic event-triggered conditions with both unshared and shared communication channels (where in the latter case a scheduling protocol is needed). Before providing the conclusions in Section 5.8, we will provide numerical examples in Section 5.7 illustrating the main developments in this chapter. Appendix A.4 contains the proofs of the lemmas and theorems.

5.1.1 Nomenclature

For a vector $x \in \mathbb{R}^n$, we denote by $\|x\| := \sqrt{x^\top x}$ its 2-norm and by $x_{\mathcal{J}}$ the subvector formed by all components of x in the index set $\mathcal{J} \subseteq \{1, \ldots, n\}$.

For a symmetric matrix $A \in \mathbb{R}^{n \times n}$, $\lambda_{\max}(A)$ and $\lambda_{\min}(A)$ denote the maximum and minimum eigenvalue of A, respectively. For a matrix $A \in \mathbb{R}^{n \times m}$, we denote by $A^\top \in \mathbb{R}^{m \times n}$ its transposed and by $\|A\| := \sqrt{\lambda_{\max}(A^\top A)}$ its induced 2-norm. Furthermore, by $A_{\mathcal{J}\bullet}$ and $A_{\bullet\mathcal{J}}$, we denote the submatrices formed by taking all the rows of A in the index set $\mathcal{J} \subseteq \{1, \ldots, n\}$, and by all the columns of A in the index set $\mathcal{J} \subseteq \{1, \ldots, m\}$, respectively. By $\mathrm{diag}(A_1, \ldots, A_N)$, we denote a block-diagonal matrix with the entries $A_1, \ldots, A_N$ on the diagonal,

and for the sake of brevity we sometimes write symmetric matrices of the form $\begin{bmatrix} A & B \\ B^\top & C \end{bmatrix}$ as $\begin{bmatrix} A & B \\ \star & C \end{bmatrix}$ or $\begin{bmatrix} A & \star \\ B^\top & C \end{bmatrix}$. We call a matrix $P \in \mathbb{R}^{n \times n}$ positive definite and write $P \succ 0$, if P is symmetric and $x^\top P x > 0$ for all $x \neq 0$. Similarly, we use $P \succeq 0$, $P \prec 0$ and $P \preceq$ to denote that P is positive semidefinite, negative definite and negative semidefinite, respectively.

For a locally integrable signal $w : \mathbb{R}_+ \to \mathbb{R}^n$, where $\mathbb{R}_+$ denotes the set of nonnegative real numbers, we denote by $\|x\|_{\mathcal{L}_2} = (\int_0^\infty \|x(t)\|^2 \mathrm{d}t)^{1/2}$ its $\mathcal{L}_2$-norm, provided the integral is finite. Furthermore, we define the set of all locally integrable signals with a finite $\mathcal{L}_2$-norm as $\mathcal{L}_2$. For a signal $w : \mathbb{R}_+ \to \mathbb{R}^n$, we denote the limit from above at time $t \in \mathbb{R}_+$ by $w^+(t) = \lim_{s \downarrow t} w(s)$, provided that it exists.

5.2 Periodic Event-Triggered Control

In this section, we introduce periodic event-triggered control (PETC) and give a precise formulation of the stability and performance analysis problems we aim to solve in this chapter.

5.2.1 The Periodic Event-Triggered Control System

To introduce PETC, let us consider a linear time-invariant (LTI) plant, given by

$$\frac{\mathrm{d}}{\mathrm{d}t} x = A^p x + B^p \hat{u} + B^w w, \tag{5.1}$$

where $x \in \mathbb{R}^{n_x}$ denotes the state of the plant, $\hat{u} \in \mathbb{R}^{n_u}$ is the input applied to the plant, and $w \in \mathbb{R}^{n_w}$ is an unknown disturbance. In a conventional sampled-data state-feedback setting, the plant is controlled using a controller

$$\hat{u}(t) = K x(t_k), \quad \text{for} \quad t \in (t_k, t_{k+1}], \tag{5.2}$$

where t_k, $k \in \mathbb{N}$, are the sampling times, which are periodic in the sense that $t_k = kh$, $k \in \mathbb{N}$, for some properly chosen sampling interval $h > 0$.

Instead of using conventional periodic sampled-data control, we propose here to use PETC, meaning that at each sampling time $t_k = kh$, $k \in \mathbb{N}$, state measurements are transmitted over a communication network and the control values are updated only when necessary from a stability or performance point of view. This modifies the controller from (5.2) to

$$\hat{u}(t) = K \hat{x}(t), \quad \text{for} \quad t \in \mathbb{R}_+, \tag{5.3}$$

where $\hat{x}$ is a left-continuous signal[2], given for $t \in (t_k, t_{k+1}]$, $k \in \mathbb{N}$, by

$$\hat{x}(t) = \begin{cases} x(t_k), & \text{when } \mathcal{C}(x(t_k), \hat{x}(t_k)) > 0 \\ \hat{x}(t_k), & \text{when } \mathcal{C}(x(t_k), \hat{x}(t_k)) \leqslant 0 \end{cases} \tag{5.4}$$

---

[2]A signal $x : \mathbb{R}_+ \to \mathbb{R}^n$ is called left-continuous, if for all $t > 0$, $\lim_{s \uparrow t} x(s) = x(t)$.
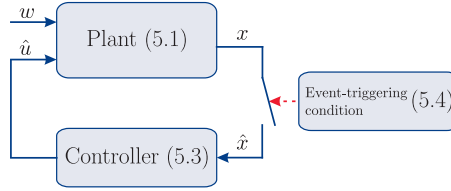
Figure 5.1: Event-triggered control schematic.

and some initial value for $\hat{x}(0)$. Hence, considering the configuration in Figure 5.1, the value $\hat{x}(t)$ can be interpreted as the most recently transmitted measurement of the state x to the controller at time t. Whether or not new state measurements are transmitted to the controller is determined by the event-triggering condition $\mathcal{C} : \mathbb{R}^{n_\xi} \to \mathbb{R}$ with $n_\xi := 2n_x$. In particular, if at time t_k it holds that $\mathcal{C}(x(t_k), \hat{x}(t_k)) > 0$, the state $x(t_k)$ is transmitted over the network to the controller and $\hat{x}$ and the control value $\hat{u}$ are updated accordingly at time t_k. In case $\mathcal{C}(x(t_k), \hat{x}(t_k)) \leqslant 0$, no new state information is sent to the controller, in which case the input $\hat{u}$ is not updated and kept the same for (at least) another sampling interval, implying that no control computations are needed and no new state measurements and control values have to be transmitted.

5.2.2   *Quadratic Event-Triggering Conditions*

In this chapter, we focus on *quadratic* event-triggering conditions, i.e., $\mathcal{C}$, as in (5.4), is given by

$$\mathcal{C}(\xi(t_k)) = \xi^\top(t_k) Q \xi(t_k) > 0, \tag{5.5}$$

where $\xi := [x^\top \ \hat{x}^\top]^\top \in \mathbb{R}^{n_\xi}$, for some symmetric matrix $Q \in \mathbb{R}^{n_\xi \times n_\xi}$. To show that these event-triggering conditions form a relevant class, we will review some existing event-triggering conditions that have been applied in the context of *continuous* event-triggered control (CETC), and show how they can be written as quadratic event-triggering conditions for PETC as in (5.5).

A) Event-Triggering Conditions Based on the State Error: An important class of event-triggering conditions, which has been applied to CETC in [126, 136], are given by

$$\|\hat{x}(t_k) - x(t_k)\| > \sigma \|x(t_k)\|, \tag{5.6}$$

for $k \in \mathbb{N}$, where $\sigma > 0$. Clearly, (5.6) is of the form (5.5) with

$$Q = \begin{bmatrix} (1 - \sigma^2)I & -I \\ -I & I \end{bmatrix}. \tag{5.7}$$

B) Event-Triggering Conditions Based on the Input Error: In [36], where the objective was to develop *output-based* CETC, an event-triggering condition was proposed that would translate for state-feedback-based PETC systems to

$$\|K\hat{x}(t_k) - Kx(t_k)\| > \sigma\|Kx(t_k)\|, \tag{5.8}$$

where $\sigma > 0$. Condition (5.8) is equivalent to $\|\hat{u}(t_k) - u(t_k)\| > \sigma\|u(t_k)\|$ in which $u(t_k) = Kx(t_k)$ is the control value determined on the basis of $x(t_k)$ as in standard periodic state-feedback (see (5.2)). The event-triggering condition (5.8) is equivalent to (5.5), in which

$$Q = \begin{bmatrix} (1 - \sigma^2)K^\top K & -K^\top K \\ -K^\top K & K^\top K \end{bmatrix}. \tag{5.9}$$

This scheme could be implemented at the sensor-to-controller channel (using (5.8)), but it is more natural to implement this particular event-triggering condition in the controller-to-actuator channel to determine whether, at time t_k, it is necessary to transmit the newly computed control value $u(t_k) = Kx(t_k)$ to the actuators, or that the latest sent value $\hat{u}(t_k)$ is still adequate.

C) Event-Triggering Conditions as in [135]: A PETC interpretation of the condition used in [135] is

$$\|\hat{u}(t_k) - u(t_k)\|^2 > (1 - \beta^2)\|x(t_k)\|^2 + \|\hat{u}(t_k)\|^2, \tag{5.10}$$

where $0 < \beta \leqslant 1$ and, again, $u(t_k) = Kx(t_k)$, which results in an event-triggering condition (5.5) with

$$Q = \begin{bmatrix} (\beta^2 - 1)I + K^\top K & -K^\top K \\ -K^\top K & 0 \end{bmatrix}, \tag{5.11}$$

as $\hat{u}(t_k) = K\hat{x}(t_k)$, $k \in \mathbb{N}$.

D) Event-Triggering Conditions Based on Lyapunov Functions: In [131, 137], in the context of CETC, and in [92], in the context of self-triggered control [130], Lyapunov-based event-triggering conditions have been proposed. For PETC, a Lyapunov-based event-triggering condition can be derived using the discretisation of (5.1), with $w = 0$, given by

$$x(t_{k+1}) = Ax(t_k) + B\hat{u}_k \tag{5.12}$$

in which $A := e^{A^p h}$, $B = \int_0^h e^{A^p s}B^p \mathrm{d}s$, and $\hat{u}_k := \lim_{t \downarrow t_k} \hat{u}(t)$ taken as $Kx(t_k)$, $k \in \mathbb{N}$, as in (5.2). In case K is designed such that (5.12) in closed loop with (5.2) is exponentially stable, which is equivalent to requiring that the matrix $A + BK$ has all its eigenvalues inside the open unit circle, there exists a

quadratic Lyapunov function of the form $V(x) = x^\top P x$, $x \in \mathbb{R}^{n_x}$, with $P \succ 0$ and

$$(A + BK)^\top P (A + BK) \preceq \lambda P, \tag{5.13}$$

for some $0 \leqslant \lambda < 1$. This implies the decrease of the Lyapunov function in the sense that $V(x(t_{k+1})) \leqslant \lambda V(x(t_k))$ for all $k \in \mathbb{N}$ along the solutions of (5.12) and (5.2). In [92, 131, 137], an event-triggering condition has been proposed (in the context of CETC) based on the existence of V by selecting $\lambda \leqslant \beta < 1$ and only updating $\hat{x}$ at time t_k to $x(t_k)$ when

$$(A x(t_k) + BK \hat{x}(t_k))^\top P (A x(t_k) + BK \hat{x}(t_k)) > \beta\ x^\top(t_k) P x(t_k). \tag{5.14}$$

Hence, only when the current input $\hat{u}(t_k) = K \hat{x}(t_k)$ no longer guarantees a decrease of the Lyapunov function V with a factor β, the signals $\hat{x}$ and $\hat{u}$ are updated. Obviously, (5.14) can be written as in (5.5) by taking

$$Q = \begin{bmatrix} A^\top P A - \beta P & A^\top P B K \\ (BK)^\top P A & (BK)^\top P B K \end{bmatrix}. \tag{5.15}$$

The interest in [92, 131, 137] for this event-triggering condition is motivated by the fact that for any choice of β, satisfying $\lambda \leqslant \beta < 1$, V is a Lyapunov function for the PETC system (5.1), with $w = 0$, (5.3) and (5.4) with event-triggering condition (5.14), and thus stability of the resulting PETC system is inherently guaranteed. Note that even though this event-triggering condition was originally proposed for the case where $w = 0$, it is certainly of interest to analyse this event-triggering condition in the new setting of PETC and in the presence of disturbances ($w \neq 0$). Namely, using the techniques developed in this chapter, closed-loop performance guarantees in terms of disturbance suppression can be made for this event-triggering condition.

The four mentioned examples show the relevance of the class of *quadratic* event-triggering conditions (5.5), as their CETC counterparts have been considered in the literature extensively.

Remark 5.2.1. *Besides on the parameter σ in (5.6) or (5.8), or on the parameter β in (5.10) or (5.14), the occurrence of events in PETC and the overall closed-loop behaviour also depends on the choice of the sampling interval h, as events can only occur at instants $t_k = kh$, $k \in \mathbb{N}$, see (5.4). Hence, given the plant (5.1) and the controller (5.3) with a given matrix K, also the sampling interval h should be chosen such that the PETC system is stable and has a certain closed-loop performance. As these properties can be guaranteed by using the techniques developed in this chapter, a framework will be offered to properly select h (and σ and β). Obviously, the sampling interval h determines directly a lower bound on the minimum inter-event time, as events can only occur at the sampling instants of the event-triggering condition, which is directly determined*

by the choice of h. However, even though h directly provides a guarantee on the minimum inter-event time, by changing the sampling interval h of the event-triggering condition, the behaviour (in terms of solutions) of the PETC system, given by (5.1), (5.3), (5.4) and (5.5), is changed and, thereby, also the sampling times t_k, $k \in \mathbb{N}$, at which the event-triggering condition holds true, generally change. How the sampling interval h influences the (average) number of events within a certain time interval is currently an unsolved problem that requires future attention. Still, a significant benefit of PETC, compared to CETC, is that the guaranteed minimum inter-event time can be directly tuned by choosing a certain h, while choosing the event-triggering condition for CETC, such that a certain minimum inter-event time is guaranteed, is much more difficult.

5.2.3 Problem Formulation

To obtain a complete model of the PETC system, we combine (5.1), (5.3), (5.4) and (5.5), and define $\xi := [x^\top \ \hat{x}^\top]^\top$ and

$$\bar{A} := \begin{bmatrix} A^p & B^p K \\ 0 & 0 \end{bmatrix}, \quad \bar{B} := \begin{bmatrix} B^w \\ 0 \end{bmatrix}, \quad J_1 := \begin{bmatrix} I & 0 \\ I & 0 \end{bmatrix}, \quad J_2 := \begin{bmatrix} I & 0 \\ 0 & I \end{bmatrix}, \qquad (5.16)$$

to arrive at an impulsive system [50, 55] given by

$$\frac{\mathrm{d}}{\mathrm{d}t} \begin{bmatrix} \xi \\ \tau \end{bmatrix} = \begin{bmatrix} \bar{A}\xi + \bar{B}w \\ 1 \end{bmatrix}, \quad \text{when } \tau \in [0, h], \tag{5.17a}$$

$$\begin{bmatrix} \xi^+ \\ \tau^+ \end{bmatrix} = \begin{cases} \begin{bmatrix} J_1 \xi \\ 0 \end{bmatrix}, & \text{when } \xi^\top Q \xi > 0, \ \tau = h \\ \begin{bmatrix} J_2 \xi \\ 0 \end{bmatrix}, & \text{when } \xi^\top Q \xi \leqslant 0, \ \tau = h \end{cases} \tag{5.17b}$$

$$z = \bar{C}\xi + \bar{D}w, \tag{5.17c}$$

where $z \in \mathbb{R}^{n_z}$ is a performance output with $\bar{C}$ and $\bar{D}$ appropriately chosen matrices, and the state τ keeps track of the time elapsed since the last sampling time.

Besides the introduction of PETC, the main objective of this chapter is to analyse and design event-triggering conditions of the form (5.5) such that the corresponding closed-loop system (5.1), (5.3), (5.4) and (5.5) is stable and has a certain closed-loop performance, both defined in an appropriate sense, while the number of transmissions between the plant and the controller is minimised. To make precise what we mean by stability and performance, let us define the notion of global exponential stability and $\mathcal{L}_2$-performance, where the latter definition is adopted from [129].

Definition 5.2.2. *The PETC system* (5.1), (5.3) (5.4) *and* (5.5) *is said to be globally exponentially stable (GES), if there exist $c > 0$ and $\rho > 0$ such that*

for all solutions to the impulsive system (5.17) *with* $\tau(0) \in [0, h]$ *and* $w = 0$, *it holds that* $\|\xi(t)\| \leqslant ce^{-\rho t}\|\xi(0)\|$ *for all* $t \in \mathbb{R}_+$. *In this case, we call* ρ *an (upper bound on the) decay rate.*

Definition 5.2.3. *The PETC system* (5.1), (5.3) (5.4) *and* (5.5), *with* (5.17c), *is said to have an* $\mathcal{L}_2$-*gain from* w *to* z *smaller than or equal to* γ, *if there is a function* $\beta : \mathbb{R}^{n_\xi} \to \mathbb{R}_+$ *such that for any* $w \in \mathcal{L}_2$, *any initial state* $\xi(0) = \xi_0 \in \mathbb{R}^{n_\xi}$ *and* $\tau(0) \in [0, h]$, *the corresponding solution satisfies*

$$\|z\|_{\mathcal{L}_2} \leqslant \beta(\xi_0) + \gamma\|w\|_{\mathcal{L}_2}. \tag{5.18}$$

In fact, as will be demonstrated below, we can take $\beta(s) = c\|s\|$, $s \in \mathbb{R}^{n_\xi}$, for some $c \geqslant 0$.

5.3 Stability and $\mathcal{L}_2$-Gain Analysis of the PETC System

In this section, we analyse stability and performance of the PETC system given by (5.1), (5.3), (5.4), (5.5) and (5.17c) using three different approaches, namely: (i) a discrete-time piecewise linear (PWL) system approach, (ii) a discrete-time perturbed linear system approach, and (iii) an impulsive system approach. In particular, in the first two approaches we will focus on GES only and, thus, take $w = 0$, while in the third approach we also analyse the $\mathcal{L}_2$-gain of the PETC system.

5.3.1 A Piecewise Linear System Approach

To obtain a discrete-time PWL model, see, e.g., [75, 120], we discretise the impulsive system (5.17), with $\tau(0) = h$ and $w = 0$, at the sampling times $t_k = kh$, $k \in \mathbb{N}$. By defining the state variable $\xi_k := \xi(t_k)$ (and assuming ξ to be left-continuous), we obtain the bimodal PWL model

$$\xi_{k+1} = \begin{cases} A_1 \xi_k, & \text{when } \xi_k^\top Q \xi_k > 0, \\ A_2 \xi_k, & \text{when } \xi_k^\top Q \xi_k \leqslant 0, \end{cases} \tag{5.19}$$

where

$$A_1 = e^{\bar{A}h} J_1 = \begin{bmatrix} A + BK & 0 \\ I & 0 \end{bmatrix}, \qquad A_2 = e^{\bar{A}h} J_2 = \begin{bmatrix} A & BK \\ 0 & I \end{bmatrix}, \tag{5.20}$$

in which $A := e^{A^p h}$ and $B := \int_0^h e^{A^p s} B^p \mathrm{d}s$.

Using the PWL model (5.19) and a piecewise quadratic (PWQ) Lyapunov function of the form

$$V(\xi) = \begin{cases} \xi^\top P_1 \xi, & \text{when } \xi^\top Q \xi > 0, \\ \xi^\top P_2 \xi, & \text{when } \xi^\top Q \xi \leqslant 0, \end{cases} \tag{5.21}$$

we can guarantee GES of the PETC system given by (5.1), (5.3) (5.4) and (5.5).

Theorem 5.3.1. *The PETC system given by* (5.1), (5.3) (5.4) *and* (5.5) *is GES with convergence rate ρ, if there exist matrices P_1, P_2 and scalars $\alpha_{ij}, \beta_{ij}, \kappa_i \geqslant 0$, $i, j \in \{1, 2\}$, satisfying*

$$e^{-2\rho h} P_i - A_i^\top P_j A_i + (-1)^i \alpha_{ij} Q + (-1)^j \beta_{ij} A_i^\top Q A_i \succeq 0, \qquad (5.22)$$

for all $i, j \in \{1, 2\}$, and

$$P_i + (-1)^i \kappa_i Q \succ 0, \qquad (5.23)$$

for all $i \in \{1, 2\}$.

Proof. The proof is given in Appendix A.4. $\qquad\qquad\qquad\qquad\square$

Remark 5.3.2. *The conditions in Theorem 5.3.1 guarantee not only GES for the discrete-time PWL model (5.19) and the impulsive system (5.17) with $w = 0$, but also for the regularisation of (5.19) as in [78], which has $\xi_{k+1} \in \{A_1 \xi_k, A_2 \xi_k\}$ when $\xi_k^\top Q \xi_k = 0$, and the Krasovskii regularisation [112] of (5.17) with $w = 0$, which uses $\xi^+ \in \{J_1 \xi, J_2 \xi\}$ when $\xi^\top Q \xi = 0$ (and $\tau = h$). Due to GES of these regularisation, we have robust stability properties for (5.17) and (5.19), see [23, 78].*

Remark 5.3.3. *Instead of the Lyapunov function (5.21), which is based on two regions defined by the sign of $\xi^\top Q \xi$, a more versatile piecewise quadratic Lyapunov function*

$$V(\xi) = \xi^\top P_i \xi \quad when \ \ \xi \in \Omega_i, \qquad (5.24)$$

where $\Omega_i \subset \mathbb{R}^{n_\xi}$, can be used. For instance,

$$\Omega_i := \left\{ \xi \in \mathbb{R}^{n_\xi} \, \middle| \, \rho_{i-1} \|\xi\|^2 \leqslant \xi^\top Q \xi < \rho_i \|\xi\|^2 \right\}, \qquad (5.25)$$

for $i \in \{1, 2, \ldots, L\}$, can be used, where $-\infty =: \rho_0 < \rho_1 < \rho_2 < \ldots < \rho_r := 0 < \rho_{r+1} < \ldots < \rho_{L-1} < \rho_L := \infty$ are fixed for the analysis. This can lead to less conservative LMI-based stability conditions that can be obtained in the similar fashion as the LMIs in Theorem 5.3.1.

5.3.2 A Perturbed Linear System Approach

An alternative approach to analyse GES of the PETC system or to design an event-triggering condition that guarantees GES is based on ℓ_2-gain techniques. This approach can be seen as the PETC counterpart of the CETC approach taken in [126] using input-to-state stability (ISS) for nonlinear plants and state-feedback controllers, which was specialized in [36] using $\mathcal{L}_2$-gain analysis in the context of linear plants and output-based controllers. Transforming the ideas

presented in [36, 126] to PETC with event-triggering condition (5.6) results in studying the ℓ_2-gain of the perturbed discrete-time linear system

$$x_{k+1} = (A + BK)x_k + BKe_k, \tag{5.26}$$

where $x_k = x(t_k)$, $\hat{x}_k = \lim_{t \downarrow t_k} \hat{x}(t)$ (recall that the signal $\hat{x}$ is piecewise constant and left-continuous, cf. (5.4)), $e_k := \hat{x}_k - x_k$, $k \in \mathbb{N}$, $A = e^{A^p h}$ and $B = \int_0^h e^{A^p s} B^p \mathrm{d}s$. The system (5.26) is obtained by discretising (5.1), with $w = 0$, and combining it with (5.3). The system expresses how the plant (5.1) with the event-triggered controller (5.3) is perturbed when compared to the original periodic sampled-data control system given by (5.1) and (5.2).

The following stability result, which could be seen as the PETC variant of the result in [126], relies on the concepts of dissipativity, storage functions and supply rates, see, e.g., [19, 139]. Note that the result we present below uses the event-triggering condition that has been used in [126], i.e., it uses (5.6). A similar result can be obtained for event-triggering condition (5.8) by modifying (5.26) into $x_{k+1} = (A+BK)x_k + Be_k$ and then $e_k := \hat{u}_k - u_k$, $k \in \mathbb{N}$. Although we will not formally establish a stability result for the event-triggering condition (5.8), we will reflect on it in Remark 5.3.5.

Theorem 5.3.4. *Suppose that the perturbed linear system* (5.26) *admits a storage function* $\bar{V}(x) = x^\top \bar{P}x$ *with* $\bar{P}$ *a symmetric positive definite matrix for supply rate[3]* $-\theta^2\|x\|^2 + \|e\|^2$, *i.e., the dissipation inequality*

$$\bar{V}(x_{k+1}) - \bar{V}(x_k) \leqslant -\theta^2\|x_k\|^2 + \|e_k\|^2, \ k \in \mathbb{N} \tag{5.27}$$

is satisfied for any disturbance sequence $\{e_k\}_{k\in\mathbb{N}}$ *and all corresponding solutions* $\{x_k\}_{k\in\mathbb{N}}$. *Then the PETC system given by* (5.1), (5.3) (5.4), *with* (5.6) *is GES for any* $0 < \sigma < \theta$.

Proof. It is possible to give a direct proof on the basis of (5.27) along the lines of [126]. For reasons of brevity, we will not give a direct proof, but point out that the proof follows from Theorem 5.4.1 below together with Theorem 5.3.1 above. $\qquad\square$

Observe that the existence of a storage function $\bar{V}$ satisfying the dissipation inequality (5.27) proves that (5.26) has an ℓ_2-gain smaller than or equal to $1/\theta$ from e to x. To obtain the largest (minimum) inter-event times, it follows from (5.6) that σ should be as large as possible and thus that θ should be maximised, while satisfying (5.27). This corresponds to determining the true ℓ_2-gain $1/\theta^*$ of (5.26) from e to x, which is equal to the $\mathcal{H}_\infty$-norm of the system (5.26), with

---

[3]We scaled the constant in front of $\|e\|^2$ to 1. Note that this is without loss of generality as P and θ can be scaled as well.

output x_k, given by $\sup_{\omega \in [0,\pi]} \|(e^{j\omega}I - A - BK)^{-1}BK)\|$. Alternatively, the $\mathcal{H}_\infty$-norm can be computed by maximising θ^2 subject to $\bar{P} \succ 0$ and

$$\begin{bmatrix} \bar{P} - (A+BK)^\top \bar{P}(A+BK) - \theta^2 I & \star \\ -(BK)^\top \bar{P}(A+BK) & I - (BK)^\top \bar{P}BK \end{bmatrix} \succ 0, \qquad (5.28)$$

see, e.g., [19]. The supremal θ^* satisfying (5.28) gives rise to the ℓ_2-gain of $1/\theta^*$ and guarantees stability of the PETC system (5.1), (5.3), (5.4), with (5.6) for any $0 < \sigma < \theta^* = 1/(\sup_{\omega \in [0,\pi]} \|(e^{j\omega}I - A - BK)^{-1}BK\|)$. Hence, a standard $\mathcal{H}_\infty$-norm calculation for a linear system provides stability bounds in terms of σ for the event-triggering condition (5.6) (or (5.8)). It is beneficial that the stability bounds can be obtained with simple $\mathcal{H}_\infty$-norm calculations. However, in Section 5.4, we will formally show that the PWL system approach, although computationally somewhat more complex, yields larger bounds on σ for which GES can be guaranteed.

Remark 5.3.5. *If $A + BK$ has all its eigenvalues inside the unit circle, then the PETC system (5.1), (5.3), (5.4), with event-triggering condition (5.6) or (5.8) is GES for sufficiently small values of σ (and thus a high number of transmissions and control updates). Indeed, if $A + BK$ has all its eigenvalues inside the unit circle, it is well known that the $\mathcal{H}_\infty$-norms given by $1/\theta^* = \sup_{\omega \in [0,\pi]} \|(e^{j\omega}I - A - BK)^{-1}BK\|$ in case of (5.6), and $1/\theta^* = \sup_{\omega \in [0,\pi]} \|K(e^{j\omega}I - A - BK)^{-1}B\|$ in case of (5.8) are finite and hence, for any $0 < \sigma < \theta^*$ GES of the corresponding PETC systems is guaranteed.*

5.3.3 An Impulsive System Approach

In this section, we will apply stability and performance analysis techniques to the impulsive system (5.17) directly. Since the impulsive model explicitly includes the behaviour of the system in between the sampling times, it allows us to analyse the performance in terms of the $\mathcal{L}_2$-gain from a disturbance w to a performance output z.

The analysis is based on a Lyapunov/storage function of the form

$$V(\xi, \tau) = \xi^\top P(\tau)\xi, \qquad (5.29)$$

for $\xi \in \mathbb{R}^{n_\xi}$ and $\tau \in [0, h]$, where $P : [0, h] \to \mathbb{R}^{n_\xi \times n_\xi}$ with $P(\tau) \succ 0$, for $\tau \in [0, h]$. The choice of Lyapunov function is inspired by the developments in [33, 50]. The function $P : [0, h] \to \mathbb{R}^{n_\xi \times n_\xi}$ will be chosen such that it becomes a candidate storage function for the system (5.17) with the supply rate $\gamma^{-2} z^\top z - w^\top w$. In particular, we will select the matrix function P to satisfy the Riccati differential equation (where we omitted τ for compactness of notation)

$$\frac{\mathrm{d}}{\mathrm{d}\tau}P = -\bar{A}^\top P - P\bar{A} - 2\rho P - \gamma^{-2}\bar{C}^\top \bar{C}$$
$$-(P\bar{B} + \gamma^{-2}\bar{C}^\top \bar{D})M(\bar{B}^\top P + \gamma^{-2}\bar{D}^\top \bar{C}), \qquad (5.30)$$

provided the solution exists on $[0, h]$ for a desired convergence rate $\rho > 0$, in which $M := (I - \gamma^{-2}\bar{D}^\top\bar{D})^{-1}$ is assumed to exist and to be positive definite, which means that $\gamma^2 > \lambda_{\max}(\bar{D}^\top\bar{D})$. As we will show in the proof of Theorem 5.3.7, this choice for the matrix function P yields the inequality

$$\frac{\mathrm{d}}{\mathrm{d}t}V \leqslant -2\rho V - \gamma^{-2}z^\top z + w^\top w, \tag{5.31}$$

during the flow (5.17a) along the solutions of the impulsive system (5.17). Combining inequality (5.31) with the conditions

$$V(J_1\xi, 0) \leqslant V(\xi, h), \text{ for all } \xi \text{ with } \xi^\top Q\xi > 0, \tag{5.32a}$$

$$V(J_2\xi, 0) \leqslant V(\xi, h), \text{ for all } \xi \text{ with } \xi^\top Q\xi \leqslant 0, \tag{5.32b}$$

which imply that the storage function does not increase during the jumps (5.17b) of the impulsive system (5.17), we can guarantee that the $\mathcal{L}_2$-gain from w to z is smaller than or equal to γ, see, e.g., [62]. The result that we present below, is based on verifying the satisfaction of (5.32) by relating $P_0 := P(0)$ to $P_h := P(h)$. To do so, we introduce the Hamiltonian matrix

$$H := \begin{bmatrix} \bar{A} + \rho I + \gamma^{-2}\bar{B}M\bar{D}^\top\bar{C} & \bar{B}M\bar{B}^\top \\ -\bar{C}^\top L\bar{C} & -(\bar{A} + \rho I + \gamma^{-2}\bar{B}M\bar{D}^\top\bar{C})^\top \end{bmatrix}, \tag{5.33}$$

with $L := (\gamma^2 I - \bar{D}\bar{D}^\top)^{-1}$, which is positive definite again if $\gamma^2 > \lambda_{\max}(\bar{D}^\top\bar{D}) = \lambda_{\max}(\bar{D}\bar{D}^\top)$, and the matrix exponential

$$F(\tau) := e^{-H\tau} = \begin{bmatrix} F_{11}(\tau) & F_{12}(\tau) \\ F_{21}(\tau) & F_{22}(\tau) \end{bmatrix}, \tag{5.34}$$

allowing us to provide the explicit solution to the Riccati differential equation (5.30), yielding

$$P_0 = (F_{21}(h) + F_{22}(h)P_h)(F_{11}(h) + F_{12}(h)P_h)^{-1}, \tag{5.35}$$

provided that the solution (5.35) is well defined on $[0, h]$. To guarantee this, we will use the following assumption.

Assumption 5.3.6. *$F_{11}(\tau)$ is invertible for all $\tau \in [0, h]$.*

Before presenting the main result, observe that Assumption 5.3.6 is always satisfied for sufficiently small h. Namely, $F(\tau) = e^{-H\tau}$ is a continuous function and we have that $F_{11}(0) = I$. Let us also introduce the notation $\bar{F}_{11} := F_{11}(h)$, $\bar{F}_{12} := F_{12}(h)$, $\bar{F}_{21} := F_{21}(h)$ and $\bar{F}_{22} := F_{22}(h)$, and a matrix $\bar{S}$ that satisfies $\bar{S}\bar{S}^\top := -\bar{F}_{11}^{-1}\bar{F}_{12}$. A matrix $\bar{S}$ exists under Assumption 5.3.6, because this assumption will guarantee that the matrix $-\bar{F}_{11}^{-1}\bar{F}_{12}$ is positive semidefinite, as we will show in the proof of the theorem presented below.

Theorem 5.3.7. *Consider the impulsive system* (5.17) *and let* $\rho > 0$, $\gamma > \sqrt{\lambda_{max}(\bar{D}^\top \bar{D})}$, *and Assumption 5.3.6 hold. Suppose that there exist a matrix* $P_h \succ 0$, *and scalars* $\mu_i \geqslant 0$, $i \in \{1, 2\}$, *such that*

$$\begin{bmatrix} P_h + (-1)^i \mu_i Q & J_i^\top \bar{F}_{11}^{-\top} P_h \bar{S} & J_i^\top (\bar{F}_{11}^{-\top} P_h \bar{F}_{11}^{-1} + \bar{F}_{21} \bar{F}_{11}^{-1}) \\ \star & I - \bar{S}^\top P_h \bar{S} & 0 \\ \star & \star & \bar{F}_{11}^{-\top} P_h \bar{F}_{11}^{-1} + \bar{F}_{21} \bar{F}_{11}^{-1} \end{bmatrix} \succ 0, \quad (5.36)$$

for $i \in \{1, 2\}$. *Then, the PETC system given by* (5.1), (5.3) (5.4), (5.5) *and* (5.17c) *is GES with convergence rate* ρ *(when* $w = 0$*) and has an* $\mathcal{L}_2$-gain *from* w *to* z *smaller than or equal to* γ.

Proof. The proof is given in Appendix A.4. □

The results of Theorem 5.3.7 guarantee both GES (for $w = 0$) and an upper bound on the $\mathcal{L}_2$-gain. In case disturbances are absent (i.e., $w = 0$), the conditions of Theorem 5.3.7 simplify and GES can be guaranteed using the following corollary.

Corollary 5.3.8. *Consider the impulsive system* (5.17) *and let* $\rho > 0$ *be given. Assume there exist a matrix* $P_h \succ 0$ *and scalars* $\mu_i \geqslant 0$, $i \in \{1, 2\}$, *such that*

$$\begin{bmatrix} e^{-2\rho h} P_h + (-1)^i \mu_i Q & J_i^\top e^{\bar{A}^\top h} P_h \\ \star & P_h \end{bmatrix} \succ 0, \quad (5.37)$$

for all $i \in \{1, 2\}$. *Then, the PETC system given by* (5.1), (5.3) (5.4) *and* (5.5) *is GES (for* $w = 0$*) with convergence rate* ρ.

Proof. The proof is given in Appendix A.4. □

5.4   Comparison of the Modelling Approaches

So far, we have developed three approaches for the analysis of the PETC system, namely (i) a discrete-time PWL system approach, (ii) a discrete-time perturbed linear system approach and (iii) an impulsive system approach. When comparing the different analysis approaches, several observations can be made.

The first observation to be made is that the perturbed linear system approach allows the PETC system to be analysed using a simple $\mathcal{H}_\infty$-norm computation (in case of event-triggering conditions (5.6) and (5.8)), which is of lower computational complexity than the other two approaches. The second observation is that the impulsive system approach is the only approach of the three that allows the $\mathcal{L}_2$-gain from w to z to be studied at this point, which makes this approach important for PETC. Note that the $\mathcal{L}_2$-gain from w to z could also be studied using a PWL approach by analysing the intersample behaviour in a way that has been done for networked control systems in [142].

However, this indirect analysis typically leads to conservative upper bounds on the $\mathcal{L}_2$-gain, as evidenced in [142]. Finally, the PWL system approach is relevant since, when comparing it to the perturbed linear system and the impulsive system approach, we can show that for stability analysis (when $w = 0$), and using Corollary 5.3.8 for the impulsive system approach, the latter two approaches can never prove GES, if the PWL system approach does not result in a GES guarantee. Hence, the PWL system approach never yields more conservative results than the other two approaches when stability is analysed. We will make this result precise in the two theorems we present below.

Based on the discussion above and the two technical results we present below, we can conclude that each of the three presented modelling approaches are of independent interest. Namely, the PWL system approach provides the least conservative LMI-based results to perform the stability analysis, the perturbed linear system approach has the lowest computational complexity (however its usage is restricted to two types of quadratic event-triggering conditions), while the impulsive system approach is the only method able to perform a direct $\mathcal{L}_2$-gain analysis.

5.4.1 Comparison between the PWL System Approach and the Perturbed Linear System Approaches

We will now formally show that for the particular event-triggering condition (5.6) (or (5.8)), the perturbed linear system approach of Section 5.3.2 can never do better, in terms of the range of σ for which GES of the PETC system can be proven, than the PWL system approach presented in Section 5.3.1.

Theorem 5.4.1. *In case the perturbed linear system approach in Section 5.3.2 guarantees GES of the PETC system, given by (5.1), (5.3), (5.4), and (5.6) (or (5.8)) for some $\sigma > 0$, using Theorem 5.3.4, then the PWL system approach of Section 5.3.1, using Theorem 5.3.1, proves GES of the PETC system for the same $\sigma > 0$. In other words, satisfaction of (5.28) for some $\bar{P} \succ 0$ and $\theta > \sigma$, implies satisfaction of (5.22) and (5.23), for some P_1, P_2 and scalars $\alpha_{ij}, \beta_{ij}, \kappa_i \geqslant 0$, $i,j \in \{1,2\}$ and with Q as in (5.7) with the same σ.*

Proof. The proof is given in Appendix A.4. □

In fact, the proof of this theorem establishes that the perturbed linear system approach results in a *quadratic* Lyapunov function (cf. (A.124)) for the PWL model and therefore does not exploit the flexibility of PWQ Lyapunov functions (5.21), as offered by the PWL system approach. Besides this, another source of conservatism in the perturbed linear system approach is that it does not truly model the PETC system as the solutions of $\hat{x}$ are not modelled explicitly (but only account for the difference between x and $\hat{x}$ through the perturbation e in (5.26)), while the PWL model does.

5.4.2 Comparison between the PWL System Approach and the Impulsive System Approach

We will now show that the impulsive system approach of Section 5.3.3 can never outperform the PWL system approach in stability analysis of Section 5.3.1 in terms of stability guarantees. In other words, if GES of the PETC system cannot be proven using the PWL system approach, it cannot be proven using the impulsive system approach. To formally prove this statement, we substitute (5.20) into (5.37), and apply a Schur complement to (5.37), yielding that

$$e^{-2\rho h} P_h + (-1)^i \mu_i Q - A_i^\top P_h A_i \succ 0, \tag{5.38}$$

for all $i \in \{1,2\}$, $P_h \succ 0$ and $\mu_i \geqslant 0$, $i \in \{1,2\}$. As these conditions are equivalent to the LMIs (5.22), with $P_1 = P_2 = P_h$, $\alpha_{ij} = \mu_i$ and $\beta_{ij} = 0$, $i,j \in \{1,2\}$, this shows that if the LMIs (5.37) are feasible, then the LMIs (5.22) are feasible. In addition, since $P_h \succ 0$ the LMIs (5.23) hold with $\kappa_1 = \kappa_2 = 0$. Hence, we have proven the following result.

Theorem 5.4.2. *In case the impulsive system approach in Section 5.3.3 guarantees GES with convergence rate ρ of the PETC system, given by (5.1), (5.3), (5.4) and (5.5), using Corollary 5.3.8, then the PWL system approach of Section 5.3.1, using Theorem 5.3.1, proves GES with convergence rate ρ of the PETC system as well. In other words, for given $\rho > 0$ satisfaction of (5.37) for some $P_h \succ 0$, $\mu_i \geqslant 0$, $i \in \{1,2\}$, implies satisfaction of (5.22) and (5.23), for some P_1, P_2 and scalars $\alpha_{ij}, \beta_{ij}, \kappa_i \geqslant 0$, $i,j \in \{1,2\}$.*

5.5 Minimum Inter-Event Times and Self-Triggered Implementations

Besides the fact that PETC is easier to implement in practice than CETC, PETC has two major additional advantages over CETC at a more technical level. The first advantage is the existence of a strictly positive minimum inter-event time, i.e., the time between two successive updates of the control signal is strictly positive, and the second is the fact that PETC can be transformed directly into self-triggered control, (at least, for the state-feedback controller (5.3)). We will elaborate on the former result in Section 5.5.1, and on the latter in Section 5.5.2.

5.5.1 Minimum Inter-Event Times

Due to the periodic sampled-data nature of PETC, the sampling interval h is always a lower bound on the time difference between two consecutive updates of the control signal in the PETC system (5.1), (5.3), (5.4) and (5.5). This

is one of the main advantages of PETC over CETC, for which such a lower bound is not always guaranteed (cf. Chapter 4). The largest lower bound on the time differences between two consecutive control updates is called the *minimum inter-event time*, which might actually be larger than h. Below we will outline how the exact minimum inter-event time can be computed, where, for ease of exposition, we restrict ourselves to the case $w = 0$. Using bounds on the disturbances, one can also obtain lower bounds on the minimum inter-event time for the case with disturbances, i.e., $w \neq 0$, by applying similar reasoning as in [36], although the bounds will not be tight, unlike in the disturbance-free case.

An expression for the minimum inter-event time can be obtained as follows. First, let us consider the PWL model (5.19). Now given that the current state $\xi_{\tilde{k}} = \xi$ and the assumption that, at time $t_{\tilde{k}}$, $\tilde{k} \in \mathbb{N}$, an update of the control signal has occurred, the next control update time is given by $t_{\tilde{k}} + ht(\xi)$, where

$$t(\xi) := \inf \left\{ l \in \mathbb{N} \backslash \{0\} \,\big|\, \xi^\top (A_2^{l-1} A_1)^\top Q A_2^{l-1} A_1 \xi > 0 \right\}. \qquad (5.39)$$

The expression in (5.39) follows from the facts that the control signal is updated when $\xi_{\tilde{k}+l}^\top Q \xi_{\tilde{k}+l} > 0$, and as long as there is no update of the control signal $\xi_{\tilde{k}+l} = A_2^{l-1} A_1 \xi_{\tilde{k}}$. Based on (5.39), it is now immediate that the minimum inter-event time for the PETC system (5.1), (5.3) and (5.4) with event-triggering condition (5.5) is given by $t_{\min,h}^r = h t_{\min,h}^* \geqslant h$, with

$$t_{\min,h}^* := \inf \{ t(\xi) \,|\, \xi \in \mathbb{R}^{n_\xi} \} \qquad (5.40)$$

and h is the sampling interval of the event-triggering condition. Interestingly, $t_{\min,h}^*$ can equivalently be characterised by the computationally friendly expression

$$t_{\min,h}^* = \inf \{ l \in \mathbb{N} \backslash \{0\} \,|\, \lambda_{\max}((A_2^{l-1} A_1)^\top Q A_2^{l-1} A_1) > 0 \}. \qquad (5.41)$$

5.5.2 Self-Triggered Implementations

The idea of self-triggered control was put forward in [130]. Like in event-triggered control, a self-triggered control algorithm for plant (5.1) essentially consist of two parts, namely: the mechanism that determines the next update times $\tilde{t}_l$ of the control signals given for $l \in \mathbb{N}$ by

$$\tilde{t}_{l+1} = \tilde{t}_l + T(x(\tilde{t}_l)), \qquad (5.42)$$

and the feedback controller

$$\hat{u}(t) = G(x(\tilde{t}_l)), \text{ for } t \in (\tilde{t}_l, \tilde{t}_{l+1}], \qquad (5.43)$$

specifying the control signal in the next time interval $(\tilde{t}_l, \tilde{t}_{l+1}]$, where $T : \mathbb{R}^{n_x} \to \mathbb{R}_+$ and $G : \mathbb{R}^{n_x} \to \mathbb{R}^{n_u}$ are appropriately selected mappings. Hence, based

on the results on the existence of a minimum inter-event time above, which focussed on the case that $w = 0$, we readily obtain that

$$G(x) = Kx \qquad \text{and} \qquad T(x) = ht(x) \tag{5.44}$$

for all $x \in \mathbb{R}^{n_x}$ with $t : \mathbb{R}^{n_x} \to \mathbb{N}$ as in (5.39), leads to a self-triggered implementation as in (5.42) and (5.43) of the PETC algorithm, given by (5.3), (5.4) and (5.5). Note that the PETC system behaves exactly the same as its self-triggered counterpart. The advantage of the self-triggered control is, however, that the event-triggering condition (5.5) does not have to be monitored at every sampling time t_k, $k \in \mathbb{N}$, but that the next update time $\tilde{t}_{l+1}$ is computed *a priori* at each update time $\tilde{t}_l$. As a consequence, in between two update times the self-triggered controller does not need to monitor, communicate or compute anything, and the control algorithm can idle.

Conclusively, the transition from PETC to self-triggered control is rather straightforward in the case of state-feedback, as was just shown, while for CETC, this transition is more complicated [92, 135].

5.6   *Output-Based Decentralised PETC*

In this section, we will extend the previous results in two directions, namely towards dynamical output-based controllers and towards *decentralised* event-triggering conditions. To do so, let us consider the linear time-invariant (LTI) plant given by

$$\begin{cases} \frac{\mathrm{d}}{\mathrm{d}t}x^p = A^p x^p + B^p \hat{u} + B^w w, \\ \quad y = C^p x^p, \end{cases} \tag{5.45}$$

where $x^p \in \mathbb{R}^{n_p}$ denotes the state[4] of the plant, $\hat{u} \in \mathbb{R}^{n_u}$ the input applied to the plant, $w \in \mathbb{R}^{n_w}$ an unknown disturbance, and $y \in \mathbb{R}^{n_y}$ the output of the plant. The plant is controlled using a discrete-time LTI controller

$$\begin{cases} x^c_{k+1} = A^c x^c_k + B^c \hat{y}_k, \\ u(t_k) = u_k = C^c x^c_k + D^c \hat{y}(t_k), \end{cases} \tag{5.46}$$

where $x^c \in \mathbb{R}^{n_c}$ denotes the state of the controller, $\hat{y} \in \mathbb{R}^{n_y}$ the input of the controller, and $u \in \mathbb{R}^{n_u}$ the output of the controller. As before, at the sampling times t_k, $k \in \mathbb{N}$, the outputs of the plant $y(t_k)$ and controller $u(t_k)$ are sampled, but which values in y and u are transmitted, thereby updating the corresponding values in $\hat{y}$ and $\hat{u}$, will be determined based on a *decentralised* event-triggering condition. Note that the states of the controller x^c_{k+1} are updated based on $\hat{y}_k := \lim_{t \downarrow t_k} \hat{y}(t)$, i.e., directly after $\hat{y}$ is updated as was also

---

[4]We added superscript p here to denote the state of the plant (cf. (5.1)), as now we have to distinguish between the plant state x^p and the controller state x^c.

done in the context of networked control systems in [34] and in Chapters 2 and 3 of this thesis. To implement the discrete-time controller (5.46) in practice, the update of the state x_k^c to x_{k+1}^c should occur somewhere in the time interval $(t_k, t_{k+1}]$, $k \in \mathbb{N}$. Note that $u(t_k)$ at time t_k is computed on the basis of $\hat{y}(t_k)$, i.e., the most recently received output of the plant at time t_k, which will be $\hat{y}_{k-1}$ as we define for $t \in (t_k, t_{k+1}]$

$$\hat{y}(t) = \hat{y}_k \quad \text{and} \quad \hat{u}(t) = \hat{u}_k. \tag{5.47}$$

Hence, $\hat{u}$ and $\hat{y}$ as continuous-time signals are left-continuous. To convert the controller states x_c^k, $k \in \mathbb{N}$, into a (left-continuous) continuous-time signal, we will adopt the convention that for $t \in (t_k, t_{k+1}]$, $k \in \mathbb{N}$, it holds that

$$x^c(t) = x_{k+1}^c = A^c x_k^c + B^c \hat{y}_k \tag{5.48}$$

indicating that the updates of x^c take place just after t_k, $k \in \mathbb{N}$. In this way, $u(t_k) = C^c x^c(t_k) + D^c \hat{y}(t_k)$, $k \in \mathbb{N}$.

Just as $\hat{x}$ was the most recently received version of x in the state-feedback case in Section 5.2, $\hat{u}$ and $\hat{y}$ are now the most recently received versions of u and y, respectively, see Figure 5.2. We choose again a sampled-data implementation corresponding to the sampling times $t_k = kh$, $k \in \mathbb{N}$, for the sampling interval $h > 0$. However, we will now use *decentralised* event-triggering conditions to determine which signals will be transmitted at t_k, see also Figure 5.2. To formalise this, we define $v = [y^\top \ u^\top]^\top \in \mathbb{R}^{n_v}$ and $\hat{v} = [\hat{y}^\top \ \hat{u}^\top]^\top \in \mathbb{R}^{n_v}$ with $n_v := n_y + n_u$, and assume that the outputs of the plant and controller, i.e., the entries in v and $\hat{v}$, are grouped into N nodes. The entries in v and $\hat{v}$ corresponding to node $j \in \{1, \ldots, N\}$ are denoted by v^j and $\hat{v}^j$, respectively. To introduce the adopted decentralised PET conditions, we focus on (5.6), although alternative PET conditions as given in Section 5.2.2 can be used as well, see also Remark 5.6.1 below. By focussing on (5.6), the decentralised version of the event-triggering condition and the decentralised update of the signals $\hat{v}$ can be described as

$$\hat{v}^j(t) = \begin{cases} v^j(t_k), & \text{if } \|v^j(t_k) - \hat{v}^j(t_k)\| > \sigma_j \|v^j(t_k)\| \\ \hat{v}^j(t_k), & \text{if } \|v^j(t_k) - \hat{v}^j(t_k)\| \leqslant \sigma_j \|v^j(t_k)\|, \end{cases} \tag{5.49}$$

for $t \in (t_k, t_{k+1}]$, $k \in \mathbb{N}$, in which $\sigma_j \geqslant 0$, $j \in \{1, \ldots, N\}$, are given constants. Hence, (5.49) expresses that at a sampling time t_k, $k \in \mathbb{N}$, each node j samples the respective outputs of plant and controller and verifies if the difference $v^j(t_k) - \hat{v}^j(t_k)$ is too large with respect to $v^j(t_k)$ (determined by σ_j). In case the difference is too large, node j will transmit its corresponding signals $v^j(t_k)$, and $\hat{v}^j$ is updated just after t_k. Note that each node has its own *local* event-triggering condition, which invokes transmission of v^j if

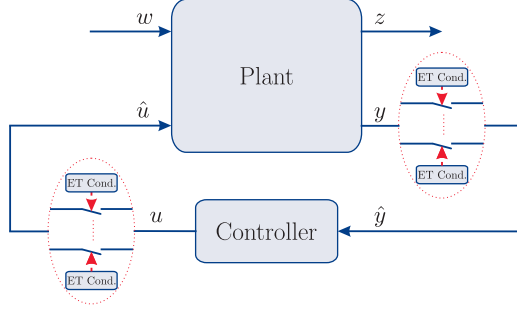$$\|v^j(t_k) - \hat{v}^j(t_k)\| > \sigma_j \|v^j(t_k)\|. \tag{5.50}$$

Figure 5.2: Decentralised event-triggered control schematic.

Interestingly, each of the local event-triggering conditions in (5.50) can be reformulated as the quadratic event-triggering condition

$$\xi^\top(t_k) Q_j \xi(t_k) > 0 \tag{5.51}$$

in terms of $\xi = [x^{p\top} \ x^{c\top} \ \hat{v}^\top]^\top = [x^{p\top} \ x^{c\top} \ \hat{y}^\top \ \hat{u}^\top]^\top$ by proper choice of Q_j, $j \in \{1, \ldots, N\}$. To show how this can be accomplished, we introduce some notational conventions. For an index set $\mathcal{J} \subseteq \{1, \ldots, N\}$, we define the diagonal matrices $\Gamma_{\mathcal{J}} \in \mathbb{R}^{n_v \times n_v}$

$$\Gamma_{\mathcal{J}} = \mathrm{diag}(\gamma_{\mathcal{J}}^1, \ldots, \gamma_{\mathcal{J}}^{n_y + n_u}), \tag{5.52}$$

where the elements $\gamma_{\mathcal{J}}^l$, with $l \in \{1, \ldots, n_y\}$, are equal to 1 if plant output y_l belongs to a node $l \in \mathcal{J}$, elements $\gamma_{\mathcal{J}}^{l+n_y}$, with $l \in \{1, \ldots, n_u\}$, are equal to 1 if controller output u_l belongs to a node $j \in \mathcal{J}$. The element $\gamma_{\mathcal{J}}^l$ is 0 otherwise. We will also sometimes use the diagonal submatrices $\Gamma_{\mathcal{J}}^y \in \mathbb{R}^{n_y \times n_y}$ and $\Gamma_{\mathcal{J}}^u \in \mathbb{R}^{n_u \times n_u}$ of $\Gamma_{\mathcal{J}}$ that satisfy $\Gamma_{\mathcal{J}} = \mathrm{diag}(\Gamma_{\mathcal{J}}^y, \Gamma_{\mathcal{J}}^u)$. Furthermore, we use the notation $\Gamma_j = \Gamma_{\{j\}}$, $\Gamma_j^y = \Gamma_{\{j\}}^y$ and $\Gamma_j^u = \Gamma_{\{j\}}^u$ for $j \in \{1, \ldots, N\}$,

$$C := \begin{bmatrix} C^p & 0 \\ 0 & C^c \end{bmatrix}, \qquad D := \begin{bmatrix} 0 & 0 \\ D^c & 0 \end{bmatrix}, \tag{5.53}$$

to obtain for $k \in \mathbb{N}$ that

$$\|v^j(t_k)\| = \|\Gamma_j [C \quad D]\xi(t_k)\|, \tag{5.54a}$$

$$\|v^j(t_k) - \hat{v}^j(t_k)\| = \|\Gamma_j [C \quad D - I]\xi(t_k)\|, \tag{5.54b}$$

which allow us to rewrite (5.50) as (5.51) with

$$Q_j := \begin{bmatrix} (1 - \sigma_j) C^\top \Gamma_j C & (1 - \sigma_j) C^\top \Gamma_j D - C^\top \Gamma_j \\ (1 - \sigma_j) D^\top \Gamma_j C - \Gamma_j C & (D - I)^\top \Gamma_j (D - I) - \sigma_j D^\top \Gamma_j D \end{bmatrix}. \tag{5.55}$$

Moreover, using the introduced notational conventions, we can now compactly write the updates of $\hat{v}$ just after time t_k as

$$\begin{aligned}
\hat{v}^+(t_k) &= \Gamma_{\mathcal{J}_k} v(t_k) + (I - \Gamma_{\mathcal{J}_k})\hat{v}(t_k) \\
&= \begin{bmatrix} \Gamma_{\mathcal{J}_k} C & \Gamma_{\mathcal{J}_k} D + I - \Gamma_{\mathcal{J}_k} \end{bmatrix} \xi(t_k).
\end{aligned} \tag{5.56}$$

where for $\xi \in \mathbb{R}^{n_\xi}$

$$\mathcal{J}(\xi) := \{ j \in \{1, \dots, N\} \mid \xi^\top Q_j \xi > 0 \}. \tag{5.57}$$

Remark 5.6.1. *Although we focus on event-triggering conditions as in* (5.50) *and show how they can be converted into event-triggering conditions as in* (5.51), *any decentralised event-triggering conditions that can be written in the form* (5.51), *e.g., the decentralised equivalents of* (5.10) *or* (5.14), *can be analysed with the tools presented below as well.*

To obtain an impulsive system model of the decentralised PETC system, given by (5.45) (5.46), (5.47), (5.48), and (5.50), we observe that due to the definition of $\mathcal{J}(\xi)$ in (5.57) we have for $k \in \mathbb{N}$ that $\mathcal{J}(\xi(t_k)) = \mathcal{J}$ if and only if

$$\xi(t_k)^\top Q_j \xi(t_k) > 0, \ j \in \mathcal{J} \text{ and } \xi(t_k)^\top Q_j \xi(t_k) \leqslant 0, \ j \in \mathcal{J}^c, \tag{5.58}$$

where we denote for any arbitrary set $J \subseteq \{1, \dots, N\}$ its complement by $\mathcal{J}^c := \{1, \dots, N\} \backslash \mathcal{J}$. Based on the above, we can obtain the impulsive model

$$\frac{\mathrm{d}}{\mathrm{d}t} \begin{bmatrix} \xi \\ \tau \end{bmatrix} = \begin{bmatrix} \bar{A}\xi + \bar{B}w \\ 1 \end{bmatrix}, \text{when } \tau \in [0, h] \tag{5.59a}$$

$$\begin{bmatrix} \xi^+ \\ \tau^+ \end{bmatrix} = \begin{bmatrix} J_{\mathcal{J}}\xi \\ 0 \end{bmatrix}, \qquad \text{when } \tau = h, \ \xi^\top Q_j \xi > 0, \ j \in \mathcal{J}, \tag{5.59b}$$

$$\text{and } \xi^\top Q_j \xi \leqslant 0, \ j \in \mathcal{J}^c, \tag{5.59c}$$

$$z = \bar{C}\xi + \bar{D}w. \tag{5.59d}$$

where $z \in \mathbb{R}^{n_z}$ is a performance output, similar to (5.17c). The matrices Q_j, $j \in \{1, \dots, N\}$, are given as in (5.55), and

$$\bar{A} = \begin{bmatrix} A^p & 0 & 0 & B^p \\ 0 & 0 & 0 & 0 \\ 0 & 0 & 0 & 0 \\ 0 & 0 & 0 & 0 \end{bmatrix}, \qquad \bar{B} = \begin{bmatrix} B^w \\ 0 \\ 0 \\ 0 \end{bmatrix}, \tag{5.60a}$$

$$J_{\mathcal{J}} = \begin{bmatrix} I & 0 & 0 & 0 \\ B^c \Gamma_{\mathcal{J}}^y C^p & A^c & B^c(I - \Gamma_{\mathcal{J}}^y) & 0 \\ \Gamma_{\mathcal{J}}^y C^p & 0 & (I - \Gamma_{\mathcal{J}}^y) & 0 \\ 0 & \Gamma_{\mathcal{J}}^u C^c & \Gamma_{\mathcal{J}}^u D^c & I - \Gamma_{\mathcal{J}}^u \end{bmatrix}. \tag{5.60b}$$

In the above output-based decentralised PETC system, we allow multiple nodes to transmit simultaneously at t_k, (i.e, $\mathcal{J}_k$ may consist of more than one element). In some cases, e.g., in case the nodes transmit their data over a shared communication medium, it might not always be realistic to assume that multiple nodes can transmit simultaneously. Therefore, we will indicate how the setup presented above can be extended in Section 5.6.3 in case communication constraints are present, i.e., in case only *one* node is allowed to transmit its data at a each sampling time t_k and a protocol is needed to schedule the transmissions.

5.6.1 A Piecewise Linear Systems Approach

To arrive at a discrete-time PWL model (for the case $w = 0$), we discretise the impulsive system (5.59), with $\tau(0) = h$ and $w = 0$, at the sampling times $t_k = kh$, $k \in \mathbb{N}$, as before. Following now the same rationale used to derive the PWL system (5.19), we again define the state $\xi_k := \xi(t_k)$, and obtain the model

$$\xi_{k+1} = A_{\mathcal{J}}\xi_k, \quad \text{when } \xi_k^\top Q_j \xi_k > 0, \ l \in \mathcal{J} \text{ and } \xi_k^\top Q_j \xi_k \leqslant 0, \ l \in \mathcal{J}^c, \quad (5.61)$$

where

$$A_{\mathcal{J}} = e^{\bar{A}h} J_{\mathcal{J}} = \begin{bmatrix} A & B\Gamma_{\mathcal{J}}^u C^c & B\Gamma_{\mathcal{J}}^u D^c & B(I - \Gamma_{\mathcal{J}}^u) \\ B^c \Gamma_{\mathcal{J}}^y C^p & A^c & B(I - \Gamma_{\mathcal{J}}^y) & 0 \\ \Gamma_{\mathcal{J}}^y C^p & 0 & I - \Gamma_{\mathcal{J}}^y & 0 \\ 0 & \Gamma_{\mathcal{J}}^u C^c & \Gamma_{\mathcal{J}}^u D^c & I - \Gamma_{\mathcal{J}}^u \end{bmatrix}, \quad (5.62)$$

in which $A = e^{A^p h}$ and $B = \int_0^h e^{A^p s} B^p \mathrm{d}s$.

In a similar fashion as we derived Theorem 5.3.1 for the state-feedback case, we can obtain the following result using the piecewise quadratic Lyapunov function

$$V(\xi) = \xi^\top P_{\mathcal{J}} \xi, \quad \text{when } \xi^\top Q_j \xi > 0, \ j \in \mathcal{J} \text{ and } \xi^\top Q_j \xi \leqslant 0, \ j \in \mathcal{J}^c. \quad (5.63)$$

Theorem 5.6.2. *The PETC system given by* (5.45), (5.46) *and* (5.49) *is GES with convergence rate $\rho > 0$, if there exist symmetric matrices $P_{\mathcal{J}}$, $\mathcal{J} \subseteq \{1, \ldots, N\}$, and scalars $\alpha_{\mathcal{J}\tilde{\mathcal{J}}j} \geqslant 0$, $\beta_{\mathcal{J}\tilde{\mathcal{J}}j} \geqslant 0$ and $\kappa_{\mathcal{J}j} \geqslant 0$, $\mathcal{J}, \tilde{\mathcal{J}} \subseteq \{1, \ldots, N\}$, $j \in \{1, \ldots, N\}$, such that*

$$A_{\mathcal{J}}^\top P_{\tilde{\mathcal{J}}} A_{\mathcal{J}} - e^{-2\rho h} P_{\mathcal{J}} + \sum_{j \in \mathcal{J}} \alpha_{\mathcal{J}\tilde{\mathcal{J}}j} Q_j - \sum_{j \in \mathcal{J}^c} \alpha_{\mathcal{J}\tilde{\mathcal{J}}j} Q_j$$
$$+ A_{\mathcal{J}}^\top \Big(\sum_{j \in \tilde{\mathcal{J}}} \beta_{\mathcal{J}\tilde{\mathcal{J}}j} Q_j - \sum_{j \in \tilde{\mathcal{J}}^c} \beta_{\mathcal{J}\tilde{\mathcal{J}}j} Q_j \Big) A_{\mathcal{J}} \preceq 0, \quad (5.64)$$

for all $\mathcal{J}, \tilde{\mathcal{J}} \subseteq \{1, \dots, N\}$, and

$$P_{\mathcal{J}} - \sum_{j \in \mathcal{J}} \kappa_{\mathcal{J}j} Q_j + \sum_{j \in \mathcal{J}^c} \kappa_{\mathcal{J}j} Q_j \succ 0. \tag{5.65}$$

for all $\mathcal{J} \subseteq \{1, \dots, N\}$

5.6.2 An Impulsive System Approach

In a similar fashion as the developments in Section 5.3.3, we can obtain the following result.

Theorem 5.6.3. *Let $\rho > 0$, $\gamma > \sqrt{\lambda_{max}(D^\top D)}$ and Assumption 5.3.6 hold, and suppose that there is a matrix $P_h \succ 0$ and scalars $\mu_{\mathcal{J}j} \geqslant 0$, $\mathcal{J} \subseteq \{1, \dots, N\}$, $j \in \{1, \dots, N\}$, such that*

$$\begin{bmatrix} P_h - \sum_{j \in \mathcal{J}} \mu_{\mathcal{J}j} Q_j + \sum_{j \in \mathcal{J}^c} \mu_{\mathcal{J}j} Q_j & J_{\mathcal{J}}^\top \bar{F}_{11}^{-\top} P_h \bar{S} & J_{\mathcal{J}}^\top (\bar{F}_{11}^{-\top} P_h \bar{F}_{11}^{-1} + \bar{F}_{21} \bar{F}_{11}^{-1}) \\ \star & I - \bar{S}^\top P_h \bar{S} & 0 \\ \star & \star & \bar{F}_{11}^{-\top} P_h \bar{F}_{11}^{-1} + \bar{F}_{21} \bar{F}_{11}^{-1} \end{bmatrix} \succ 0, \tag{5.66}$$

for all $\mathcal{J} \subseteq \{1, \dots, N\}$, where $\bar{F}_{ij} = F_{ij}(h)$, $i, j \in \{1, 2\}$ as in (5.34) with H in (5.33) for $\bar{A}$, $\bar{B}$ as in (5.60a), and a matrix $\bar{S}$ satisfying $\bar{S}\bar{S}^\top = -\bar{F}_{11}^{-1} \bar{F}_{12}$. Then, the PETC system given by (5.45), (5.46), (5.49) and (5.59d) is GES with convergence rate ρ (when $w = 0$) and has an $\mathcal{L}_2$-gain from w to z smaller than or equal to γ,

5.6.3 Extensions for Communication Constraints

We will now briefly indicate how the output-based decentralised PETC system presented above can be extended in case it is not possible that more than one node transmits its data at a sampling time t_k. In principle, this communication constraint requires one element $j^* \in \mathcal{J}_k$ to be selected at time t_k from the index set $\mathcal{J}_k$ in (5.57) whenever $\mathcal{J}_k$ contains more than one element. Selecting one element from the set $\mathcal{J}_k$ requires a scheduling protocol, on top of the local event-triggering conditions, to determine which of the nodes $j^* \in \mathcal{J}_k$ is allowed to transmit. The problem of scheduling transmissions has been studied for networked control systems in, e.g., [40, 62, 103, 133].

To show how scheduling protocols can be included in the framework of output-based decentralised PETC, let us consider the class of quadratic protocols, which have been introduced in the context of networked control systems in [40]. We can show that for quadratic protocols, the framework presented above applies directly. Namely, a quadratic protocol invokes transmission of the data in node $j^\star$ at sample time t_k, if

$$j^\star = \arg \max_{j \in \mathcal{J}_k} \xi^\top(t_k) R_j \xi(t_k) \tag{5.67}$$

where R_j, $j \in \{1, \ldots, N\}$ are given symmetric matrices. In fact, the Try-Once-Discard (TOD) protocol, sometimes also called the Maximum-Error-First (MEF) protocol, that has been studied in, e.g., [40, 62, 103, 133], is a quadratic protocol. In the TOD protocol, the node with the largest difference between $v^j(t_k)$ and $\hat{v}^j(t_k)$ is allowed to transmit its data. To be more precise, at time t_k, node $j^\star \in \mathcal{J}_k$ is allowed to transmit if

$$j^\star = \arg \max_{j \in \mathcal{J}_k} \| v^j(t_k) - \hat{v}^j(t_k) \|. \tag{5.68}$$

This expression can be written in the form (5.67), by taking

$$R_j = \begin{bmatrix} C^\top \Gamma_j C & C^\top \Gamma_j (D - I) \\ (D - I)^\top \Gamma_j C & (D - I)^\top \Gamma_j (D - I) \end{bmatrix}, \tag{5.69}$$

for all $j \in \{1, \ldots, N\}$. Since (5.67) involves quadratic conditions in selecting the node that is allowed to transmit, it can be modelled and analysed in the framework presented in this chapter.

In particular, to obtain an impulsive model of the output-based decentralised PETC system including the quadratic protocols (5.67), we have to observe that (5.59c) has to be modified to indicate which node $j^\star \in \mathcal{J}_k$ is selected to transmit its data, resulting in an impulsive system of the form (5.59), where (5.59c) is replaced by

$$\begin{bmatrix} \xi^+ \\ \tau^+ \end{bmatrix} = \begin{cases} \begin{bmatrix} J_\emptyset \xi \\ 0 \end{bmatrix}, & \text{when } \tau = h, \ \xi^\top Q_j \xi \leqslant 0, \ \text{for all } j \in \{1, \ldots, N\}, \\[2ex] \begin{bmatrix} J_{\{j^\star\}} \xi \\ 0 \end{bmatrix}, & \text{when } \tau = h, \ \text{and there exists a set } \mathcal{J} \text{ with } j^\star \in \mathcal{J} \\[2ex] & \text{such that } \xi^\top Q_j \xi > 0, \ j \in \mathcal{J}, \ \xi^\top Q_j \xi \leqslant 0, \ j \in \mathcal{J}^c \\ & \text{and } \xi^\top (R_{j^\star} - R_j) \xi \geqslant 0, \ j \in \mathcal{J}. \end{cases}$$
$$\tag{5.70}$$

The PWL model (5.61) will be modified in a similar fashion with $A_{\mathcal{J}}$ becoming $A_{\{j^\star\}}$ and the regional conditions in (5.61) becoming the ones in the right-hand side of (5.70). Since the basic structure of both the impulsive model and the PWL model is not changed, i.e., it still has linear dynamics and quadratic regional conditions, the analysis in Section 5.6.1 and Section 5.6.2 can be applied *mutatis mutandis*.

Other protocols could also be included in the presented PETC system framework, such as the Round-Robin protocol [40, 62, 103, 133]. In this case, time-dependent priorities can be assigned to each node, which are updated at each sampling interval t_k based on which node $j^\star$ transmits its data. In particular, the node $j^\star$ that transmits at time t_k might be assigned the lowest priority for the next transmission. To model this situation, the PETC system

model (5.59) has to be extended by including a list of time-dependent priorities. Although this and the inclusion of other protocols require future research, the above considerations already show the versatility and relevance of the presented framework, also in case the PETC system is subject to communication constraints.

5.7   Illustrative Examples

In this section, we illustrate the presented theory using two numerical examples. The first example is taken from [126] and uses state-feedback control. For this example, we will apply all the three developed approaches for stability analysis for both the event-triggering condition (5.6), as well as for (5.8). Furthermore, we will analyse the $\mathcal{L}_2$-gain for the case (5.8). In the second example, we consider a well-known benchmark example in the networked control system literature [133], consisting of a model of a batch reactor, see, e.g., [40, 62, 103, 133], to illustrate output-based decentralised PETC.

Example 1   Let us consider the example taken from [126] with plant (5.1) given by

$$\frac{\mathrm{d}}{\mathrm{d}t} x = \begin{bmatrix} 0 & 1 \\ -2 & 3 \end{bmatrix} x + \begin{bmatrix} 0 \\ 1 \end{bmatrix} u + \begin{bmatrix} 1 \\ 0 \end{bmatrix} w, \tag{5.71}$$

and state-feedback controller (5.3), where we take $K = \begin{bmatrix} 1 & -4 \end{bmatrix}$ and $t_k = kh$, $k \in \mathbb{N}$, with sampling interval $h = 0.05$. In this example, we first consider the situation where the event-triggering condition is given by (5.6) and, later, by (5.8). For this PETC system, we will apply all the three developed approaches for stability analysis (for $w = 0$), and the impulsive system approach for performance analysis. For all methods, we aim at constructing the largest value of σ in (5.6) and (5.8) such that GES or a certain $\mathcal{L}_2$-gain can be guaranteed. The reason for striving for large values of σ is that then large (minimum) inter-event times are obtained, due to the forms of (5.6) and (5.8).

For the case that the event-triggering condition is given by (5.6), the perturbed linear systems approach of Section 5.3.2 yields the maximum value of σ, while still guaranteeing GES, equal to $\sigma_{\mathrm{lin}} := 0.1728$, as the $\mathcal{H}_\infty$-norm of (5.26) from e to x is equal to $1/0.1728$. The discrete-time PWL system approach using Theorem 5.3.1 yields a maximum value of $\sigma = \sigma_{\mathrm{PWL}} := 0.2425$. Finally, using the impulsive system approach (Corollary 5.3.8) we obtain $\sigma_{\mathrm{IS}} = 0.2425$. Note that the facts $\sigma_{\mathrm{lin}} \leqslant \sigma_{\mathrm{PWL}}$ and $\sigma_{\mathrm{IS}} \leqslant \sigma_{\mathrm{PWL}}$ (note that the latter inequality holds with equality in this case) are in accordance with Theorem 5.4.1 and Theorem 5.4.2, respectively. Obviously, for all these values of σ a lower bound on the minimum inter-event time of $h = 0.05$ is guaranteed. However, in absence of disturbances we can use the expression in (5.41) to obtain the exact minimum inter-event times for all these three cases, which result for

$\sigma = \sigma_{\text{PWL}} = \sigma_{\text{IS}} = 0.2425$ in a minimum inter-event time of $3h = 0.15$ and for $\sigma = \sigma_{\text{lin}}$ in a minimum inter-event time of $2h = 0.10$.

Let us now consider the event-triggering condition given by (5.8). In this case, the PWL system approach (using Theorem 5.3.1) yields a maximum value for σ of $\sigma_{\text{PWL}} = 0.2550$, while still guaranteeing stability of the PETC system. The perturbed linear system approach gives a maximum value of $\sigma_{\text{lin}} = 0.2506$, while the impulsive system approach results in the maximum $\sigma_{\text{IS}} = 0.2532$ in this case. Hence, as expected, we again see that $\sigma_{\text{lin}} \leqslant \sigma_{\text{PWL}}$ and $\sigma_{\text{IS}} \leqslant \sigma_{\text{PWL}}$, although the values are rather close. In fact, the minimum inter-event time according to (5.41) is equal to $h = 0.05$ for all values σ_{PWL}, σ_{IS} and σ_{lin} in the event-triggering condition (5.8). When analysing the $\mathcal{L}_2$-gain from the disturbance w to the output variable z as in (5.17c) where $z = [0\ 1\ 0\ 0]\xi$, we obtain Figure 5.3a, in which the smallest upper bound on the $\mathcal{L}_2$-gain that can be guaranteed on the basis of Theorem 5.3.7 is given as function of σ. This figure clearly demonstrates that better control performance (i.e., smaller γ), necessitates more updates (i.e., smaller σ), allowing us to make tradeoffs between these two competing objectives. Note that for $\gamma \to \infty$ (meaning no performance requirements), the value of σ approaches the value obtained using Corollary 5.3.8 equal to $\sigma_{\text{IS}} = 0.2532$. On the other hand, for $\sigma \to 0$, we recover an upper bound on the $\mathcal{L}_2$-gain for the periodic sampled-data system, given by (5.1) of the controller (5.2) with sampling interval $h = 0.05$ and $t_k = kh$, $k \in \mathbb{N}$.

Figure 5.3b shows the response of the performance output z of the PETC system with $\sigma = 0.2$ subject to a disturbance w, which is also depicted in Figure 5.3b. For the same situation, Figure 5.3c shows the evolution of the inter-event times. We see inter-event times ranging from $h = 0.05$, up to 0.85 (17 times the sampling interval h). Hence, this figure illustrates that using PETC instead of periodic sampled-data control, a significant reduction in the number of transmissions/controller computations can be achieved.

Example 2 Let us now consider the model of a linearised batch reactor. The details of the linearised model of the batch reactor model and a continuous-time controller can be found in [40, 62, 103, 133]. The controller considered in this example will be obtained from this continuous-time controller by discretising it using a zero-order-hold for the sampling interval $h = 0.05$, resulting in a controller of the form (5.46) with

$$A^c = \begin{bmatrix} 1 & 0 \\ 0 & 1 \end{bmatrix}, \quad B^c = \begin{bmatrix} 0 & 0.05 \\ 0.05 & 0 \end{bmatrix}, \quad C^c = \begin{bmatrix} -2 & 0 \\ 0 & 8 \end{bmatrix}, \quad D^c = \begin{bmatrix} 0 & -2 \\ 5 & 0 \end{bmatrix}. \quad (5.72)$$

For this plant and controller, we will illustrate the decentralised event-triggering condition (5.49), in which we assume that each individual plant input and output is in a different node. Hence, this decentralised PETC system has 4 nodes. Using the result of Theorem 5.3.1, in which we take $\sigma_1 = \sigma_2 = \sigma_3 = \sigma_4$
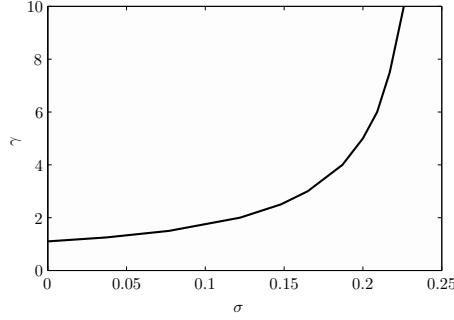
(a) $\mathcal{L}_2$-gain versus event-triggering condition.
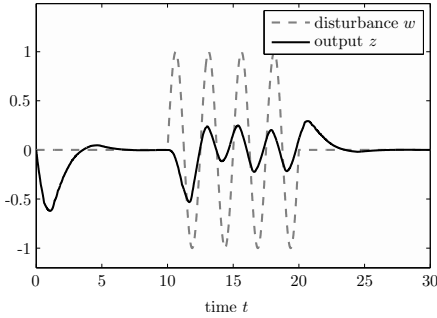
(b) The evolution of the disturbances and the output z as a function of time
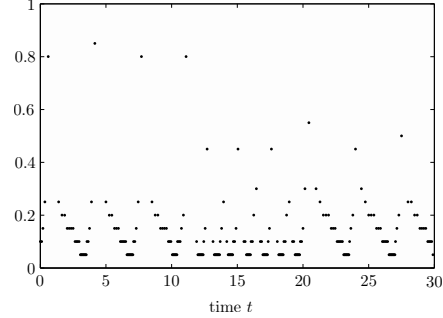
(c) The inter-event times as a function of time.

Figure 5.3: Example 1, with $\sigma = 0.2$.

for simplicity, we obtain that the PETC system (5.59) is GES for $\sigma_1 = \sigma_2 = \sigma_3 = \sigma_4 \leqslant 0.5$. This is illustrated also in Figure 5.4a, in which the simulated response of the PETC system (5.59) is given for the initial condition $\xi(0) = [1 \ -1 \ -1 \ 1 \ 0 \ 0 \ 0 \ 0 \ 0 \ 0]^\top$, for $\sigma_1 = \sigma_2 = \sigma_3 = \sigma_4 = 0.5$. The corresponding event times at which the individual nodes transmit their data are provided in Figure 5.4b. In fact, the outputs y_1, y_2, u_1 and u_2 are transmitted 45, 27, 22 and 44 times, respectively, during the first 5 units of time. This makes the total number of transmissions equal to 138. If a standard periodic sampled-data implementation would have been used, 400 transmissions would have occurred during the first 5 units of time ($h = 0.05$ results in 100 transmissions for each of the 4 channels in a time span of 5 units of time). Hence, the PETC implementation leads to a reduction in the number of transmissions of more than 65%, while still resulting in a closed-loop system that is GES. This clearly shows the relevance of the PETC algorithms proposed in this chapter.
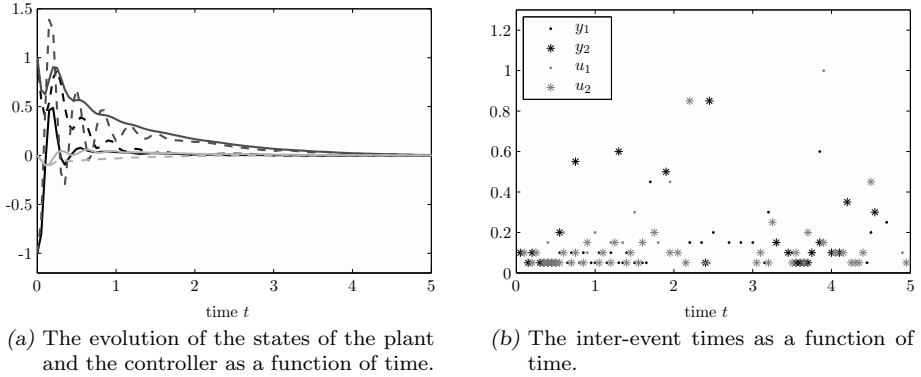
(a) The evolution of the states of the plant and the controller as a function of time.

(b) The inter-event times as a function of time.

Figure 5.4: Example 2, with $\sigma_1 = \sigma_2 = \sigma_3 = \sigma_4 = 0.5$.

5.8 Conclusions

In this chapter, we proposed a novel event-triggered control (ETC) strategy, which aims at combining the benefits that periodic sampled-data control and ETC offer. In particular, the ETC strategy is based on the idea of having an event-triggering condition that is verified only periodically, and at every time it is decided whether or not to transmit new measurements and control signals. Only when necessary from a stability or performance point of view, the communication or computation resources are used. This control strategy, for which we propose to use the term *periodic event-triggered control* (PETC), preserves the benefits of reduced resource utilisation as transmissions and controller computations are not performed periodically, while the event-triggering conditions still have a periodic character. The latter aspect leads to several benefits as the event-triggering condition has to be verified only at the periodic sampling times, instead of continuously, which makes it suitable for implementation in standard time-sliced embedded system architectures. Moreover, the strategy has an inherently guaranteed minimum inter-event time of (at least) one sampling interval of the event-triggering condition, and can easily be converted into self-triggered implementations [130], at least in the case of state feedback.

In this chapter, PETC was developed for both static state-feedback controllers, and dynamical output-based controllers considering also decentralised event-triggering conditions. To analyse the stability and $\mathcal{L}_2$-gain properties of the PETC systems, we used three approaches: (i) a discrete-time piecewise linear (PWL) system approach, (ii) a discrete-time perturbed linear system approach, and (iii) an impulsive system approach. We discussed the advantages and disadvantages of all the three approaches, showing that each of the three presented modelling approaches is of independent interest. Namely, the

PWL system approach provides the least conservative LMI-based results in case of stability analysis only, the perturbed linear system approach has the lowest computational complexity, while the impulsive system approach provides $\mathcal{L}_2$-gain analyses. Besides presenting the three analysis methodologies, we also provided techniques to compute (tight) lower bounds on the minimum inter-event times. We illustrated the theory using two numerical examples and showed that PETC is able to reduce the utilisation of communication and computation resources significantly.

6

On the Minimum Attention and the Anytime Attention Control Problem for Linear Systems: A Linear Programming Approach[1]

Abstract – In this chapter, we present two control laws that are tailored for control applications in which computational and/or communication resources are scarce. Namely, we consider minimum attention control, where the 'attention' that a control task requires is minimised given certain performance requirements, and anytime attention control, where the performance under the 'attention' given by a scheduler is maximised. Here, we interpret 'attention' as the inverse of the time elapsed between two consecutive executions of a control task. Instrumental for the solution will be a novel extension of the notion of a control Lyapunov function. By focussing on linear plants, by allowing for only a finite number of possible intervals between two subsequent executions of the control task and by taking the extended control Lyapunov function to be ∞-norm based, we can formulate the aforementioned control problems as linear programs, which can be solved efficiently online. Furthermore, we provide techniques to construct suitable ∞-norm-based (extended) control Lyapunov functions for our purposes. Finally, we illustrate the theory using two numerical examples. In particular, we show that minimum attention control outperforms an alternative implementation-aware control law available in the literature.

---

[1]This chapter is based on [42].

6.1 Introduction

A current trend in control engineering is to no longer implement controllers on dedicated platforms having dedicated communication channels, but in embedded microprocessors and using (shared) communication networks. Since in such an environment the control task has to share computational and communication resources with other tasks, the availability of these resources is limited and might even be time-varying. Despite the fact that resources are scarce, controllers are typically still implemented in a time-triggered fashion, in which the control task is executed periodically. This design choice is motivated by the fact that it enables the use of the well-developed theory on sampled-data systems, e.g., [8, 27], to design controllers and analyse the resulting closed-loop systems. This design choice, however, leads to over-utilisation of the available resources and requires over-provisioned hardware, as it might not be necessary to execute the control task every period. For this reason, several alternative control strategies have been developed to reduce the required computation and communication resources needed to execute the control task.

Two of such approaches are event-triggered control, see, e.g., [60, 66, 90, 126], and self-triggered control, see, e.g., [92, 130, 135]. In event-triggered control and self-triggered control, the control law consists of two elements: namely, a feedback controller that computes the control input, and a triggering mechanism that determines when the control task should be executed. The difference between event-triggered control and self-triggered control is that in the former the triggering mechanism uses current measurements, while in the latter it uses predictions using previously sampled and transmitted data and knowledge on the plant dynamics, meaning that it is the controller itself that triggers the execution of the control task. Current design methods for event-triggered control and self-triggered control are emulation-based approaches, by which we mean that the feedback controller is designed for an ideal implementation, while subsequently the triggering mechanism is designed (based on the given controller). Since the feedback controller is designed before the triggering mechanism, it is difficult, if not impossible, to obtain an optimal design of the combined feedback controller and triggering mechanism in the sense that the minimum number of controller executions is achieved while guaranteeing stability and a certain level of closed-loop performance. Hence, no solution to the codesign problem currently exists.

An alternative way to handle limited computation and communication resources is by using so-called *anytime control* methods, see, e.g., [52, 53, 54]. These are control laws that are able to compute a control input, given a certain minimum amount of computation resources allotted by a scheduler, while providing a 'better' control input whenever more computation resources are available. What is meant by 'better', varies from computing more control inputs [53], computing more future control inputs [54], or computing the control

input using a higher-order dynamical controller [52].

In this chapter, we consider two methodologies that are able to handle scarcity in computation and communication resources. The first methodology adopts minimum attention control (MAC), see [21], in which the objective is to minimise the attention the control loop requires, i.e., MAC maximises the next execution instant, while guaranteeing a certain level of closed-loop performance. Note that this control strategy is similar to self-triggered control, where also the objective is to have as few control task executions as possible, given a certain closed-loop performance requirement. However, contrary to self-triggered control, MAC is typically not designed using emulation-based approaches in the sense that it does not require a separate feedback controller to be available before the triggering mechanism can be designed. Clearly, this joint design procedure is more likely to yield a (close to) optimal design than a sequential design procedure would. The second methodology proposed in this chapter is more in line with anytime control, as discussed above. Namely, by assuming that after each execution of the control task, the control input cannot be recomputed for a certain amount of time that is specified by a scheduler, anytime attention control (AAC) finds a control input that maximises the performance of the closed-loop system, given this time-varying computation constraint. This setting is realistic in many embedded and networked systems, where a real-time scheduler distributes the available resources among all tasks, and hence, determines online, the execution instants of the control task.

The control problems studied in this chapter are similar to the ones studied in [3]. However, by focussing on linear systems, we will propose an alternative approach to solve the control problems at hand. As was already observed in [3], the MAC and the AAC problem are related and the same solution strategy can be used to solve both problems. We will also use the same solution strategy, yet a different one than used in [3], to solve the both problems in this chapter. In the solution strategy we propose, we focus on linear plants, as already mentioned, and consider only a finite number of possible interexecution times. Furthermore, we will employ control Lyapunov functions (CLFs) that can be seen as an extension of the CLFs for sampled-data systems, which will enable us to guarantee a certain level of performance. These extended CLFs will first be formulated for general sampled-data systems and will later be particularised to ∞-norm-based functions, see, e.g., [80, 108]. Namely, by using ∞-norm-based extended CLFs, we can formulate both the MAC and the AAC problem as linear programs (LPs), which can be efficiently solved online, thereby alleviating the computational burden as experienced in [3]. Furthermore, we provide techniques to construct suitable ∞-norm-based (extended) control Lyapunov functions for the control objectives under consideration. We will illustrate the theory using two numerical examples. In particular, we will show that MAC outperforms the self-triggered control strategy of [92].

The remainder of this chapter is organised as follows. After introducing the

necessary notational conventions used in this chapter, we formulate the MAC and the AAC problem in Section 6.2. In Section 6.3, we show how the control problems can be solved using extended CLFs, in Section 6.4, we show how to guarantee well-defined solutions, and, in Section 6.5, we present computationally tractable algorithms to solve the control problems efficiently. Finally, the presented theory is illustrated using numerical examples in Section 6.6 and we draw conclusions in Section 6.7. Appendix A.5 contains the proofs of the lemmas and theorems.

6.1.1 Nomenclature

The following notational conventions will be used. For a vector $x \in \mathbb{R}^n$, we denote by $[x]_i$ its i-th element and by $\|x\|_p := \sqrt[p]{\sum_{i=1}^n |x_i|^p}$ its p-norm, $p \in \mathbb{N}$, and by $\|x\|_\infty = \max_{i=\{1,\ldots,N\}} |x_i|$, its ∞-norm. For a matrix $A \in \mathbb{R}^{n \times m}$, we denote by $[A]_{ij}$ its i,j-th element, by $A^\top \in \mathbb{R}^{m \times n}$ its transposed and by $\|A\|_p := \max_{x \neq 0} \frac{\|Ax\|_p}{\|x\|_p}$, its induced p-norm, $p \in \mathbb{N} \cup \{\infty\}$. In particular, $\|A\|_\infty := \max_{i \in \{1,\ldots,n\}} \sum_{j=1}^m |[A]_{ij}|$. We denote the set of nonnegative real numbers by $\mathbb{R}_+ := [0, \infty)$, and for a function $f : \mathbb{R}_+ \to \mathbb{R}^n$, we denote the limit from above for time $t \in \mathbb{R}_+$ by $\lim_{s \downarrow t} f(s)$, provided that it exists. Finally, to denote a set-valued function F from $\mathbb{R}^n$ to $\mathbb{R}^m$, we write $F : \mathbb{R}^n \hookrightarrow \mathbb{R}^m$, meaning that $F(x) \subseteq \mathbb{R}^m$ for each $x \in \mathbb{R}^n$.

6.2 Problem Formulation

In this section, we formulate the minimum attention and the anytime attention control problem. To do so, let us consider a linear time-invariant (LTI) plant given by

$$\tfrac{\mathrm{d}}{\mathrm{d}t} x = Ax + Bu, \tag{6.1}$$

where $x \in \mathbb{R}^{n_x}$ denotes the state of the plant and $u \in \mathbb{R}^{n_u}$ the input applied to the plant. The plant is controlled in a sampled-data fashion, using a zero-order hold (ZOH), which leads to

$$u(t) = \hat{u}_k, \quad \text{for all } t \in [t_k, t_{k+1}), \tag{6.2}$$

where the discrete-time control inputs $\hat{u}_k$, $k \in \mathbb{N}$, and the strictly increasing sequence of execution instants $\{t_k\}_{k \in \mathbb{N}}$ are given by either one of the solutions to the following two control problems:

- The minimum attention control (MAC) Problem: *Find a set-valued function $F_{\mathrm{MAC}} : \mathbb{R}^{n_x} \hookrightarrow \mathbb{R}^{n_u}$ and a function $h : \mathbb{R}^{n_x} \to \mathbb{R}_+$, such that*

$$\begin{cases} \hat{u}_k \in F_{\mathrm{MAC}}(x(t_k)) \\ t_{k+1} = t_k + h(x(t_k)), \end{cases} \tag{6.3}$$

for all $k \in \mathbb{N}$, renders the plant (6.1) with ZOH (6.2) stable and guarantees a certain level of performance, both defined in an appropriate sense, while, for each $x \in \mathbb{R}^{n_x}$, $h(x)$ is as large as possible.

- The anytime attention control (AAC) Problem: *Find a set-valued function* $F_{\text{AAC}} : \mathbb{R}^{n_x} \times \mathbb{R}_+ \hookrightarrow \mathbb{R}^{n_u}$, such that

$$\begin{cases} \hat{u}_k \in F_{\text{AAC}}(x(t_k), h_k) \\ t_{k+1} = t_k + h_k, \end{cases} \tag{6.4}$$

for all $k \in \mathbb{N}$, renders the plant (6.1) with ZOH (6.2) stable and maximises performance in an appropriate sense, assuming that h_k, $k \in \mathbb{N}$, is given at time t_k by the real-time scheduler.

Note that the mappings F_{MAC} and F_{AAC} in the problems above are set-valued functions, i.e., $F_{\text{MAC}}(x) \subseteq \mathbb{R}^{n_u}$, for all $x \in \mathbb{R}^{n_x}$, and $F_{\text{AAC}}(x, h) \subseteq \mathbb{R}^{n_u}$, for all $x \in \mathbb{R}^{n_x}$ and $h \in \mathbb{R}_+$. This means that $\hat{u}_k$, $k \in \mathbb{N}$, can be chosen from a subset $F_{\text{MAC}}(x(t_k))$ or $F_{\text{AAC}}(x(t_k), h_k)$ of $\mathbb{R}^{n_u}$, while still guaranteeing the required properties of the MAC and the AAC problem.

To make the preceding problems well defined we need to give a precise meaning to the terms stability and performance qualifying the solutions of the closed-loop system given by (6.1), (6.2), with (6.3) or (6.4).

Definition 6.2.1. *The system* (6.1), (6.2), *with* (6.3) *or* (6.4), *is said to be* globally exponentially stable *(GES) with a convergence rate* $\alpha > 0$ *and a gain* $c > 0$, *if for any initial condition* $x(0)$, *the corresponding solutions satisfy*

$$\|x(t)\| \leqslant c e^{-\alpha t} \|x(0)\|, \tag{6.5}$$

for all $t \in \mathbb{R}_+$.

The notion of performance used in this chapter is explicitly expressed in terms of the convergence rate α as well as the gain c. Only requiring a desired convergence rate α (in the MAC problem), or maximising it (in the AAC problem), could yield a very large gain c and, thus, could yield unacceptable closed-loop behaviour. As we will show below (see Lemma 6.3.2), the guaranteed gain c typically becomes large when the time between two controller executions, i.e., $t_{k+1} - t_k$, is large. Therefore, special measures have to be taken to prevent the gain c from becoming unacceptably large.

6.3 Formulating the Control Problems using Control Lyapunov Functions

In this section, we will propose a solution to the two considered control problems by formulating them as optimisation problems. In these optimisation problems,

we will use an extension to the notion of a control Lyapunov function (CLF). Before doing so, we will briefly revisit some existing results on CLFs, see, e.g., [77, 121], and show how they can be used to design control laws that render the plant (6.1) with ZOH (6.2) GES with a certain convergence rate $\alpha > 0$ and a certain gain $c > 0$.

6.3.1 Preliminary Results on CLFs

Let us now introduce the notion of a CLF, which has been applied to discrete-time systems in [77] and will now be applied to periodic sampled-data systems, given by the plant (6.1) with ZOH (6.2), in which $t_{k+1} = t_k + h$, $k \in \mathbb{N}$, for some fixed $h > 0$.

Definition 6.3.1. *Consider the plant* (6.1) *with ZOH* (6.2). *The function* $V : \mathbb{R}^{n_x} \to \mathbb{R}$ *is said to be a* control Lyapunov function *(CLF) for* (6.1) *and* (6.2), *a convergence rate* $\alpha > 0$, *a control gain bound* $\beta > 0$ *and an interexecution time* $h > 0$, *if there exist constants* $\underline{a}, \overline{a} \in \mathbb{R}_+$ *and* $q \in \mathbb{N}$, *such that for all* $x \in \mathbb{R}^{n_x}$

$$\underline{a}\|x\|^q \leqslant V(x) \leqslant \overline{a}\|x\|^q, \tag{6.6}$$

and, for all $x \in \mathbb{R}^{n_x}$, *there exists a control input* $\hat{u} \in \mathbb{R}^{n_u}$, *satisfying* $\|\hat{u}\| \leqslant \beta\|x\|$ *and*

$$V(e^{Ah}x + \int_0^h e^{As}\mathrm{d}s B\hat{u}) \leqslant e^{-\alpha qh}V(x). \tag{6.7}$$

Based on a CLF for a convergence rate $\alpha > 0$, a control gain bound $\beta > 0$ and an interexecution time $h > 0$, as in Definition 6.3.1, the control law

$$\begin{cases} \hat{u}_k \in F(x) := \{u \in \mathbb{R}^{n_u} \,|\, f(x, u, h, \alpha) \leqslant 0 \text{ and } \|u\| \leqslant \beta\|x\|\}, \\ t_{k+1} = t_k + h, \end{cases} \tag{6.8}$$

in which

$$f(x, u, h, \alpha) := V(e^{Ah}x + \int_0^h e^{As}B\mathrm{d}s\, u) - e^{-\alpha qh}V(x), \tag{6.9}$$

renders the plant (6.1) with ZOH (6.2) GES with a convergence rate $\alpha > 0$ and a certain gain $c > 0$, as we will show in the following lemma.

Lemma 6.3.2. *Assume there exists a CLF for* (6.1) *with* (6.2), *a convergence rate* $\alpha > 0$, *a control gain bound* $\beta > 0$ *and an interexecution time* $h > 0$, *in the sense of Definition 6.3.1. Then, the control law* (6.8) *renders the plant* (6.1) *with ZOH* (6.2) *GES with the convergence rate* α *and the gain* $c = \bar{c}(\alpha, \beta, h)$, *where*

$$\bar{c}(\alpha, \beta, h) := \sqrt[q]{\frac{\overline{a}}{\underline{a}}} \Big(e^{\|A\|h} + \beta \int_0^h e^{\|A\|s}\mathrm{d}s\|B\| \Big) e^{\alpha h}. \tag{6.10}$$

Proof. This lemma is a special case of Lemma 6.3.4 that we will present and prove below. □

Lemma 6.3.2 illustrates why it is important to express the notion of performance both in terms of the convergence rate α as well as the gain c, as was mentioned at the end of Section 6.2. Namely, even though a CLF could guarantee GES with a certain convergence rate α, for some control gain bound β and for any arbitrarily large h, by using a corresponding CLF in the control law (6.8), the consequence is that the guaranteed gain c becomes extremely large, see Lemma 6.3.2. In particular, c grows exponentially as h becomes larger, which (potentially) yields undesirably large responses for large interexecution times $h = t_{k+1} - t_k$, $k \in \mathbb{N}$. To avoid having such unacceptable behaviour, we propose a control design methodology that is able to guarantee a desired convergence rate α, as well as a desired gain c, even for large interexecution times h. This requires an extension of the CLF defined above.

6.3.2 Extended Control Lyapunov Functions

The observation that the interexecution time h influences the gain c is important to allow the MAC and the AAC problem to be formalised using CLFs. Namely, in order to achieve sufficiently high performance (meaning a sufficiently large α and a sufficiently small c), Lemma 6.3.2 indicates that the interexecution time h has to be selected sufficiently small. This, however, contradicts the MAC and the AAC problem, where in the former the interexecution time is to be maximised and in the latter it is time varying and specified by a scheduler. We therefore propose an extended control Lyapunov function (eCLF), which we will subsequently use to solve the MAC and the AAC problem. Roughly speaking, the eCLF is such that it does not only decrease from t_k to t_{k+1}, but also from t_k to intermediate time instants $t_k + \hbar_l$, for some (well-chosen) $\hbar_l > 0$ satisfying $t_{k+1} - t_k > \hbar_l$, $k \in \mathbb{N}$, $l \in \{1, \dots, L - 1\}$. The existence of such an eCLF guarantees high performance, even though the interexecution time $\hbar_L := t_{k+1} - t_k$, $k \in \mathbb{N}$, can be large, as we will show after giving the formal definition of the eCLF.

Definition 6.3.3. *Consider the plant* (6.1) *with ZOH* (6.2). *The function* $V : \mathbb{R}^{n_x} \to \mathbb{R}$ *is said to be an* extended control Lyapunov function *(eCLF) for* (6.1) *and* (6.2), *a convergence rate* $\alpha > 0$, *a control gain bound* $\beta > 0$, *and a set* $\mathcal{H} := \{\hbar_1, \dots, \hbar_L\}$, $L \in \mathbb{N}$, *satisfying* $\hbar_{l+1} > \hbar_l > 0$ *for all* $l \in \{1, \dots, L - 1\}$, *if there exist constants* $\underline{a}, \overline{a} \in \mathbb{R}_+$ *and* $q \in \mathbb{N}$, *such that for all* $x \in \mathbb{R}^{n_x}$

$$\underline{a}\|x\|^q \leqslant V(x) \leqslant \overline{a}\|x\|^q \tag{6.11}$$

and, for all $x \in \mathbb{R}^{n_x}$, *there exists a control input* $\hat{u} \in \mathbb{R}^{n_u}$, *satisfying* $\|\hat{u}\| \leqslant \beta\|x\|$ *and*

$$V\big(e^{A\hbar_l}x + \int_0^{\hbar_l} e^{As}\mathrm{d}sB\hat{u}\big) \leqslant e^{-\alpha q\hbar_l}V(x) \tag{6.12}$$

for all $l \in \{1, \dots, L\}$.

As before, based on an eCLF for a convergence rate $\alpha > 0$, a control gain bound $\beta > 0$ and a set $\mathcal{H}$ as in Definition 6.3.3, the control law

$$\begin{cases} \hat{u}_k \in F(x) := \big\{ u \in \mathbb{R}^{n_u} \,\big|\, f(x, u, \hbar_l, \alpha) \leqslant 0 \,\forall l \in \{1, \ldots, L\} \text{ and } \|u\| < \beta \|x\| \big\}, \\ t_{k+1} = t_k + \hbar_L, \end{cases}$$

$$(6.13)$$

with $f(x, u, \hbar_l, \alpha)$ as defined in (6.9), renders the plant (6.1) with ZOH (6.2) GES with a convergence rate $\alpha > 0$ and a certain gain $c > 0$ that is typically smaller than the gain obtained using an ordinary CLF, as we will show in the following lemma.

Lemma 6.3.4. *Assume there exists an eCLF for* (6.1) *with* (6.2), *a convergence rate* $\alpha > 0$, *a control gain bound* $\beta > 0$ *and a set* $\mathcal{H} := \{\hbar_1, \ldots, \hbar_L\}$, $L \in \mathbb{N}$, *satisfying* $\hbar_{l+1} > \hbar_l > 0$ *for all* $l \in \{1, \ldots, L-1\}$, *in the sense of Definition 6.3.3. Then, the control law* (6.13) *renders the plant* (6.1) *with ZOH* (6.2) *GES with the convergence rate* α *and the gain* $c = \bar{c}(\alpha, \beta, \Delta_\hbar, \hbar_L)$, *where*

$$\bar{c}(\alpha, \beta, \Delta_\hbar, \hbar_L) := \sqrt[q]{\frac{\bar{a}}{\underline{a}}} \Big(e^{\|A\|\Delta_\hbar} + \beta e^{\alpha(\hbar_L - \Delta_\hbar)} \int_0^{\Delta_\hbar} e^{\|A\|s} \mathrm{d}s \|B\| \Big) e^{\alpha\Delta_\hbar}, \quad (6.14)$$

with $\Delta_\hbar := \max_{l \in \{1, \ldots, L\}} (\hbar_l - \hbar_{l-1})$, *in which* $\hbar_0 := 0$.

Proof. The proof can be found in Appendix A.5. $\qquad\square$

The existence of an eCLF for a well-chosen set $\mathcal{H}$ (i.e., realising a sufficiently small $\Delta_\hbar$) guarantees high performance in terms of the convergence rate α and the gain c, while still allowing for large interexecution times $\hbar_L = t_{k+1} - t_k$, $k \in \mathbb{N}$. Indeed, by using the intermediate time instants $t_k + \hbar_l$, the gain c in Lemma 6.3.4 is generally much smaller than the gain c in Lemma 6.3.2. However, making $\Delta_\hbar$ too small might lead to infeasibility of the control law, as decreasing $\Delta_\hbar$ for a fixed interexecution time $t_{k+1} - t_k$ means taking more intermediate times $\hbar_l$ and, thus, that more inequality constraints are added to the set-valued function F in (6.13), which, besides resulting in a much more complicated control law, might cause $F(x) = \emptyset$ for some $x \in \mathbb{R}^{n_x}$. Hence, a tradeoff can be made between the magnitude of the gain c and the number of constraints in $F(x)$ and we will exactly exploit this fact in the solution to the MAC and the AAC problem, as we will show below.

6.3.3 Solving the MAC Problem using eCLFs

We will now propose a solution to the MAC problem. As a starting point, we consider the control law (6.13), which is based on an eCLF. Indeed, the existence of an eCLF for a convergence rate $\alpha > 0$, a control gain bound $\beta > 0$ and a set $\mathcal{H}$ implies GES with convergence rate α and gain c of the plant (6.1) with ZOH (6.2) and the control law (6.13), according to Lemma 6.3.4. However,

given the function V, a convergence rate α, a control gain bound β and a set $\mathcal{H}$, it might not always be possible to ensure that $F(x) \neq \emptyset$ for all $x \in \mathbb{R}^{n_x}$. To resolve this issue, we take subsets of $\mathcal{H}$ of the form $\mathcal{H}_{\bar{L}} := \{\hbar_1, \ldots, \hbar_{\bar{L}}\}$, for $\bar{L} \in \{1, \ldots, L\}$, such that $\mathcal{H}_1 \subseteq \mathcal{H}_2 \subseteq \ldots \subseteq \mathcal{H}_L = \mathcal{H}$, and propose MAC, in which the objective is to maximise $\bar{L} \in \{1, \ldots, L\}$ for each given $x \in \mathbb{R}^{n_x}$. In other words, for each given $x \in \mathbb{R}^{n_x}$, $\bar{L}$ is maximised such that $F_{\bar{L}}(x) \neq \emptyset$, in which

$$F_{\bar{L}}(x) := \big\{ u \in \mathbb{R}^{n_u} \,|\, f(x, u, \hbar_l, \alpha) \leqslant 0 \ \forall \, l \in \{1, \ldots, \bar{L}\} \text{ and } \|u\| \leqslant \beta\|x\| \big\}, \quad (6.15)$$

with $f(x, u, \hbar_l, \alpha)$ as defined in (6.9). We maximise $\bar{L}$ to make the interexecution times $\hbar_{\bar{L}} = t_{k+1} - t_k$ maximal, yielding that the control law requires minimum attention. Hence, this MAC law is given by (6.3), in which we take

$$\begin{cases} F_{\mathrm{MAC}}(x) := F_{\bar{L}^\star(x)}(x) \\ h(x) := \hbar_{\bar{L}^\star(x)} \end{cases} \quad (6.16)$$

and

$$\bar{L}^\star(x) := \max\{l \in \{1, \ldots, L\} \,|\, F_l(x) \neq \emptyset\}. \quad (6.17)$$

Indeed, the control law (6.3) with (6.16) and (6.17) is a solution to the MAC problem, as every control input $\hat{u}_k$ is chosen such that the interexecution time $t_{k+1} - t_k = \hbar_{\bar{L}^\star(x(t_k))}$ is the largest one in the set $\mathcal{H}$ for which $F_{\bar{L}^\star(x(t_k))}(x(t_k)) \neq \emptyset$. Note that this control law is well defined if $F_{\mathrm{MAC}}(x) \neq \emptyset$, for all $x \in \mathbb{R}^{n_x}$. This condition is equivalent to requiring that $F_1(x) \neq \emptyset$ for all $x \in \mathbb{R}^{n_x}$. Namely, for each $x \in \mathbb{R}^{n_x}$, it holds that $F_1(x) \supseteq F_2(x) \supseteq \ldots \supseteq F_L(x)$, which gives that, for each $x \in \mathbb{R}^{n_x}$, $F_{\mathrm{MAC}}(x) \neq \emptyset$ implies that $F_1(x) \neq \emptyset$, while the fact that $F_1(x) \neq \emptyset$ implies that $F_{\mathrm{MAC}}(x) \neq \emptyset$ follows directly from (6.16) and (6.17). Hence, (6.16) is well defined if $F_1(x) \neq \emptyset$ for all $x \in \mathbb{R}^{n_x}$, which is guaranteed if the function V is an ordinary CLF for (6.1) with (6.2), a convergence rate $\alpha > 0$, a control gain bound $\beta > 0$ and an interexecution time $\hbar_1$, in the sense of Definition 6.3.2.

We will now formally show that the proposed MAC law renders the plant (6.1) with ZOH (6.2) GES with convergence rate α and a certain gain c.

Theorem 6.3.5. *Assume there exist a set $\mathcal{H} := \{\hbar_1, \ldots, \hbar_L\}$, $L \in \mathbb{N}$, satisfying $\hbar_{l+1} > \hbar_l > 0$ for all $l \in \{1, \ldots, L-1\}$, and an ordinary CLF for (6.1) with (6.2), a convergence rate $\alpha > 0$, a control gain bound $\beta > 0$ and the interexecution time $\hbar_1$, in the sense of Definition 6.3.1. Then, the MAC law (6.3), with (6.9), (6.15), (6.16) and (6.17), renders the plant (6.1) with ZOH (6.2) GES with the convergence rate α and the gain $c = \bar{c}(\alpha, \beta, \Delta_\hbar, \hbar_L)$ as in (6.14).*

Proof. The proof can be found in Appendix A.5. □

6.3.4   Solving the AAC Problem using eCLFs

We will now propose a solution to the AAC problem, in which the objective is to 'maximise performance' for an interexecution time h_k given by the real-time scheduler at time t_k, $k \in \mathbb{N}$. The solution is again based on allowing only a finite number of possible interexecution times, i.e., $h_k \in \mathcal{H} := \{\hbar_1, \ldots, \hbar_L\}$, $L \in \mathbb{N}$. Moreover, we consider only a finite number of possible convergence rates, i.e., $\alpha_k \in \mathcal{A} := \{\bar{\alpha}_1, \ldots, \bar{\alpha}_J\}$, $k \in \mathbb{N}$, where each $\bar{\alpha}_{j+1} > \bar{\alpha}_j > 0$, $j \in \{1, \ldots, J-1\}$, $J \in \mathbb{N}$. A consequence of these choices is that the notion of 'maximising performance' is actually relaxed to (approximately) maximising the local convergence rate $\alpha_k \in \mathcal{A}$ of the solutions of the closed-loop system (6.1), (6.2) with (6.4), in the sense that $V(x(t_{k+1})) \leqslant e^{-\alpha_k q h_k} V(x(t_k))$, for all $k \in \mathbb{N}$. In the proposed solution to the AAC problem, the local convergence rate α_k, $k \in \mathbb{N}$ is maximised, by maximising $\bar{J} \in \{1, \ldots, J\}$, (so that $\bar{\alpha}_{\bar{J}} \in \mathcal{A}$ is maximised), while guaranteeing a certain gain c (cf. Theorem 6.3.6), for each given $x \in \mathbb{R}^{n_x}$ and for each given $h \in \mathcal{H}$. In other words, for each given $x \in \mathbb{R}^{n_x}$ and each given $h \in \mathcal{H}$, $\bar{J}$ is maximised such that $F_{\bar{L}(h), \bar{J}}(x) \neq \emptyset$, in which

$$F_{\bar{L}, \bar{J}}(x) := \{u \in \mathbb{R}^{n_u} \mid f(x, u, \hbar_l, \bar{\alpha}_{\bar{J}}) \leqslant 0 \ \forall \ l \in \{1, \ldots, \bar{L}\} \text{ and } \|u\| \leqslant \beta \|x\|\}, \tag{6.18}$$

with $f(x, u, \hbar_l, \alpha)$ as defined in (6.9) and where $\bar{L}(h)$ is a function that, for all $h \in \mathcal{H}$, satisfies $\bar{L}(h) = \bar{L}$ if $h = \hbar_{\bar{L}}$. Hence, this AAC law is given by (6.4), for a given value of $h \in \mathcal{H}$ by the scheduler, where we take

$$F_{\text{AAC}}(x, h) := F_{\bar{L}(h), \bar{J}^\star(x, h)}(x), \tag{6.19}$$

with

$$\bar{J}^\star(x, h) = \max\{j \in \{1, \ldots, J\} \mid F_{\bar{L}(h), j}(x) \neq \emptyset\}. \tag{6.20}$$

The control law (6.4), with (6.19) and (6.20) is an AAC law, as for a given interexecution time, $t_{k+1} - t_k = h_k \in \mathcal{H}$, a control control input $\hat{u}_k$ is chosen such that the local convergence rate α_k is maximal and a bound on the gain c is guaranteed. Note that, similar to the solution to the MAC problem, this control law is well defined if $F_{\text{AAC}}(x, h) \neq \emptyset$ for all $x \in \mathbb{R}^{n_x}$ and all $h \in \mathcal{H}$, which is equivalent to requiring that $F_{L,1}(x) \neq \emptyset$ for all $x \in \mathbb{R}^{n_x}$. This is due to the fact that for each $x \in \mathbb{R}^{n_x}$, for all $l_1, l_2 \in \{1, \ldots, L\}$ and for all $j_1, j_2 \in \{1, \ldots, J\}$, it holds that $F_{l_1, j_1}(x) \supseteq F_{l_2, j_2}(x)$, if $l_1 \geqslant l_2$ and $j_1 \leqslant j_2$, which means that, for each $x \in \mathbb{R}^{n_x}$, $F_{\text{AAC}}(x) \neq \emptyset$ implies that $F_{L,1}(x) \neq \emptyset$, while the fact that $F_{L,1}(x) \neq \emptyset$ implies that $F_{\text{MAC}}(x) \neq \emptyset$ follows from that the fact that $F_{L,1}(x) \neq \emptyset$ implies that $F_{l,1}(x) \neq \emptyset$ for all $l \in \{1, \ldots, L\}$ and from (6.19) and (6.20). Hence, (6.19) is well defined if $F_{L,1}(x) \neq \emptyset$ for all $x \in \mathbb{R}^{n_x}$, which is guaranteed if the function V is an eCLF for (6.1) with (6.2), a convergence rate $\alpha = \bar{\alpha}_1$, a control gain bound β and the set $\mathcal{H}$.

We will now formally show that the proposed AAC law renders the plant (6.1) with ZOH (6.2) GES with at least convergence rate $\alpha = \bar{\alpha}_1$, and possibly a better convergence rate, and a certain gain c.

Theorem 6.3.6. *Assume there exist a set $\mathcal{A} := \{\bar{\alpha}_1, \ldots, \bar{\alpha}_J\}$, $J \in \mathbb{N}$, satisfying $\bar{\alpha}_{j+1} > \bar{\alpha}_j > 0$ for all $j \in \{1, \ldots, J-1\}$, and an eCLF for (6.1) with (6.2), the convergence rate $\alpha = \bar{\alpha}_1$, a control gain bound β and a set $\mathcal{H} := \{\hbar_1, \ldots, \hbar_L\}$, $L \in \mathbb{N}$, satisfying $\hbar_{l+1} > \hbar_l > 0$ for all $l \in \{1, \ldots, L-1\}$. Then, the AAC law (6.4), with (6.9), (6.18), (6.19) and (6.20), renders the plant (6.1) with ZOH (6.2) GES with (at least) the convergence rate $\alpha = \bar{\alpha}_1$ and the gain $c = \bar{c}(\bar{\alpha}_1, \beta, \Delta_\hbar, \hbar_L)$, as in (6.14).*

Proof. The proof can be found in Appendix A.5. $\qquad\square$

6.4 **Obtaining Well-Defined Solutions**

In this section, we will address the issue of how to guarantee that the solutions to the MAC and the AAC problem are *well defined*, i.e., that $F_{\mathrm{MAC}}(x) \neq \emptyset$ for all $x \in \mathbb{R}^{n_x}$ and that $F_{\mathrm{AAC}}(x, h) \neq \emptyset$ for all $x \in \mathbb{R}^{n_x}$ and all $h \in \mathcal{H}$. As was observed in the previous section, the existence of a CLF or an eCLF for (6.1) with (6.2), a convergence rate α, a control gain bound β and, for the CLF, an interexecution time h, and, for the eCLF, a set $\mathcal{H}$, ensures that the MAC law and the AAC law, respectively, are well defined. To obtain such a CLF or an eCLF, and to guarantee that the two control problems can be solved efficiently (as we will show in the next section), we focus in this section on ∞-norm-based (e)CLFs of the form

$$V(x) = \|Px\|_\infty, \tag{6.21}$$

with $P \in \mathbb{R}^{m \times n_x}$ satisfying $\mathrm{rank}(P) = n_x$. Note that (6.21) is a suitable candidate (e)CLF, in the sense of Definition 6.3.3, with $q = 1$, since (6.6) and (6.11) are satisfied with

$$\bar{a} = \|P\|_\infty, \quad \text{and} \quad \underline{a} = \max\{a > 0 \,|\, a\|x\| \leqslant \|Px\| \text{ for all } x \in \mathbb{R}^{n_x}\}. \tag{6.22}$$

In fact, $\mathrm{rank}(P) = n_x$ ensures that $\underline{a} > 0$.

We will now provide a two-step procedure to obtain a suitable (e)CLF. The first step is to consider an auxiliary control law of the form

$$u(t) = Kx(t) \tag{6.23}$$

that renders the plant (6.1) GES. To avoid any misunderstanding, (6.23) is not the control law being used; it is just an auxiliary control law that is useful to construct a candidate (e)CLF. The actual MAC law will be given by (6.3), with (6.16) and (6.17), and the AAC law will be given by (6.4), (6.19) and (6.20) based on (6.21), and neither one of these uses a matrix K.

Using the auxiliary control law, we can find a Lyapunov function for the plant (6.1) with control law (6.23) (without ZOH (6.2)) by employing the following intermediate result. This intermediate result can be seen as a slight extension of the results presented in [80, 108] to allow GES to be guaranteed, instead of only global asymptotic stability.

Lemma 6.4.1. *Assume that there exist a matrix $P \in \mathbb{R}^{m \times n_x}$, with $\mathrm{rank}(P) = n_x$, a matrix $Q \in \mathbb{R}^{m \times m}$ and a scalar $\hat{\alpha} > 0$ satisfying*

$$P(A + BK) - QP = 0 \tag{6.24a}$$

$$[Q]_{ii} + \sum_{j \in \{1, \dots, m\} \setminus \{i\}} \big|[Q]_{ij}\big| \leqslant -\hat{\alpha}, \tag{6.24b}$$

for all $i \in \{1, \dots, m\}$. Then, control law (6.23) renders the plant (6.1) GES with convergence rate $\hat{\alpha}$ and gain $\hat{c} = \overline{a}/\underline{a}$, with $\overline{a}$ and $\underline{a}$ as in (6.22).

Proof. The proof can be found in Appendix A.5. □

Note that it is always possible, given stabilisability of the pair (A, B), to find a matrix P satisfying the hypotheses of Lemma 6.4.1, and constructive methods to obtain a matrix P are given in [80, 108]. The second step in the procedure is to show that a matrix P satisfying the conditions of Lemma 6.4.1, renders the plant (6.1) with ZOH (6.2) GES in case the auxiliary control law is given, for all $k \in \mathbb{N}$, by

$$\begin{cases} \hat{u}_k = Kx(t_k) \\ t_{k+1} = t_k + h \end{cases} \tag{6.25}$$

provided that $h > 0$ is well chosen.

Lemma 6.4.2. *Suppose the conditions of Lemma 6.4.1 are satisfied. Then, for each $\alpha > 0$ satisfying $\alpha < \hat{\alpha}$, the system given by (6.1), (6.2) and (6.25) is GES with convergence rate α and gain $c = \bar{c}(\alpha, \|K\|, h)$ as in (6.10), for all $h < h_{\max}(\alpha)$ with*

$$h_{\max}(\alpha) = \min\big\{\hat{h} > 0 \,\big|\, \|P(e^{A\hat{h}} + \int_0^{\hat{h}} e^{As} \mathrm{d}s BK)(P^\top P)^{-1} P^\top\|_\infty > e^{-\alpha\hat{h}}\big\}. \tag{6.26}$$

Proof. The proof can be found in Appendix A.5. □

Using the matrix P and the function $h_{\max}(\alpha)$ obtained from Lemmas 6.4.1 and 6.4.2, we can now formally state the conditions under which the proposed solutions to the MAC and the AAC problem are well defined and how to achieve a desired convergence rate α and a desired gain c.

Theorem 6.4.3. *Assume there exist matrices $P \in \mathbb{R}^{m \times n_x}$, $K \in \mathbb{R}^{n_u \times n_x}$, and a scalar $\hat{\alpha} > 0$ satisfying the conditions of Lemma 6.4.1, and let $0 < \alpha < \hat{\alpha}$ and $c > \hat{c}$. If the control gain bound β satisfies $\beta \geqslant \|K\|_\infty$ and the*

set $\mathcal{H} := \{\hbar_1, \ldots, \hbar_L\}$, $L \in \mathbb{N}$, *is such that* $\hbar_1 < h_{\max}(\alpha)$ *as in* (6.26), *and* $c \geqslant \bar{c}(\alpha, \beta, \Delta_\hbar, \hbar_L)$ *as in* (6.14), *then the MAC law* (6.3), *with* (6.9), (6.15), (6.16), (6.17) *and* (6.21), *is well defined and renders the plant* (6.1) *with ZOH* (6.2) *GES with the convergence rate* α *and the gain* c.

Proof. The proof can be found in Appendix A.5. □

Theorem 6.4.4. *Assume there exist matrices* $P \in \mathbb{R}^{m \times n_x}$, $K \in \mathbb{R}^{n_u \times n_x}$, *and a scalar* $\hat{\alpha} > 0$ *satisfying the conditions of Lemma 6.4.1, and let* $0 < \alpha < \hat{\alpha}$ *and* $c > \hat{c}$ *be given. If the control gain bound* β, *satisfies* $\beta \geqslant \|K\|_\infty$, *the set* $\mathcal{A} := \{\bar{\alpha}_1, \ldots, \bar{\alpha}_J\}$, $J \in \mathbb{N}$, *is such that* $\alpha \leqslant \bar{\alpha}_1 < \hat{\alpha}$, *the set* $\mathcal{H} := \{\hbar_1, \ldots, \hbar_L\}$, $L \in \mathbb{N}$, *is such that* $\hbar_L < h_{\max}(\bar{\alpha}_1)$ *as in* (6.26), *and* $c \geqslant \bar{c}(\bar{\alpha}_1, \beta, \Delta_\hbar, \hbar_L)$ *as in* (6.14), *then the AAC law* (6.4), *with* (6.9), (6.18), (6.19), (6.20) *and* (6.21), *is well defined and renders the plant* (6.1) *with ZOH* (6.2) *GES with at least convergence rate* $\alpha = \bar{\alpha}_1$, *and possibly a better convergence rate, and a certain gain* c.

Proof. The proof can be found in Appendix A.5. □

These theorems formally show how to choose the scalar β, and the sets $\mathcal{A}$ and $\mathcal{H}$ to make each of the proposed solutions to the two control problems well defined and to achieve a desired convergence rate α and a desired gain c.

6.5 Making the Solutions to the MAC and the AAC Problem Computationally Tractable

As a final step in providing a complete solution to the MAC and the AAC problem, we will now propose computationally efficient algorithms to compute the control inputs generated by the MAC and AAC laws using online optimisation. To do so, note that the ∞-norm-based (e)CLFs as in (6.21) allow us to rewrite (6.9) as

$$f(x, u, h, \alpha) = \left\| P e^{Ah} x + \int_0^h P e^{As} B \mathrm{d}s\, u \right\|_\infty - e^{-\alpha h} \|Px\|_\infty. \qquad (6.27)$$

We can now observe that the constraint $f(x, u, h, \alpha) \leqslant 0$, which appears in (6.16) and (6.19), is equivalent to

$$\left| [P e^{A\hbar_l} x + \int_0^h P e^{As} B \mathrm{d}s\, u]_i \right| - e^{-\alpha h} \|Px\|_\infty \leqslant 0, \qquad (6.28)$$

for all $i \in \{1, \ldots, m\}$, which is equivalent to $\bar{f}(x, u, h, \alpha) \leqslant 0$, where

$$\bar{f}(x, u, h, \alpha) := \begin{bmatrix} P e^{Ah} x + P \int_0^h e^{As} \mathrm{d}s B u \\ -P e^{Ah} x - P \int_0^h e^{As} \mathrm{d}s B u \end{bmatrix} - e^{-\alpha h} \|Px\|_\infty \begin{bmatrix} 1 \\ \vdots \\ 1 \end{bmatrix} \qquad (6.29)$$

and the inequality is assumed to be taken elementwise, which results in $2m$ linear scalar constraints for u.

Equation (6.29) reveals that ∞-norm-based (e)CLFs convert the two considered problems into feasibility problems with linear constraints, allowing us to propose an algorithmic solution to the MAC and the AAC problem. The algorithms are based on solving the maximisation that appears in (6.17) and (6.20) by incrementally increasing $\bar{L}$ and $\bar{J}$, respectively.

Algorithm 6.5.1 (Minimum Attention Control). *Let the matrix $P \in \mathbb{R}^{m \times n_x}$, the scalars $\alpha, \beta > 0$ and the set $\mathcal{H}$, satisfying the conditions of Theorem 6.4.3, be given. At each t_k, $k \in \mathbb{N}$, given state $x(t_k)$:*

1. Set $l := 0$ and define $\mathcal{U}_0^{MAC} := \left\{ u \in \mathbb{R}^{n_u} \mid \begin{bmatrix} u \\ -u \end{bmatrix} - \beta \|x(t_k)\|_\infty \begin{bmatrix} 1 \\ \vdots \\ 1 \end{bmatrix} \leqslant 0 \right\}$

2. While $\mathcal{U}_l^{MAC} \neq \emptyset$, and $l < L$

   - *$\mathcal{U}_{l+1}^{MAC} := \mathcal{U}_l^{MAC} \cap \{ u \in \mathbb{R}^{n_u} \mid \bar{f}(x(t_k), u, \hbar_{l+1}, \alpha) \leqslant 0 \}$*
   - *$l := l + 1$*

3. If $l = L$ and $\mathcal{U}_L^{MAC} \neq \emptyset$, take $\hat{u}_k \in \mathcal{U}_L^{MAC}$, and $t_{k+1} = t_k + \hbar_L$

4. Or else, if $\mathcal{U}_l^{MAC} = \emptyset$, take $\hat{u}_k \in \mathcal{U}_{l-1}^{MAC}$, and $t_{k+1} = t_k + \hbar_{l-1}$.

Algorithm 6.5.2 (Anytime Attention Control). *Let the matrix $P \in \mathbb{R}^{m \times n_x}$, the scalar $\beta > 0$, and the sets $\mathcal{A}$ and $\mathcal{H}$, satisfying the conditions of Theorem 6.4.4, be given. At each t_k, $k \in \mathbb{N}$, given state $x(t_k)$ and given $h_k \in \mathcal{H}$, let $\bar{L} \in \{1, \ldots, L\}$ be such that $h_k = \hbar_{\bar{L}}$, and:*

1. Set $j := 0$ and define $\mathcal{U}_0^{AAC} := \left\{ u \in \mathbb{R}^{n_u} \mid \begin{bmatrix} u \\ -u \end{bmatrix} - \beta \|x(t_k)\|_\infty \begin{bmatrix} 1 \\ \vdots \\ 1 \end{bmatrix} \leqslant 0 \right\}$

2. While $\mathcal{U}_j^{AAC} \neq \emptyset$, and $j < J$,

   - *$\mathcal{U}_{j+1}^{AAC} := \mathcal{U}_0^{AAC} \cap \{ u \in \mathbb{R}^{n_u} \mid \bar{f}(x(t_k), u, \hbar_l, \alpha_{j+1}) \leqslant 0 \ \forall \, l \in \{1, \ldots, \bar{L}\} \}$*
   - *$j := j + 1$*

3. If $j = J$ and $\mathcal{U}_J^{AAC} \neq \emptyset$, take $\hat{u}_k \in \mathcal{U}_J^{AAC}$

4. Or else, if $\mathcal{U}_j^{AAC} = \emptyset$, take $\hat{u}_k \in \mathcal{U}_{j-1}^{AAC}$.

Remark 6.5.3. *Since verifying that $\mathcal{U}_l^{MAC} \neq \emptyset$, for some $l \in \{1, \ldots, L\}$, is a feasibility test for linear constraints, the algorithm can be efficiently implemented online using existing solvers for linear programs.*

6.6 Illustrative Examples

In this section, we illustrate the presented theory using a well-known example in the NCS literature, see, e.g., [40, 62, 103, 133], consisting of a linearised model of a batch reactor. For this example, we solve both the MAC and the AAC problem. The linearised batch reactor is given by (6.1) with

$$
\begin{bmatrix} A|B \end{bmatrix} = \left[\begin{array}{cccc|cc} 1.380 & -0.208 & 6.715 & -5.676 & 0 & 0 \\ -0.581 & -4.290 & 0 & 0.675 & 5.679 & 0 \\ 1.067 & 4.273 & -6.654 & 5.893 & 1.136 & -3.146 \\ 0.048 & 4.273 & 1.343 & -2.104 & 1.136 & 0 \end{array}\right]. \tag{6.30}
$$

In order to solve the two control problems discussed in this chapter, we need a suitable (e)CLF. To obtain such a (e)CLF, we use the results from Section 6.4, and use an auxiliary control law (6.23), with

$$
K = \begin{bmatrix} 0.0360 & -0.5373 & -0.3344 & -0.0147 \\ 1.6301 & 0.5716 & 0.8285 & -0.2821 \end{bmatrix} \tag{6.31}
$$

yielding that the eigenvalues $A + BK$ are all real valued, distinct, and smaller than or equal to -2. This allows us to find a Lyapunov function of the form (6.21) using Lemma 6.4.1, with P being the inverse of the matrix consisting of the eigenvectors of $A + BK$, Q being a diagonal matrix consisting of the eigenvalues of $A + BK$, $\hat{\alpha} = 2$ and $\hat{c} \approx 23.9$. This Lyapunov function will serve as an eCLF in the two control problems.

6.6.1 The Minimum Attention Control Problem

Given this eCLF, we can solve the MAC problem using Algorithm 6.5.1. Before doing so, we use the result of Theorem 6.4.3 to guarantee that the MAC law is well defined and renders the closed-loop system GES with desired convergence rate $\alpha = 0.98\hat{\alpha} = 1.96$ and desired gain $c = 4\hat{c} \approx 95.7$. According to Theorem 6.4.3, this convergence rate α and this gain c can be achieved by taking $\beta = \|K\|_\infty \approx 3.1$ and

$$
\mathcal{H} = \{\hbar_1, \ldots, \hbar_{10}\} = \{\tfrac{1.5}{1000}, \tfrac{7.5}{100}, \tfrac{15}{100}, \tfrac{22.5}{100}, \tfrac{30}{100}, \tfrac{37.5}{100}, \tfrac{45}{100}, \tfrac{52.5}{100}, \tfrac{60}{100}, \tfrac{67.5}{100}\}, \tag{6.32}
$$

because it holds that $\hbar_1 < h_{\max}(\alpha)$ and that $\bar{c}(\alpha, \beta, \Delta_\hbar, \hbar_L) \leqslant c$. To implement Algorithm 6.5.1 in MATLAB, we use the routine `polytope` of the MPT-toolbox [82], to create the sets $\mathcal{U}_l^{\mathrm{MAC}}$, to remove redundant constraints and to check if the set $\mathcal{U}_l^{\mathrm{MAC}}$, $l \in \{1, \ldots, 10\}$, is nonempty.

When we simulate the response of the plant with the resulting MAC law for the initial condition $x(0) = [1\ 0\ 1\ 0]^\top$, we can observe that the closed-loop system is indeed GES, see Figure 6.1a, and satisfies the required convergence rate α, see Figure 6.1c. To show the effectiveness of the theory, we compare

(a) Evolution of the states of the plant using MAC.

(b) Evolution of the states of the plant using self-triggered control.

(c) The decay of the Lyapunov function using MAC and self-triggered control.

(d) The interexecution times using MAC and self-triggered control.
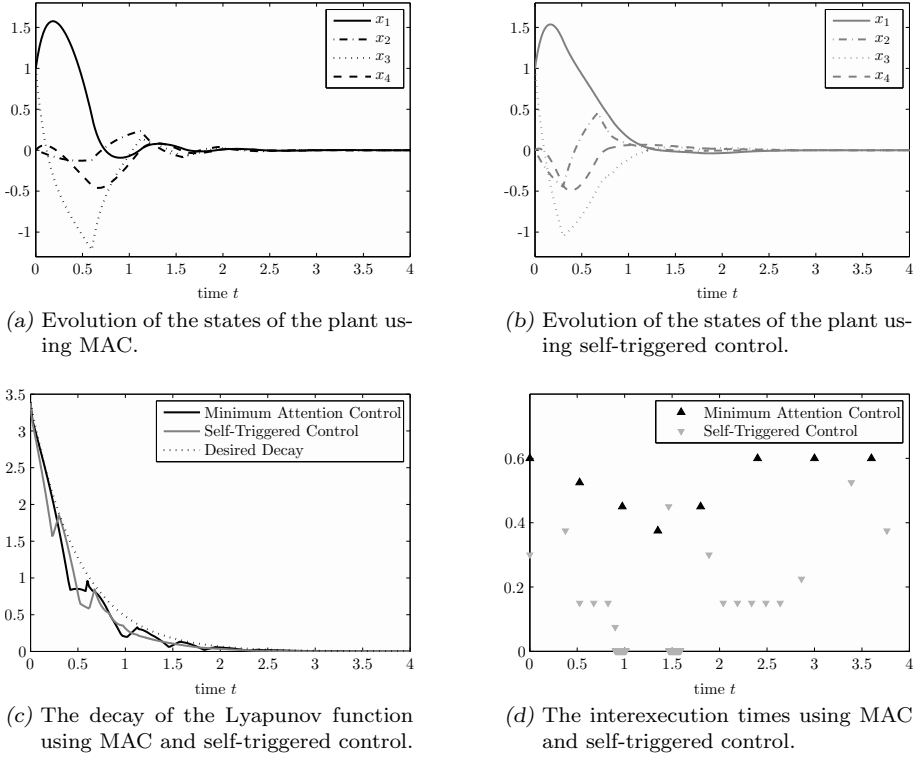
Figure 6.1: Minimum Attention Control.

our results with the self-triggered control strategy in the spirit of [92], however tailored to work with ∞-norm-based Lyapunov functions, resulting (by using the notation used in this chapter) in a control law (6.2) with $\hat{u}_k = Kx(t_k)$, and $t_{k+1} = t_k + \hbar_{\bar{L}(x(t_k))}$, where

$$\bar{L}(x(t_k)) = \max\{\hat{L} \in \{1, \dots, L\} \mid f(x(t_k), Kx(t_k), \hbar_l, \alpha) \leqslant 0 \ \forall \ l \in \{1, \dots, \hat{L}\}\}.$$
(6.33)

To illustrate that also this control strategy renders the plant (6.1) GES, we show the response of the plant to the initial condition $x(0) = [1 \ 0 \ 1 \ 0]^\top$ in Figure 6.1b, and the decay of the Lyapunov function in Figure 6.1c. Note that the decay of the Lyapunov function for MAC is comparable to the decay of the Lyapunov function for self-triggered control. However, when we compare the resulting interexecution times as depicted in Figure 6.1d, we can observe that the MAC yields much larger interexecution times. Hence, from a resource utilisation point of view, the proposed MAC outperforms the self-triggered

(a) Evolution of the states of the plant using AAC.

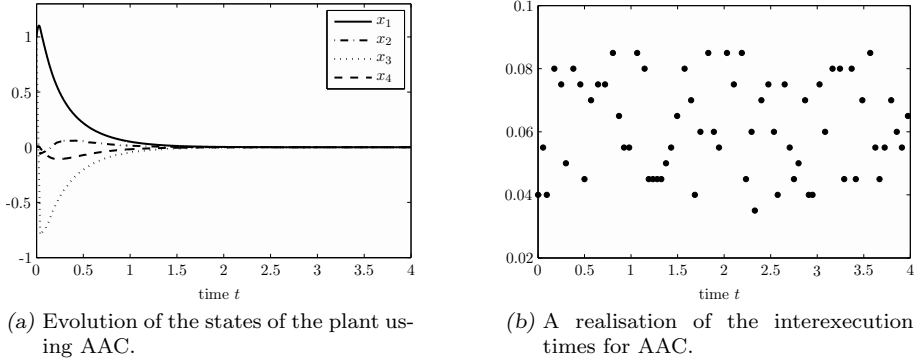(b) A realisation of the interexecution times for AAC.

Figure 6.2: Anytime Attention Control.

control law.

6.6.2 The Anytime Attention Control Problem

Let us now illustrate the AAC problem, which can be solved using Algorithm 6.5.2. In this case, Theorem 6.4.4 provides conditions under which the AAC law is well defined and renders the closed-loop system GES with guaranteed convergence rate $\alpha = 0.5$ and gain $c = 1.05\hat{c} \approx 25$. According to Theorem 6.4.4, this desired convergence rate α and this desired gain c can be achieved by taking $\beta = 1.4\|K\|_\infty \approx 4.6$, $\mathcal{A} = \{\bar{\alpha}_1, \ldots, \bar{\alpha}_{12}\}$, with $\bar{\alpha}_j = \frac{j}{2}$ for $j \in \{1, \ldots, 12\}$, and $\mathcal{H} = \{\hbar_1, \ldots, \hbar_6\} = \{0.011, 0.021, 0.031, 0.041, 0.051, 0.061\}$, because it holds that $\hbar_6 < h_{\max}(\bar{\alpha}_1)$ and that $\bar{c}(\bar{\alpha}_1, \beta, \Delta_\hbar, \hbar_L) \leqslant c$.

When we simulate the response of the plant with the AAC law to the initial condition $x(0) = [1\ 0\ 1\ 0]^\top$, and we take $h_k \in \mathcal{H}$, where h_k, $k \in \mathbb{N}$, is given by an independent and identically distributed sequence of discrete random variables having a uniform probability distribution, we can observe that the closed-loop system is indeed GES, see Figure 6.2a. We also depict the corresponding realisation of h_k for the interval $t \in [0, 4]$ in Figure 6.2b. We conclude that AAC is able to yield high performance, even though the execution times are time-varying and given by a scheduler.

6.7 Conclusion

In this chapter, we proposed a novel way to solve the minimum attention and the anytime attention control problem. Instrumental for the solutions is a novel extension to the notion of a control Lyapunov function. We solved the two control problems by focussing on linear plants, by considering only a finite

number of possible intervals between two subsequent executions of the control task and by choosing the extended control Lyapunov function (eCLF) to be ∞-norm-based, which allowed the two control problems to be formulated as linear programs. We provided a technique to obtain suitable eCLFs that render the solution to the minimum attention control problem feasible with a guaranteed upper bound on the attention (i.e., an lower bound on the inter-execution times), while guaranteeing an *a priori* selected performance level, and that renders solution to the anytime attention control problem feasible with a lower bound on the performance (in terms of a lower bound on the convergence rates), while guaranteeing a minimum level of performance. We illustrated the theory using two numerical examples. In particular, the first example showed that the proposed methodology outperforms a self-triggered control strategy that is available in the literature.

7

Conclusions, Recommendations and Final Thoughts

7.1   Concluding Remarks

In this thesis, control strategies have been studied that are tailored for platforms where only limited computation and/or communication resources are available for control. These considered control strategies contribute to the fields of networked control systems (NCSs) and event-triggered control systems (ETCSs). The main contributions of this thesis are summarised below.

- A modelling and analysis framework has been developed that allows the study of stability of NCSs that simultaneously subject to time-varying transmission intervals, time-varying delays, and communication constraints. Packet dropouts can be accommodated for, as well, by modelling them as a prolongations of the transmission intervals. The framework focusses on linear plants and controllers and is based on discrete-time switched linear parameter-varying models for NCSs. Two cases have been considered for the modelling of time-varying transmission intervals and delays; namely, the case where the transmission intervals and delays are simply assumed to be upper and lower bounded (Chapter 2), and the case where they are described by a sequence of continuous random variables (Chapter 3). The former case requires a less detailed description of the network behaviour than the latter case, while the latter case results in a less conservative stability analysis than the former, as has been shown in Chapter 3. For both cases, techniques have been provided for assessing the stability of the NCS using polytopic overapproximations and using linear matrix inequalities (LMIs). The presented framework reduces conservatism significantly with respect to existing results in the literature, as has been shown on the benchmark example of a chemical batch reactor in

Chapter 2, in the sense that stability can now be guaranteed for considerably larger ranges of transmission intervals and delays. Furthermore, the presented framework allows to study discrete-time dynamical output-based controllers, which could not be done before. Hence, the presented framework is an important and practically relevant contribution to the field of NCSs.

- Several contributions to the theory on event-triggered control (ETC) have been made. The first contribution (Chapter 4) has been the proposal of an ETC strategy that uses dynamical output-based controllers, instead of static state-feedback controllers, as is commonly done in the literature on ETC. Furthermore, decentralised event triggering has been considered to be able to handle large-scale systems, in which sensors, actuators and controllers can be physically distributed. A modelling framework has been provided based on impulsive systems to study the closed-loop stability and the $\mathcal{L}_\infty$-gain from disturbance inputs to performance outputs. Furthermore, guarantees on the minimum time between two subsequent events in each node, the so-called minimum inter-event time of a node, have been provided. The second contribution (Chapter 5) has been the proposition of the new class of periodic event-triggered control (PETC) algorithms, which aims at combining the benefits that, on the one hand, periodic control and, on the other hand, ETC offer. In PETC, the event-triggering condition is monitored periodically and at each sampling instant it is decided whether or not to transmit the sensor and/or actuator data and to use computation resources for the control task. Methodologies have been provided to analyse the stability and the $\mathcal{L}_2$-gain from disturbance inputs to performance outputs of this class of PETC algorithms. Finally, a preliminary contribution has been made in solving the codesign problem for ETC (Chapter 6). In particular, a novel way to solve the minimum attention and anytime attention control problem in one unifying framework has been proposed. The two control problems have been solved by formulating them as linear programs, which can be solved efficiently in an online fashion. With these three contributions, a significant step towards a comprehensive theory on ETC has been made.

These contributions are discussed in more detail below.

7.1.1   (Robust) Stability Analysis of NCSs

Chapter 2 discussed the stability analysis of NCSs that are subject to communication constraints, time-varying transmission intervals and time-varying delays, and (although more implicitly) packet dropouts. The stability of the NCS has been analysed for communication sequences that are determined by protocols in the newly introduced classes of quadratic protocols or periodic protocols,

having the well-known try-once-discard (TOD) and the round-robin (RR) as special cases. The analysis has been based on a discrete-time switched linear uncertain model of the NCS. A new and efficient convex overapproximation has been proposed that allows to analyse stability using a finite number of linear matrix inequalities (LMIs). On a benchmark example, the advantages and the effectiveness of the developed theory have been illustrated. In particular, it has been shown that stability can be guaranteed for a much larger maximum allowable transmission interval and maximum allowable transmission delay, when compared to the existing results in the literature. In addition, the results of Chapter 2 can be applied for stability analysis of NCSs with *discrete-time dynamic output-based controllers* and *nonzero* lower bounds on the transmission intervals and delays, which could not be analysed before even though they are highly relevant for practical implementations of networked controllers.

7.1.2 Stability Analysis of Stochastic NCSs

Chapter 3 also discussed stability analysis of NCSs that are subject to communication constraints, time-varying transmission intervals and time-varying delays, and packet dropouts. Contrary to Chapter 2, the stability of the NCS is analysed for the case where the transmission intervals and the transmission delays are described by a sequence of *continuous* random variables and the occurrence of packet dropouts is described by a Markov chain. Besides quadratic and periodic protocols, as studied in Chapter 2, also stochastic protocols are considered. The analysis has been based on a discrete-time switched linear stochastically parameter-varying model of the NCS. Conditions for stability (in the mean-square sense) have been derived by extending the convex overapproximation techniques of Chapter 2, such that the probabilistic information as present in the continuous probability distribution is preserved. This has also led to LMI-based conditions for stability. On a benchmark example, it has been shown that by incorporating probabilistic information on the transmission intervals and delays, stability can now be guaranteed for situations neither covered by existing results in the literature, nor by the results in Chapter 2.

7.1.3 Output-Based Decentralised ETC

Chapter 4 studied the stability and the $\mathcal{L}_\infty$-performance of ETC for dynamical output-based controllers having decentralised event triggering. The proposed event-triggering mechanism (ETM) unifies earlier proposals for ETMs, which have been mainly applied to state-feedback controllers. To analyse the resulting closed-loop system, it has been modelled as an impulsive system. This allows the stability and the $\mathcal{L}_\infty$-gains to be analysed using LMIs. Explicit expressions for lower bounds on the inter-event times have been provided and it has been formally proved that by using an impulsive systems approach, stability

and performance can be guaranteed for ETC algorithms with larger inter-event times than for existing results in literature, and, thus, using fewer communication resources. Using three numerical examples, the presented theory has been illustrated. These examples have shown that larger inter-event times can be obtained compared to existing results in the literature, that for unstable systems the outputs of the plants and controllers have to be transmitted less often when the state approaches the origin, and that for stable systems the outputs of the plant and controller only seem to be transmitted when disturbances are acting on the system and during transients.

7.1.4   Periodic Event-Triggered Control

In Chapter 5, a novel ETC strategy has been proposed, which aims at combining the benefits that periodic sampled-data control and ETC offer. In particular, the ETC strategy is based on the idea of having an event-triggering condition that is verified only periodically, and at each time it is decided whether or not to transmit new measurements and control signals. This control strategy, for which the term *periodic event-triggered control* (PETC) has been proposed, preserves the benefits of reduced resource utilisation as transmissions and controller computations are not performed periodically, while the event-triggering conditions still have a periodic character. The fact that the event-triggering condition only has to be verified at the periodic sampling times, instead of continuously, has the favourable property that this strategy can be implemented using standard time-sliced embedded software architectures. In addition, this strategy has the appealing feature of an inherent guaranteed minimum inter-event time of (at least) one sampling interval of the event-triggering condition, which can be tuned as desired during the design process. To analyse the stability and $\mathcal{L}_2$-gain properties of the PETC system, three approaches have been used: (i) a discrete-time piecewise linear (PWL) system approach, (ii) a discrete-time perturbed linear system approach, and (iii) an impulsive system approach. A comparison between all the three approaches has been provided, showing that each of the three presented modelling approaches have their own benefits and are therefore of independent interest. The theory has been illustrated using two numerical examples, showing that PETC is able to reduce the utilisation of communication and computation resources significantly.

7.1.5   Minimum Attention & Anytime Attention Control

Chapter 6 discussed a novel way to solve the minimum attention and anytime attention control problems. Instrumental for the solutions is a novel extension to the notion of a control Lyapunov function. The two control problems have been solved by focussing on linear plants, by considering only a finite number of possible inter-event times (and in the case of anytime attention control also

a finite number of performance levels), and by choosing the extended control Lyapunov function (eCLF) to be ∞-norm-based, which allowed the two control problems to be reformulated as linear programs. A technique has been provided to obtain suitable eCLFs that renders the solution to the minimum attention control problem feasible with a guaranteed upper bound on the attention (i.e., an lower bound on the inter-execution times), while guaranteeing an *a priori* selected performance level, and renders solution to the anytime attention control problem feasible with a lower bound on the performance (in terms of a lower bound on the convergence rates), while guaranteeing a minimum level of performance. In the case of anytime attention control algorithm receives more attention, higher levels of performance are automatically selected by the control algorithm. The theory has been illustrated using numerical examples. In particular, the first example showed that the proposed methodology outperforms an existing self-triggered control strategy.

7.2   Recommendations for Future Research

In the introduction, it has been acknowledged that both fields of NCSs and ETCSs have major open problems and that the system theory on NCSs and ETCSs is far from being comprehensive. Although several contributions to the system theory on NCSs and ETCS have been made in this thesis, several important questions remain that need to be addressed in future research. This section comments on some of these open problems for NCSs and ETCSs.

7.2.1   Networked Control Systems

Even though the NCS model presented in Chapter 2 and Chapter 3 is already general in the sense that it is one of the first that allows stability of NCSs to be studied in the joint presence of time-varying transmission intervals, time-varying transmission delays and communication constraints, while the occurrence of packet-dropouts can be including by modelling them (implicitly) as prolongations of the transmission intervals, the modelling framework is still not complete. In fact, it would be of interest to extend the framework in the following directions.

Including the effects of quantisation: Since the presented framework considers the four network-induced phenomena, the first natural extension of the framework could be the inclusion of the remaining network-induced phenomenon, namely, quantisation. Since quantisation effectively results in a discrepancy between the actual output of the plant or controller and the transmitted output, it can be modelled as a disturbance. Hence, the modelling framework presented in this thesis can be extended by modelling quantisation as a disturbance having certain properties and by exploiting ideas from, e.g.,

input-to-state stability analysis or $\mathcal{L}_p$-gain analysis, $p \in \mathbb{N}$, [79] to the analyse of the resulting model. Initial ideas in this direction are reported in [89].

Allowing the delays to be larger than the transmission interval: The framework presented in this thesis assumes that the delays are smaller than the transmission intervals, implying that the previous packet arrived before the new one is transmitted. In this way, packets do not arrive out of order. Since this cannot always be guaranteed in practice, it is of interest to extend the modelling framework to accommodate for the case that delays are larger than the transmission interval. This situation is sometimes referred to as the 'large delay'-case. Even though some results on large delays exist, e.g., see [29, 31], they have never been studied in combination with communication constraints and network protocols. Furthermore, the existing results on large delays use state-feedback controllers, whereas the framework presented in this thesis uses general dynamical output-based controllers. The fact that dynamical output-based controllers are used and communication constraints are present complicates the analysis significantly. For instance, it is not straightforward how the states of the controller should be updated in case a packet arrives before an earlier transmitted packet, i.e., when one packet 'overtakes' the other. Nevertheless, since in practical NCSs large delays might occur, the extension of the current framework to include large delays constitutes an interesting topic for future research.

Analysing closed-loop performance: The framework presented in the first part of the thesis focusses on stability analysis of NCSs. Even though stability is one of the most important and basic properties a control system should have, a control system also has to satisfy certain closed-loop performance requirements. Since it is well known that the insertion of a communication network deteriorates the closed-loop performance of the control system, it would be beneficial to have performance analysis tools for NCSs as well. Hence, it is of interest to generalise the analysis framework presented in the first part of this thesis towards the analysis of the $\mathcal{L}_p$-gain, for some $p \in \mathbb{N}$, from disturbance inputs to performance outputs of the NCS. To achieve this, efficient methods to include intersample behaviour in the discrete-time framework presented in this thesis are needed in order to arrive at nonconservative tools for closed-loop performance analysis.

Allowing for more detailed network models: In this thesis, the delays and transmission intervals are either assumed to be upper and lower bounded, or assumed to be given by an independent and identically distributed (iid) sequence of random variables. Even though the latter is already a more detailed description of the network behaviour than the former, it is still a simplified description of reality. For instance, the communication channels can exhibit a

time-varying reliability, which means that the sequence of random variables describing the transmission intervals and the transmission delays can no longer be assumed to be iid. In particular, there might exist a correlation between transmission delays at two successive transmission intervals. Hence, it is of interest to extend the modelling and analysis framework to include the consequences of this time-varying reliability.

Furthermore, it has been assumed in this thesis that the bounds on, or the probability distribution of, the transmission intervals, the transmission intervals delays and packet dropouts are given, while in fact they are a consequence of, e.g., the underlying communication technology, the network topology, and the fact that other (i.e., not control-related) tasks make use of the network. Even though these bounds, or this joint probability distribution, only provide an abstract description of the network, it has been shown that they are extremely valuable for the analysis of the closed-loop system for different network protocols. However, in some occasions, these network models might be too abstract and more detailed models of the underlying network are needed. This is an other important topic of research as it might allow the consequences of choosing a certain network topology and communication technology to be analysed more directly.

Controller and protocol codesign: The work presented in this thesis allows stability to be studied given a controller and a scheduling protocol, while the controller/protocol codesign problem is not studied. The controller synthesis problem for NCSs without communication constraints and for state-feedback control laws is solved in [29], and the (decentralised) controller synthesis problem for NCSs with a given periodic protocol for dynamical output-based controllers is studied in [13, 14]. The cited papers assume that the transmission interval and delays can be upper and lower bounded and either do not consider communication constraints at all or assume a particular, and given, scheduling protocol. Furthermore, the controller and (quadratic) protocol synthesis problem for NCSs *without* time-varying transmission intervals and delays is studied in [34]. Hence, the important problem of controller/protocol codesign for general classes of protocols is not solved yet and, therefore, forms an important topic for future research.

7.2.2   *Event-Triggered Control Systems*

Although various relevant contributions to the field of ETCSs are made in this thesis, a comprehensive system theory for ETC is currently not yet available. Therefore, several recommendations for future research are given below that will contribute to a comprehensive system theory for ETC that will support the deployment of ETC in a large variety of control applications.

Reducing conservatism in the analysis: The illustrative examples in Chapter 4 have shown that the upper bound on the magnitude of the ultimate bounds and the $\mathcal{L}_\infty$-gain, based on the theory, were larger than what was expected from the simulations, and the lower bounds on the inter-event times, again based on the theory, were smaller than the inter-event times observed in the simulations. Furthermore, the theoretical upper bounds on the $\mathcal{L}_2$-gain in the illustrative examples in Chapter 6 were larger than what could be concluded from the simulations. Therefore, future work on (P)ETC should focus on improving the upper bound on the magnitude of the ultimate bound, the upper bound on the $\mathcal{L}_\infty$-gain or $\mathcal{L}_2$-gain, and the lower bound on the inter-event times to become closer to the true value of the ultimate bound, the $\mathcal{L}_\infty$-gain, the $\mathcal{L}_2$-gain and the minimum inter-event times, respectively.

Including network-induced artifacts: The fact that ETC aims at saving communication resources, makes it a very useful control strategy to be implemented over a multipurpose communication network. Hence, ETC provides an alternative to the conventional sampled-data controller used in the NCS literature. However, in the case that ETC is used in the context of NCSs, the control system again becomes subject to time-varying transmission delays, packet dropouts and perhaps even communication constraints, and the robustness of the ETC algorithm against these phenomena has to be quantified. In the case of PETC, the control system might also become subject to time-varying transmission intervals, as the local clocks might not be synchronised exactly, and the the robustness of the PETC algorithm against time-varying transmission intervals has to be quantified as well. Therefore, future work could focus on extending the framework presented in Chapter 4 and Chapter 5 to include the case where the ETC system is subject to the network-induced phenomena studied in the first part of this thesis. In fact, the theory developed in the first part of the thesis can provide a good starting point to achieve this. Once this task is accomplished successfully, ETC might be the natural control strategy for many NCS applications.

Solving the controller and ETM codesign problem: Even though Chapter 6 presented an approach to solve the minimum attention and the anytime attention control problems, and the former can be seen as a solution to the controller and ETM codesign problem, the general codesign problem is largely unexplored. Namely, the minimum attention control problem solved in Chapter 6 focusses on state-feedback controllers and yields a self-triggered control algorithm, thereby providing only a solution to very particular codesign problem in ETC. Furthermore, the solution of the control problem has the form of an online optimisation problem. Even though these linear programs can be solved efficiently using existing solvers, the computations are numerically more demanding than, for instance, a conventional state-feedback control algorithm,

which might not be desirable from an implementation point of view. If instead the optimisation problem can be solved explicitly, e.g., using multiparametric linear programming as has been done in explicit model predictive control (MPC) in [15], this computational burden might be alleviated. Therefore, future research on minimum attention control and anytime attention control could focus on obtaining explicit solutions to the optimisation problem and on formulating the problem for the case in which not all the states can be measured directly.

7.3 Final Thoughts

The contributions of this thesis can form a basis for future research explorations, possibly along the lines of the recommendations given above. These contributions and future explorations can lead to a mature system theory for both NCSs and ETCSs, thereby supporting their deployment in a large variety of practical control applications, such as chemical plants, water distribution networks, distributed power generation systems, unmanned aerial vehicles, vehicle platoons on motorways, tele-operated haptic systems, and so on. In particular, ETC can have an enormous potential to revolutionise the control field as it advocates the abandonment of the conventional periodic time-triggered feedback control paradigm. The benefits of ETC being that it naturally results in less communication and, thereby, in less delay and fewer packet dropouts makes this control strategy very well suited for NCSs. If the ideas put forward in Part II of this thesis are combined with the results on NCSs in Part I of this thesis leading to ETCSs that are able to deal with the network-induced imperfections, ETC can become an important component in the design of the NCSs of the future.

<div style="text-align: center">

A

Proofs of Theorems and Lemmas

</div>

A.1   Chapter 2

Proof of Lemma 2.2.4. In Theorem 4 of [104], it was shown that a sampled-data system is UGES if and only if its corresponding discretised model is UGES and the intersample behaviour is so-called linearly uniformly globally bounded over T (LUGBT), where T is the sampling interval. This means, roughly speaking, that the intersample behaviour can be bounded by a linear function of the state of the system at the transmission instants. To show that the sampled-data model is indeed LUGBT, let us introduce an additional variable $\tilde{t} := t - t_k$, for all $t \in (t_k, t_{k+1}]$. Solving the differential equation (2.1) on the interval $\tilde{t} \in (0, \tau_k]$ yields

$$x^p(t_k + \tilde{t}) = e^{A^p \tilde{t}} x^p(t_k) + \int_0^{\tilde{t}} e^{A^p(\tilde{t}-s)} \mathrm{d}s B^p \hat{u}(t_k) \tag{A.1}$$

and on the interval $\tilde{t} \in (\tau_k, h_k]$

$$x^p(t_k + \tilde{t}) = e^{A^p \tilde{t}} x^p(t_k) + \int_0^{\tau_k} e^{A^p(\tilde{t}-s)} \mathrm{d}s B^p \hat{u}(t_k) + \int_{\tau_k}^{\tilde{t}} e^{A^p(\tilde{t}-s)} \mathrm{d}s B^p \lim_{t \downarrow r_k} \hat{u}(t). \tag{A.2}$$

Or equivalently, when expressed in states at the sample instants, for $\tilde{t} \in (0, \tau_k]$,

$$x^p(t_k + \tilde{t}) = e^{A^p \tilde{t}} x_k^p + \int_0^{\tilde{t}} e^{A^p s} \mathrm{d}s B^p (D^c C^p x_k^p + C^c x_k^c + D^c e_k^y + e_k^u) \tag{A.3}$$

and for $\tilde{t} \in (\tau_k, h_k]$,

$$x^p(t_k + \tilde{t}) = e^{A^p \tilde{t}} x_k^p + \int_0^{\tilde{t}} e^{A^p s} \mathrm{d}s B^p (D^c C^p x_k^p + C^c x_k^c + e_k^u + D^c e_k^y)$$
$$- \int_0^{\tilde{t} - \tau_k} e^{A^p s} \mathrm{d}s B^p \Gamma_{\sigma_k}^u e_k^u. \quad \text{(A.4)}$$

Using (A.3) and (A.4), we can bound the intersample behaviour on the interval $\tilde{t} \in (0, h_k]$ by

$$\|x^p(t_k + \tilde{t})\| \leqslant \|e^{A^p \tilde{t}}\| \|x_k^p\| + \left\| \int_0^{\tilde{t} - \tau_k} e^{A^p s} \mathrm{d}s B^p \Gamma_{\sigma_k}^u \right\| \|e_k^u\|$$
$$+ \left\| \int_0^{\tilde{t}} e^{A^p s} \mathrm{d}s B^p \right\| \left(\|C^c\| \|x_k^c\| + \|D^c C^p\| \|x_k^p\| + \|D^c\| \|e_k^y\| + \|e_k^u\| \right). \quad \text{(A.5)}$$

Similar inequalities can be derived that bound the intersample behaviour for the state evolution $x^c(t)$ of (2.2a) and for the network-induced error given by (2.7). Therefore, by using the bounds on h_k and τ_k, the continuous-time NCS (2.1), (2.2a) or (2.2b), (2.3), and (2.7) is LUGBT. Consequently, Theorem 4 of [104] guarantees that the continuous-time NCS is UGES if and only if the discrete-time model (2.12). $\qquad \square$

Proof of Theorem 2.3.2. The proof is based on showing that Procedure 2.3.1 yields that system (2.25) is an overapproximation of (2.12) in the sense that (2.27) holds, and that this overapproximation is tight in the sense that (2.30) holds for a $\varepsilon > 0$, satisfying $\varepsilon \leqslant \varepsilon_u$ for some ε_u.

In order for (2.27) to hold, considering a fixed $\sigma \in \{1, \ldots, N\}$, we should have that for all $(h, \tau) \in \Theta$, there exist an $\alpha \in \mathcal{A}$ and a $\Delta \in \boldsymbol{\Delta}$, such that (2.29) holds, i.e.,

$$\tilde{A}_{\sigma, h, \tau} = \sum_{l=1}^{L} \alpha^l \bar{A}_{\sigma, l} + \bar{B} \Delta \bar{C}_\sigma. \quad \text{(A.6)}$$

Therefore, given L distinct pairs $(\tilde{h}_l, \tilde{\tau}_l) \in \Theta$, $l \in \{1, \ldots, L\}$, and $\bar{A}_{\sigma, l}$ as in (2.32), we can write the approximation error between $\tilde{A}_{\sigma, h, \tau}$ of (2.12) and $\sum_{l=1}^{L} \alpha^l \bar{A}_{\sigma, l}$ of (2.28) as

$$\tilde{A}_{\sigma, h, \tau} - \sum_{l=1}^{L} \alpha^l \bar{A}_{\sigma, l} = \underbrace{\begin{bmatrix} T^\top & -(CT)^\top \\ T^\top & -(CT)^\top \\ T^\top & -(CT)^\top \end{bmatrix}^\top}_{=:\tilde{B}} \tilde{\Delta}_{\alpha, h, \tau} \underbrace{\begin{bmatrix} T^{-1} & 0 \\ T^{-1}BDC & T^{-1}BD \\ 0 & -T^{-1}B\Gamma_\sigma \end{bmatrix}}_{=:\bar{C}_\sigma},$$
$$\text{(A.7)}$$

where

$$\tilde{\Delta}_{\alpha,h,\tau} = \text{diag}\left(T^{-1}\left(A_h - \sum_{l=1}^{L}\alpha^l A_{\tilde{h}_l}\right)T, T^{-1}\left(E_h - \sum_{l=1}^{L}\alpha^l E_{\tilde{h}_l}\right)T,\right.$$
$$\left. T^{-1}\left(E_{h-\tau} - \sum_{l=1}^{L}\alpha^l E_{\tilde{h}_l-\tilde{\tau}_l}\right)T\right), \quad \text{(A.8)}$$

in which A_h, E_h, $E_{h-\tau}$ are defined as in Section 2.2.1.A, 2.2.1.B or 2.2.1.C. Using the real Jordan form of (2.33), we can observe that

$$T^{-1}\left(A_h - \sum_{l=1}^{L}\alpha^l A_{\tilde{h}_l}\right)T = e^{\Lambda h} - \sum_{l=1}^{L}\alpha^l e^{\Lambda \tilde{h}_l}, \quad \text{(A.9a)}$$

$$T^{-1}\left(E_h - \sum_{l=1}^{L}\alpha^l E_{\tilde{h}_l}\right)T = \sum_{l=1}^{L}\alpha^l \int_{\tilde{h}_l}^{h} e^{\Lambda s}\mathrm{d}s, \quad \text{(A.9b)}$$

$$T^{-1}\left(E_{h-\tau} - \sum_{l=1}^{L}\alpha^l E_{\tilde{h}_l-\tilde{\tau}_l}\right)T = \sum_{l=1}^{L}\alpha^l \int_{\tilde{h}_l-\tilde{\tau}_l}^{h-\tau} e^{\Lambda s}\mathrm{d}s \quad \text{(A.9c)}$$

hold for all $\alpha \in \mathcal{A}$ if A_h, E_h, and $E_{h-\tau}$ are defined as in Section 2.2.1.A and 2.2.1.C. Since E_h and $E_{h-\tau}$, when defined as in Section 2.2.1.B, contain identity matrices in the lower-right part, the left-hand side of (A.9b) and (A.9c) contain zero blocks. Therefore, in case of E_h and $E_{h-\tau}$ being defined as in Section 2.2.1, equality in (A.9b) and (A.9c) do not automatically hold and we have to impose additional requirements on $\alpha \in \mathcal{A}$ to ensure that the appropriate Jordan blocks of the right-hand side of (A.9b) and (A.9c) also equal zero. These additional requirements are that

$$\sum_{l=1}^{L}\alpha^l \tilde{h}_l = h, \qquad \text{and} \qquad \sum_{l=1}^{L}\alpha^l(\tilde{h}_l - \tilde{\tau}_l) = h - \tau, \quad \text{(A.10)}$$

since substituting (A.10) into (A.9) indeed results in zero-blocks at the appropriate places in the left-hand side of (A.9). Now, combining (A.8) and (A.9) yields

$$\tilde{\Delta}_{\alpha,h,\tau} = \sum_{l=1}^{L}\alpha^l \text{ diag}(e^{\Lambda h} - e^{\Lambda \tilde{h}_l}, \int_{\tilde{h}_l}^{h} e^{\Lambda s}\mathrm{d}s, \int_{\tilde{h}_l-\tilde{\tau}_l}^{h-\tau} e^{\Lambda s}\mathrm{d}s), \quad \text{(A.11)}$$

provided that (A.10) holds.

As an intermediate step in the proof, we aim at finding a set $\tilde{\boldsymbol{\Delta}}$ of matrices, such that for all $(h,\tau) \in \Theta$ there is an $\alpha \in \mathcal{A}$ such that $\tilde{\Delta}_{\alpha,h,\tau} \in \tilde{\boldsymbol{\Delta}}$. Since $\Theta = \cup_{m=1}^{M}\mathcal{S}_m$, we wil perform the construction of $\tilde{\boldsymbol{\Delta}}$ per triangle $\mathcal{S}_m$, $m \in$

$\{1\ldots,M\}$, and combine them later. Hence, for each $m \in \{1,\ldots,M\}$, we now aim at constructing $\tilde{\boldsymbol{\Delta}}^m$ such that for all $(h,\tau) \in \mathcal{S}_m$, $m \in \{1,\ldots,M\}$, there is an $\alpha \in \mathcal{A}$ such that $\tilde{\Delta}_{\alpha,h,\tau} \in \tilde{\boldsymbol{\Delta}}^m$. In particular, for $(h,\tau) \in \mathcal{S}_m$, $m \in \{1,\ldots,M\}$, with $\mathcal{S}_m$ as in (2.31), take $\bar{\alpha}^{l_j^m} = \tilde{\alpha}^j$, $j = \{1,2,3\}$, and $\bar{\alpha}^i = 0$, $i \notin \{l_1^m, l_2^m, l_3^m\}$, where $\sum_{j=1}^3 \tilde{\alpha}^j(\tilde{h}_j^m, \tilde{\tau}_j^m) = (h,\tau)$, $\sum_{j=1}^3 \tilde{\alpha}^j = 1$, and $\tilde{\alpha}^j \geqslant 0$, $j \in \{1,2,3\}$. Let us now bound the norm of (A.11) for triangle $\mathcal{S}_m$, $m \in \{1,\ldots,M\}$, and per Jordan block Λ_i, $i \in \{1,\ldots,K\}$ using this particular choice $\bar{\alpha}$ for α. Hence, for all $(h,\tau) \in \mathcal{S}_m$, $\tilde{\Delta}_{\bar{\alpha},h,\tau} \in \tilde{\boldsymbol{\Delta}}^m$ with

$$
\begin{aligned}
\tilde{\boldsymbol{\Delta}}^m := \Big\{ &\text{diag}(\tilde{\Delta}_1^A,\ldots,\tilde{\Delta}_K^A,\tilde{\Delta}_1^{E_h},\ldots,\tilde{\Delta}_K^{E_h},\tilde{\Delta}_1^{E_h-\tau},\ldots,\tilde{\Delta}_K^{E_h-\tau})\Big| \\
&\|\tilde{\Delta}_i^A\| \leqslant \max_{\substack{\sum_{j=1}^3 \tilde{\alpha}^j = 1, \\ \tilde{\alpha}^j \geqslant 0}} \tilde{\delta}_{i,m,\tilde{\alpha}}^A, \ \|\tilde{\Delta}_i^{E_h}\| \leqslant \max_{\substack{\sum_{j=1}^3 \tilde{\alpha}^j = 1, \\ \tilde{\alpha}^j \geqslant 0}} \tilde{\delta}_{i,m,\tilde{\alpha}}^{E_h}, \\
&\|\tilde{\Delta}_i^{E_h-\tau}\| \leqslant \max_{\substack{\sum_{j=1}^3 \tilde{\alpha}^j = 1, \\ \tilde{\alpha}^j \geqslant 0}} \tilde{\delta}_{i,m,\tilde{\alpha}}^{E_h-\tau}, i \in \{1,\ldots,K\}\Big\}, \quad \text{(A.12)}
\end{aligned}
$$

for $m \in \{1,\ldots,M\}$ in which $\tilde{\delta}_{i,m,\tilde{\alpha}}^A$, $\tilde{\delta}_{i,m,\tilde{\alpha}}^{E_h}$, and $\tilde{\delta}_{i,m,\tilde{\alpha}}^{E_h-\tau}$ are given by (2.36). This upper bound on the approximation errors allows us to write

$$
\begin{aligned}
\big\{\tilde{A}_{\sigma,h,\tau} \mid (h,\tau) \in \mathcal{S}_m\big\} \subseteq & \\
\Big\{\sum_{j=1}^3 \tilde{\alpha}^j \bar{A}_{\sigma,l_j^m} + \bar{B}\tilde{\Delta}^m \bar{C}_\sigma \ \Big| \ \sum_{j=1}^3 \tilde{\alpha}^j = 1, \tilde{\alpha}^j \geqslant 0, & j \in \{1,2,3\}, \tilde{\Delta}^m \in \tilde{\boldsymbol{\Delta}}^m\Big\}. \ \text{(A.13)}
\end{aligned}
$$

To obtain $\boldsymbol{\Delta}$ independent of m, as in (2.44), let us now introduce the scaling matrix

$$
U := \text{diag}(\delta_1^A I_1,\ldots,\delta_K^A I_K, \delta_1^{E_h} I_1,\ldots,\delta_K^{E_h} I_K, \delta_1^{E_h-\tau} I_1,\ldots,\delta_K^{E_h-\tau} I_K) \quad \text{(A.14)}
$$

in which I_i is an identity matrix of size n_i, complying with the size of the $\tilde{\Delta}_i$ and observe that $\tilde{\boldsymbol{\Delta}}^m \subseteq U\boldsymbol{\Delta}$, with $\boldsymbol{\Delta}$ as in (2.44). Now due to (2.35) and (2.38), $\bar{B} = \tilde{B} \cdot U$, and this allows us to rewrite (A.13) as

$$
\begin{aligned}
\big\{\tilde{A}_{\sigma,h,\tau} \mid (h,\tau) &\in \mathcal{S}_m\big\} \\
&\subseteq \Big\{\sum_{j=1}^3 \tilde{\alpha}^j \bar{A}_{\sigma,l_j^m} + \bar{B}\Delta\bar{C}_\sigma \Big| \sum_{j=1}^3 \tilde{\alpha}^j = 1, \tilde{\alpha}^j \geqslant 0, j \in \{1,2,3\}, \Delta \in \boldsymbol{\Delta}\Big\} \\
&\subseteq \Big\{\sum_{l=1}^L \alpha^l \bar{A}_{\sigma,l} + \bar{B}\Delta\bar{C}_\sigma \Big| \alpha \in \mathcal{A}, \Delta \in \boldsymbol{\Delta}\Big\}, \quad \text{(A.15)}
\end{aligned}
$$

with $\mathcal{A}$ as in (2.26) and $\boldsymbol{\Delta}$ as in (2.44), which is . By taking the convex hull over all $m \in \{1,\ldots,M\}$ in the left-hand-side and observing that the right-hand-side is independent of m, we obtain (2.27).

To show that (2.30) holds for ε as in (2.39), we consider a fixed $\sigma \in \{1, \ldots, N\}$ and show that for all $\alpha \in \mathcal{A}$ and $\Delta \in \mathbf{\Delta}$, there exist a pair $(h, \tau) \in \Theta$ and a $\bar{\Delta}$, satisfying $\|\bar{\Delta}\| \leqslant \varepsilon$, such that

$$\sum_{l=1}^{L} \alpha^l \bar{A}_{\sigma,l} + \bar{B} \Delta \bar{C}_\sigma \in \mathrm{co}\{\tilde{A}_{\sigma,h,\tau} \,|\, (h, \tau) \in \Theta\} + \{\bar{\Delta} \,|\, \|\bar{\Delta}\| \leqslant \varepsilon\}. \qquad (A.16)$$

Since by definition it holds that

$$\sum_{l=1}^{L} \alpha^l \bar{A}_{\sigma,l} = \sum_{l=1}^{L} \alpha^l \bar{A}_{\sigma,\tilde{h}_l,\tilde{\tau}_l} \in \mathrm{co}\{\bar{A}_{\sigma,h,\tau} \,|\, (h, \tau) \in \Theta\}, \qquad (A.17)$$

this inclusion is satisfied if $\left\|\bar{B}\Delta\bar{C}_\sigma\right\| \leqslant \varepsilon$, which holds for $\varepsilon \leqslant \varepsilon_u$ as in (2.39), due to the fact that Procedure 2.3.1 terminates not until $\varepsilon \leqslant \varepsilon_u$. $\qquad \square$

Proof of Theorem 2.4.1. The proof is based on showing that V as in (2.46) is a Lyapunov function for the switched uncertain system (2.25) with switching law (2.18). Note that $V(\bar{x}_k) = \bar{x}_k^\top P_i \bar{x}_k$, with $i = \sigma_k$, due to (2.18). Now, we obtain using (2.46) and (2.25) that

$$V(\bar{x}_{k+1}) = \min_{\nu \in \mathcal{N}} \bar{x}_{k+1}^\top \sum_{j=1}^{N} \nu_j P_j \bar{x}_{k+1}$$

$$= \min_{\nu \in \mathcal{N}} \bar{x}_k^\top \Big(\sum_{l_1=1}^{L} \alpha_k^{l_1} \bar{A}_{\sigma_k,l_1} + \bar{B}\Delta_k \bar{C}_{\sigma_k} \Big)^\top$$

$$\sum_{j=1}^{N} \nu_j P_j \Big(\sum_{l_2=1}^{L} \alpha_k^{l_2} \bar{A}_{\sigma_k,l_2} + \bar{B}\Delta_k \bar{C}_{\sigma_k} \Big) \bar{x}_k$$

$$\leqslant \bar{x}_k^\top \Big(\sum_{l_1=1}^{L} \alpha_k^{l_1} \bar{A}_{i,l_1} + \bar{B}\Delta_k \bar{C}_i \Big)^\top \sum_{j=1}^{N} \pi_{ji} P_j \Big(\sum_{l_2=1}^{L} \alpha_k^{l_2} \bar{A}_{i,l_2} + \bar{B}\Delta_k \bar{C}_i \Big) \bar{x}_k,$$

$$(A.18)$$

where $\{\pi_{ji}\} \in \mathcal{M}$, with $\mathcal{M}$ as in (2.48). To obtain UGES, it is sufficient to require that the Lyapunov function is strictly decreasing in the sense that (due to (A.18))

$$\Big(\sum_{l_1=1}^{L} \alpha_k^{l_1} \bar{A}_{i,l_1} + \bar{B}\Delta \bar{C}_i \Big)^\top \sum_{j=1}^{N} \pi_{ji} P_j \Big(\sum_{l_2=1}^{L} \alpha_k^{l_2} \bar{A}_{i,l_2} + \bar{B}\Delta \bar{C}_i \Big) - P_i \prec 0. \quad (A.19)$$

for all $\alpha \in \mathcal{A}$, $\Delta \in \mathbf{\Delta}$, and $i \in \{1, \ldots, N\}$. By taking a Schur complement, realising that $\sum_{j=1}^{N} \pi_{ji} P_j \succ 0$, and using that $\alpha_k \in \mathcal{A}$, we obtain that (A.19)

is equivalent to

$$\sum_{l=1}^{L} \alpha_k^l \underbrace{\begin{bmatrix} P_i & (\bar{A}_{i,l} + \bar{B}\Delta\bar{C}_i)^\top \sum_{j=1}^{N} \pi_{ji} P_j \\ \sum_{j=1}^{N} \pi_{ji} P_j (\bar{A}_{i,l} + \bar{B}\Delta\bar{C}_i) & \sum_{j=1}^{N} \pi_{ji} P_j \end{bmatrix}}_{G_{i,l}} \succ 0, \quad \text{(A.20)}$$

for all $\alpha \in \mathcal{A}$, $\Delta \in \boldsymbol{\Delta}$, and $i \in \{1, \ldots, N\}$. A necessary and sufficient condition for positive definiteness of (A.20), for all $\alpha_k \in \mathcal{A}$, is that $G_{i,l} \succ 0$ for all $i \in \{1, \ldots, N\}$ and $l \in \{1, \ldots, L\}$. Now observe that for all $\Delta \in \boldsymbol{\Delta}$, it holds that $\bar{C}_i^\top (R_{i,l} - \Delta^\top R_{i,l} \Delta) \bar{C}_i \succeq 0$, for all $R_{i,l} \in \mathcal{R}$, $i \in \{1, \ldots, N\}$ and $l \in \{1, \ldots, L\}$. Hence, $G_{i,l} \succ 0$ if

$$\begin{bmatrix} P_i & (\bar{A}_{i,l} + \bar{B}\Delta\bar{C}_i)^\top \sum_{j=1}^{N} \pi_{ji} P_j \\ \sum_{j=1}^{N} \pi_{ji} P_j (\bar{A}_{i,l} + \bar{B}\Delta\bar{C}_i) & \sum_{j=1}^{N} \pi_{ji} P_j \end{bmatrix}$$
$$\succ \begin{bmatrix} \bar{C}_i^\top (R_{i,l} - \Delta^\top R_{i,l} \Delta) \bar{C}_i & 0 \\ 0 & 0 \end{bmatrix}, \quad \text{(A.21)}$$

or equivalently if

$$\begin{bmatrix} I & 0 \\ \Delta\bar{C}_i & 0 \\ 0 & I \\ -\bar{C}_i & 0 \end{bmatrix}^\top \begin{bmatrix} P_i & 0 & \bar{A}_{i,l}^\top \sum_{j=1}^{N} \pi_{ji} P_j & \bar{C}_i^\top R_{i,l} \\ \star & R_{i,l} & \bar{B}^\top \sum_{j=1}^{N} \pi_{ji} P_j & 0 \\ \star & \star & \sum_{j=1}^{N} \pi_{ji} P_j & 0 \\ \star & \star & \star & R_{i,l} \end{bmatrix} \begin{bmatrix} I & 0 \\ \Delta\bar{C}_i & 0 \\ 0 & I \\ -\bar{C}_i & 0 \end{bmatrix} \succ 0, \quad \text{(A.22)}$$

which is implied by the satisfaction of (2.50) for all $i \in \{1, \ldots, N\}$ and $l \in \{1, \ldots, L\}$, because the matrix $\begin{bmatrix} I & (\Delta\bar{C}_i)^\top & 0 & -\bar{C}_i^\top \\ 0 & 0 & I & 0 \end{bmatrix}^\top$ has full column rank.

Since (2.50) holds by the hypothesis of the theorem, we can conclude that V is strictly decreasing in spite of the presence of the uncertainty. Standard Lyapunov-based stability arguments now prove that (2.25) with (2.18) is UGES. Using that (2.25) is an overapproximation of (2.12) as proven in Theorem 2.3.2 and subsequently, using the result of Lemma 2.2.4, it follows that the NCS system given by (2.1), (2.2a) or (2.2b), (2.3), and (2.7) is UGES. $\qquad\square$

Proof of Theorem 2.5.1: Since (2.55) holds for all pairs $(h, \tau) \in \Theta$ and, therefore, for all $(\tilde{h}_l, \tilde{\tau}_l) \in \Theta$, $l \in \{1, \ldots, L\}$, we have that

$$\begin{bmatrix} \bar{A}_{i,l}^\top \sum_{j=1}^{N} \pi_{ji} P_j \bar{A}_{i,l} - P_i + \gamma I & 0 \\ 0 & 0 \end{bmatrix} \preceq 0, \quad \text{(A.23)}$$

for all $i \in \{1, \ldots, N\}$ and $l \in \{1, \ldots, L\}$. Note that (A.23) holds irrespective of the choice of $(\tilde{h}_l, \tilde{\tau}_l) \in \Theta$, $l \in \{1, \ldots, L\}$. Now suppose that we would establish

that there exist matrices $R_{i,l} \in \mathcal{R}$, $i \in \{1, \ldots, N\}$ and $l \in \{1, \ldots, L\}$, such that

$$\sum_{j=1}^{N} \pi_{ji} \begin{bmatrix} \bar{C}_i^\top R_{i,l} \bar{C}_i - \gamma I & \bar{A}_{i,l}^\top P_j \bar{B} \\ \bar{B}^\top P_j \bar{A}_{i,l} & \bar{B}^\top P_j \bar{B} - R_{i,l} \end{bmatrix} \prec 0, \tag{A.24}$$

for all $i \in \{1, \ldots, N\}$ and $l \in \{1, \ldots, L\}$. Then, combining this expression with (A.23) yields, after taking a Schur complement, the conditions of Theorem 2.4.1. Hence, if the fact that (2.30) holds for a sufficiently small ε, implies that (A.24) holds for some $R_{i,l} \in \mathcal{R}$, we completed the proof.

Therefore, it remains to show that there exists an ε_0, such that for any $0 < \varepsilon \leqslant \varepsilon_0$, (A.24) is satisfied for some $R_{i,l} \in \mathcal{R}$. Note that (A.24) holds if

$$\bar{C}_i^\top R_{i,l} \bar{C}_i + \bar{A}_{i,l}^\top P_j \bar{B} \big(R_{i,l} - \bar{B}^\top P_j \bar{B}\big)^{-1} \bar{B}^\top P_j \bar{A}_{i,l} \prec \gamma I, \tag{A.25}$$

and $\bar{B}^\top P_j \bar{B} \prec R_{i,l}$, for some $R_{i,l} \in \mathcal{R}$, and for all $i, j \in \{1, \ldots, N\}$ and $l \in \{1, \ldots, L\}$. By choosing $R_{i,l} = rI$, for all $i \in \{1, \ldots, N\}$ and $l \in \{1, \ldots, L\}$ with $r > 0$, we can observe that (A.25) is implied by

$$\frac{\|P_j \bar{A}_{i,l}\|^2 \|\bar{B}\|^2}{r - \lambda_{\min}(\bar{B}^\top P_j \bar{B})} < \gamma - r\|\bar{C}_i\|^2, \tag{A.26}$$

where $\lambda_{\min}(\bar{B}^\top P_j \bar{B})$ denotes the minimum eigenvalue of $\bar{B}^\top P_j \bar{B}$. Since it holds that $\lambda_{\min}(\bar{B}^\top P_j \bar{B}) \leqslant \|\bar{B}\|^2 \|P_j\|$, (A.26) is implied by

$$\|P_j \bar{A}_{i,l}\|^2 \|\bar{B}\|^2 < (\gamma - r\|\bar{C}_i\|^2)(r - \|\bar{B}\|^2 \|P_j\|), \tag{A.27}$$

Furthermore, $\bar{B}^\top P_j \bar{B} \prec R_{i,l}$ is implied by $\|\bar{B}\|^2 \|P_j\| < r$, for some $r > 0$ and all $i, j \in \{1, \ldots, N\}$ and $l \in \{1, \ldots, L\}$. Now choosing $r = \frac{\gamma}{2\|\bar{C}_i\|^2}$, multiplying the left-hand and the right-hand side of (A.27) by $\|\bar{C}_i\|^2$, and realising that $\|\bar{B}\| \|\bar{C}_i\| \leqslant \varepsilon$ yields that (A.27), and thereby (A.25), is satisfied if

$$\varepsilon^2 \|P_j \bar{A}_{i,l}\|^2 < \tfrac{1}{4}\gamma^2 - \tfrac{1}{2}\gamma \varepsilon^2 \|P_j\|, \tag{A.28}$$

and that $\bar{B}^\top P_j \bar{B} \prec R_{i,l}$ is satisfied if $\varepsilon^2 \|P_j\| < \tfrac{1}{2}\gamma$, which can be satisfied by choosing ε sufficiently small.

Therefore, if (2.46) is a Lyapunov function for system (2.12), with protocol (2.20), then there exists an $\varepsilon_0 > 0$, such that for any overapproximation satisfying (2.30) with $0 < \varepsilon \leqslant \varepsilon_0$, the conditions of Theorem 2.4.1 hold, which completes the proof. $\qquad \square$

A.2 Chapter 3

Proof of Lemma 3.2.4. As a first step in the proof, let us define the renewal process

$$s(t) = \sup\{k \in \mathbb{N} \mid \textstyle\sum_{l=0}^{k-1} h_l \leqslant t\}, \tag{A.29}$$

which allows us to write

$$\mathbb{E}(\|\bar{x}(t)\|^2) = \sum_{k \in \mathbb{N}} \mathbb{E}\big(\|\bar{x}(t)\|^2 \,|s(t) = k\big) \Pr(s(t) = k), \qquad (A.30)$$

where $\mathbb{E}\big(\|\bar{x}(t)\|^2 \,|s(t) = k\big)$ denotes the conditional expectation of $\|\bar{x}(t)\|^2$ given that $s(t) = k$. Furthermore, we have that

$$\begin{aligned}
\mathbb{E}\big(\|\bar{x}(t)\|^2 \,|s(t) = k\big) &\leqslant \mathbb{E}\big(\gamma(h_k)\|\bar{x}(t_k)\|^2 \,|s(t) = k\big) \\
&= \mathbb{E}\big(\gamma(h_k)\|\bar{x}(t_k)\|^2\big) \leqslant c_\gamma \mathbb{E}\big(\|\bar{x}(t_k)\|^2\big) \qquad (A.31)
\end{aligned}$$

due to the fact that (3.26) holds, the fact that h_k and t_k are independent of $s(t)$, the fact that $\gamma(h_k)$ and $\|\bar{x}(t_k)\|^2$ are mutually independent, and $\mathbb{E}\big(\gamma(h_k)\big) < c_\gamma$, for some $c_\gamma > 0$. Now using (A.31), (A.30) becomes

$$\begin{aligned}
\mathbb{E}(\|\bar{x}(t)\|^2) &\leqslant \sum_{k \in \mathbb{N}} c_\gamma \mathbb{E}\big(\|\bar{x}(t_k)\|^2\big) \Pr(s(t) = k) \\
&= \sum_{k \in \mathbb{N} \setminus \mathcal{K}} c_\gamma \mathbb{E}\big(\|\bar{x}(t_k)\|^2\big) \Pr(s(t) = k) \\
&\quad + \sum_{k \in \mathcal{K}} c_\gamma \mathbb{E}\big(\|\bar{x}(t_k)\|^2\big) \Pr(s(t) = k), \qquad (A.32)
\end{aligned}$$

in which $\mathcal{K} = \{k \in \mathbb{N} \,|\, k \geqslant t\big(\frac{1}{\mathbb{E}(h)} - \epsilon\big)\}$, for some ϵ, satisfying $\frac{1}{\mathbb{E}(h)} > \epsilon > 0$. The first term of the right-hand side of the last line of (A.32) can be bounded as follows:

$$\begin{aligned}
\sum_{k \in \mathbb{N} \setminus \mathcal{K}} c_\gamma \mathbb{E}\big(\|\bar{x}(t_k)\|^2\big) \Pr(s(t) = k) &\leqslant \sum_{k \in \mathbb{N} \setminus \mathcal{K}} c_\gamma c_d \|\bar{x}(0)\|^2 \Pr(s(t) = k) \\
&\leqslant c_\gamma c_d \|\bar{x}(0)\|^2 \Pr\big(s(t) < t\big(\frac{1}{\mathbb{E}(h)} - \epsilon\big)\big) \\
&\leqslant c_\gamma c_d \|\bar{x}(0)\|^2 c_{\bar{\lambda}} e^{-\bar{\lambda} t}, \qquad (A.33)
\end{aligned}$$

for some $c_{\bar{\lambda}} > 0$, because of (3.25) and the exponential rate of convergence in the law of large numbers under the existence of exponential moments, see [28] or [116, §4.5]. Furthermore, the second term in the right-hand side of (A.32) can be bounded as follows:

$$\begin{aligned}
\sum_{k \in \mathcal{K}} c_\gamma \mathbb{E}\big(\|\bar{x}(t_k)\|^2\big) \Pr(s(t) = k) &\leqslant \sum_{k \in \mathcal{K}} c_\gamma c_d \|\bar{x}(0)\|^2 e^{-\beta_d k} \Pr(s(t) = k) \\
&\leqslant \sum_{k \in \mathcal{K}} c_\gamma c_d \|\bar{x}(0)\|^2 e^{-\beta_d k} \\
&\leqslant c_\gamma c_d \|\bar{x}(0)\|^2 \frac{1}{1 - e^{-\beta_d}} e^{-\beta_d t\big(\frac{1}{\mathbb{E}(h)} - \epsilon\big)}, \quad (A.34)
\end{aligned}$$

since (3.25) holds, $\Pr(s(t) = k) \leqslant 1$ for all $t \in \mathbb{R}_+$ and $k \in \mathbb{N}$, and the fact that the summation of the exponential function forms a geometric series. Now substituting (A.33) and (A.34) into (A.32) yields

$$\begin{aligned}
\mathbb{E}(\|\bar{x}(t)\|^2) &\leqslant c_\gamma c_d \|\bar{x}(0)\|^2 \left(c_{\bar{\lambda}} e^{-\bar{\lambda} t} + \frac{1}{1 - e^{-\beta_d}} e^{-\beta_d t\big(\frac{1}{\mathbb{E}(h)} - \epsilon\big)} \right) \\
&\leqslant 2 c_\gamma c_d \|\bar{x}(0)\|^2 \max\{c_{\bar{\lambda}}, \tfrac{1}{1 - e^{-\beta_d}}\} \max\{e^{-\bar{\lambda} t}, e^{-\beta_d t\big(\frac{1}{\mathbb{E}(h)} - \epsilon\big)}\} \\
&\leqslant 2 c_\gamma c_d \|\bar{x}(0)\|^2 \max\{c_{\bar{\lambda}}, \tfrac{1}{1 - e^{-\beta_d}}\} e^{-\min\{\bar{\lambda}, \beta_d\big(\frac{1}{\mathbb{E}(h)} - \epsilon\big)\} t}, \qquad (A.35)
\end{aligned}$$

since $\frac{1}{1-e^{-\beta_d}} > 1$, for all $\beta_d > 0$. Now observe that (A.35) has the form of (3.24), with $c_c = 2c_\gamma c_d \|\bar{x}(0)\|^2 \max\{c_{\bar{\lambda}}, \frac{1}{1-e^{-\beta_d}}\}$ and $\beta_c = \min\{\bar{\lambda}, \beta_d(\frac{1}{\mathbb{E}(h)} - \epsilon)\}$, for some $\epsilon > 0$ and $c_{\bar{\lambda}} > 0$. This completes the proof. □

Proof of Theorem 3.2.6. The proof is based on showing that the conditions of Lemma 3.2.4 are satisfied. Because of Assumption 3.2.5, it holds that $\mathbb{E}(e^{\bar{\lambda}h}) < c_h$, for some $c_h > 0$. Therefore, it remains to show that there exists a function $\gamma : \mathbb{R}_+ \to \mathbb{R}_+$ satisfying (3.26) and $\mathbb{E}(\gamma(h)) < c_\gamma$, for some $c_\gamma > 0$. To do so, let us introduce an auxiliary variable $\tilde{t} := t - t_k$, for all $t \in (t_k, t_{k+1}]$. Now solving the differential equation resulting from combining (3.1), (3.2a) or (3.2b), (3.3), and (3.8), on the interval $\tilde{t} \in (0, \tau_k]$ yields

$$\bar{x}(t_k + \tilde{t}) = \begin{bmatrix} A_{\tilde{t}} + E_{\tilde{t}} BDC & E_{\tilde{t}} BD \\ C(I - A_{\tilde{t}} - E_{\tilde{t}} BDC) & I - CE_{\tilde{t}} BD \end{bmatrix} \bar{x}(t_k) \qquad (A.36)$$

where $A_{\tilde{t}}$, B, C, D, and $E_{\tilde{t}}$, $\tilde{t} \in \mathbb{R}_+$, are defined according to (3.13), (3.14) or (3.17), depending on the chosen setup for the NCS. Equation (A.36) can be rewritten as

$$\bar{x}(t_k + \tilde{t}) = \left(\tilde{A}_{\sigma_k, 0, 0} + \tilde{B} \text{diag}(A_{\tilde{t}} - A_0, E_{\tilde{t}} - E_0, 0) \tilde{C}_{\sigma_k} \right) \bar{x}(t_k), \qquad (A.37)$$

in which $\tilde{A}_{\sigma, h, \tau}$ is defined in (3.12) and $\tilde{B}$ and $\tilde{C}_\sigma$ as in (3.45). Similarly, solving (3.1), (3.2a) or (3.2b), (3.3), and (3.8) on the interval $\tilde{t} \in (\tau_k, h_k]$ yields

$$\bar{x}(t_k + \tilde{t}) = \left(\tilde{A}_{\sigma_k, 0, 0} + \tilde{B} \tilde{\Delta}_{\tilde{t}, \tau_k} \tilde{C}_{\sigma_k} \right) \bar{x}(t_k), \qquad (A.38)$$

in which

$$\tilde{\Delta}_{\tilde{t}, \tau_k} := \text{diag}(A_{\tilde{t}} - A_0, E_{\tilde{t}} - E_0, E_{\tilde{t}-\tau_k} - E_0). \qquad (A.39)$$

Using (A.37) and (A.38), we can bound the intersample behaviour on the interval $\tilde{t} \in (0, h_k]$ by

$$\|\bar{x}(t_k + \tilde{t})\|^2 \leqslant \max_{\substack{\tilde{t} \in (0, h_k], \tau_k \in (0, h_k], \\ \sigma \in \{1, \ldots, N\}}} \left(\|\tilde{A}_{\sigma, 0, 0}\| + \|\tilde{B}\| \|\tilde{\Delta}_{\tilde{t}, \tau}\| \|\tilde{C}_\sigma\| \right)^2 \|\bar{x}(t_k)\|^2$$

$$\leqslant \gamma(h_k) \|\bar{x}(t_k)\|^2 \qquad (A.40)$$

in which

$$\gamma(h_k) = \max_{\sigma \in \{1, \ldots, N\}} \left(\|\tilde{A}_{\sigma, 0, 0}\| + \|\tilde{B}\| \|\tilde{C}_\sigma\| \right)^2$$

$$\max_{\tilde{t} \in (0, h_k], \tau_k \in (0, h_k]} \max \left\{ 1, \|A_{\tilde{t}} - A_0\|^2, \|E_{\tilde{t}} - E_0\|^2, \|E_{\tilde{t}-\tau_k} - E_0\|^2 \right\}.$$

$$(A.41)$$

To prove that $\mathbb{E}(\gamma(h)) < c_\gamma$, for some $c_\gamma > 0$, we use that

$$\|A_{\tilde{t}} - A_0\|^2 \leqslant (e^{\frac{1}{2}\lambda_{\max}(\bar{\Lambda}^\top + \bar{\Lambda})\tilde{t}} + 1)^2 \leqslant (e^{\frac{1}{2}\lambda_{\max}(\bar{\Lambda}^\top + \bar{\Lambda})h} + 1)^2 \qquad \text{(A.42a)}$$

$$\|E_{\tilde{t}} - E_0\|^2 \leqslant \int_0^{\tilde{t}} e^{\lambda_{\max}(\bar{\Lambda}^\top + \bar{\Lambda})s}\mathrm{d}s \leqslant \int_0^h e^{\lambda_{\max}(\bar{\Lambda}^\top + \bar{\Lambda})s}\mathrm{d}s \qquad \text{(A.42b)}$$

$$\|E_{\tilde{t}-\tau} - E_0\|^2 \leqslant \int_0^{\tilde{t}-\tau} e^{\lambda_{\max}(\bar{\Lambda}^\top + \bar{\Lambda})s}\mathrm{d}s \leqslant \int_0^h e^{\lambda_{\max}(\bar{\Lambda}^\top + \bar{\Lambda})s}\mathrm{d}s, \qquad \text{(A.42c)}$$

due to Wazewski's inequality, i.e., $\|e^{\Lambda s}\| \leqslant e^{\frac{1}{2}\lambda_{\max}(\bar{\Lambda}^\top + \bar{\Lambda})s}$. Therefore, due to Assumption 3.2.5, it holds that $\mathbb{E}(\gamma(h)) < c_\gamma$ for some $c_\gamma > 0$, and consequently the conditions of Lemma 3.2.4 hold. This completes the proof. $\qquad\square$

Proof of Lemma 3.4.1. The proof is based on showing that for system (3.12), the inequalities (3.42a) and (3.42b) imply (3.25). First observe that because of (3.42a) and (3.42b), it holds that

$$b_1\mathbb{E}(\|\tilde{A}_{\sigma_k,h,\tau}\bar{x}\|^2) \leqslant \mathbb{E}[V(\tilde{A}_{\sigma_k,h,\tau}\bar{x}, k+1)] \leqslant (b_2 - b_3)\|\bar{x}\|^2, \qquad \text{(A.43)}$$

and because the left-hand side of the expression is nonnegative, we have that $b_2 \geqslant b_3$. Now using that $b_2 \geqslant b_3$ and (3.42a), we can rewrite (3.42b) as

$$\mathbb{E}[V(\tilde{A}_{\sigma,h,\tau}\bar{x}, k+1)] \leqslant (1 - \tfrac{b_3}{b_2})V(\bar{x}, k), \qquad \text{(A.44)}$$

which implies that

$$\mathbb{E}[V(\bar{x}_k, k)] \leqslant (1 - \tfrac{b_3}{b_2})^k V(\bar{x}_0, 0), \qquad \text{(A.45)}$$

for all $k \in \mathbb{N}$. Finally, using the bounds (3.42a), we obtain (3.25) with $c_d = \frac{b_2}{b_1} > 0$ and $\beta_d > \ln(\frac{b_2}{b_2-b_3}) > 0$. $\qquad\square$

Proof of Lemma 3.4.2. First, observe that for each $i \in \{1, \ldots, N\}$, the left-hand side of (3.43) satisfies

$$\mathbb{E}\big(\tilde{A}_{i,h,\tau}^\top \tilde{P}\tilde{A}_{i,h,\tau}\mathbf{1}_{\mathcal{Q}}(h,\tau)\big) \preceq \lambda_{\max}(\tilde{P})\mathbb{E}\big(\|\tilde{A}_{i,h,\tau}\|^2\mathbf{1}_{\mathcal{Q}}(h,\tau)\big). \qquad \text{(A.46)}$$

We can now upper bound the right-hand side of (A.46) using

$$\|\tilde{A}_{i,h,\tau}\|^2 \leqslant \big(\|\tilde{A}_{i,0,0}\| + \|\tilde{B}\|\|\tilde{\Delta}_{h,\tau}\|\|\tilde{C}_i\|\big)^2 \leqslant \upsilon_i\big(\max\{\|\tilde{\Delta}_{h,\tau}\|, 1\}\big)^2, \quad \text{(A.47)}$$

where $\tilde{A}_{i,h,\tau}$ is given in (3.12), $\tilde{B}$ and $\tilde{C}$ in (3.45) and $\tilde{\Delta}_{h,\tau}$ in (A.39). Using the bounds derived in (A.42), we have that

$$\max\{\|\tilde{\Delta}_{h,\tau}\|^2, 1\} = \max\{\|A_h - A_0\|^2, \|E_h - E_0\|^2, \|E_{h-\tau} - E_0\|^2, 1\} \leqslant \rho(h).$$
$$\text{(A.48)}$$

Now substituting (A.47), with (A.48) into (A.46), we obtain (3.43), which completes the proof. $\qquad\square$

Proof of Theorem 3.4.3. The proof is based on showing that (3.47) is a Lyapunov function for system (3.12) with switching law (3.18), see Lemma 3.4.1. Note that $V(\bar{x}_k) = \bar{x}_k^\top P_i \bar{x}_k$, with $i = \sigma_k$, due to (3.18). Now using (3.47) and (3.12), we have that

$$\mathbb{E}[V(\tilde{A}_{i,h_k,\tau_k}\bar{x})] = \mathbb{E}[\min_{\nu \in \mathcal{N}} \sum_{j=1}^{N} \bar{x}^\top \tilde{A}_{i,h_k,\tau_k}^\top \nu_j P_j \tilde{A}_{i,h_k,\tau_k} \bar{x}]$$

$$\leqslant \mathbb{E}[\bar{x}^\top \tilde{A}_{i,h_k,\tau_k}^\top \sum_{j=1}^{N} \pi_{ji} P_j \tilde{A}_{i,h_k,\tau_k} \bar{x}],$$

$$\leqslant \sum_{m=1}^{M} \mathbb{E}[\bar{x}^\top \tilde{A}_{i,h_k,\tau_k}^\top \sum_{j=1}^{N} \pi_{ji} P_j \tilde{A}_{i,h_k,\tau_k} \bar{x} \, \mathbf{1}_{\mathcal{S}_m}(h_k,\tau_k)]$$

$$+ \mathbb{E}[\bar{x}^\top \tilde{A}_{i,h_k,\tau_k}^\top \sum_{j=1}^{N} \pi_{ji} P_j \tilde{A}_{i,h_k,\tau_k} \bar{x} \, \mathbf{1}_{\mathcal{Q}}(h_k,\tau_k)], \quad \text{(A.49)}$$

for all $i \in \{1, \ldots, N\}$ and $\bar{x} \in \mathbb{R}^n$. Since we have the following inequality

$$\mathbb{E}[\bar{x}^\top \tilde{A}_{i,h_k,\tau_k}^\top \sum_{j=1}^{N} \pi_{ji} P_j \tilde{A}_{i,h_k,\tau_k} \bar{x} \, \mathbf{1}_{\mathcal{S}_m}(h_k,\tau_k)]$$

$$\leqslant \sum_{m=1}^{M} \bar{p}_m \max_{(h_k,\tau_k) \in \mathcal{S}_m} \bar{x}^\top \tilde{A}_{i,h_k,\tau_k}^\top \sum_{j=1}^{N} \pi_{ji} P_j \tilde{A}_{i,h_k,\tau_k} \bar{x} \quad \text{(A.50)}$$

for all $i \in \{1, \ldots, N\}$, $m \in \{1, \ldots, M\}$, and $\bar{x} \in \mathbb{R}^n$, UGMSES can now be shown using Lemma 3.4.1. Because of (3.47), condition (3.42a) is satisfied and, using (A.49), condition (3.42b) is implied by

$$\sum_{m=1}^{M} \bar{p}_m \tilde{A}_{i,\bar{h}_m,\bar{\tau}_m}^\top \sum_{j=1}^{N} \pi_{ji} P_j \tilde{A}_{i,\bar{h}_m,\bar{\tau}_m} + \mathbb{E}\big(\tilde{A}_{i,h,\tau}^\top \sum_{j=1}^{N} \pi_{ji} P_j \tilde{A}_{i,h,\tau} \mathbf{1}_{\mathcal{Q}}(h,\tau)\big) - P_i \prec 0,$$

$$\text{(A.51)}$$

for all $(\bar{h}_m, \bar{\tau}_m) \in \mathcal{S}_m$, $m \in \{1, \ldots, M\}$, and all $i \in \{1, \ldots, N\}$. This condition is satisfied if there exist matrices $U_{i,m}$, $i \in \{1, \ldots, N\}$, $m \in \{1, \ldots, M\}$, such that

$$\bar{p}_m \tilde{A}_{i,\bar{h}_m,\bar{\tau}_m}^\top \sum_{j=1}^{N} \pi_{ji} P_j \tilde{A}_{i,\bar{h}_m,\bar{\tau}_m} - U_{i,m} \prec 0 \quad \text{(A.52)}$$

for all $i \in \{1, \ldots, N\}$ and all $(\bar{h}_m, \bar{\tau}_m) \in \mathcal{S}_m$, $m \in \{1, \ldots, M\}$, and

$$\mathbb{E}\big(\tilde{A}_{i,h,\tau}^\top \sum_{j=1}^{N} \pi_{ji} P_j \tilde{A}_{i,h,\tau} \mathbf{1}_{\mathcal{Q}}(h,\tau)\big) - P_i + \sum_{m=1}^{M} U_{i,m} \preceq 0, \quad \text{(A.53)}$$

for all $i \in \{1, \ldots, N\}$. Hence, if we can now show that (3.51) and (3.52) imply (A.52) and (A.53), the proof is complete.

Equation (A.52) still yields an infinite number of LMIs (due to the fact that $(\bar{h}_m, \bar{\tau}_m)$ can take an infinite number of values in $\mathcal{S}_m$). This can be resolved by employing the hypothesis of the theorem, implying that (3.32) holds. Indeed, (A.52) is satisfied, if

$$\bar{p}_m (\sum_{l_1=1}^{L} \alpha^{l_1} \bar{A}_{i,m,l_1} + \bar{B}_m \Delta \bar{C}_i)^\top \sum_{j=1}^{N} \pi_{ji} P_j (\sum_{l_2=1}^{L} \alpha^{l_2} \bar{A}_{i,m,l_2} + \bar{B}_m \Delta \bar{C}_i) - U_{i,m} \prec 0,$$
(A.54)

for all $\alpha \in \mathcal{A}$, $\Delta \in \boldsymbol{\Delta}$, $i \in \{1, \ldots, N\}$, and $m \in \{1, \ldots, M\}$. By taking a Schur complement, realising that $\sum_{j=1}^{N} \pi_{ji} P_j \succ 0$, and using that $\alpha_k \in \mathcal{A}$, we obtain that (A.54) is equivalent to stating that $\sum_{l=1}^{L} \alpha^l G_{i,m,l} \succ 0$, where

$$G_{i,m,l} = \begin{bmatrix} U_{i,m} & \sqrt{\bar{p}_m} \left(\bar{A}_{i,m,l} + \bar{B}_l \Delta \bar{C}_i \right)^\top \sum_{j=1}^{N} \pi_{ji} P_j \\ \star & \sum_{j=1}^{N} \pi_{ji} P_j \end{bmatrix},$$
(A.55)

for all $\alpha \in \mathcal{A}$, $\Delta \in \boldsymbol{\Delta}$, $i \in \{1, \ldots, N\}$, $m \in \{1, \ldots, M\}$, and $l \in \{1, \ldots, L\}$. A necessary and sufficient condition for positive definiteness of $\sum_{l=1}^{L} \alpha^l G_{i,m,l}$, for all $\alpha \in \mathcal{A}$, is that $G_{i,m,l} \succ 0$ for all $i \in \{1, \ldots, N\}$, $m \in \{1, \ldots, M\}$ and $l \in \{1, \ldots, L\}$. Using again a Schur complement, we can rewrite the condition $G_{i,m,l} \succ 0$ as follows:

$$U_{i,m} - \bar{p}_m \left(\bar{A}_{i,m,l} + \bar{B}_m \Delta \bar{C}_i \right)^\top \sum_{j=1}^{N} \pi_{ji} P_j \left(\bar{A}_{i,m,l} + \bar{B}_m \Delta \bar{C}_i \right) \succ 0.$$
(A.56)

Now observe that for all $\Delta \in \boldsymbol{\Delta}$, it holds that $\bar{C}_i^\top (R_{i,m,l} - \Delta^\top R_{i,m,l} \Delta) C_i \succeq 0$, for all $R_{i,m,l} \in \mathcal{R}$, $i \in \{1, \ldots, N\}$, $m \in \{1, \ldots, M\}$ and $l \in \{1, \ldots, L\}$. Hence, (A.56) is satisfied if

$$U_{i,m} - \bar{p}_m \left(\bar{A}_{i,m,l} + \bar{B}_m \Delta \bar{C}_i \right)^\top \sum_{j=1}^{N} \pi_{ji} P_j \left(\bar{A}_{i,m,l} + \bar{B}_m \Delta \bar{C}_i \right) \succ$$

$$\bar{C}_i^\top (R_{i,m,l} - \Delta^\top R_{i,m,l} \Delta) C_i, \quad \text{(A.57)}$$

or equivalently that $[I \ (\Delta \bar{C}_i)^\top] \bar{G}_{i,m,l} [I \ (\Delta \bar{C}_i)^\top]^\top \succ 0$, for all $\Delta \in \boldsymbol{\Delta}$, $i \in \{1, \ldots, N\}$, $m \in \{1, \ldots, M\}$ and $l \in \{1, \ldots, L\}$, in which

$\bar{G}_{i,m,l} :=$

$$\begin{bmatrix} U_{i,m} - \bar{p}_m \bar{A}_{i,m,l}^\top \sum_{j=1}^{N} \pi_{ji} P_j \bar{A}_{i,m,l} - \bar{C}_i^\top R_{i,m,l} \bar{C}_i & \bar{p}_m \bar{A}_{i,m,l}^\top \sum_{j=1}^{N} \pi_{ji} P_j \bar{B}_m \\ \star & R_{i,m,l} - \bar{B}_m^\top \sum_{j=1}^{N} \pi_{ji} P_j \bar{B}_m \end{bmatrix}$$
(A.58)

which is implied by the requirement that $\bar{G}_{i,m,l} \succ 0$, for all $i \in \{1, \ldots, N\}$, $m \in \{1, \ldots, M\}$ and all $l \in \{1, \ldots, L\}$, which is equivalent to (3.51) after a Schur complement.

It remains to show that (3.52) implies (A.53). To do so, we use the result of Lemma 3.4.2 with $\bar{P} = \sum_{j=1}^{N} \pi_{ji} P_j$, thus $\lambda_{\max}(\bar{P}) \leqslant \mu_i$, and $\mathcal{Q} := \Theta \backslash (\cup_{m=1}^{M} \mathcal{S}_m)$. Therefore, using inequality (3.43), we have that (A.53) is satisfied if (3.52) satisfied. $\qquad \square$

Proof of Theorem 3.5.1. The fact that (3.57) holds implies that there exist matrices $U_{i,m}$, $i \in \{1, \ldots, N\}$, $m \in \{1, \ldots, M\}$, such that

$$U_{i,m} - \bar{\gamma}_m I - \mathbb{E}\big(\tilde{A}_{i,h,\tau}^\top \sum_{j=1}^{N} \pi_{ji} P_j \tilde{A}_{i,h,\tau} \mathbf{1}_{\mathcal{S}_m}(h, \tau)\big) \succeq 0, \qquad (A.59)$$

for all $i \in \{1, \ldots, N\}$ and $m \in \{1, \ldots, M\}$, and

$$P_i - \sum_{m=1}^{M} U_{i,m} - \bar{\gamma}_{\mathcal{Q}} I - \mathbb{E}\big(\tilde{A}_{i,h,\tau}^\top \sum_{j=1}^{N} \pi_{ji} P_j \tilde{A}_{i,h,\tau} \mathbf{1}_{\mathcal{Q}}(h, \tau)\big) \succeq 0, \qquad (A.60)$$

for all $i \in \{1, \ldots, N\}$, with $\bar{\gamma}_m := \frac{\bar{p}_m \gamma}{3}$ for all $m \in \{1, \ldots, M\}$ satisfying $\bar{p}_m \neq 0$ and $\bar{\gamma}_m := \frac{\gamma}{3M}$ for all $m \in \{1, \ldots, M\}$ satisfying $\bar{p}_m = 0$, and $\bar{\gamma}_{\mathcal{Q}} = \frac{\gamma}{3}$, since $\big(\bigcup_{m=1}^{M} \mathcal{S}_m\big) \cup \mathcal{Q} = \Theta$ by definition of $\mathcal{Q}$. Note that (A.59) and (A.60) hold independent of the particular choice of the partitioning $\{\mathcal{S}_1, \ldots, \mathcal{S}_M, \mathcal{Q}\}$. Now suppose that we would establish the existence of matrices $R_{i,m,l} \in \mathcal{R}$, $i \in \{1, \ldots, N\}$, $m \in \{1, \ldots, M\}$, and $l \in \{1, 2, 3\}$, such that

$$\sum_{j=1}^{N} \pi_{ji} \begin{bmatrix} \bar{\gamma}_m I + \mathbb{E}(\tilde{A}_{i,h,\tau}^\top P_j \tilde{A}_{i,h,\tau} \mathbf{1}_{\mathcal{S}_m}(h, \tau)) & 0 & \sqrt{\bar{p}_m} \tilde{A}_{i,m,l}^\top P_j & \bar{C}_i^\top R_{i,m,l} \\ \star & R_{i,m,l} & \sqrt{\bar{p}_m} \bar{B}_m^\top P_j & 0 \\ \star & \star & P_j & 0 \\ \star & \star & \star & R_{i,m,l} \end{bmatrix} \succ 0, \quad (A.61)$$

for all $i \in \{1, \ldots, N\}$, $m \in \{1, \ldots, M\}$, $l \in \{1, 2, 3\}$, and

$$\mathbb{E}\big(\tilde{A}_{i,h,\tau}^\top \sum_{j=1}^{N} \pi_{ji} P_j \tilde{A}_{i,h,\tau} \mathbf{1}_{\mathcal{Q}}(h, \tau)\big) + \bar{\gamma}_{\mathcal{Q}} I - \mu_i \upsilon_i \mathbb{E}\big(\rho(h) \mathbf{1}_{\mathcal{Q}}(h, \tau)\big) I \succeq 0, \quad (A.62)$$

for all $i \in \{1, \ldots, N\}$. Then, combining these expressions with (A.59) and (A.60), respectively, yields the conditions of Theorem 3.4.3.

Therefore, if we can show that there exists an $h_0^\star > 0$, such that for any $h^\star > h_0^\star$ there is an ε_0 such that for any $0 < \varepsilon < \varepsilon_0$, it holds that (A.61) and (A.62) are satisfied for some $R_{i,l} \in \mathcal{R}$, the proof is complete. Before doing so, we present two intermediate steps. The first step is to show that for all $i, j \in \{1, \ldots, N\}$, $l \in \{1, 2, 3\}$, for all $(h, \tau) \in \mathcal{S}_m$, $m \in \{1, \ldots, M\}$ and for any $h^\star > 0$, there exists a continuous function $\chi_{h^\star} : \mathbb{R}_+ \to \mathbb{R}_+$ with $\chi_{h^\star}(0) = 0$,

satisfying for all $i \in \{1, \ldots, N\}$, $l \in \{1, 2, 3\}$, $(h, \tau) \in \mathcal{S}_m$ and $m \in \{1, \ldots, M\}$, that

$$\|\bar{A}_{i,m,l}^\top P_j \bar{A}_{i,m,l} - \tilde{A}_{i,h,\tau}^\top P_j \tilde{A}_{i,h,\tau}\| \leqslant \chi_{h^\star}(\varepsilon). \tag{A.63}$$

Observe that we can write $\tilde{A}_{i,h,\tau}$ as

$$\tilde{A}_{i,h,\tau} = \bar{A}_{i,m,l} + \tilde{B}\bar{\Delta}_{h,\tau,\tilde{h}_{m,l},\tilde{\tau}_{m,l}}\tilde{C}_i \tag{A.64}$$

with $\tilde{B}$ and $\tilde{C}_i$ as in (3.45), and

$$\bar{\Delta}_{h,\tau,\tilde{h}_{m,l},\tilde{\tau}_{m,l}} := \operatorname{diag}(A_h - A_{\tilde{h}_{m,l}}, E_h - E_{\tilde{h}_{m,l}}, E_{h-\tau} - E_{\tilde{h}_{m,l}-\tilde{\tau}_{m,l}}). \tag{A.65}$$

We can bound $\bar{\Delta}_{h,\tau,\tilde{h}_{m,l},\tilde{\tau}_{m,l}}$, for all $(h, \tau) \in \mathcal{S}_m$, using

$$\|A_h - A_{\tilde{h}_{m,l}}\| \leqslant e^{\|\bar{\Lambda}\|(\tilde{h}_{m,l}+\varepsilon)}\|\bar{\Lambda}\|\varepsilon, \tag{A.66a}$$

$$\|E_h - E_{\tilde{h}_{m,l}}\| \leqslant \left|\int_{\tilde{h}_{m,l}}^h e^{\|\bar{\Lambda}\|s}\mathrm{d}s\right| \leqslant e^{\|\bar{\Lambda}\|(\tilde{h}_{m,l}+\varepsilon)}\varepsilon, \tag{A.66b}$$

$$\|E_{h-\tau} - E_{\tilde{h}_{m,l}-\tilde{\tau}_{m,l}}\| \leqslant e^{\|\bar{\Lambda}\|(\tilde{h}_{m,l}+\varepsilon)}\varepsilon, \tag{A.66c}$$

with $\bar{\Lambda}$ as in (3.27). Equation (A.66) are all continuous and equal to zero at $\varepsilon = 0$. Furthermore, as $\cup_{m=1}^M \mathcal{S}_m := \{(h, \tau) \in \Theta \mid h \leqslant h^\star\}$, it holds that $e^{\|\bar{\Lambda}\|(\tilde{h}_{m,l}+\varepsilon)}\|\bar{\Lambda}\|\varepsilon \leqslant e^{\|\bar{\Lambda}\|(h^\star+\varepsilon)}\|\bar{\Lambda}\|\varepsilon$, for all $(h, \tau) \in \mathcal{S}_m$, $m \in \{1, \ldots, M\}$. This inequality allows us to bound the left-hand side of (A.66) by a continuous function that is zero at $\varepsilon = 0$ for any $h^\star > 0$, which allows us to bound $\bar{\Delta}_{h,\tau,\tilde{h}_{m,l},\tilde{\tau}_{m,l}}$ by a continuous function that is zero at $\varepsilon = 0$ for any $h^\star > 0$, and therefore, there exists a continuous function $\chi_{h^\star} : \mathbb{R}_+ \to \mathbb{R}_+$ with $\chi_{h^\star}(0) = 0$ satisfying (A.63). The second intermediate step is to show that there exists a continuous function $\varphi_{h^\star} : \mathbb{R}_+ \to \mathbb{R}_+$ with $\varphi_{h^\star}(0) = 0$, satisfying $\max_{m \in \{1, \ldots, M\}} \|\bar{B}_m\|^2 \leqslant \varphi_{h^\star}(\varepsilon)$, with $\bar{B}_m$ as in (3.39), and $\varphi_{h^\star}(0) = 0$ for any $h^\star > 0$, since we have that, similarly to (A.66), that the terms in (3.37) can be bounded for all $i \in \{1, \ldots, N\}$ and all $m \in \{1, \ldots, M\}$ as

$$\delta_{i,m}^A \leqslant \max_{l \in \{1,2,3\}} e^{\|\Lambda_i\|(\tilde{h}_{m,l}+\varepsilon)}\|\bar{\Lambda}_i\|\varepsilon \leqslant e^{\|\Lambda_i\|(h^\star+\varepsilon)}\|\bar{\Lambda}_i\|\varepsilon, \tag{A.67a}$$

$$\delta_{i,m}^{E_h} \leqslant \max_{l \in \{1,2,3\}} e^{\|\Lambda_i\|(\tilde{h}_{m,l}+\varepsilon)}\varepsilon \leqslant e^{\|\Lambda_i\|(h^\star+\varepsilon)}\|\bar{\Lambda}_i\|\varepsilon, \tag{A.67b}$$

$$\delta_{i,m}^{E_{h-\tau}} \leqslant \max_{l \in \{1,2,3\}} e^{\|\Lambda_i\|(\tilde{h}_{m,l}+\varepsilon)}\varepsilon \leqslant e^{\|\Lambda_i\|(h^\star+\varepsilon)}\|\bar{\Lambda}_i\|\varepsilon, \tag{A.67c}$$

which are all continuous functions and equal to zero at $\varepsilon = 0$ for any $h^\star > 0$, and thereby $\|\bar{B}_m\|^2$, with $\bar{B}_m$ as in (3.39), is bounded by a continuous function $\varphi_{h^\star}$ satisfying $\varphi_{h^\star}(0) = 0$.

We can now show that for any $h^\star > 0$, there exists an $\varepsilon_0 > 0$, such that for any $0 < \varepsilon < \varepsilon_0$, (A.61) is satisfied. First observe that (A.61) is implied by

$$
\begin{bmatrix}
\bar{\gamma}_m I + \mathbb{E}\big(\tilde{A}_{i,h,\tau}^\top P_j \tilde{A}_{i,h,\tau} \mathbf{1}_{\mathcal{S}_m}(h,\tau)\big) & 0 & \sqrt{\bar{p}_m}\bar{A}_{i,m,l}^\top P_j & \bar{C}_i^\top R_{i,m,l} \\
\star & R_{i,m,l} & \sqrt{\bar{p}_m}\bar{B}_m^\top P_j & 0 \\
\star & \star & P_j & 0 \\
\star & \star & \star & R_{i,m,l}
\end{bmatrix} \succ 0, \quad \text{(A.68)}
$$

for all $i,j \in \{1,\ldots,N\}$, $l \in \{1,2,3\}$, and $m \in \{1,\ldots,M\}$. After taking a Schur complement, we can observe that (A.68) is equivalent to requiring that

$$
\begin{bmatrix}
\bar{\gamma}_m I + \mathbb{E}\big(\tilde{A}_{i,h,\tau}^\top P_j \tilde{A}_{i,h,\tau} \mathbf{1}_{\mathcal{S}_m}(h,\tau)\big) - \bar{p}_m \bar{A}_{i,m,l}^\top P_j \bar{A}_{i,m,l} - \bar{C}_i^\top R_{i,m,l}\bar{C}_i & -\bar{p}_m \bar{A}_{i,m,l}^\top P_j \bar{B}_m \\
\star & R_{i,m,l} - \bar{p}_m \bar{B}_m^\top P_j \bar{B}_m
\end{bmatrix}
$$
$$\text{(A.69)}$$

is positive semidefinite. Now taking another Schur complement yields that (A.68) is implied by

$$
\bar{\gamma}_m I + \mathbb{E}\big(\tilde{A}_{i,h,\tau}^\top P_j \tilde{A}_{i,h,\tau} \mathbf{1}_{\mathcal{S}_m}(h,\tau)\big) - \bar{p}_m \bar{A}_{i,m,l}^\top P_j \bar{A}_{i,m,l} - \bar{C}_i^\top R_{i,m,l}\bar{C}_i
$$
$$
-\bar{p}_m^2 \bar{A}_{i,m,l}^\top P_j \bar{B}_m (R_{i,m,l} - \bar{p}_m \bar{B}_m^\top P_j \bar{B}_m)^{-1} \bar{B}_m^\top P_j \bar{A}_{i,m,l} \succ 0, \quad \text{(A.70)}
$$

and $R_{i,l,m} - \bar{p}_m \bar{B}_m^\top P_j \bar{B}_m \succ 0$, for all $i,j \in \{1,\ldots,N\}$, $l \in \{1,2,3\}$, and $m \in \{1,\ldots,M\}$. Now for all $m \in \{1,\ldots,M\}$ for which $\bar{p}_m = 0$, the inequality (A.70) can be satisfied by choosing $R_{i,m,l}$ sufficiently small. For all $m \in \{1,\ldots,M\}$ for which $\bar{p}_m \neq 0$, we have that (A.70) is implied by

$$
\mathbb{E}\big(\big(\tfrac{\bar{\gamma}_m}{\bar{p}_m} I + \tilde{A}_{i,h,\tau}^\top P_j \tilde{A}_{i,h,\tau} - \bar{A}_{i,m,l}^\top P_j \bar{A}_{i,m,l} - \tfrac{1}{\bar{p}_m}\bar{C}_i^\top R_{i,m,l}\bar{C}_i
$$
$$
-\bar{A}_{i,m,l}^\top P_j \bar{B}_m (\tfrac{1}{\bar{p}_m} R_{i,m,l} - \bar{B}_m^\top P_j \bar{B}_m)^{-1} \bar{B}_m^\top P_j \bar{A}_{i,m,l}\big)\mathbf{1}_{\mathcal{S}_m}(h,\tau)\big) \succ 0, \quad \text{(A.71)}
$$

which is, due to continuity of the argument of the expected value and compactness of $\mathcal{S}_m$, implied by

$$
\tfrac{\bar{\gamma}_m}{\bar{p}_m} I + \tilde{A}_{i,h,\tau}^\top P_j \tilde{A}_{i,h,\tau} - \bar{A}_{i,m,l}^\top P_j \bar{A}_{i,m,l} - \tfrac{1}{\bar{p}_m}\bar{C}_i^\top R_{i,m,l}\bar{C}_i
$$
$$
-\bar{A}_{i,m,l}^\top P_j \bar{B}_m (\tfrac{1}{\bar{p}_m} R_{i,m,l} - \bar{B}_m^\top P_j \bar{B}_m)^{-1} \bar{B}_m^\top P_j \bar{A}_{i,m,l} \succ 0, \quad \text{(A.72)}
$$

for all $(h,\tau) \in \mathcal{S}_m$. By choosing $\mathcal{R}_{i,m,l} = rI$ for all $i \in \{1,\ldots,N\}$, $l \in \{1,2,3\}$, and $m \in \{1,\ldots,M\}$, with $r > 0$, we can observe that (A.72) is implied by

$$
\|\bar{A}_{i,m,l}^\top P_j \bar{A}_{i,m,l} - \tilde{A}_{i,h,\tau}^\top P_j \tilde{A}_{i,h,\tau}\| + \tfrac{r}{\bar{p}_m}\|\bar{C}_i\|^2 + \frac{\|\bar{A}_{i,m,l}^\top P_j\|^2\|\bar{B}_m\|^2}{\frac{r}{\bar{p}_m} - \lambda_{\max}(\bar{B}_m^\top P_j \bar{B}_m)} < \tfrac{\bar{\gamma}_m}{\bar{p}_m},
$$
$$\text{(A.73)}$$

which is, using and the intermediate steps given above and the fact that $\lambda_{\max}(\bar{B}_m^\top P_j \bar{B}_m) \leqslant \|\bar{B}_m\|^2\|P_j\| \leqslant \varphi_{h^\star}(\varepsilon)\|P_j\|$, implied by

$$
\|\bar{A}_{i,m,l}^\top P_j\|^2 \varphi_{h^\star}(\varepsilon) < \big(\tfrac{\bar{\gamma}_m}{\bar{p}_m} - \tfrac{r}{\bar{p}_m}\|\bar{C}_i\|^2 - \chi_{h^\star}(\varepsilon)\big)\big(\tfrac{r}{\bar{p}_m} - \|P_j\|\varphi_{h^\star}(\varepsilon)\big). \quad \text{(A.74)}
$$

By choosing $r = \frac{\bar{\gamma}_m}{2\|\bar{C}_i\|^2}$, multiplying the left-hand and the right-hand sides by $\|\bar{C}_i\|^2$, and substituting $\bar{\gamma}_m := \frac{\bar{p}_m \gamma}{3}$, (A.74) can be rewritten as

$$\|\bar{C}_i\|^2 \|\bar{A}_{i,m,l}^\top P_j\|^2 \varphi_{h^\star}(\varepsilon) < \left(\tfrac{\gamma}{6} - \chi_{h^\star}(\varepsilon)\right)\left(\tfrac{\gamma}{6} - \|\bar{C}_i\|^2 \|P_j\| \varphi_{h^\star}(\varepsilon)\right), \qquad \text{(A.75)}$$

which can be satisfied for any $\gamma > 0$ by making $\chi_{h^\star}(\varepsilon)$ and $\varphi_{h^\star}(\varepsilon)$ sufficiently small, which can be achieved by making the triangles $\mathcal{S}_m$ sufficiently small, i.e., $\text{diam}\mathcal{S}_m \leqslant \varepsilon$, $m \in \{1, \ldots, M\}$, for a sufficiently small ε. Furthermore, by the same choice of $R_{i,l,m}$, the condition $R_{i,l,m} - \bar{p}_m \bar{B}_m^\top P_j \bar{B}_m \succ 0$ is implied by $\varphi_{h^\star}(\varepsilon)\|\bar{C}_i\|^2 \|P_j\| < \tfrac{1}{6}\gamma$, which can be satisfied by making $\varphi_{h^\star}(\varepsilon)$ sufficiently small by making ε sufficiently small. Therefore, these expressions imply satisfaction of (A.61), ε is chosen sufficiently small.

It now only remains to show that there exists an $h_0^\star > 0$ such that for any $h^\star > h_0^\star$, (A.62) is satisfied. First, note that (A.62) is satisfied if

$$\bar{\gamma}_\mathcal{Q} - \mu_i \upsilon_i \mathbb{E}(\rho(h)\mathbf{1}_\mathcal{Q}(h, \tau)) \geqslant 0. \qquad \text{(A.76)}$$

Now since $\rho(h) > 0$, for all $h > 0$, and because $\mathbb{E}(\rho(h))$ is finite, we can make $\mathbb{E}(\rho(h)\mathbf{1}_\mathcal{Q}(h, \tau))$ arbitrary small by choosing $h^\star$ sufficiently large. Hence, (A.76), and thereby (A.62), can be satisfied if $h^\star$ is chosen sufficiently large.

Therefore, if (3.47) is a Lyapunov function for system (3.12), with protocol (3.20), then there exists an $h_0^\star$, such that for all $h^\star > h_0^\star$ there is an $\varepsilon_0 > 0$, such that for an overapproximation according to Procedure 3.3.1, with $0 < \varepsilon < \varepsilon_0$, the conditions of Theorem 3.4.3 hold. This completes the proof. $\qquad \square$

A.3   Chapter 4

Proof of Lemma 4.3.3. The proof follows directly from Theorem 20 of [50], adopted for linear flow and jump dynamics as in (4.10). Since we have that $\bar{x}^+ = G_i \bar{x}$ for all $\bar{x} \in \mathcal{D}_i$, $i \in \{1, \ldots, N\}$, the condition $W(g) - W(\bar{x}) < 0$ for all $\bar{x} \in \mathcal{D}\backslash\mathcal{A}$ and all $g \in \{\bar{G}_i \bar{x} \,|\, \bar{x} \in \mathcal{D}_i\}$ in Theorem 20 of [50] is implied by requiring that

$$W(\bar{G}_i \bar{x}) - W(\bar{x}) < 0, \quad \text{for all} \ \ \bar{x} \in \mathcal{D}_i\backslash\mathcal{A}, \ i \in \{1, \ldots, N\}. \qquad \text{(A.77)}$$

Furthermore, since $t_{k_i+1}^i - t_{k_i}^i \geqslant h_{\min}^i > 0$ for all $k_i \in \mathbb{N}$, it holds that the set of event times $\{t_k \,|\, k \in \mathbb{N}\} = \cup_{i=1}^N \{t_{k_i}^i \,|\, k_i \in \mathbb{N}\}$, chosen such that $t_{k+1} > t_k$, $k \in \mathbb{N}$, does not contain accumulation points, i.e., there is an $\tau > 0$ such that $(t_k - \tau, t_k + \tau) \cap \{t_k \,|\, k \in \mathbb{N}\} = \{t_k\}$ for all $k \in \mathbb{N}$, (therefore Zeno behaviour is excluded). In fact we have that $\bigcup_{k \in \mathbb{N}}(t_k, t_{k+1}] = \mathbb{R}_+$. The observation that $\{t_k \,|\, k \in \mathbb{N}\}$ does not have accumulation points and the fact that at each event time t_k, $k \in \mathbb{N}$, at most N jumps take place yields that we can relax (A.77) to (4.19b) as the Lyapunov function candidate W is strictly decreasing along solutions as long as the set $\mathcal{A}$ has not been reached. $\qquad \square$

Proof of Theorem 4.3.5. The proof is based on showing that the hypotheses of Theorem 4.3.5 lead to a particular Lyapunov function candidate satisfying the conditions of Lemma 4.3.3 thereby establishing global asymptotic stability. Subsequently, we will show that the hypotheses of Theorem 4.3.5 also lead to an upper bound on the $\mathcal{L}_\infty$-gain as defined in Definition 4.3.4. To do so, let us define $V(\bar{x}) = \bar{x}^\top P \bar{x}$, for $\bar{x} \in \mathbb{R}^{n_x}$, and observe that (4.22a) is equivalent to

$$\tfrac{\mathrm{d}V(\bar{x})}{\mathrm{d}\bar{x}}(\bar{A}\bar{x} + \bar{B}w) \leqslant -\alpha V(\bar{x}) + \beta\|w\|^2 + \sum_{i=1}^N \mu_i \bar{x}^\top Q_i \bar{x}, \tag{A.78}$$

for all $\bar{x} \in \mathbb{R}^{n_x}$ and $w \in \mathbb{R}^{n_w}$, which can be rewritten as

$$\tfrac{\mathrm{d}V(\bar{x})}{\mathrm{d}\bar{x}}(\bar{A}\bar{x} + \bar{B}w) \leqslant -\alpha V(\bar{x}) + \beta\|w\|^2 + \sum_{i=1}^N \mu_i(\bar{x}^\top Q_i \bar{x} - \varepsilon_i) + \sum_{i=1}^N \mu_i \varepsilon_i, \tag{A.79}$$

for all $\bar{x} \in \mathbb{R}^{n_x}$ and $w \in \mathbb{R}^{n_w}$. Furthermore, since $(\bar{x}^\top Q_i \bar{x} - \varepsilon_i) \leqslant 0$, for all $\bar{x} \in \mathcal{C}$ and $\mu_i \geqslant 0$, $i \in \{1, \ldots, N\}$, we have that

$$\tfrac{\mathrm{d}V(\bar{x})}{\mathrm{d}\bar{x}}(\bar{A}\bar{x} + \bar{B}w) \leqslant -\alpha V(\bar{x}) + \beta\|w\|^2 + \sum_{i=1}^N \mu_i \varepsilon_i, \tag{A.80}$$

for all $\bar{x} \in \mathcal{C}$. Similarly, using the definition of $V(\bar{x})$, we have that (4.22c) implies that

$$V(\bar{G}_i \bar{x}) - V(\bar{x}) \leqslant -\nu_i(\bar{x}^\top Q_i \bar{x} - \varepsilon_i) - \nu_i \varepsilon_i, \tag{A.81}$$

for all $i \in \{1, \ldots, N\}$. Since for all $\bar{x} \in \mathcal{D}_i$, it holds that $\bar{x}^\top Q_i \bar{x} - \varepsilon_i = 0$ and $\nu_i \geqslant 0$, $i \in \{1, \ldots, N\}$, (A.81) implies that

$$V(\bar{G}_i \bar{x}) - V(\bar{x}) \leqslant 0, \tag{A.82}$$

for all $\bar{x} \in \mathcal{D}_i$, $i \in \{1, \ldots, N\}$.

We will now show global asymptotic stability of the set $\mathcal{A}$, as in (4.23), for (4.10) with $w = 0$, using

$$W(\bar{x}) = \max\{V(\bar{x}) - \sum_{i=1}^N \tfrac{\mu_i \varepsilon_i}{\alpha}, 0\} \tag{A.83}$$

as the Lyapunov function candidate. It can be verified that (A.83) defines a proper Lyapunov function candidate. Indeed, the function W satisfies (i) of Definition 4.3.2, since for all $\bar{x} \in (\mathcal{C} \cup \bigcup_{i=1}^N \mathcal{D}_i)\backslash\mathcal{A}$, it holds that $W(\bar{x}) = \bar{x}^\top P \bar{x} - \sum_{i=1}^N \tfrac{\mu_i \varepsilon_i}{\alpha} \geqslant 0$, due to (4.23). In addition, W is continuous and nonnegative on $(\mathcal{C} \cup \bigcup_{i=1}^N \mathcal{D}_i)\backslash\mathcal{A}$. Furthermore, (ii) of Definition 4.3.2 is satisfied since W is

locally Lipschitz and (iii) is satisfied as W is continuous and $W(\bar{x}) = 0$ for all $\bar{x} \in \mathcal{A}$. To show that (iv) of Definition 4.3.2 is satisfied, i.e., to show that all the sublevel sets of W are compact, let us suppose that $W(\bar{x}) \leqslant c_W$, for some $c_W \geqslant 0$, which implies that $V(\bar{x}) = x^\top P x + \bar{x}^\top U \bar{x} \leqslant c_W + \sum_{i=1}^N \frac{\mu_i \varepsilon_i}{\alpha}$ and thus that $\|x\|^2 \leqslant c_x$, with $c_x := \frac{1}{\lambda_{\min}(P)}(c_W + \sum_{i=1}^N \frac{\mu_i \varepsilon_i}{\alpha})$, (due to $P \succ 0$ and $U \succeq 0$). Now since (4.8) holds for all $t \in \mathbb{R}_+$, we have that $\|e_{\mathcal{J}_i}\|^2 \leqslant \sigma_i \|v_{\mathcal{J}_i}\|^2 + \varepsilon_i \leqslant \sigma_i \|C\|^2 c_x + \varepsilon_i$, and thus that $\|\bar{x}\|^2 = \|x\|^2 + \|e\|^2 \leqslant \|x\|^2 + \sum_{i=1}^N \|e_{\mathcal{J}_i}\|^2 \leqslant c_{\bar{x}}$, (since $\|e\|^2 \leqslant \sum_{i=1}^N \|e_{\mathcal{J}_i}\|^2$, due to the assumption that $\sum_{i=1}^N \gamma_i^j > 0$ for all $j \in \{1, \ldots, n_y + n_u\}$), with $c_{\bar{x}} := c_x + \sum_{i=1}^N (\sigma_i \|C\|^2 c_x + \varepsilon_i)$. Hence, as $W(\bar{x}) \leqslant c_W$ implies that $\|\bar{x}\| \leqslant \sqrt{c_{\bar{x}}}$, we have that all the sublevel sets of W are compact on $\mathcal{X}$. Now that we concluded that (A.83) is a proper Lyapunov function candidate for the event-triggered control system, global asymptotic stability of the set $\mathcal{A}$, as in (4.23), can be proven by observing that for all $\bar{x} \in (\mathcal{C} \cup \bigcup_{i=1}^N \mathcal{D}_i) \backslash \mathcal{A}$, it holds that $\bar{x}^\top \bar{P} \bar{x} > \sum_{i=1}^N \frac{\mu_i \varepsilon_i}{\alpha}$ and, thus, $W(\bar{x}) = V(\bar{x}) - \sum_{i=1}^N \frac{\mu_i \varepsilon_i}{\alpha}$. Therefore, (4.19a) is implied by (A.80) with $w = 0$, while (4.19b) is implied by (A.82). Furthermore, the fact that $\bar{G}_i \bar{x} \in \mathcal{A}$ holds for all $\bar{x} \in \mathcal{D}_i \cap \mathcal{A}$, $i \in \{1, \ldots, N\}$, is implied by (4.19b), (which followed from (A.82).) Hence, all conditions of Lemma 4.3.3 are satisfied and the set $\mathcal{A}$ is a globally asymptotically stable set for the system (4.10) with $w = 0$.

To show that the $\mathcal{L}_\infty$-gain of the system is equal to or smaller than κ, we use the hypothesis that, for all $\bar{x}(0) \in \mathcal{X}$ and all $w \in \mathcal{L}_\infty$, a minimum inter-event time $h_{\min}^i > 0$ exists for each $i \in \{1, \ldots, N\}$. Namely, as in the proof of Lemma 4.3.3, due to the fact that $h_{\min}^i > 0$, the set of event times $\{t_k \mid k \in \mathbb{N}\} = \cup_{i=1}^N \{t_{k_i}^i \mid k_i \in \mathbb{N}\}$, chosen such that $t_{k+1} > t_k$, $k \in \mathbb{N}$, does not contain accumulation points and it holds that $\bigcup_{k \in \mathbb{N}} (t_k, t_{k+1}] = \mathbb{R}_+$. Furthermore, at each event time t_k, $k \in \mathbb{N}$, at most N jumps take place according to (4.10b) take place, which are all known to satisfy (4.19b). Now by observing that (A.80) is equivalent to

$$\frac{\mathrm{d}}{\mathrm{d}t} V(\bar{x}(t)) \leqslant -\alpha V(\bar{x}(t)) + \beta \|w(t)\|^2 + \sum_{i=1}^N \mu_i \varepsilon_i, \qquad \text{(A.84)}$$

for all $t \in (t_k, t_{k+1}]$, $k \in \mathbb{N}$. Using the Comparison Lemma, see, e.g., Lemma 3.4 in [79], we can observe that (A.84) implies that

$$V(\bar{x}(t)) \leqslant e^{-\alpha(t-t_k)} V(\bar{x}^+(t_k)) + \int_{t_k}^t e^{-\alpha(t-s)} (\beta \|w(s)\|^2 + \sum_{i=1}^N \mu_i \varepsilon_i) \mathrm{d}s, \quad \text{(A.85)}$$

for all $t \in (t_k, t_{k+1}]$, $k \in \mathbb{N}$. Using (A.82) and (A.85) repeatedly, and the fact that $\{t_k \mid k \in \mathbb{N}\}$ does not have accumulation points, we obtain that

$$V(\bar{x}(t)) \leqslant e^{-\alpha t} V(\bar{x}(0)) + \int_0^t e^{-\alpha(t-s)} (\beta \|w(s)\|^2 + \sum_{i=1}^N \mu_i \varepsilon_i) \mathrm{d}s, \qquad \text{(A.86)}$$

for all $t \in \mathbb{R}_+$, and thus

$$V(\bar{x}(t)) \leqslant e^{-\alpha t} V(\bar{x}(0)) + \sum_{i=1}^{N} \tfrac{\mu_i \varepsilon_i}{\alpha} + \tfrac{\beta}{\alpha} \|w\|_{\mathcal{L}_\infty}^2, \qquad \text{(A.87)}$$

for all $t \in \mathbb{R}_+$. Now observe that (4.22b) implies that

$$\|z(t)\|^2 \leqslant \alpha V(\bar{x}(t)) + (\kappa^2 - \beta)\|w(t)\|^2, \qquad \text{(A.88)}$$

for all $t \in \mathbb{R}_+$ and that $\kappa^2 \geqslant \beta$. Based on ideas presented in [1], we substitute (A.87) into (A.88) and observe that $\|w(t)\| \leqslant \|w\|_{\mathcal{L}_\infty}$, for all $t \in \mathbb{R}_+$, yielding

$$\|z(t)\|^2 \leqslant \alpha e^{-\alpha t} V(\bar{x}(0)) + \sum_{i=1}^{N} \mu_i \varepsilon_i + \kappa^2 \|w\|_{\mathcal{L}_\infty}^2, \qquad \text{(A.89)}$$

for all $t \in \mathbb{R}_+$. Taking now the supremum of the left-hand and the right-hand side of (A.89) over all time $t \in \mathbb{R}_+$, we have that

$$\|z\|_{\mathcal{L}_\infty}^2 \leqslant (\delta(\bar{x}(0))^2 + \kappa^2 \|w\|_{\mathcal{L}_\infty}^2 \leqslant (\delta(\bar{x}(0)) + \kappa \|w\|_{\mathcal{L}_\infty})^2, \qquad \text{(A.90)}$$

with $\delta(\bar{x}(0))$ as defined in the hypothesis of the theorem. Taking the square-root of the left-hand and right-hand side shows that the $\mathcal{L}_\infty$-gain as defined in (4.21) is smaller than κ. This completes the proof. $\qquad \square$

Proof of Theorem 4.4.1. Let $\delta_x \geqslant 0$ and $\delta_w \geqslant 0$ be given and take $\bar{x}(0) \in \mathcal{X}$ such that $\|\bar{x}(0)\| \leqslant \delta_x$ and take $w \in \mathcal{L}_\infty$, such that $\|w\|_{\mathcal{L}_\infty} \leqslant \delta_w$. Since the existence of solutions for each $\bar{x}(0) \in \mathcal{X}$ and each $w \in \mathcal{L}_\infty$ for all $t \in \mathbb{R}_+$ is not proven yet, suppose that $[0,T)$ is the supremal interval on which solutions to (4.10) are defined. Note that, for linear flow and jump dynamics, global existence problems (i.e., $T < \infty$) can only be caused by an accumulation point in the set of the event times $\{t_k \mid k \in \mathbb{N}\} = \bigcup_{i=1}^{N} \{t_{k_i}^i \mid k_i \in \mathbb{N}\}$, with $t_{k+1} > t_k$, $k \in \mathbb{N}$. Since $\|w\|_{\mathcal{L}_\infty}$ is bounded, $\varepsilon_i > 0$ for all $i \in \{1, \ldots, N\}$, and $e(0) = 0$, it is clear on the basis of (4.8) that the first transmission occurs at a (strictly) positive time and, thus, that $T > 0$. Following the reasoning in the proof of Theorem 4.3.5, the bound (A.87) holds for all $t \in [0,T)$, which implies that

$$V(\bar{x}(t)) \leqslant \lambda_{\max}(\bar{P})\|\bar{x}(0)\|^2 + \sum_{i=1}^{N} \tfrac{\mu_i \varepsilon_i}{\alpha} + \tfrac{\beta}{\alpha} \|w\|_{\mathcal{L}_\infty}^2, \qquad \text{(A.91)}$$

for all $\bar{x}(t) \in \mathcal{X}$, $t \in [0,T)$. Therefore, it holds that

$$\|x(t)\|^2 \leqslant \tfrac{1}{\lambda_{\min}(P)}(x^\top(t)Px(t) + \bar{x}^\top(t)U\bar{x}(t)) = \tfrac{1}{\lambda_{\min}(P)} V(\bar{x}(t)) \leqslant \eta, \quad \text{(A.92)}$$

for all $t \in [0,T)$, with η as defined in the hypothesis of the theorem. We now consider two event-times $t_{k_i+1}^i, t_{k_i}^i \in [0,T)$ and show that we can guarantee

that $t^i_{k_i+1} \geqslant t^i_{k_i} + h^i_{\min}$, for all $k_i \in \mathbb{N}$ and some $h^i_{\min} > 0$, $i \in \{1, \ldots, N\}$. After establishing this result, we will prove that $T = \infty$, meaning that all solutions are defined for all $t \in \mathbb{R}_+$.

To compute a guaranteed $h^i_{\min} > 0$, we compute the event time $t^i_{k_i+1}$, of node i given by (4.6), or equivalently,

$$t^i_{k_i+1} = \inf\left\{ t > t^i_{k_i} \,\Big|\, \begin{bmatrix} x(t) \\ e_{\mathcal{J}_i}(t) \end{bmatrix}^\top \begin{bmatrix} I & 0 \\ 0 & \bar{\Gamma}^\top_i \end{bmatrix} Q_i \begin{bmatrix} I & 0 \\ 0 & \bar{\Gamma}_i \end{bmatrix} \begin{bmatrix} x(t) \\ e_{\mathcal{J}_i}(t) \end{bmatrix} = \varepsilon_i \right\}. \tag{A.93}$$

We will use the fact that the solution of the event-triggered control system satisfies (4.27). Since $\bar{\Gamma}_i \bar{\Gamma}^\top_i = \Gamma_i$, and therefore

$$\left(\begin{bmatrix} I & 0 \\ 0 & \bar{\Gamma}^\top_i \end{bmatrix} \bar{A} \begin{bmatrix} I & 0 \\ 0 & \bar{\Gamma}_i \end{bmatrix} \right)^k \begin{bmatrix} I & 0 \\ 0 & \bar{\Gamma}^\top_i \end{bmatrix} = \begin{bmatrix} I & 0 \\ 0 & \bar{\Gamma}^\top_i \end{bmatrix} \left(\bar{A} \begin{bmatrix} I & 0 \\ 0 & \Gamma_i \end{bmatrix} \right)^k, \tag{A.94}$$

for all $k \in \mathbb{N}$, it holds for any $s \in \mathbb{R}_+$ that

$$e^{\left(\begin{bmatrix} I & 0 \\ 0 & \bar{\Gamma}^\top_i \end{bmatrix} \bar{A} \begin{bmatrix} I & 0 \\ 0 & \bar{\Gamma}_i \end{bmatrix} s \right)} \begin{bmatrix} I & 0 \\ 0 & \bar{\Gamma}^\top_i \end{bmatrix} = \begin{bmatrix} I & 0 \\ 0 & \bar{\Gamma}^\top_i \end{bmatrix} e^{\left(\bar{A} \begin{bmatrix} I & 0 \\ 0 & \Gamma_i \end{bmatrix} s \right)}. \tag{A.95}$$

Solving the differential equation (4.27) from $t^i_{k_i}$ to $t > t^i_{k_i}$ and using (A.95), the fact that $\bar{\Gamma}^\top_i \bar{\Gamma}_i = I$ and $e^+_{\mathcal{J}_i}(t^i_{k_i}) = 0$, yield

$$\begin{bmatrix} x(t) \\ e_{\mathcal{J}_i}(t) \end{bmatrix} = \begin{bmatrix} I & 0 \\ 0 & \bar{\Gamma}^\top_i \end{bmatrix} \left(e^{\bar{A} \begin{bmatrix} I & 0 \\ 0 & \Gamma_i \end{bmatrix}(t - t^i_{k_i})} \begin{bmatrix} I & 0 \\ 0 & \bar{\Gamma}_i \end{bmatrix} \begin{bmatrix} I \\ 0 \end{bmatrix} x(t^i_{k_i}) \right.$$
$$\left. + \int_{t^i_{k_i}}^t e^{\bar{A} \begin{bmatrix} I & 0 \\ 0 & \Gamma_i \end{bmatrix}(t - s)} \left(\bar{A} \begin{bmatrix} 0 \\ \bar{\Gamma}^c_i \end{bmatrix} e_{\mathcal{J}^c_i}(s) + \bar{B} w(s) \right) \mathrm{d}s \right), \tag{A.96}$$

with $\|w\|_{\mathcal{L}_\infty} \leqslant \delta_w$ and $e_{\mathcal{J}^c_i}(t)$ satisfying (4.8) for all $t \in [0, T)$. Given (A.93), we can conclude that, given $x(t^i_{k_i})$, no events are triggered by node $i \in \{1, \ldots, N\}$ as long as $t \geqslant t^i_{k_i}$ satisfies

$$x^\top(t^i_{k_i}) \begin{bmatrix} I \\ 0 \end{bmatrix}^\top e^{\begin{bmatrix} I & 0 \\ 0 & \Gamma_i \end{bmatrix} \bar{A}^\top (t - t^i_{k_i})} Q_i e^{\bar{A} \begin{bmatrix} I & 0 \\ 0 & \Gamma_i \end{bmatrix}(t - t^i_{k_i})} \begin{bmatrix} I \\ 0 \end{bmatrix} x(t^i_{k_i})$$

$$+ \int_{t^i_{k_i}}^t \left(\bar{A} \begin{bmatrix} 0 \\ \bar{\Gamma}^c_i \end{bmatrix} e_{\mathcal{J}^c_i}(s) + \bar{B} w(s) \right)^\top e^{\begin{bmatrix} I & 0 \\ 0 & \Gamma_i \end{bmatrix} \bar{A}^\top (t - s)} \mathrm{d}s \, Q_i$$

$$\left(\int_{t^i_{k_i}}^t e^{\bar{A} \begin{bmatrix} I & 0 \\ 0 & \Gamma_i \end{bmatrix}(t - s)} \left(\bar{A} \begin{bmatrix} 0 \\ \bar{\Gamma}^c_i \end{bmatrix} e_{\mathcal{J}^c_i}(s) + \bar{B} w(s) \right) \mathrm{d}s + 2 e^{\bar{A} \begin{bmatrix} I & 0 \\ 0 & \Gamma_i \end{bmatrix}(t - t^i_{k_i})} \begin{bmatrix} I \\ 0 \end{bmatrix} x(t^i_{k_i}) \right) < \varepsilon_i. \tag{A.97}$$

Now observe that

$$\Big\| \int_{t^i_{k_i}}^{t} e^{\bar A \left[\begin{smallmatrix} I & 0 \\ 0 & \Gamma_i \end{smallmatrix}\right](t-s)} \big(\bar A \left[\begin{smallmatrix} 0 \\ \bar\Gamma^c_i \end{smallmatrix}\right] e_{\mathcal{J}^c_i}(s) + \bar B w(s) \big) \mathrm{d}s \Big\|^2$$

$$\leqslant \int_{t^i_{k_i}}^{t} e^{\vartheta(t-s)} \mathrm{d}s \int_{t^i_{k_i}}^{t} \| \big(\bar A \left[\begin{smallmatrix} 0 \\ \bar\Gamma^c_i \end{smallmatrix}\right] e_{\mathcal{J}^c_i}(s) + \bar B w(s) \big) \|^2 \mathrm{d}s$$

$$\leqslant \int_{0}^{t-t^i_{k_i}} e^{\vartheta s} \mathrm{d}s \int_{t^i_{k_i}}^{t} 1 \mathrm{d}s \sup_{s \in (t^i_{k_i}, t]} \| \bar A \left[\begin{smallmatrix} 0 \\ \bar\Gamma^c_i \end{smallmatrix}\right] e_{\mathcal{J}^c_i}(s) + \bar B w(s) \|^2, \quad \text{(A.98)}$$

due to Hölder's inequality (applied twice) and Wazewski's inequality. It also holds that

$$\sup_{s \in (t^i_{k_i}, t]} \| \bar A \left[\begin{smallmatrix} 0 \\ \Gamma^c_i \end{smallmatrix}\right] e_{\mathcal{J}^c_i}(s) + \bar B w(s) \|^2$$

$$\leqslant (\| \bar A \left[\begin{smallmatrix} 0 \\ \Gamma^c_i \end{smallmatrix}\right] \| \sup_{s \in (t^i_{k_i}, t]} \| e_{\mathcal{J}^c_i}(s) \| + \| \bar B \| \delta_w)^2$$

$$\leqslant \Big(\| \bar A \left[\begin{smallmatrix} 0 \\ \Gamma^c_i \end{smallmatrix}\right] \| \sqrt{ \sup_{s \in (t^i_{k_i}, t]} \sum_{j \in \mathcal{I}_i} \| \Gamma_j e(s) \|^2 } + \| \bar B \| \delta_w \Big)^2$$

$$\leqslant \Big(\| \bar A \left[\begin{smallmatrix} 0 \\ \Gamma^c_i \end{smallmatrix}\right] \| \sqrt{ \sum_{j \in \mathcal{I}_i} \sigma_j \| \Gamma_j C \|^2 \eta + \varepsilon_j } + \| \bar B \| \delta_w \Big)^2, \quad \text{(A.99)}$$

with $\mathcal{I}_i$ as in the hypothesis of the theorem, due to the fact that the network induced error satisfies (4.8) and we have the bound (A.92). Therefore, the left-hand side of (A.98) can be upper bounded by $\rho_i(t - t^i_{k_i})$, as in (4.30). Hence,

$$x^\top(t^i_{k_i}) \left[\begin{smallmatrix} I \\ 0 \end{smallmatrix}\right]^\top e^{\left[\begin{smallmatrix} I & 0 \\ 0 & \Gamma_i \end{smallmatrix}\right] \bar A^\top (t-t^i_{k_i})} Q_i e^{\bar A \left[\begin{smallmatrix} I & 0 \\ 0 & \Gamma_i \end{smallmatrix}\right](t-t^i_{k_i})} \left[\begin{smallmatrix} I \\ 0 \end{smallmatrix}\right] x(t^i_{k_i}) < \zeta_i(t - t^i_{k_i}) \quad \text{(A.100)}$$

for some $x(t^i_{k_i}) \in \mathbb{R}^{n_p + n_c}$ and $t > t^i_{k_i}$, implies satisfaction of (A.97). Hence, given $\bar x(t^i_{k_i}) \in \mathcal{X}$, no events are triggered in node $i \in \{1, \ldots, N\}$ as long as $t > t^i_{k_i}$ satisfies (A.100). Now the solution to (4.28) is the smallest value $h^i_{\min} := t - t^i_{k_i}$, such that

$$x^\top \left[\begin{smallmatrix} I \\ 0 \end{smallmatrix}\right]^\top e^{\left[\begin{smallmatrix} I & 0 \\ 0 & \Gamma_i \end{smallmatrix}\right] \bar A^\top h^i_{\min}} Q_i e^{\bar A \left[\begin{smallmatrix} I & 0 \\ 0 & \Gamma_i \end{smallmatrix}\right] h^i_{\min}} \left[\begin{smallmatrix} I \\ 0 \end{smallmatrix}\right] x = \tfrac{\zeta_i(h^i_{\min}) \| \bar x \|^2}{\eta} \quad \text{(A.101)}$$

for some $x \in \mathbb{R}^{n_p + n_c}$ satisfying (A.92), in which we have used that $\| x \|^2 \leqslant \| \bar x \|^2$. Hence, we have that (A.100) is guaranteed to be satisfied for all $x \in \mathbb{R}^{n_p + n_c}$ as long as $t < t^i_{k_i} + h^i_{\min}$ and thus no events are triggered by node i under these conditions. This provides a lower bound on the inter-event time. Now

observe that for $h = 0$, the left-hand side of the condition in (4.28) reduces to $\lambda_{\max}(-\sigma_i C^\top \Gamma_i C)$ (which is smaller than or equal to zero) and the right-hand side to ε_i (which is strictly greater than zero) and, hence, the inequality in the condition in (4.28) is not (yet) satisfied for $h = 0$. Besides the fact that this shows that (A.100) can always be satisfied for some $x(t_{k_i}^i) \in \mathbb{R}^{n_p + n_c}$ and $t > t_{k_i}^i$, it also allows us to prove that the minimum in (4.28) always exists. Indeed, due to continuity of the matrix exponential, and the fact that for $h = 0$ the inequality in (4.28) is not (yet) satisfied, the minimum in (4.28) exists and is strictly positive.

It now only remains to show that $T = \infty$ and, thus, that the computed minimal inter-event times hold on the time interval $[0, \infty)$, thereby completing the proof. We proceed by contradiction and, therefore, suppose that $T < \infty$. If $T < \infty$, we have that the sequence $\{t_k\}_{k \in \mathbb{N}}$ has an accumulation point at T, implying that there must be a node $i \in \{1, \ldots, N\}$, for which the sequence $\{t_{k_i}\}_{k_i \in \mathbb{N}}$ has an accumulation point at time T, as well. Hence, node i transmits *infinitely often* in the time interval $[T - \tau, T)$ for any $\tau \in (0, T]$. Hence, there exist a τ and a $\bar\tau$, satisfying $0 < \tau \leqslant \bar\tau < T$ and $\bar\tau - \tau < h_{\min}^i$, such that on the interval $(\tau, \bar\tau)$ at least two transmissions of node i take place, i.e., $t_{k_i}^i, t_{k_i+1}^i \in (\tau, \bar\tau)$ for some $k_i \in \mathbb{N}$. However, $t_{k_i+1}^i - t_{k_i}^i \leqslant \bar\tau - \tau < h_{\min}^i$, which would contradict the minimal inter-event time of $h_{\min}^i$ on $[0, T)$ that we computed above. Hence, $T = \infty$ and $\bar x(t)$ is defined for all $t \in \mathbb{R}_+$, which completes the proof. $\qquad\square$

Proof of Theorem 4.5.2. The proof is based on showing that the positive definite matrix P, the scalars $\alpha, \beta, \kappa > 0$, and the scalars $\sigma_i \geqslant 0$, $i \in \{1, \ldots, N\}$, satisfying (4.36), also leads to a solution of the LMIs in Theorem 4.3.5, as formulated in Theorem 4.5.2. To do so, we take $\bar P$ in Theorem 4.3.5 as $\bar P := \mathrm{diag}(P, 0)$, (i.e., take $U = 0$). Now, because of the particular structure of $\bar P$, the left-hand side of (4.22a) becomes

$$\begin{bmatrix} -Z - \alpha P - C^\top \sum_{i=1}^N \mu_i \sigma_i \Gamma_i C & \star & \star \\ B^\top P & \sum_{i=1}^N \mu_i \Gamma_i & \star \\ E^\top P & 0 & \beta I \end{bmatrix}, \qquad (A.102)$$

where $Z := (A + BC)^\top P + P(A + BC)$. Note that (A.102) should be positive semidefinite. Now by selecting $\mu_i = \frac{1}{\sigma_i}$, for all $i \in \{1, \ldots, N\}$, (A.102) is equal to (4.36a), which is positive semidefinite by assumption. Therefore, (A.102) is also positive semidefinite and (4.22a) is satisfied. Then, by choosing $\nu_i = 0$, for all $i \in \{1, \ldots, N\}$, and using the particular structure in $\bar P$ and $\bar G_i$, results in zero-matrices on the left-hand side of (4.22c) for all $i \in \{1, \ldots, N\}$, which satisfies the inequality. Finally, using the particular structure of $\bar P$ and $\bar C = [C_x\ 0]$, we can conclude that (4.36b) is equal to (4.22b), and that the obtained set $\mathcal{A}$ of (4.37) is equal to (4.23), since we have taken $\mu_i = \frac{1}{\sigma_i}$ for all $i \in \{1, \ldots, N\}$. $\qquad\square$

A.4   Chapter 5

Proof of Theorem 5.3.1. From (5.23), it follows that $P_i \succ -(-1)^i \kappa_i Q$ for $i \in \{1, 2\}$. Since this implies that $\xi^\top (P_1 - \kappa_1 Q)\xi \geqslant \lambda_{\min}(P_1 - \kappa_1 Q)\|\xi\|^2$ and that $\xi^\top (P_2 + \kappa_2 Q)\xi \geqslant \lambda_{\min}(P_2 + \kappa_2 Q)\|\xi\|^2$, with $\lambda_{\min}(P_1 - \kappa_1 Q), \lambda_{\min}(P_2 - \kappa_2 Q) > 0$, we have that $V(\xi) = \xi^\top P_1 \xi \geqslant \lambda_{\min}(P_1 - \kappa_1 Q)\|\xi\|^2 + \kappa_1 \xi^\top Q\xi \geqslant \lambda_{\min}(P_1 - \kappa_1 Q)\|\xi\|^2$ for all ξ satisfying $\xi^\top Q\xi > 0$ and that $V(\xi) = \xi^\top P_2 \xi \geqslant \lambda_{\min}(P_2 + \kappa_2 Q)\|\xi\|^2 - \kappa_2 \xi^\top Q\xi \geqslant \lambda_{\min}(P_2 + \kappa_2 Q)\|\xi\|^2$ for all ξ satisfying $\xi^\top Q\xi \leqslant 0$. This proves that for the candidate Lyapunov function (5.21), there exists a $c_1 = \min\{\lambda_{\min}(P_1 - \kappa_1 Q), \lambda_{\min}(P_2 + \kappa_2 Q)\} > 0$ and some $c_2 \geqslant c_1$ such that $c_1 \|\xi\|^2 \leqslant V(\xi) \leqslant c_2 \|\xi\|^2$ for all $\xi \in \mathbb{R}^{n_\xi}$.

Furthermore, note that if $V(\xi) = \xi^\top P_i \xi$, it holds that

$$(-1)^i \xi^\top Q\xi \leqslant 0, \tag{A.103}$$

and if $V(A_i \xi) = (A_i \xi)^\top P_j (A_i \xi)$, then

$$(-1)^j \xi^\top A_i^\top Q A_i \xi \leqslant 0, \tag{A.104}$$

for $i, j \in \{1, 2\}$. Hence, using this and (5.22)

$$\begin{aligned} V(A_i \xi) &= \xi^\top A_i^\top P_j A_i \xi \\ &\leqslant e^{-2\rho h} \xi^\top P_i \xi + (-1)^i \alpha_{ij} \xi^\top Q\xi + (-1)^j \beta_{ij} \xi^\top A_i^\top Q A_i \xi \\ &\leqslant e^{-2\rho h} \xi^\top P_i \xi = e^{-2\rho h} V(\xi), \end{aligned} \tag{A.105}$$

where in the latter inequality we used that (A.103) and (A.104) hold and that $\alpha_{ij}, \beta_{ij} \geqslant 0$. By standard Lyapunov arguments this proves GES of the discrete-time PWL system (5.19) with decay factor $e^{-\rho h}$. Now, by including the inter-sample behaviour in a straightforward fashion, as was done in, e.g., [40], this also implies GES with decay rate ρ of the (continuous-time) PETC system, given by (5.1), (5.3), (5.4), and (5.5). $\square$

Proof of Theorem 5.3.7. The proof is based on showing that (5.30) guarantees that (5.31) holds, and that the hypotheses of the theorem guarantee that the conditions in (5.32) hold and that (5.29) is a well-defined storage function candidate. This would complete the proof as, provided that (5.29) is a well-defined storage function candidate, (5.31) and (5.32) prove GES and an upper bound on the $\mathcal{L}_2$-gain of γ, see, e.g., [62]. Proving that (5.30) guarantees that (5.31) holds for the function (5.29) will be the first step in the proof. To prove that the hypotheses of the theorem guarantee that the conditions in (5.32) hold, we need to relate $P_0 := P(0)$ to $P_h := P(h)$ and doing so will be the second step of the proof. The final step in the proof is to show how this relation can be used to show that the conditions in the theorem guarantee that (5.32) hold and that (5.29) is indeed a well-defined storage function candidate.

To show that (5.30) yields that the derivative of (5.29) along the flow part (5.17a) of the impulsive system (5.17) satisfies (5.31), we observe that

$$\frac{\mathrm{d}}{\mathrm{d}t}V = w^\top \bar{B}^\top P \xi + \xi^\top P \bar{B} w - \xi^\top (2\rho P + \gamma^{-2}\bar{C}^\top \bar{C})\xi$$
$$-\xi^\top(P\bar{B} + \gamma^{-2}\bar{C}^\top \bar{D})M(\bar{B}^\top P + \gamma^{-2}\bar{D}^\top \bar{C})\xi. \quad \text{(A.106)}$$

Now using the fact that $(G\xi - M^{-1}w)^\top M(G\xi - M^{-1}w) \geqslant 0$, with $G := \bar{B}^\top P + \gamma^{-2}\bar{D}^\top \bar{C}$, we have that $-\xi^\top G^\top M G \xi \leqslant -\xi G^\top w - w^\top G \xi + w^\top M^{-1}w$, and, therefore, it holds that

$$\frac{\mathrm{d}}{\mathrm{d}t}V \leqslant -\xi^\top(2\rho P + \gamma^{-2}\bar{C}^\top \bar{C})\xi - \gamma^{-2}\xi^\top \bar{C}^\top \bar{D} w - \gamma^{-2}w^\top \bar{D}^\top \bar{C}\xi + w^\top M^{-1}w, \tag{A.107}$$

or, equivalently,

$$\frac{\mathrm{d}}{\mathrm{d}t}V \leqslant -\xi^\top 2\rho P \xi + \begin{bmatrix} \xi \\ w \end{bmatrix}^\top \begin{bmatrix} \bar{C} & \bar{D} \\ 0 & I \end{bmatrix}^\top \begin{bmatrix} -\gamma^{-2}I & 0 \\ 0 & I \end{bmatrix} \begin{bmatrix} \bar{C} & \bar{D} \\ 0 & I \end{bmatrix} \begin{bmatrix} \xi \\ w \end{bmatrix}. \tag{A.108}$$

By using (5.17c), we have that (A.108) shows that (5.31) is satisfied. This completes the first step in the proof.

We will now relate $P_0 := P(0)$ to $P_h := P(h)$. To do so, we first reverse the time in the Riccati differential equation (5.30) by introducing $\tilde{P}(\tau) := P(h-\tau)$, $\tau \in [0, h]$. This results in

$$\frac{\mathrm{d}}{\mathrm{d}\tau}\tilde{P} = (\bar{A} + \rho I)^\top \tilde{P} + \tilde{P}(\bar{A} + \rho I) + \gamma^{-2}\bar{C}^\top \bar{C}$$
$$+(\tilde{P}\bar{B} + \gamma^{-2}\bar{C}^\top \bar{D})M(\bar{B}^\top \tilde{P} + \gamma^{-2}\bar{D}^\top \bar{C}), \tag{A.109}$$

or equivalently,

$$\frac{\mathrm{d}}{\mathrm{d}\tau}\tilde{P} = (\bar{A} + \rho I + \gamma^{-2}\bar{B}M\bar{D}^\top \bar{C})^\top \tilde{P} + \tilde{P}(\bar{A} + \rho I + \gamma^{-2}\bar{B}M\bar{D}^\top \bar{C})$$
$$+\gamma^{-2}\bar{C}^\top(I + \gamma^{-2}\bar{D}M\bar{D}^\top)\bar{C} + \tilde{P}\bar{B}M\bar{B}^\top \tilde{P}, \tag{A.110}$$

in which we have exploited the fact that M is symmetric. Note that $I + \gamma^{-2}\bar{D}M\bar{D}^\top = I + \gamma^{-2}\bar{D}(I - \gamma^{-2}\bar{D}^\top \bar{D})^{-1}\bar{D}^\top = I + \gamma^{-2}\bar{D}\bar{D}^\top(I - \gamma^{-2}\bar{D}\bar{D}^\top)^{-1}$, because for any matrix Z it holds that $(I + Z^\top Z)^{-1}Z^\top = Z^\top(I + ZZ^\top)^{-1}$. Furthermore, because for any matrix Z for which $I-Z$ is invertible, it holds that $I + Z(I - Z)^{-1} = (I - Z)^{-1}$, we have that $I + \gamma^{-2}\bar{D}\bar{D}^\top(I - \gamma^{-2}\bar{D}\bar{D}^\top)^{-1} = L$, where $L := (I - \gamma^{-2}\bar{D}\bar{D}^\top)^{-1}$ as was also used in the definition of the Hamiltonian matrix (5.33). Furthermore, observe that $\tilde{P}(0) := \tilde{P}_0 = P_h$ and $\tilde{P}(h) := \tilde{P}_h = P_0$. To link $\tilde{P}_0$ to $\tilde{P}_h$, and thereby P_h to P_0, we use the Hamiltonian matrix (5.33), which allows us to find explicitly the solution to the Riccati differential equation (A.110). Indeed by using (5.34), we can express the solution to (A.110) as

$$\tilde{P}(\tau) = (F_{21}(\tau) + F_{22}(\tau)\tilde{P}_0)(F_{11}(\tau) + F_{12}(\tau)\tilde{P}_0)^{-1}, \tag{A.111}$$

which requires that $F_{11}(\tau) + F_{12}(\tau)\tilde{P}_0$ is invertible. This fact can be easily verified, see, e.g., [11, Lemma 8.2]. Since (A.111) relates $\tilde{P}_0$ to $\tilde{P}_h$ (by taking $\tau = h$), provided that (A.111) is well defined for all $\tau \in [0, h]$, and thereby relates P_h to P_0, this completes the second step of the proof.

It now only remains to show how the expression (A.111) and the hypotheses can be used to show that the candidate storage function is well defined on $[0, h]$ and satisfies (5.32). To do so, we will use the fact that $F(\tau)$ is simplectic, i.e., $F^\top(\tau)\Omega F(\tau) = \Omega$ for all $\tau \in [0, h]$, where

$$\Omega = \begin{bmatrix} 0 & I \\ -I & 0 \end{bmatrix}, \tag{A.112}$$

and thus $\Omega^{-1} = -\Omega$. This fact follows from observing that $F^\top(0)\Omega F(0) = \Omega$ holds and $\frac{\mathrm{d}}{\mathrm{d}\tau}F^\top(\tau)\Omega F(\tau) = 0$ for all $\tau \in \mathbb{R}$, by exploiting the structure in the Hamiltonian (5.33) giving $H^\top\Omega + \Omega H = 0$. From $F^\top(\tau)\Omega F(\tau) = \Omega$, we obtain that

$$0 = F_{11}^\top F_{21} - F_{21}^\top F_{11} \tag{A.113a}$$

$$0 = F_{22}^\top F_{12} - F_{12}^\top F_{22} \tag{A.113b}$$

$$I = F_{11}^\top F_{22} - F_{21}^\top F_{12}, \tag{A.113c}$$

where we have again omitted the argument τ for compactness of notation. We will use these relations to rewrite (A.111). In particular, under Assumption 5.3.6, we have for all τ for which $F_{11}(\tau) + F_{12}(\tau)\tilde{P}_0 = F_{11}(\tau) + F_{12}(\tau)P_h$ is invertible,

$$
\begin{aligned}
P(h - \tau) = \tilde{P}(\tau) &\overset{\text{(A.111)}}{=} (F_{21} + F_{22}P_h)(F_{11} + F_{12}P_h)^{-1} \\
&= (F_{21} + F_{22}P_h)(I + F_{11}^{-1}F_{12}P_h)^{-1}F_{11}^{-1} \\
&\overset{\text{(A.113c)}}{=} (F_{21} + F_{11}^{-\top}(I + F_{21}^\top F_{12})P_h)(I + F_{11}^{-1}F_{12}P_h)^{-1}F_{11}^{-1} \\
&\overset{\text{(A.113a)}}{=} (F_{21} + F_{11}^{-\top}P_h + F_{21}F_{11}^{-1}F_{12}P_h)(I + F_{11}^{-1}F_{12}P_h)^{-1}F_{11}^{-1} \\
&= (F_{21}(I + F_{11}^{-1}F_{12}P_h) + F_{11}^{-\top}P_h)(I + F_{11}^{-1}F_{12}P_h)^{-1}F_{11}^{-1} \\
&= F_{21}F_{11}^{-1} + F_{11}^{-\top}P_h(I + F_{11}^{-1}F_{12}P_h)^{-1}F_{11}^{-1} \\
&= F_{21}F_{11}^{-1} + F_{11}^{-\top}\big(P_h - P_h(I + F_{11}^{-1}F_{12}P_h)^{-1}F_{11}^{-1}F_{12}P_h\big)F_{11}^{-1}, \tag{A.114}
\end{aligned}
$$

where the fact that $X^{-1} = X^{-1}Y^{-1}Y = (XY)^{-1}X$ for $X = F_{11}$ and $Y = F_{11} + F_{12}P_h$ was used in the third equality and the fact that $(I - Z)^{-1} = I + (I - Z)^{-1}Z$ for $Z = -F_{11}^{-1}F_{12}P_h$ was used in the last equality. Now since Lemma A.4.1 below states that $-F_{11}^{-1}F_{12}$ is positive semidefinite, there exists a (τ-dependent) matrix S that satisfies $-F_{11}^{-1}F_{12} = SS^\top$. This leads to

$$P(h - \tau) = F_{21}F_{11}^{-1} + F_{11}^{-\top}\big(P_h + P_hS(I - S^\top P_hS)^{-1}S^\top P_h\big)F_{11}^{-1}, \tag{A.115}$$

for all τ for which $P(h - \tau)$ is defined, as $(I + SS^\top P_h)^{-1}SS^\top = S(I + S^\top P_h S)^{-1}S^\top$.

Now (A.115) will be used to show that the candidate Lyapunov/storage function is well defined for all $\tau \in [0, h]$ and that the conditions in (5.32) hold, if the hypotheses in the theorem are satisfied. Namely, (A.115) shows that having $P(h - \tau)$ defined for all $\tau \in [0, h]$ is equivalent to the existence of $(I - S^\top(\tau)P_h S(\tau))^{-1}$ for all $\tau \in [0, h]$. Now observe that the existence of the inverse of $I - S^\top(\tau)P_h S(\tau)$ for all $\tau \in [0, h]$ is guaranteed if $I - S^\top(\tau)P_h S(\tau) \succ 0$ for all $\tau \in [0, h]$, or, equivalently (by applying a Schur complement twice and using that $P_h \succ 0$), if $P_h^{-1} - S(\tau)S^\top(\tau) \succ 0$ for all $\tau \in [0, h]$. The fact that Lemma A.4.1 guarantees that $U(\tau) = -F_{11}^{-1}(\tau)F_{12}(\tau)$ is nondecreasing, i.e., $S(\tau)S^\top(\tau) \preceq S(h)S^\top(h)$ for all $\tau \leqslant h$, gives that $P_h^{-1} - S(h)S^\top(h) \succ 0$ implies that $P_h^{-1} - S(\tau)S^\top(\tau) \succ 0$, for all $\tau \in [0, h]$. Furthermore, using the reasoning in the proof of Proposition 8.1 of [11], we can show that $P(\tau) \succ 0$ for $\tau \in [0, h]$ under Assumption 5.3.6. Now since by the hypotheses of the theorem (in particular, (5.36)), $P_h \succ 0$ and $I - S^\top(h)P_h S(h) \succ 0$, the function (5.29) satisfies ToS

$$c_1\|\xi\|^2 \leqslant V(\tau, \xi) \leqslant c_2\|\xi\|^2, \tag{A.116}$$

for some $0 < c_1 \leqslant c_2$, for all $\xi \in \mathbb{R}^{n_\xi}$ and for all $\tau \in [0, h]$, and is therefore a well-defined storage function candidate.

It now only remains to show that the conditions in the theorem guarantee that the conditions (5.32) hold. To do so, we choose $\tau = h$ in (A.115) to obtain

$$P_0 = \bar{F}_{21}\bar{F}_{11}^{-1} + \bar{F}_{11}^{-\top}\big(P_h + P_h\bar{S}(I - \bar{S}^\top P_h \bar{S})^{-1}\bar{S}^\top P_h\big)\bar{F}_{11}^{-1}, \tag{A.117}$$

where $\bar{F}_{ij} := F_{ij}(h)$ for $i, j \in \{1, 2\}$, and $\bar{S} := S(h)$. Substituting (A.117) into (5.32a), and using an S-procedure to encode that $\xi^\top Q\xi > 0$, yield that (5.32a) with $i = 1$ holds if

$$P_h - \mu_1 Q - J_1^\top\big(\bar{F}_{21}\bar{F}_{11}^{-1} + \bar{F}_{11}^{-\top}\big(P_h + P_h\bar{S}(I - \bar{S}^\top P_h\bar{S})^{-1}\bar{S}^\top P_h\big)\bar{F}_{11}^{-1}\big)J_1 \tag{A.118}$$

is positive semidefinite for some $\mu_1 \geqslant 0$, which is implied by (5.36) for $i = 1$. Using a similar reasoning, satisfaction of (5.32b) is implied by (5.36) with $i = 2$ as $\mu_2 \geqslant 0$. This completes the proof. $\qquad\square$

Lemma A.4.1. *Consider $F(\tau)$ as in (5.34). Under Assumption 5.3.6, it holds that $U(\tau) := -F_{11}^{-1}(\tau)F_{12}(\tau)$ and $R(\tau) := F_{21}(\tau)F_{11}^{-1}(\tau)$ are positive semidefinite and nondecreasing for all $\tau \in [0, h]$, i.e., $U(\tau_1) \preceq U(\tau_2)$ and $R(\tau_1) \preceq R(\tau_2)$, when $0 \leqslant \tau_1 \leqslant \tau_2 \leqslant h$.*

Proof of Lemma A.4.1. Note that $R(\tau)$ is the solution to (A.110) for $\tilde{P}(0) = R(0) = 0$ according to (A.111). In particular,

$$\frac{\mathrm{d}}{\mathrm{d}\tau}R = \tilde{A}^\top R + R\tilde{A} + \bar{C}^\top L\bar{C} \tag{A.119}$$

where $\tilde{A} = \bar{A} + \rho I + \gamma^{-2} \bar{B} M \bar{D}^\top C + \frac{1}{2} \bar{B} M \bar{B}^\top R$, which depends on τ. Applying now Proposition 8.1 of [11] yields that $R(\tau) \succeq 0$, $\tau \in [0, h]$. Since $R(\tau)$ satisfies (A.119), $\frac{\mathrm{d}}{\mathrm{d}\tau} R(\tau)$ satisfies

$$
\begin{aligned}
\frac{\mathrm{d}^2}{\mathrm{d}\tau^2} R &= \tilde{A}^\top \frac{\mathrm{d}R}{\mathrm{d}\tau} + \frac{\mathrm{d}\tilde{A}^\top}{\mathrm{d}\tau} R + \frac{\mathrm{d}R}{\mathrm{d}\tau} \tilde{A} + R \frac{\mathrm{d}\tilde{A}}{\mathrm{d}\tau} \\
&= (\bar{A} + \rho I + \gamma^{-2} \bar{B} M \bar{D}^\top C + \tfrac{1}{2} \bar{B} M \bar{B}^\top R)^\top \frac{\mathrm{d}R}{\mathrm{d}\tau} + (\tfrac{1}{2} \bar{B} M \bar{B}^\top \tfrac{\mathrm{d}R}{\mathrm{d}\tau})^\top R \\
&\qquad + \frac{\mathrm{d}R}{\mathrm{d}\tau} (\bar{A} + \rho I + \gamma^{-2} \bar{B} M \bar{D}^\top C + \tfrac{1}{2} \bar{B} M \bar{B}^\top R) + R(\tfrac{1}{2} \bar{B} M \bar{B}^\top \tfrac{\mathrm{d}R}{\mathrm{d}\tau}) \\
&= (\bar{A} + \rho I + \bar{B} M \bar{D}^\top \bar{C} + \bar{B} M \bar{B}^\top R)^\top \frac{\mathrm{d}R}{\mathrm{d}\tau} \\
&\qquad + \frac{\mathrm{d}R}{\mathrm{d}\tau} (\bar{A} + \rho I + \bar{B} M \bar{D}^\top \bar{C} + \bar{B} M \bar{B}^\top R). \quad \text{(A.120)}
\end{aligned}
$$

Since $\frac{\mathrm{d}}{\mathrm{d}\tau} R(0) \stackrel{\text{(A.119)}}{=} C^\top L C \succeq 0$, applying Proposition 8.1 of [11] once more shows that $\frac{\mathrm{d}}{\mathrm{d}\tau} R(\tau) \succeq 0$ for $\tau \in [0, h]$. This shows that R is nondecreasing.

A similar reasoning applies to $U(\tau)$ for a somewhat modified Riccati differential equation corresponding to the Hamiltonian $\tilde{H} = V^{-1} H^\top V$ with $V = \mathrm{diag}(I, -I)$. Defining

$$
\tilde{F}(\tau) := e^{-\tilde{H}\tau} = \begin{bmatrix} \tilde{F}_{11}(\tau) & \tilde{F}_{12}(\tau) \\ \tilde{F}_{21}(\tau) & \tilde{F}_{22}(\tau) \end{bmatrix} \quad \text{(A.121)}
$$

and using that $\tilde{F}(\tau) = V^{-1} F(\tau)^\top V$, we can show that $\tilde{R}(\tau) := \tilde{F}_{21}(\tau) \tilde{F}_{11}^{-1}(\tau) = -F_{11}^{-1}(\tau) F_{12}(\tau) = U(\tau)$ (exploiting symmetry of solutions to Riccati differential equations of the type (A.110) for symmetric initial conditions). Applying the same reasoning to $\tilde{R}(\tau)$ as for $R(\tau)$ using the Riccati differential equation corresponding to the Hamiltonian $\tilde{H}$, the facts that $U(\tau) \succeq 0$ and $U(\tau)$ is nondecreasing follow. $\qquad \square$

Proof of Corollary 5.3.8. The proof follows from a slight modification of the reasoning in Section 5.3.3 and the proof of Theorem 5.3.7. Namely, instead of the dissipation inequality (5.31), we require $\frac{\mathrm{d}}{\mathrm{d}t} V = -2\rho V$ along the solutions of (5.17a) with $w = 0$. Using the same Lyapunov function candidate as in (5.29), this is satisfied if the matrix differential equation $\frac{\mathrm{d}}{\mathrm{d}t} P = -(\bar{A}^\top + \rho I) P - P(\bar{A} + \rho I)$ holds, which has the solution $P(\tau) = e^{2\rho(h-\tau)} e^{\bar{A}^\top (h-\tau)} P_h e^{\bar{A}(h-\tau)}$ and thus $P(0) = e^{2\rho h} e^{\bar{A}^\top h} P_h e^{\bar{A} h}$. Substituting this in the jump conditions (5.32) yields

$$
e^{2\rho h} \xi^\top J_1^\top e^{\bar{A}^\top h} P_h e^{\bar{A} h} J_1 \xi \leqslant \xi^\top P_h \xi, \quad \text{(A.122)}
$$

when $\xi^\top Q \xi > 0$, and

$$
e^{2\rho h} \xi^\top J_2^\top e^{\bar{A}^\top h} P_h e^{\bar{A} h} J_2 \xi \leqslant \xi^\top P_h \xi, \quad \text{(A.123)}
$$

when $\xi^\top Q \xi \leqslant 0$. These conditions are guaranteed by the hypotheses of the theorem. $\qquad \square$

Proof of Theorem 5.4.1. We will only give the proof for the triggering condition (5.6), as the proof is similar for (5.8). The proof will be based on showing that if the LMIs (5.28) are feasible for $\bar{P} \succ 0$ for some $\sigma < \theta$, then

$$P_1 = P_2 = P := \begin{bmatrix} \bar{P} & 0 \\ 0 & \delta I \end{bmatrix} \tag{A.124}$$

is a solution to the LMIs (5.22) and (5.23), with the matrix Q as in (5.7), for some scalars $\alpha_{ij}, \beta_{ij}, \kappa_i \geqslant 0$, $i, j \in \{1, 2\}$, for some (sufficiently small) $\delta > 0$. To do so, we first observe that (5.23) is satisfied for all $\delta > 0$ with $\kappa_1 = \kappa_2 = 0$. Focussing on (5.22) with $i = 1$, we observe that for $\alpha_{11} = \alpha_{12} = \beta_{11} = \beta_{12} = 0$, (5.22) with $i = 1$ and P_1 as in (A.124) is equivalent to

$$e^{-2\rho h}P - A_1^\top P A_1 = \begin{bmatrix} e^{-2\rho h}\bar{P} - (A+BK)^\top \bar{P}(A+BK) - \delta I & 0 \\ 0 & e^{-2\rho h}\delta I \end{bmatrix} \succeq 0, \tag{A.125}$$

where A_1 is given as in (5.20). Clearly, due to (5.28), for sufficiently small $\delta > 0$ and $\rho > 0$, we have that $e^{-2\rho h}\bar{P} - (A + BK)^\top \bar{P}(A + BK) - \delta I$ and $e^{-2\rho h}\delta I$ are positive semidefinite matrices. Hence, the matrix inequality in (A.125) is satisfied and thus (5.22) with $i = 1$ is satisfied for P as in (A.124) for $\alpha_{11} = \alpha_{12} = \beta_{11} = \beta_{12} = 0$ and a sufficiently small value of $\delta > 0$. Focussing now on (5.22) with $i = 2$, we observe that by taking $\alpha_{21} = \alpha_{22} = 1$ and $\beta_{21} = \beta_{22} = 0$, we obtain

$$\begin{aligned} &e^{-2\rho h}P + Q - A_2^\top P A_2 \\ &= \begin{bmatrix} e^{-2\rho h}\bar{P} + (1-\sigma^2)I - A^\top \bar{P}A & -I - A^\top \bar{P}BK \\ -I - (BK)^\top \bar{P}A & I + (e^{-2\rho h} - 1)\delta I - (BK)^\top \bar{P}BK \end{bmatrix} \succeq 0, \end{aligned} \tag{A.126}$$

where A_1 is given as in (5.20) and Q is given as in (5.6). This expression is equivalent to

$$\begin{bmatrix} I & -I \\ 0 & I \end{bmatrix} R(\sigma) \begin{bmatrix} I & 0 \\ -I & I \end{bmatrix} \succeq \begin{bmatrix} (1 - e^{-2\rho h})\bar{P} & 0 \\ 0 & (1 - e^{-2\rho h})\delta I \end{bmatrix} \succ 0, \tag{A.127}$$

with

$$R(\sigma) := \begin{bmatrix} \bar{P} - \sigma^2 I - (A + BK)^\top \bar{P}(A + BK) & \star \\ -(BK)^\top \bar{P}(A + BK) & I - (BK)^\top \bar{P}BK \end{bmatrix}. \tag{A.128}$$

To guarantee now that (A.127) is satisfied for some (arbitrary small) $\rho > 0$, we have to show that $R(\sigma) \succ 0$ for the given σ. Since $\sigma < \theta$, (5.28) implies that $R(\sigma) \succ 0$ and, hence, that the matrix inequality in (A.127) is satisfied and thus (5.22) with $i = 2$ is satisfied for P as in (A.124) for $\alpha_{21} = \alpha_{22} = 1$ and $\beta_{21} = \beta_{22} = 0$. This completes the proof. $\qquad \square$

A.5   Chapter 6

Proof of Lemma 6.3.4. Since (6.12) holds, and since the solutions to (6.1) with (6.2) satisfy

$$x(t_k + \hbar_l) = e^{A\hbar_l}x(t_k) + \int_0^{\hbar_l}e^{As}B\mathrm{d}s\,\hat{u}_k, \tag{A.129}$$

we have that

$$V(x(t_k + \hbar_l)) \leqslant e^{-\alpha q(t_k + \hbar_l)}V(x(0)). \tag{A.130}$$

for all $l \in \{0, \ldots, L-1\}$ and for all t_k, $k \in \mathbb{N}$, with $\hbar_0 = 0$. Now using (6.11), we have that (A.130) implies

$$\|x(t_k + \hbar_l)\| \leqslant \sqrt[q]{\frac{\bar{a}}{\underline{a}}}e^{-\alpha(t_k + \hbar_l)}\|x(0)\|, \tag{A.131}$$

for all $l \in \{0, \ldots, L-1\}$ and for all t_k, $k \in \mathbb{N}$, with $\hbar_0 = 0$. Moreover, because it holds that $\|\hat{u}_k\| \leqslant \beta\|x(t_k)\|$, the solutions to (6.1) with (6.2) also satisfy

$$\|x(t)\| \leqslant \|e^{A(t-t_k-\hbar_l)}\|\,\|x(t_k + \hbar_l)\| + \int_{t_k+\hbar_l}^{t}\|e^{A(t-s)}\|\mathrm{d}s\,\|B\|\|\hat{u}_k\|$$
$$\leqslant e^{\|A\|\Delta_\hbar}\|x(t_k+\hbar_l)\| + \beta\int_0^{\Delta_\hbar}e^{\|A\|s}\mathrm{d}s\,\|B\|\,\|x(t_k)\|, \tag{A.132}$$

for all $t \in [t_k + \hbar_l, t_k + \hbar_{l+1})$, $k \in \mathbb{N}$, $l \in \{0, \ldots, L-1\}$, with $\Delta_\hbar$ as defined in the hypothesis of the lemma. Substituting (A.131) into this expression (twice) yields

$$\|x(t)\| \leqslant \sqrt[q]{\frac{\bar{a}}{\underline{a}}}\Big(e^{\|A\|\Delta_\hbar}\,e^{-\alpha(t_k+\hbar_l)} + \beta\int_0^{\Delta_\hbar}e^{\|A\|s}\mathrm{d}s\,\|B\|\,e^{-\alpha t_k}\Big)\|x(0)\|, \tag{A.133}$$

for all $t \in [t_k + \hbar_l, t_k + \hbar_{l+1})$, $k \in \mathbb{N}$, $l \in \{0, \ldots, L-1\}$. Now realising that for all $t \in [t_k + \hbar_l, t_k + \hbar_{l+1})$, $k \in \mathbb{N}$, $l \in \{0, \ldots, L-1\}$, it holds that $e^{-\alpha(t_k+\hbar_l)} < e^{-\alpha t + \alpha\Delta_\hbar}$ and that $e^{-\alpha t_k} < e^{-\alpha t + \alpha\hbar_L}$ we have (6.5) with c as given in the hypothesis of the Lemma 6.3.4. $\qquad\square$

Proof of Theorem 6.3.5. Using the arguments given in Section 6.3.3, we have that the hypotheses of the theorem guarantee that $F_{\mathrm{MAC}}(x) \neq \emptyset$ for all $x \in \mathbb{R}^{n_x}$. By following a similar reasoning as done in the proof of Lemma 6.3.4, we can show that the MAC law guarantees that (A.133) holds for all $t \in [t_k + \hbar_l, t_k + \hbar_{l+1})$, $k \in \mathbb{N}$, $l \in \{0, \ldots, \bar{L}^\star(x(t_k)) - 1\}$, with $\hbar_0 = 0$, and all $x \in \mathbb{R}^{n_x}$. Again realising that for all $t \in [t_k + \hbar_l, t_k + \hbar_{l+1})$, $k \in \mathbb{N}$, $l \in \{0, \ldots, \bar{L}^\star(x(t_k)) - 1\}$, it holds that $e^{-\alpha(t_k+\hbar_l)} < e^{-\alpha t + \alpha\Delta_\hbar}$ and that $e^{-\alpha t_k} < e^{-\alpha t + \alpha\hbar_{\bar{L}^\star(x(t_k))}} \leqslant e^{-\alpha t + \alpha\hbar_L}$ yields (6.5) with gain $c = \bar{c}(\alpha, \beta, \Delta_\hbar, \hbar_L)$ as in (6.14). $\qquad\square$

Proof of Theorem 6.3.6. Using the arguments given in Section 6.3.4, we have that the hypotheses of the theorem guarantee that $F_{\mathrm{AAC}}(x, h) \neq \emptyset$ for all $x \in \mathbb{R}^{n_x}$ and all $h \in \mathcal{H}$. Moreover, as also argued in Section 6.3.4, the proposed

AAC law guarantees that the solutions of the system (6.1), (6.2) with (6.4) satisfy

$$V(x(t_k + \hbar_l)) \leqslant e^{-\bar{\alpha}_{J^\star(x(t_k), h_k)} q\hbar_l} V(x(t_k)) \leqslant e^{-\bar{\alpha}_1 q\hbar_l} V(x(t_k)) \qquad (A.134)$$

for all $l \in \{0, \ldots, \bar{L}(h_k) - 1\}$, $k \in \mathbb{N}$. Now using the reasoning of the proof of Lemma 6.3.4, we can show that this implies that (A.133) holds for all $t \in [t_k + \hbar_l, t_k + \hbar_{l+1})$, $l \in \{0, \ldots, \bar{L}(h_k)) - 1\}$, with $\hbar_0 = 0$, $k \in \mathbb{N}$, and for all $x \in \mathbb{R}^{n_x}$. Again realising that for all $t \in [t_k + \hbar_l, t_k + \hbar_{l+1})$, $l \in \{0, \ldots, \bar{L}(h_k) - 1\}$, $k \in \mathbb{N}$, it holds that $e^{-\bar{\alpha}_1(t_k + \hbar_l)} < e^{-\bar{\alpha}_1 t + \bar{\alpha}_1 \Delta_\hbar}$ and that $e^{-\bar{\alpha}_1 t_k} < e^{-\bar{\alpha}_1 t + \bar{\alpha}_1 \hbar_{\bar{L}(h)}} \leqslant e^{-\bar{\alpha}_1 t + \bar{\alpha}_1 \hbar_L}$ yields (6.5) with gain $c = \bar{c}(\bar{\alpha}_1, \beta, \Delta_\hbar, \hbar_L)$ as in (6.14). $\qquad \square$

Proof of Lemma 6.4.1. The proof follows the same line of reasoning as in [80, 108]. GES of (6.1) with (6.23) with convergence rate $\hat{\alpha}$ and gain $\hat{c} = \bar{a}/\underline{a}$ is implied by the existence of a positive definite function, satisfying (6.11) and

$$\lim_{s \downarrow 0} \tfrac{1}{s} \big(V(x(t+s)) - V(x(t))\big) \leqslant -\hat{\alpha} V(x(t)), \qquad (A.135)$$

for all $t \in \mathbb{R}_+$, which follows from the Comparison Lemma, see, e.g., [79]. Now using the fact that the solutions to (6.1) with (6.23) satisfy $\frac{\mathrm{d}}{\mathrm{d}t} x = (A + BK)x$, and using (6.21), we obtain that (A.135) is implied by

$$\lim_{s \downarrow 0} \tfrac{1}{s} (\|P(I + s(A + BK))x(t)\|_\infty - \|Px(t)\|_\infty) \leqslant -\hat{\alpha} \|Px(t)\|_\infty, \quad (A.136)$$

for all $t \in \mathbb{R}_+$. Using (6.24a), we have that, for all $t \in \mathbb{R}_+$, (A.136) implied by

$$\lim_{s \downarrow 0} \tfrac{1}{s} (\|(I + sQ)\|_\infty - 1) \|Px(t)\|_\infty \leqslant -\hat{\alpha} \|Px(t)\|_\infty, \qquad (A.137)$$

which is, due to positivity of $\|Px\|_\infty$ for all $x \neq 0$, equivalent to $\lim_{s \downarrow 0} \tfrac{1}{s} (\|(I + sQ)\|_\infty - 1) \leqslant -\hat{\alpha}$, which is implied by (6.24b). This completes the proof. $\quad \square$

Proof of Lemma 6.4.2. The proof is based on showing that the Lyapunov function obtained using Lemma 6.4.1 also guarantees (6.1) and (6.2), with (6.25) and $t_{k+1} = t_k + h$, $k \in \mathbb{N}$, to be GES with convergence rate α and gain $c := \bar{c}(\alpha, \beta, h)$, where $\bar{c}(\alpha, \beta, h)$ as in (6.10), for all $h < h_{\max}(\alpha)$ as in (6.26). To do so, observe that the solutions of (6.1) and (6.2), with (6.25) and $t_{k+1} = t_k + h$, $k \in \mathbb{N}$, satisfy

$$x(t) = (e^{A(t - t_k)} + \int_0^{t - t_k} e^{As} BK \mathrm{d}s) x(t_k), \qquad (A.138)$$

for all $t \in [t_k, t_k + h)$, $k \in \mathbb{N}$, which can be bounded as

$$\|x(t)\| \leqslant \big(e^{\|A\| h} + \int_0^h e^{\|A\| s} \mathrm{d}s \, \|B\| \, \|K\|\big) \|x(t_k)\|, \qquad (A.139)$$

for all $t \in [t_k, t_k + h)$, $k \in \mathbb{N}$. Now by following the ideas used in the proof of Lemma 6.3.4, and the candidate Lyapunov function of the form (6.21), we have

that GES with convergence rate α and gain c of (6.1) and (6.2), with (6.25) and $t_{k+1} = t_k + h$, $k \in \mathbb{N}$, is implied by requiring that

$$\|Px(t_k + h)\|_\infty - e^{-\alpha h}\|Px(t_k)\|_\infty \leqslant 0, \qquad (A.140)$$

for all t_k, $k \in \mathbb{N}$, and some well-chosen $h > 0$. Substituting (A.138) and defining $\hat{x} := Px$, yielding $x = (P^\top P)^{-1} P^\top \hat{x}$, yields that that (A.140) is implied by

$$(\|P(e^{Ah} + \int_0^h e^{As} BK \mathrm{d}s)(P^\top P)^{-1}P^\top\|_\infty - e^{-\alpha h})\|\hat{x}(t_k)\|_\infty \leqslant 0, \qquad (A.141)$$

for all $\hat{x}(t_k) \in \mathbb{R}^m$, which holds for all $h > 0$, satisfying $h < h_{\max}(\alpha)$, as given in the hypothesis of the lemma, meaning that (A.140) holds for all $\hat{x}(t_k) \in \mathbb{R}^m$ and for all $h > 0$, satisfying $h < h_{\max}(\alpha)$. This completes the proof. $\qquad\square$

Proof of Theorem 6.4.3. As a result of Lemma 6.4.2, we have that the control input given by (6.25) renders the plant (6.1) with ZOH (6.2) GES with convergence rate α and gain $c := \bar{c}(\alpha, \|K\|_\infty, h)$ as in (6.10), for any interexecution time $h < h_{\max}(\alpha)$ as in (6.26). To obtain a well-defined control law, we need that $F_{\mathrm{MAC}}(x) \neq \emptyset$, for all $x \in \mathbb{R}^{n_x}$, which is guaranteed if and only if (6.15) satisfies $F_1(x) \neq \emptyset$ for all $x \in \mathbb{R}^{n_x}$, as argued in Section 6.3.3. This can be achieved by choosing $\beta \geqslant \|K\|_\infty$ and choosing the set $\mathcal{H} := \{\hbar_1, \ldots, \hbar_L\}$, $L \in \mathbb{N}$, such that $\hbar_1 < h_{\max}(\alpha)$, as this yields that $F_1(x) \supseteq \{Kx\} \neq \emptyset$, if V is chosen as in (6.21). GES with the convergence rate α and the gain $c \geqslant \bar{c}(\alpha, \beta, \Delta_\hbar, \hbar_L)$ of (6.1) with ZOH (6.2) and (6.3), with (6.9), (6.15), (6.16), (6.17) and (6.21), follows directly from Theorem 6.3.5. This completes the proof. $\qquad\square$

Proof of Theorem 6.4.4. As a result of Lemma 6.4.2, we have that the control input given by (6.25), renders the plant (6.1) with ZOH (6.2) GES with a convergence rate α, a gain $c := \bar{c}(\alpha, \|K\|_\infty, h)$ as in (6.10), for any execution interval smaller than $h_{\max}(\alpha)$, as in (6.26). To obtain a well-defined control law, we need that $F_{\mathrm{AAC}}(x) \neq \emptyset$, for all $x \in \mathbb{R}^{n_x}$, which is guaranteed if and only if (6.18) satisfies $F_{L,1}(x) \neq \emptyset$ for all $x \in \mathbb{R}^{n_x}$, as argued in Section 6.3.4. This can be achieved by choosing $\alpha \leqslant \bar{\alpha}_1 < \hat{\alpha}$, the control gain bound $\beta \geqslant \|K\|_\infty$ and choosing the set $\mathcal{H} := \{\hbar_1, \ldots, \hbar_L\}$, $L \in \mathbb{N}$, such that $\hbar_L < h_{\max}(\alpha)$, as this yields that $F_{L,1}(x) \supseteq \{Kx\} \neq \emptyset$, if V is chosen as in (6.21). GES with the convergence rate α and the gain $c \geqslant \bar{c}(\bar{\alpha}_1, \beta, \Delta_\hbar, \hbar_L)$ of (6.1) with ZOH (6.2) and (6.4), with (6.9), (6.18), (6.19), (6.20) and (6.21), follows directly from Theorem 6.3.6. This completes the proof. $\qquad\square$

Bibliography

[1] J. Abedor, K. Nagpal, and K. Poolla. A linear matrix inequality approach to peak-to-peak gain minimization. *Int. J. Robust Nonlinear Control*, 6:899–927, 1996.

[2] P. Almstrom, M. Rabi, and M. Johansson. Networked state estimation over a Gilbert-Elliot type channel. In *Proc. IEEE Conf. Decision & Control*, pages 2711–2716, 2009.

[3] A. Anta and P. Tabuada. On the minimum attention and anytime attention problems for nonlinear systems. In *Proc. Conf. Decision & Control*, pages 3234–3239, 2010.

[4] P. Antsaklis and J. Baillieul. Special issue on technology of networked control systems. *Proc. IEEE*, 95, 2007.

[5] D. Antunes, J.P. Hespanha, and C. Silvestre. Volterra integral approach to impulsive renewal systems: Application to networked control. *IEEE Trans. Autom. Control*, 2011.

[6] K.-E. Arzén. A simple event-based PID controller. In *Preprints IFAC World Conf.*, volume 18, pages 423–428, 1999.

[7] S. Asmussen. *Applied Probability and Queues*. Springer, 2003.

[8] K. J. Åström and B. Wittenmark. *Computer Controlled Systems*. Prentice Hall, 1997.

[9] K.J. Åström and B.M. Bernhardsson. Comparison of periodic and event based sampling for first order stochastic systems. In *Proc. IFAC World Conf.*, pages 301–306, 1999.

[10] K.J. Åström and B.M. Bernhardsson. Comparison of Riemann and Lebesgue sampling for first order stochastic systems. In *Proc. Conf. Decision & Control*, pages 2011–2016, 2002.

[11] T. Başar and P. Bernhard. H_∞-*optimal control and related minimax design problems: A dynamic game approach*. Systems & Control: Foundations & Applications. Birkhäuser, Boston, 1991.

[12] A. Balluchi, P. Murrieri, and A. L. Sangiovanni-Vincentelli. Controller synthesis on non-uniform and uncertain discrete-time domains. In *Proc. Conf. Hybrid Systems: Computation and Control*, pages 118–133, 2005.

[13] N.W. Bauer, M.C.F. Donkers, W.P.M.H. Heemels, and N. van de Wouw. An approach to observer-based decentralized control under periodic protocols. In *Proc. American Control Conf.*, pages 2125–2131, 2010.

[14] N.W. Bauer, M.C.F. Donkers, W.P.M.H. Heemels, and N. van de Wouw. Decentralized observer-based control via networked communication. *Submitted for journal publication*, 2011.

[15] A. Bemporad, F. Borrelli, and M. Morari. Model predictive control based on linear programming the explicit solution. *IEEE Trans. Autom. Control*, 47:1974 – 1985, 2002.

[16] A. Bemporad, W.P.M.H. Heemels, and M. Johanssen. *Networked Control Systems*. Springer, 2010.

[17] D. Bernadini, M.C.F. Donkers, A. Bemporad, and W.P.M.H. Heemels. A model predictive control approach for stochastic networked control systems. In *Proc. IFAC Workshop Distributed Estimation & Control in Networked Systems*, pages 7–12, 2010.

[18] F. Blaabjerg, R. Teodorescu, M. Liserre, and A.V. Timbus. Overview of control and grid synchronization for distributed power generation systems. *IEEE Trans. Industrial Electronics,*, 53:1398–1409, oct. 2006.

[19] S. Boyd, L. El Ghaoui, E. Feron, and V. Balakrishnan. *Linear Matrix Inequalities in System and Control Theory*. SIAM, 1994.

[20] R.W. Brockett. Stabilization of motor networks. In *Proc. IEEE Conf. Decision & Control*, volume 2, pages 1484–1488, 1995.

[21] R.W. Brockett. Minimum attention control. In *Proc. Conf. Decision & Control*, pages 2628–2632, 1997.

[22] R.W. Brockett and D. Liberzon. Quantized feedback stabilization of linear systems. *IEEE Trans. Autom. Control*, 45:1279–1289, 2000.

[23] C. Cai, R. Goebel, and A.R. Teel. Smooth Lyapunov functions for hybrid systems part II: (Pre)Asymptotically stable compact sets. *IEEE Trans. Autom. Control*, 53:734 – 748, 2008.

[24] D. Carnevale, A.R. Teel, and D. Nešić. A Lyapunov proof of improved maximum allowable transfer interval for networked control systems. *IEEE Trans. Autom. Control*, 52:892–897, 2007.

[25] G. Cembrano, G. Wells, J. Quevedo, R. Prez, and R. Argelaguet. Optimal control of a water distribution network in a supervisory control system. *Control Engineering Practice*, 8:1177–1188, 2000.

[26] A. Chaillet and A. Bicchi. Delay compensation in packet-switching networked controlled sytems. In *Proc. IEEE Conf. Decision & Control*, pages 3620–3625, 2008.

[27] T. Chen and B.A. Francis. *Optimal Sampled-Data Control Systems*. Springer-Verlag, 1995.

[28] H. Chernoff. A measure of asymptotic efficiency test of a hypothesis based on the sum of observations. *Ann. Math. Stat*, 23:493–507, 1952.

[29] M.B.G. Cloosterman, L. Hetel, N. van de Wouw, W.P.M.H. Heemels, J. Daafouz, and H. Nijmeijer. Controller synthesis for networked control systems. *Automatica*, 46:1584–1594, 2010.

[30] M.B.G. Cloosterman, N. van de Wouw, W.P.M.H. Heemels, and H. Nijmeijer. Stabilization of networked control systems with large delays and packet dropouts. In *Proc. American Control Conf.*, pages 4991–4996, 2008.

[31] M.B.G. Cloosterman, N. van de Wouw, W.P.M.H. Heemels, and H. Nijmeijer. Stability of networked control systems with uncertain time-varying delays. *IEEE Trans. Autom. Control*, 54:1575 – 1580, 2009.

[32] O.L.V. Costa, M.D. Fragoso, and R.P. Marques. *Discrete-Time Markov Jump Linear Systems*. Springer-Verlag, 2005.

[33] D. Dai, T. Hu, A.R. Teel, and L. Zaccarian. Output feedback synthesis for sampled-data system with input saturation. In *Proc. American Control Conf.*, pages 1797 – 1802, 2010.

[34] D.B. Dačić and D. Nešić. Quadratic stabilization of linear networked control systems via simultaneous protocol and controller design. *Automatica*, 43:1145–1155, 2007.

[35] D.F. Delchamps. Stabilizing a linear system with quantized state feedback. *IEEE Trans. Autom. Control*, 35:916–924, 1990.

[36] M.C.F. Donkers and W.P.M.H. Heemels. Output-based event-triggered control with guaranteed $\mathcal{L}_\infty$-gain and improved event-triggering. In *Proc. IEEE Conf. Decision & Control*, pages 3246–3251, 2010.

[37] M.C.F. Donkers and W.P.M.H. Heemels. Output-based event-triggered control with guaranteed $\mathcal{L}_\infty$-gain and improved and decentralised event-triggering. *Conditionally accepted for IEEE Trans. Autom. Control*, 2011.

[38] M.C.F. Donkers, W.P.M.H. Heemels, D. Bernadini, A. Bemporad, and V. Shneer. Stability analysis of stochastic networked control systems. In *Proc. American Control Conf.*, pages 3684–3689, 2010.

[39] M.C.F. Donkers, W.P.M.H. Heemels, D. Bernadini, A. Bemporad, and V. Shneer. Stability analysis of stochastic networked control systems. *Accepted for Automatica*, 2011.

[40] M.C.F. Donkers, W.P.M.H. Heemels, N. van de Wouw, and L. Hetel. Stability analysis of networked control systems using a switched linear systems approach. *IEEE Trans. Autom. Control*, 56:2101 – 2115, 2011.

[41] M.C.F. Donkers, L. Hetel, W.P.M.H. Heemels, N. van de Wouw, and M. Steinbuch. Stability analysis of networked control systems using a switched linear systems approach. In *Proc. Conf. Hybrid Systems: Computation and Control*, pages 150–164, 2009.

[42] M.C.F. Donkers, P. Tabuada, and W.P.M.H. Heemels. On the minimum attention control problem for linear systems: A linear programming approach. In *Proc. IEEE Conf. Decision & Control*, 2011.

[43] L. Dritsas and A. Tzes. Robust stability analysis of networked systems with varying delays. *Int. J. Control*, 82:2347–2355, 2009.

[44] T. Estrada and P.J. Antsaklis. Stability of discrete-time plants using model-based control with intermittent feedback. In *Proc. Mediterranean Conf. Control & Autom.*, pages 1130–1136, 2008.

[45] H. Fujioka. A discrete-time approach to stability analysis of systems with aperiodic sample-and-hold devices. *IEEE Trans. Autom. Control*, 54:2440–2445, 2009.

[46] P.J. Gawthrop and L.B. Wang. Event-driven intermittent control. *Int. J. Control*, 82:2235–2248, 2009.

[47] J.C. Geromel and P. Colaneri. Stability and stabilization of discrete time switched systems. *Int. J. Control*, 79:719–728, 2006.

[48] R. Ghabcheloo, A.P. Aguiar, A. Pascoal, C. Silvestre, I. Kaminer, and J.P. Hespanha. Coordinated path-following in the presence of communication losses and time delays. SIAM J. Contr. Optimization, *Special Issue: Control and Optimization on Cooperative Networks*, 48:234–265, 2009.

[49] R. Gielen, S. Olaru, M. Lazar, W.P.M.H. Heemels, N. van de Wouw, and S. Niculescu. On polytopic inclusions as a modeling framework for systems with time-varying delays. *Automatica*, 46:615–619, 2010.

[50] R. Goebel, R. Sanfelice, and A.R. Teel. Hybrid dynamical systems. *IEEE Control Syst. Mag.*, 29:28–93, 2009.

[51] K.-C. Goh, M.G. Safonov, and G.P. Papavassilopoulos. A global optimization approach for the BMI problem. In *Proc. IEEE Conf. Decision & Control*, volume 3, pages 2009–2014, 1994.

[52] L. Greco, D. Fontanelli, and A. Bicchi. Design and stability analysis for anytime control via stochastic scheduling. *IEEE Trans. Autom. Control*, 2011.

[53] V. Gupta. On an anytime algorithm for control. In *Proc. Conf. Decision & Control*, pages 6218–6223, 2009.

[54] V. Gupta and D.E. Quevedo. On anytime control of nonlinear processes though calculation of control sequences. In *Proc. Conf. Decision & Control*, pages 7564–7569, 2010.

[55] W.M. Haddad, V. Chellaboina, and S.G. Nersesov. *Impulsive and Hybrid Dynamical Systems: Stability, Dissipativity, and Control*. Princeton University Press, 2006.

[56] A. Hassibi, J. How, and S. Boyd. A path-following method for solving BMI problems in control. In *Proc. American Control Conf.*, volume 2, pages 1385–1389, 1999.

[57] W.P.M.H. Heemels, M.C.F. Donkers, and A.R. Teel. Periodic event-triggered control. *Submitted for journal publication*, 2011.

[58] W.P.M.H. Heemels, M.C.F. Donkers, and A.R. Teel. Periodic event-triggered control based on state feedback. In *Proc. IEEE Conf. Decision & Control*, 2011.

[59] W.P.M.H. Heemels, R.J.A. Gorter, A. van Zijl, P.P.J. v.d. Bosch, S. Weiland, W.H.A. Hendrix, and M.R. Vonder. Asynchronous measurement and control: a case study on motor synchronisation. *Control Eng. Prac.*, 7:1467–1482, 1999.

[60] W.P.M.H. Heemels, J.H. Sandee, and P.P.J. van den Bosch. Analysis of event-driven controllers for linear systems. *Int. J. Control*, 81:571–590, 2008.

[61] W.P.M.H. Heemels, H. Siahaan, A. Juloski, and S. Weiland. Control of quantized linear systems: an l_1-optimal control approach. In *Proc. American Control Conference*, pages 3502–3507, 2003.

[62] W.P.M.H. Heemels, A.R. Teel, N. van de Wouw, and D. Nešić. Networked control systems with communication constraints: Tradeoffs between transmission intervals, delays and performance. *IEEE Trans. Autom. Control*, 55:1781–1796, 2010.

[63] W.P.M.H. Heemels, N. van de Wouw, R. Gielen, M.C.F. Donkers, L. Hetel, S. Olaru, M. Lazar, J. Daafouz, and S. I. Niculescu. Comparison of overapproximation methods for stability analysis of networked control systems. In *Proc. Conf. Hybrid Systems: Computation and Control*, pages 181–190, 2010.

[64] E. Hendricks, M. Jensen, A. Chevalier, and T. Vesterholm. Problems in event based engine control. In *Proc. American Control Conf.*, volume 2, pages 1585–1587, 1994.

[65] T. Henningsson and A. Cervin. Comparison of LTI and event-based control for a moving cart with quantized position measurements. In *Proc. European Control Conf.*, 2009.

[66] T. Henningsson, E. Johannesson, and A. Cervin. Sporadic event-based control of first-order linear stochastic systems. *Automatica*, 44:2890–2895, 2008.

[67] J.P. Hespanha, P. Naghshtabrizi, and Y. Xu. A survey of recent results in networked control systems. *Proc. IEEE*, pages 138–162, 2007.

[68] L. Hetel, J. Daafouz, and C. Iung. Stabilization of arbitrary switched linear systems with unknown time-varying delays. *IEEE Trans. Autom. Control*, 51:1668–1674, 2006.

[69] L. Hetel, J. Daafouz, and C. Iung. Analysis and control of LTI and switched systems in digital loops via an event-based modeling. *Int. J. Control*, 81:1125–1138, 2008.

[70] K. Hikichi, H. Morino, I. Arimoto, K. Sezaki, and Y. Yasuda. The evaluation of delay jitter for haptics collaboration over the internet. In *Proc. IEEE Global Telecomm. Conf.*, pages 1492–1496, 2002.

[71] R. Horn and C.R. Johnson. *Matrix Analysis*. Cambridge University Press, 1985.

[72] D. Hristu and K. Morgansen. Limited communication control. *Syst. Control Lett.*, 37:193–205, 1999.

[73] T. Iwasaki and R.E. Skelton. The XY-centring algorithm for the dual LMI problem: a new approach to fixed-order control design. *Int. J. Control*, 62:1257–1272, 1995.

[74] Z. Jin, V. Gupta, and R.M. Murray. State estimation over packet dropping networks using multiple description coding. *Automatica*, 42:1441 – 1452, 2006.

[75] M. Johansson. *Piecewise Linear Control Systems*, volume 284. Springer, Berlin, Germany, 2003.

[76] C.-Y. Kao and B. Lincoln. Simple stability criteria for systems with time-varying delays. *Automatica*, 40:1429–1434, 2004.

[77] C. M. Kellett and A. R. Teel. Discrete-time asymptotic controllability implies smooth control-lyapunov function. *Syst. & Control Lett.*, 51:349–359, 2004.

[78] C.M. Kellett and A.R. Teel. Smooth Lyapunov functions and robustness of stability for difference inclusions. *Systems & Control Letters*, 52:395–405, 2004.

[79] H. K. Khalil. *Nonlinear Systems*. Prentice Hall, 1996.

[80] H. Kiendl, J. Adamy, and P. Stelzner. Vector norms as Lyapunov function for linear systems. *IEEE Trans. Autom. Control*, 37:839–842, 1992.

[81] E. Kofman and J.H. Braslavsky. Level crossing sampling in feedback stabilization under data-rate constraints. In *Proc. IEEE Conf. Decision & Control*, pages 4423–4428, 2006.

[82] M. Kvasnica, P. Grieder, and M. Baotić. Multi-Parametric Toolbox (MPT), 2004.

[83] W.H. Kwon, Y.H. Kim, S.J. Lee, and K.-N. Paek. Event-based modeling and control for the burnthrough point in sintering processes. *IEEE Trans. Control Syst. Technol.*, 7:31–41, 1999.

[84] W. Lawrenz. *CAN System Engineering: From Theory to Practical Applications*. New York: Springer-Verlag, 1997.

[85] D. Lehmann and J. Lunze. Extension and experimental evaluation of an event-based state-feedback approach. *Control Engineering Practice*, 19:101 – 112, 2011.

[86] D. Liberzon. On stabilization of linear systems with limited information. *IEEE Trans. Autom. Control*, 48:304–307, 2003.

[87] D. Liberzon. Quantization, time delays, and nonlinear stabilization. *IEEE Trans. Autom. Control*, 51:1190–1195, 2006.

[88] X. Liu and A. Goldsmith. Kalman filtering with partial observation losses. *Proc. IEEE Conf. Decision & Control*, 4:4180–4186, 2004.

[89] S.J.L.M. van Loon, M.C.F. Donkers, W.P.M.H. Heemels, and N. van de Wouw. Stability analysis of networked and quantized control systems: a switched linear systems approach. *Submitted for journal publication*, 2011.

[90] J. Lunze and D. Lehmann. A state-feedback approach to event-based control. *Automatica*, 46:211–215, 2010.

[91] R. Marau, P. Leite, M. Velasco, P. Marti, L. Almeida, P. Pedreiras, and J.M. Fuertes. Performing flexible control on low-cost microcontrollers using a minimal real-time kernel. *IEEE Trans. Industrial Informatics*, 4:125–133, 2008.

[92] M. Mazo Jr., A. Anta, and P. Tabuada. An ISS self-triggered implementation of linear controllers. *Automatica*, 46:1310–1314, 2010.

[93] C. Meng, T. Wang, W. Chou, S. Luan, Y. Zhang, and Z. Tian. Remote surgery case: Robot-assisted teleneurosurgery. In *IEEE Int. Conf. Robotics & Automation*, pages 819–823, 2004.

[94] M. Miskowicz. Send-on-delta concept: An event-based data-reporting strategy. *Sensors*, 6:49–63, 2006.

[95] L.A. Montestruque and P. Antsaklis. Stochastic stability for model-based networked control systems. In *Proc. American Control Conf.*, pages 4119 – 4124, 2003.

[96] L.A. Montestruque and P. Antsaklis. Stability of model-based networked control systems with time-varying transmission times. *IEEE Trans. Autom. Control*, 49:1562–1572, 2004.

[97] J.R. Moyne and D.M. Tilbury. The emergence of industrial control networks for manufacturing control, diagnostics, and safety data. *Proc. IEEE*, 95:29–47, 2007.

[98] R.M. Murray, K.J. Åström, S.P. Boyd, R.W. Brockett, and G. Stein. Future directions in control in an information-rich world. *Control Syst. Mag.*, pages 20–33, 2003.

[99] P. Naghshtabrizi and J.P. Hespanha. Stability of networked control systems with variable sampling and delay. In *44th Allerton Conf. Communications, Control & Computing*, 2006.

[100] P. Naghshtabrizi, J.P. Hespanha, and A.R. Teel. Stability of delay impulsive systems with application to networked control systems. In *Proc. American Control Conf.*, pages 4899–4904, New York, USA, 2007.

[101] G.N. Nair and R.J. Evans. Stabilizability of stochastic linear systems with finite feedback data rates. *SIAM J. Control Optim.*, 43:413–436, 2004.

[102] D. Nešić and D. Liberzon. A unified framework for design and analysis of networked and quantized control systems. *IEEE Trans. Autom. Control*, 54:732–747, 2009.

[103] D. Nešić and A.R. Teel. Input-output stability properties of networked control systems. *IEEE Trans. Autom. Control*, 49:1650–1667, 2004.

[104] D. Nešić, A.R.. Teel, and E. Sontag. Formulas relating $\mathcal{KL}$ stability estimates of discrete-time and sampled-data nonlinear systems. *Syst. Control Lett.*, 38:49–60, 1999.

[105] J. Nilsson, B.M. Bernhardsson, and B. Wittenmark. Stochastic analysis and control of real-time systems with random time delays. *Automatica*, 34:57 – 64, 1998.

[106] S. Öncü, N. van de Wouw, and H. Nijmeijer. Cooperative adaptive cruise control: Tradeoffs between control and network specifications. In *Proc. Intelligent Transportation Syst.*, 2011.

[107] P.G. Otanez, J.R. Moyne, and D.M. Tilbury. Using deadbands to reduce communication in networked control systems. In *Proc. American Control Conf.*, pages 3015 – 3020, 2002.

[108] A. Polański. On infinity norms as Lyapunov functions for linear systems. *IEEE Trans. Autom. Control*, 40:1270–1274, 1995.

[109] H. Rehbinder and M. Sanfridson. Scheduling of a limited communication channel for optimal control. *Automatica*, 40:491–500, 2004.

[110] T. Samad, J.S. Bay, and D. Godbole. Network-centric systems for military operations in urban terrain: The role of uavs. *Proc. IEEE*, pages 92–107, 2007.

[111] J.H. Sandee, W.P.M.H. Heemels, S.B.F. Hulsenboom, and P.P.J. van den Bosch. Analysis and experimental validation of a sensor-based event-driven controller. In *Proc. American Control Conf.*, pages 2867–2874, 2007.

[112] R. Sanfelice, R. Goebel, and A.R. Teel. Generalized solutions to hybrid dynamical systems. *ESAIM: Control, Optimisation and Calculus of Variations*, 14:699–724, 2008.

[113] J.J.C. van Schendel, M.C.F. Donkers, W.P.M.H. Heemels, and N. van de Wouw. On dropout modelling for stability analysis of networked control systems. In *Proc. American Control Conf.*, pages 555–561, 2010.

[114] P. Seiler and R. Sengupta. An $\mathcal{H}_\infty$ approach to networked control. *IEEE Trans. Autom. Control*, 50:356 – 364, 2005.

[115] Y. Shi and B. Yu. Output feedback stabilization of networked control systems with random delays modeled by markov chains. *IEEE Trans. Autom. Control*, 54:1668 – 1674, 2009.

[116] A. N. Shiryaev. *Probability*. Springer-Verlag, 1984.

[117] B. Sinopoli, L. Schenato, M. Franceschetti, K. Poolla, M.I. Jordan, and S.S. Sastry. Kalman filtering with intermittent observations. *IEEE Trans. Autom. Control*, 49:1453–1464, 2004.

[118] S. Skogestad and I. Postlethwaite. *Multivariable Feedback Control*. John Wiley & Sons, Ltd., 2005.

[119] S.C. Smith and P. Seiler. Estimation with lossy measurements: jump estimators for jump systems. *IEEE Trans. Autom. Control*, 48:2163–2171, 2003.

[120] E.D. Sontag. Nonlinear regulation: The piecewise linear approach. *IEEE Trans. Automat. Contr.*, 26:346–357, 1981.

[121] E.D. Sontag. A Lyapunov-like characterization of asymptotic controllability. *SIAM J. Control Optim.*, 21:462–471, 1983.

[122] Y.S. Suh. Stability and stabilization of nonuniform sampling systems. *Automatica*, 44:3222–3226, 2008.

[123] Y. Sun and N.H. El-Farra. Quasi-decentralized model-based networked control of process systems. *Computers & Chemical Engineering*, 32:2016–2029, 2008.

[124] M. Tabbara and D. Nešić. Input−output stability of networked control systems with stochastic protocols and channels. *IEEE Trans. Autom. Control*, 53:1160–1175, 2008.

[125] M. Tabbara, D. Nešić, and A.R. Teel. Stability of wireless and wireline networked control systems. *IEEE Trans. Autom. Control*, 52:1615–1630, 2007.

[126] P. Tabuada. Event-triggered real-time scheduling of stabilizing control tasks. *IEEE Trans. Autom. Control*, 52:1680–1685, 2007.

[127] T.-J. Tarn, N. Xi, and A.K. Bejczy. Path-based approach to integrated planning and control for robotic systems. *Automatica*, 32:1675–1687, 1996.

[128] Y. Tipsuwan and M.-Y. Chow. Control methodologies in networked control systems. *Control Eng. Pract.*, 11:1099–1111, 2003.

[129] A. van der Schaft. $\mathcal{L}_2$-*Gain and Passivity Techniques in Nonlinear Control*. Springer, 2000.

[130] M. Velasco, J.M. Fuertes, and P. Marti. The self triggered task model for real-time control systems. In *Proc. IEEE Real-Time Systems Symposium*, pages 67–70, 2003.

[131] M. Velasco, P. Marti, and E. Bini. On Lyapunov sampling for event-driven controllers. In *Proc. IEEE Conf. Decision & Control*, pages 6238–6243, 2009.

[132] G.C. Walsh, O. Belidman, and L.G. Bushnell. Asymptotic behavior of nonlinear networked control systems. *IEEE Trans. Autom. Control*, 46:1093–1097, 2001.

[133] G.C. Walsh and H. Ye. Scheduling of networked control systems. *IEEE Control Syst. Mag.*, 21:57–65, 2001.

[134] G.C. Walsh, H. Ye, and L.G. Bushnell. Stability analysis of networked control systems. *IEEE Trans. Control Syst. Technology*, 10:438–446, 2002.

[135] X. Wang and M. Lemmon. Self-triggered feedback control systems with finite-gain $\mathcal{L}_2$ stability. *IEEE Trans. Autom. Control*, 45:452–467, 2009.

[136] X. Wang and M. D. Lemmon. Event-triggering in distributed networked systems with data dropouts and delays. *IEEE Trans. Autom. Control*, pages 586–601, 2011.

[137] X. Wang and M.D. Lemmon. Event design in event-triggered feedback control systems. In *Proc. IEEE Conf. Decision & Control*, pages 2105–2110, 2008.

[138] G. Wei, Z. Wang, X. He, and H. Shu. Filtering for networked stochastic time-delay systems with sector nonlinearity. *IEEE Trans. Circuits and Systems II: Express Briefs*, 56:71 – 75, 2009.

[139] J. C. Willems. Dissipative dynamical systems part I: General theory. *Arch. Ration. Mech. Anal.*, 45:321–351, 1972.

[140] A. Willig, M. Kubisch, C. Hoene, and A. Wolisz. Measurements of a wireless link in an industrial environment using an ieee 802.11-compliant physical layer. *IEEE Trans. Industrial Electronics*, 43:1265–1282, 2002.

[141] E. Witrant, A. D'Innocenzo, G. Sandou, F. Santucci, M.D. Di Benedetto, A. J. Isaksson, K.H. Johansson, S.-I. Niculescu, S. Olaru, E. Serra, S. Tennina, and U. Tiberi. Wireless ventilation control for large-scale systems: The mining industrial case. *Int. J. Robust Nonlinear Control*, 20:226–251, 2010.

[142] N. van de Wouw, P. Naghshtabrizi, M.B.G. Cloosterman, and J.P. Hespanha. Tracking control for sampled-data systems with uncertain sampling intervals and delays. *Int. J. Robust & Nonlinear Control*, 20:387–411, 2010.

[143] F. Yang, Z. Wang, Y.S. Hung, and M. Gani. $\mathcal{H}_\infty$ control for networked systems with random communication delays. *IEEE Trans. Autom. Control*, 51:511 – 518, 2006.

[144] T.C. Yang. Networked control system: a brief survey. *IEE Proc. Control Theory & Applications*, 153:403–412, 2006.

[145] M. Yu, L. Wang, T. Chu, and F. Hao. An LMI approach to networked control systems with data packet dropout and transmission delays. *Proc. IEEE Conf. Decision & Control*, 4:3545–3550, 2004.

[146] L. Zhang, Y. Shi, T. Chen, and B. Huang. A new method for stabilization of networked control systems with random delays. *IEEE Trans. Autom. Control*, 50:1177–1181, 2005.

[147] W. Zhang, M.S. Branicky, and S.M. Phillips. Stability of networked control systems. *IEEE Control Syst. Mag.*, 21:84–99, 2001.

[148] K. Zhou, J.C. Doyle, and K. Glover. *Robust and Optimal Control*. Prentice Hall, 1996.

Acknowledgements (Dankwoord)

Hoewel alleen mijn naam op de voorkant van dit proefschrift staat, heeft het niet alleen mij 'bloed, zweet en tranen' gekost om tot dit proefschrift te komen. Ik ben daarom een aantal mensen dank verschuldigd.

Op de eerste plaats wil ik mijn promotor Maurice Heemels en mijn copromotor Nathan van de Wouw bedanken. Ik heb jullie begeleiding en advies als erg plezierig ervaren. Dankzij jullie enthousiasme, creativiteit, scherpte en immense hoeveelheid kennis is het mij gelukt om tot dit proefschrift te komen. Ook wil ik graag Maarten Steinbuch bedanken voor de kans die hij me heeft gegeven om aan dit promotieonderzoek te kunnen beginnen.

Then, I would like to thank Paulo Tabuada for hosting me at the University of California at Los Angeles. It has been my pleasure to have worked with one of the leading experts on event-triggered control and alongside such a group of wonderful people.

Ook wil ik de afstudeerders bedanken, die ik in de afgelopen jaren heb mogen begeleiden. Bas van Loon, Emile Demarteau en Jos van Schendel, hartstikke bedankt voor al het werk dat jullie hebben verzet. Ik hoop dat jullie veel geleerd hebben; ik heb in ieder geval veel van jullie geleerd!

Although it might seem that the research presented in this thesis is carried out by a single person, many of the ideas presented in my thesis have been conceived at various places and in collaboration with other people. In addition to the people already acknowledged above, I would like to thank (in no particular order) Okko Bosgra, Jeroen van de Wijdeven, Laurentiu Hetel, Nick Bauer, Daniele Bernardini, Alberto Bemporad, Seva Shneer, Andy Teel, Jamal Daafouz, Rob Gielen, Mircea Lazar, Sorin Olaru and Silviu Niculescu for sharing ideas and for giving advice.

I would also like to thank Siep Weiland and Claudio De Persis for being part of the reading committee and for giving detailed comments on the draft version of my thesis.

Om goed werk te kunnen leveren, is het hebben van een plezierige werksfeer ook enorm belangrijk. Collega's van de HNS, CST en D&C-groepen, en in het bijzonder Thijs van Keulen, Nick Bauer en Bram Hunnekens, hartelijk dank voor het creëren van die plezierige werksfeer. Ik heb ongelooflijk genoten van alle groepsuitjes, borrels en congresbezoeken (waarbij deze laatste een aantal beruchte uitspraken heeft opgeleverd, zoals 'Coco Bongo tonight?' en 'Oké, één biertje dan...' en zo kan ik nog wel even doorgaan).

Ook wil ik de mensen bedanken die in mijn leven buiten de muren van de universiteit voor mij onmisbaar zijn. Op de eerste plaats, iedereen van de Kleats (spreek uit: Klets) bedankt voor de vriendenweekenden, carnavalsoptochten,

festivals, etc., maar vooral voor het steeds weer vragen wanneer ik nou eens eindelijk zou afstuderen. Ook wil ik de mensen van KlaarWakker bedanken voor al het plezier dat we samen hebben in het maken van muziek en voor het 'eigen leeftijd delen door twee plus zeven'-criterium.

En dan tot slotte, de mensen die het meest bepalend zijn geweest voor wie ik nu ben: mijn ouders en mijn broer. Anja, Jos en Roel, hartstikke bedankt voor jullie onvoorwaardelijke steun en liefde!

Tijs Donkers
September 2011

Curriculum Vitae

Tijs Donkers was born on 31 August 1981 in Eindhoven, the Netherlands. He received his Bachelor's degree in Mechanical Engineering from Fontys Hogescholen, Eindhoven, the Netherlands, in 2004, and his Master's degree (*cum laude*) in Systems and Control in 2007 from the Eindhoven University of Technology, the Netherlands, in 2007. His Master's thesis was entitled 'Accommodating Model Uncertainty in Iterative Learning Control' and was written under the supervision of Prof Okko Bosgra and Dr Jeroen van de Wijdeven of the Control Systems Technology group.

In November 2007, Tijs Donkers started his PhD research within the Hybrid and Networked Systems group of the department of Mechanical Engineering of Eindhoven University, the Netherlands. The results of his research are presented in this thesis. As part of the PhD programme, he visited the Cyber-Physical Systems laboratory of the University of California, at Los Angeles, CA, USA, in 2010.